

Practical Kinetics and Mechanisms of Chemical and Enzymatic Reactions

Practical Kinetics and Mechanisms of Chemical and Enzymatic Reactions

By

Alexander D. Ryabov

Cambridge
Scholars
Publishing



Practical Kinetics and Mechanisms of Chemical
and Enzymatic Reactions

By Alexander D. Ryabov

This book first published 2021

Cambridge Scholars Publishing

Lady Stephenson Library, Newcastle upon Tyne, NE6 2PA, UK

British Library Cataloguing in Publication Data

A catalogue record for this book is available from the British Library

Copyright © 2021 by Alexander D. Ryabov

All rights for this book reserved. No part of this book may be reproduced, stored in a retrieval system, or transmitted, in any form or by any means, electronic, mechanical, photocopying, recording or otherwise, without the prior permission of the copyright owner.

ISBN (10): 1-5275-6212-3

ISBN (13): 978-1-5275-6212-7

*To my parents,
Nina and Dmitry*

CONTENTS

Solutions of Selected Problems..... xiii

1. Key Definitions 1

- 1.1. A reaction mechanism. What is it?
- 1.2. Rates of chemical reactions and the mass law
- 1.3. Transition state theory (activated complex)
- 1.4. Transition state is by now not initial state but it is not product yet!
- 1.5. Transition states and their formulation
- 1.6. Diffusion and collision theory
- 1.7. Arrhenius equation
- 1.8. Problems

2. Kinetics of Simple Reactions 19

- 2.1. Irreversible first-order reactions
- 2.2. Reversible first-order reactions
 - 2.2.1. Pseudo-first-order reactions. Scatchard equation
- 2.3. Parallel first-order reactions
- 2.4. Consecutive irreversible first-order reactions
- 2.5. Second-order reactions: simplest cases
- 2.6. Zero-order reactions
- 2.7. Problems

3. From Simple Reactions to More Complicated

Kinetic Schemes 41

- 3.1. The steady-state approximation (SSA)
- 3.2. The Michaelis-Menten equation and its numerous analogs
 - 3.2.1. Integration of the Michaelis-Menten equation
 - 3.2.2. Michaelis-Menten versus Henri controversy
 - 3.2.3. Hill equation
- 3.3. pH-Dependent reactions
- 3.4. Autocatalytic (product-catalyzed) reactions
- 3.5. Mechanistic interpretation of rate laws
- 3.6. Belousov-Zhabotinsky oscillating reactions
- 3.7. Problems

4. Inhibition in Chemistry and Enzymology	69
4.1. Substrate inhibition	
4.2. Competitive inhibition	
4.3. Noncompetitive inhibition	
4.4. Uncompetitive and mixed inhibition	
4.5. Problems	
5. Irreversible Inactivation of Catalysts in Chemistry and Enzymology	83
5.1. Enzymology	
5.1.1. Case (i): Resting state inactivation	
5.1.2. Case (ii): Inactivation of enzyme-substrate complex	
5.2. Chemistry	
5.3. Problems	
6. Basic Tools of Chemical Kinetics	91
6.1. Kinetic isotope effects	
6.2. Linear free energy relationships (LFER)	
6.2.1. Hammett and Taft equations	
6.2.2. Brønsted equation	
6.2.3. Solvent and medium effects on rates. Empiric approaches and separation of the ground and transition state effects	
6.3. Activation parameters and mechanisms	
6.3.1. Enthalpy and entropy of activation	
6.3.2. Volume of activation as a mechanistic indicator	
6.4. Problems	
7. Catalysis	113
7.1. Specific acid catalysis (catalysis by proton)	
7.2. Specific base catalysis (catalysis by hydroxide)	
7.3. General acid-base and nucleophilic catalysis	
7.4. Electrophilic catalysis	
7.5. Proximal catalysis	
7.6. Micellar catalysis	
7.7. Problems	
8. Electron Transfer	129
8.1. Introduction	
8.1.1. Reduction potentials and Nernst equation	
8.1.2. Cyclic voltammetry	

- 8.2. Inner- and outer-sphere electron transfer
- 8.3. Marcus electron transfer theory
- 8.4. Important predictions
- 8.5. Problems

9. Oxidations by Metal Ions 143

- 9.1. Metal ions as one-electron oxidants: Co^{III} , Ce^{IV} , Fe^{III} , V^{V} , Mn^{III} and Ag^{I}
- 9.2. KMnO_4 and $\text{K}_2\text{Cr}_2\text{O}_7$
- 9.3. Key reduction potentials of O_2 and H_2O_2
- 9.4. Oxidation of hydrocarbons by “hard” metal oxidants
 - 9.4.1. Oxidation of toluene by Co^{III} in acetic acid at 90-100 °C
 - 9.4.2. Green oxidation of isopropylbenzene to phenol and acetone
 - 9.4.3. Oxidation of benzene
 - 9.4.4. Autoxidation of alkanes
 - 9.4.5. Initiators and antioxidants
- 9.5. Problems

10. Fenton Chemistry and Other Oxidations by Hydrogen Peroxide 159

- 10.1. Fenton Oxidations
 - 10.1.1. Introduction to Fenton Oxidations
 - 10.1.2. Scope of Fenton oxidations: *t*-butanol
 - 10.1.3. Unsaturated hydrocarbons
 - 10.1.4. Generally accepted Fenton mechanism
 - 10.1.5. Mechanisms of major pathways
 - 10.1.6. Mechanistic pathways of arenes
 - 10.1.7. Competing reactions of HO^\bullet
 - 10.1.8. Relative reactivity of aliphatic C–H bonds
 - 10.1.9. Catalase activity in Fenton systems
 - 10.1.10. Alternative mechanistic views on Fenton systems
- 10.2. Heterolytic oxidations by H_2O_2
 - 10.2.1. Oxidations catalyzed by carboxylic acids
 - 10.2.2. Oxidations catalyzed by metal oxides
 - 10.2.3. Baeyer-Villiger oxidation (ketones into esters)
 - 10.2.4. Sharpless asymmetric oxidation
- 10.3. Problems

11. Biooxidation: Peroxidases, Cytochromes P450 and Catalases	173
11.1. Horseradish peroxidase (HRP) oxidations	
11.1.1. Introduction	
11.1.2. Composition of HRP (isozyme C)	
11.1.3. Kinetics and mechanism of HRP	
11.1.4. How to measure reactivities of Compounds I and II?	
11.1.5. Intimate mechanism of activation of H ₂ O ₂ by HRP	
11.2. Cytochromes P450: functions and biological role	
11.2.1. General features	
11.2.2. Reactions of cytochromes P450	
11.2.3. Composition of cytochrome P450 (<i>Pseudomonas putida</i>)	
11.2.4. Mechanism of cytochrome P450	
11.2.5. Reactivity of cytochrome P450 Compound I	
11.2.6. Mechanism of hydroxylation of C-H bonds	
11.2.7. Peroxidases versus cytochromes P450	
11.3. Catalase: H ₂ O ₂ → ½O ₂ + H ₂ O	
11.4. Mononuclear non-heme iron enzymes	
11.4.1. Overview	
11.4.2. Prolyl hydroxylase domain dioxygenase	
11.5. Problems	
12. Alcohol Dehydrogenase (ADH) and Glucose Oxidase (GO)	197
12.1. Alcohol dehydrogenases	
12.1.1. Introduction	
12.1.2. Human alcohol dehydrogenase	
12.1.3. Mechanism of catalysis by alcohol dehydrogenase	
12.2. Glucose oxidase	
12.2.1. Chemistry and structure	
12.2.2. Oxidation of glucose: chemical and enzymatic	
12.2.3. Hydride mechanism of "glucose" half reaction	
12.2.4. Mechanism of FADH ₂ into FAD reoxidation by dioxygen	
12.2.5. Applications of glucose oxidase	

13. Copper Proteins: Tyrosinase and Laccase. Biological Generation of O₂	213
13.1. Tyrosinase	
13.2. Laccases: a family of blue proteins	
13.3. Biological generation of O ₂	
13.4. Problems	
14. Kinases and Phosphatases	223
14.1. Hexo- and glucokinases	
14.2. Protein kinases	
14.3. Phosphatases	
9.3.1. Alkaline Phosphatases	
9.3.2. Acid Phosphatase	
14.4. Problems	

SOLUTIONS OF SELECTED PROBLEMS

1-2. $k_{AB+C} = \frac{\bar{k}T}{h} e^{-\frac{\Delta G_{AB+C}^\ddagger}{RT}}$. Hence

$$\Delta G_{AB+C}^\ddagger = RT \left(\ln \frac{\bar{k}T}{h} - \ln k_{AB+C} \right);$$

$$\Delta G_{A+BC}^\ddagger = \Delta G_{AB+C}^\ddagger + \Delta G^0 = \Delta G_{AB+C}^\ddagger - RT \ln K.$$

1-3. If $k_{\text{obs}} = kK$, $k = k_{\text{obs}}/K = 10^6/10^{20} = 10^{26} \text{ M}^{-1} \text{ s}^{-1}$. This is far above diffusion limit.

1-4. Arrhenius: $\ln k = \ln A - E_A/RT$; $\frac{\partial \ln k}{\partial T} = \frac{E_A}{RT^2}$.

Eyring: $\ln k = \ln T + \ln \frac{\bar{k}}{h} - \frac{\Delta H^\ddagger}{RT} + \frac{\Delta S^\ddagger}{R}$; $\frac{\partial \ln k}{\partial T} = \frac{1}{T} + \frac{\Delta H^\ddagger}{RT^2}$.

Therefore

$$\frac{\partial \ln k}{\partial T} = \frac{E_A}{RT^2} = \frac{1}{T} + \frac{\Delta H^\ddagger}{RT^2}$$

Finally

$$E_A = \Delta H^\ddagger + RT$$

1-5. $k_1 = Ae^{-\frac{E_A}{RT}}$; $k_2 = Ae^{-\frac{(E_A+5.85)}{RT}}$; $\frac{k_1}{k_2} e^{-\frac{5.85(\text{kJ mol}^{-1})}{RT}} \sim 10$.

1-7. The sphere volume is $\frac{4}{3}\pi r^3$. The density $\rho = M/V = \frac{3M}{4\pi r^3}$. Hence, $r = \sqrt[3]{\frac{3M}{4\pi\rho}}$. $D = \frac{\bar{k}T}{6\pi\eta r}$. Therefore $D \sim M^{-1/3}$.

1-8. One in both decaborane and alcohol. Two overall.

2-1. $A_0 = \varepsilon_A a_0$; $A_\infty = \varepsilon_B a_0$; $A_t = \varepsilon_A a_0 e^{-kt} + \varepsilon_B a_0 (1 - e^{-kt}) = a_0 \Delta \varepsilon e^{-kt} + \varepsilon_B a_0$ with $\Delta \varepsilon = \varepsilon_A - \varepsilon_B$. Therefore

$$\ln\{(A_0 - A_\infty)/(A_t - A_\infty)\} = \ln \frac{\varepsilon_A a_0 - \varepsilon_B a_0}{a_0 \Delta \varepsilon e^{-kt}} = \ln e^{kt} = kt$$

2-2. $k = 0.3 \text{ min}^{-1}$.

2-3. At $t = t$, $[A] = (a_0 - x)$ and $[B] = b_0 + x$. Correspondingly

$$-\frac{d(a_0 - x)}{dt} = k_1(a_0 - x) - k_{-1}(b_0 + x) = k_1 a_0 - k_{-1} b_0 - x(k_1 + k_{-1}) = \alpha - \beta x$$

with $\alpha = k_1 a_0 - k_{-1} b_0$ and $\beta = k_1 + k_{-1}$. Therefore

$$-\frac{1}{\beta} \times \frac{d(\alpha - \beta x)}{(\alpha - \beta x)} = dt; \quad \ln(\alpha - \beta x) = c + \beta t$$

At $t = 0$ $x = 0$, $\alpha = c$ and hence

$$\alpha - \beta x = \alpha e^{-\beta t} \quad \text{and} \quad x = \frac{\alpha}{\beta} (1 - e^{-\beta t})$$

Substitution gives

$$x = \frac{a_0 k_1 - b_0 k_{-1}}{k_1 + k_{-1}} (1 - e^{-(k_1 + k_{-1})t})$$

At $t \rightarrow \infty$

$$x_{\text{eq}} = (k_1 a_0 - k_{-1} b_0) / (k_1 + k_{-1}).$$

Finally

$$x = x_{\text{eq}} (1 - e^{-(k_1 + k_{-1})t}).$$

2-5. If Mechanism 1. holds, the amount of B formed should depend on the concentration of X_t (see eq 2.2.3) and the equilibrium constant $K = k_1/k_{-1}$ could be calculated. This should correspond to the ratio of k_1 and k_{-1} found in the kinetic experiment. If Mechanism 2. holds, the amount of B formed is always constant and equal A_t .

2-6. Apply the condition $k_1 = k_2 = k$ to eq 2.4.4. Then

$$d(z \times e^{kt}) = k a_0 dt$$

Integration and application of the boundary condition $z = 0$ at $t = 0$ results in

$$z = a_0 k t e^{-kt} \quad \text{and} \quad y = x - z = a_0(1 - e^{-kt} - k t e^{-kt})$$

Differentiation gives the expression for the steady-state time.

2-7. The differential equation for the consumption of A:

$$-d(a_0 - x)/dt = k_1(a_0 - x) + k_2(a_0 - x)^2$$

If $y = (a_0 - x)$, after rearrangement

$$-\frac{dy}{y(k_1 + yk_2)} = dt$$

and

$$\frac{1}{y(k_1 + yk_2)} = \frac{m}{y} + \frac{n}{k_1 + yk_2}$$

Coefficients m and n are found as for the second-order reaction: $m = 1/k_1$ and $-n = k_2/k_1$. Thus, the function easy to integrate is

$$-\frac{1}{k_1} \frac{dy}{y} + \frac{k_2}{k_1} \times \frac{dy}{k_1 + yk_2} = dt$$

And

$$-\frac{1}{k_1} \frac{dy}{y} + \frac{1}{k_1} \times \frac{d(k_1 + yk_2)}{k_1 + yk_2} = dt$$

followed

$$-\frac{1}{k_1} (\ln y + \ln(k_1 + yk_2)) = t + c$$

Using the boundary conditions $y = a_0$ at $t = 0$ one gets

$$\ln \frac{a_0[k_1 + (a_0 - x)k_2]}{(a_0 - x)(k_1 + a_0k_2)} = k_1 t; \quad a_0 - x = \frac{a_0 k_1 e^{-k_1 t}}{k_1 + a_0 k_2 e^{-k_1 t}}$$

2-10. At any time $\frac{b}{c} = \frac{k_1}{k_2}$ and $x = b + c$. Combining these two equations one obtains

$$x = \frac{k_1 + k_2}{k_1} b$$

Substitution of the expression for x into $x = a_0(1 - e^{-(k_1+k_2)t})$ affords

$$b = a_0 \frac{k_1}{k_1 + k_2} (1 - e^{-(k_1+k_2)t})$$

2-11. It should be confirmed that the relations

$$-\frac{d(a_0 - x)}{dt} = k_1 a_0 e^{-k_1 t} = \frac{dz}{dt} = \frac{k_1 k_2 a_0}{k_1 - k_2} (e^{-k_2 t} - e^{-k_1 t})$$

hold at the steady state. It follows

$$k_1 a_0 e^{-k_1 t} = \frac{k_1 k_2 a_0}{k_1 - k_2} (e^{-k_2 t} - e^{-k_1 t})$$

and

$$e^{-k_1 t} = \frac{k_2}{k_1 - k_2} (e^{-k_2 t} - e^{-k_1 t})$$

Rearrangement affords

$$k_1 e^{-k_1 t} - k_2 e^{-k_1 t} = k_2 e^{-k_2 t} - k_2 e^{-k_1 t}$$

Finally

$$k_1 e^{-k_1 t} = k_2 e^{-k_2 t}$$

2-12.

$$x = \frac{a_0(1 - e^{(a_0 - b_0)kt})}{1 - \frac{a_0}{b_0} e^{(a_0 - b_0)kt}}$$

$$1) a_0 > b_0 \quad x = \frac{-a_0 e^{(a_0 - b_0)kt}}{-\frac{a_0}{b_0} e^{(a_0 - b_0)kt}} = b_0$$

$$2) a_0 < b_0 \quad x = a_0.$$

3-1. Mass balance $A_t = [A] + [AL]$; SSA:

$$0 \sim d[AL]/dt = k_1[A][L] - [AL](k_{-1} + k_2)$$

Two equations, two unknowns. Find expressions for [A] and [AL] at the steady-state

$$d[P]/dt = k_2[AL] + k_3[A]$$

Working with the mass balance equations, one obtains

$$A_t = [A] \left(1 + \frac{k_1 L}{k_{-1} + k_2} \right)$$

And

$$[A] = \frac{k_{-1} + k_2}{k_1 L + k_{-1} + k_2} A_t; \quad [AL] = \frac{k_1 L}{k_1 L + k_{-1} + k_2} A_t$$

Finally

$$k_{\text{obs}} = \frac{k_3(k_{-1} + k_2) + k_1 k_2 L}{k_1 L + k_{-1} + k_2} = \frac{k_3 + \frac{k_1 k_2}{k_{-1} + k_2} L}{1 + \frac{k_1 L}{k_{-1} + k_2}}$$

3-2. Mass balance $Fe_t = [Fe^{III}] + [\text{Oxidized}]$; SSA with respect to Oxidized TAML:

$$0 \sim d[\text{Oxidized}]/dt = k_1[Fe^{III}][H_2O_2] - [\text{Oxidized}](k_{-1} + k_2[S])$$

Since

$$d[P]/dt = k_2[\text{Oxidized}][S]$$

one obtains

$$\frac{d[P]}{dt} = \frac{k_1 k_2 [H_2O_2][S]}{k_{-1} + k_1 [H_2O_2] + k_2 [S]} Fe_t$$

Plotting inverse rate versus $[HOOH]^{-1}$ or $[S]^{-1}$ allows to calculate k_1 and k_2 from the slope and intercept if $k_{-1} \sim 0$.

3-3. Mass balance $E_t = [E] + [ES]$; $K_s = [E][S_t]/[ES]$. Therefore $[ES] = E_t S_t / (K_s + S_t)$ and $v = k_2 E_t S_t / (K_s + S_t)$.

$$K_m = \frac{k_{-1}}{k_1} + \frac{k_2}{k_1}; K_S = \frac{k_{-1}}{k_1}. \text{ Hence } K_m = K_S + \frac{k_2}{k_1}.$$

3-4. Mass balance $E_t = [E] + [ES] + [EA]$; SSA:

$$0 \sim d[ES]/dt = k_1[E][S] - [ES](k_{-1} + k_2)$$

$$0 \sim d[EA]/dt = k_2[ES] - k_3[EA]$$

Three equations, three unknowns. Find expression for $[EA]$ because

$$d[P]/dt = k_3[EA]$$

Working with the mass balance equations, one obtains

$$\begin{aligned} E_t &= [E] + [ES] + [EA] = [EA] \frac{k_3}{k_2} \left(1 + \frac{k_{-1} + k_2}{k_1 S_t} \right) + [EA] = \\ &= [EA] \left(1 + \frac{k_3}{k_2} + \frac{k_3}{k_2} \times \frac{k_{-1} + k_2}{k_1 S_t} \right) = \\ &= [EA] \left(\frac{k_1 k_2 S_t + k_1 k_3 S_t + k_{-1} k_3 + k_2 k_3}{k_1 k_2 S_t} \right) \end{aligned}$$

Hence

$$[EA] = \frac{k_1 k_2 S_t}{k_1 k_2 S_t + k_1 k_3 S_t + k_{-1} k_3 + k_2 k_3} E_t$$

And

$$\frac{d[P]}{dt} = \frac{k_1 k_2 k_3 S_t}{k_1 k_2 S_t + k_1 k_3 S_t + k_{-1} k_3 + k_2 k_3} E_t = \frac{\frac{k_2 k_3}{k_2 + k_3} S_t E_t}{\frac{k_3(k_{-1} + k_2)}{k_1(k_2 + k_3)} + S_t}$$

$$\mathbf{3-5.} \quad v = \frac{k_2 k_4 E_t G_t F_c^+}{k_4 K_M^{Gl} F_c^+ + k_2 K_M^{Fc} G_t + (k_2 + k_4) G_t F_c^+}; K_M^{Fc} = \frac{k_4 + k_{-3}}{k_3} \text{ and } K_M^{Gl} = \frac{k_2 + k_{-1}}{k_1}.$$

3-6. Mass balance $E_t = [E] + [CI] + [CII]$; SSAs:

$$0 \sim d[CI]/dt = k_1[E][P] - k_2[CI][S]$$

$$0 \sim d[CII]/dt = k_2[CI][S] - k_3[CII][S]$$

Three equations, three unknowns. Find expressions for $[CI]$ and $[CII]$ because

$$d[P]/dt = k_2[CI][S] + k_3[CII][S]$$

Using the mass balance equations, one obtains

$$E_t = [CI] \left(1 + \frac{k_2}{k_3} + \frac{k_2 S_t}{k_1 [P]} \right) = [CI] \left(\frac{k_1 k_2 [P] + k_1 k_3 [P] + k_2 k_3 S_t}{k_1 k_3 [P]} \right)$$

Hence

$$[CI] = \frac{k_1 k_3 [P] E_t}{k_1 k_2 [P] + k_1 k_3 [P] + k_2 k_3 S_t}$$

and

$$[CII] = \frac{k_1 k_2 [P] E_t}{k_1 k_2 [P] + k_1 k_3 [P] + k_2 k_3 S_t}$$

Finally

$$\frac{d[P]}{dt} = \frac{2k_1 k_2 k_3 [P] E_t S_t}{k_1 k_2 [P] + k_1 k_3 [P] + k_2 k_3 S_t}$$

3-7. The expression for k_{obs} in this case is:

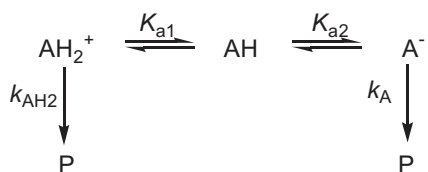
$$k_{obs} = \frac{k_{AH} K_{a1} [H^+]}{[H^+]^2 + K_{a1} [H^+] + K_{a1} K_{a2}}$$

The horizontal part of the curve, when k_{obs} is pH independent, is given by

$$k_{obs} = \frac{k_{AH} K_{a1} [H^+]}{K_{a1} [H^+]} = k_{AH}$$

Left and right straight lines are given by: $k_{obs} = \frac{k_{AH} K_{a1} [H^+]}{[H^+]^2} = \frac{k_{AH} K_{a1}}{[H^+]}$ and $k_{obs} = \frac{k_{AH} K_{a1} [H^+]}{K_{a1} K_{a2}} = \frac{k_{AH} [H^+]}{K_{a2}}$, respectively. Correspondingly, $\log k_{obs} = \log k_{AH}$; $\log k_{obs} = \log k_{AH} - pK_{a1} + \text{pH}$ and $\log k_{obs} = \log k_{AH} - \text{pH} + pK_{a2}$ for the three straight lines. The values of $\log k_{obs}$ are equal at the intersections points. This leads to $pK_{a1} = \text{pH}$ and $pK_{a2} = \text{pH}$.

3-8. The corresponding scheme is:



Mass balance:

$$A_t = [\text{AH}_2^+] + [\text{AH}] + [\text{A}^-];$$

$$K_{a1} = [\text{AH}][\text{H}^+]/[\text{AH}_2^+]; \quad K_{a2} = [\text{A}^-][\text{H}^+]/[\text{AH}]$$

Substitution affords

$$\begin{aligned}
 A_t &= [\text{AH}] \left(1 + \frac{[\text{H}^+]}{K_{a1}} \right) + [\text{A}^-] = \frac{[\text{A}^-][\text{H}^+]}{K_{a2}} \left(1 + \frac{[\text{H}^+]}{K_{a1}} \right) + [\text{A}^-] = \\
 &= [\text{A}^-] \left(1 + \frac{[\text{H}^+]}{K_{a2}} + \frac{[\text{H}^+]^2}{K_{a1}K_{a2}} \right)
 \end{aligned}$$

Equilibrium concentrations are

$$[\text{A}^-] = \frac{K_{a1}K_{a2}}{[\text{H}^+]^2 + K_{a1}[\text{H}^+] + K_{a1}K_{a2}} A_t$$

$$[\text{AH}_2^+] = \frac{[\text{H}^+]^2}{[\text{H}^+]^2 + K_{a1}[\text{H}^+] + K_{a1}K_{a2}} A_t$$

Since $d[\text{P}]/dt = k_{\text{A}}[\text{A}^-] + k_{\text{AH2}}[\text{AH}_2^+]$

$$k_{\text{obs}} = \frac{k_{\text{AH2}}[\text{H}^+]^2 + k_{\text{A}}K_{a1}K_{a2}}{[\text{H}^+]^2 + K_{a1}[\text{H}^+] + K_{a1}K_{a2}}$$

3-10. The time corresponding to the inflection point is found from the equation $\frac{d^2x}{dt^2} = 0$. The solution of the corresponding equation affords $t = \frac{\ln(a/c)}{k(a+c)}$. Assuming that $A = (a + c)$, one obtains $\frac{dx}{dt} = \frac{acA^2ke^{-Akt}}{(c+ae^{-Akt})^2}$. The slope of the straight line when $t = \frac{\ln(a/c)}{k(a+c)}$, i.e. after substitution of this expression for t into $\frac{dx}{dt}$ gives:

$$\frac{dx}{dt} = \frac{acA^2ke^{-Akt}}{(c + ae^{-Akt})^2} = \frac{acA^2ke^{-\frac{Ak \ln(a/c)}{Ak}}}{(c + ae^{-\ln(a/c)})^2} = \frac{c^2A^2k}{(c+c)^2} = \frac{A^2k}{4} = \alpha$$

Check that the units of α are $\{M s^{-1}\}$, cf. with "slope". The value of x ("y" at y axis) at $t = \frac{\ln(a/c)}{k(a+c)}$ is

$$"y" = \frac{ac \left(1 - \frac{c}{a}\right)}{2c} = \frac{a-c}{2}$$

The equation for the straight line $y = \alpha t + \beta$ passing through the inflection point is

$$\frac{a-c}{2} = \frac{A^2k}{4} \times \frac{\ln(a/c)}{k(a+c)} + \beta$$

This allows to find β as

$$\beta = \frac{2(a-c) - A \ln(a/c)}{4}$$

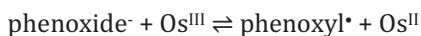
Using this expression one can find time τ , at which "y" equals zero

$$0 = \frac{A^2k}{4} \tau + \frac{2(a-c) - A \ln(a/c)}{4} \quad \text{and} \quad \tau A^2k = A \ln(a/c) - 2(a-c)$$

Finally

$$\tau = \frac{\ln(a/c) - 2 \frac{a-c}{a+c}}{k(a+c)}$$

3-12. Show that the following mechanism works, if both rapidly established equilibria are strongly shifted to the left.¹



¹ Adapted from Song N, Stanbury DM, *Inorg Chem*, **2012**, 51, 4909.

2 phenoxyI* → biphenquinone

3-13. Lineweaver-Burk: $v^{-1} = V_M^{-1} + K_M/(V_M[S])$. When $v^{-1} = 0$, $[S] = -K_M$.

3-14. The Michaelis-Menten equation in a linear form is

$$vK_M + v[S] = V_M[S]$$

After dividing both sides by $[S]$ and rearrangement one arrives to

$$v = V_M - K_M v[S]^{-1}$$

The slope and intercept of a linear v vs. $v[S]^{-1}$ plot equal $-K_M$ and V_M , respectively.

3-15. $y = 0$ when $[S_0] = [S]$. Then $0 = V_M - K_M/t$ and $t = K_M/V_M$.

4-1. $E_t = [E] + [ES] + [ES']$; $K_s = [E][S]/[ES]$; $K'_s = [E][S]/[ES']$; $E_t = [E_s]\{K_s/[S] + 1 + (K_s/[S]) \times ([S]/K'_s)\}$ and hence $[ES] = E_t[S]K'_s/\{K_sK'_s + [S](K_s + K'_s)\}$; $v = k[ES]$. Substitution of the expression for $[ES]$ into the equation for v affords

$$v = \frac{k \frac{K'_s}{K_s + K'_s} [S][E]}{\frac{K_s K'_s}{K_s + K'_s} + [S]}$$

4.2. In this case $v = k[ES] + k'[ES_2]$. $[ES] = E_t[S]/\{K_s + [S] + [S]^2/K_{2s}\}$ (see footnote to page 4-2). $E_t = [ES_2]\{(K_s/[S]) \times (K_{2s}/[S]) + K_{2s}/[S] + 1\}$; $[ES_2] = E_t\{[S]^2 \times K_{2s}^{-1}/[K_s + [S] + [S]^2 \times K_{2s}^{-1}]\}$. Correspondingly

$$v = \frac{k[S] + k' \frac{[S]^2}{K_{2s}}}{K_s + [S] + \frac{[S]^2}{K_{2s}}} E_t$$

When $[S]$ is relatively small and the term $[S]^2 \times K_{2s}^{-1}$ is negligible, $v \sim kE_t$. When $[S]$ is large, $v \sim k'E_t$. Therefore the rate will never drop at high $[S]$, if $k' > k$.

4-3. The noncompetitive inhibition.

4.4. In this case

$$v = \frac{k_{\text{cat}} \frac{K_i}{K_i + [I]} E_t [S]}{K_s + [S]}$$

At $[I] = i_{0.5}$ $v = \frac{1}{2}v$, i.e.

$$\frac{1}{2}v = \frac{k_{\text{cat}} \frac{K_i}{K_i + [i_{0.5}]} E_t [S]}{K_s + [S]}$$

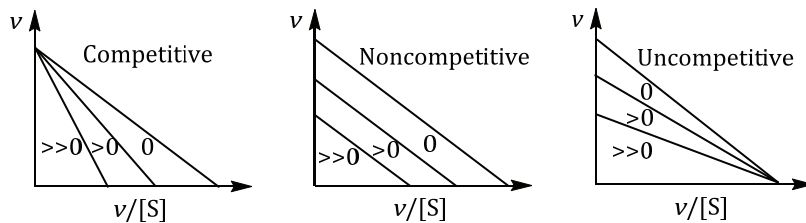
Without inhibition

$$v = \frac{k_{\text{cat}} E_t [S]}{K_s + [S]}$$

Dividing the latter by the former affords

$$2 = \frac{K_i + [i_{0.5}]}{K_i}$$

4-5.



5.1. Under the steady-state conditions (see problem 3-2 when $k_{-1} \approx 0$)

$$\frac{d[P]}{dt} = \frac{k_1 k_2 [\text{oxidant}][S]}{k_1 [\text{oxidant}] + k_2 [S]} C_t$$

One should find the condition when all R_c is rapidly and quantitatively converted to A_c , i.e. the overall rate is determined by k_2 only. This occurs when $k_1 [\text{oxidant}] \gg k_2 [S]$ because in this case

$$\frac{d[P]}{dt} \approx \frac{k_1 k_2 [\text{oxidant}][S]}{k_1 [\text{oxidant}]} C_t = k_2 [\text{oxidant}][S] C_t$$

5-2. It comes from eq 5.2.4 that

$$\frac{S_t}{S_t - x_\infty} = e^{\frac{k_{II}C_t}{k_I}}$$

Therefore

$$x_\infty = S_t(1 - e^{-\frac{k_{II}C_t}{k_I}})$$

See ref. 3 in Lecture 5 for details.

6-2. Since $\frac{\partial \ln k}{\partial p} = -\frac{\Delta V^\ddagger}{RT}$, a two-fold increase in the rate constant means $\partial \ln k = \Delta \ln k = \ln 2k - \ln k = \ln 2$. This corresponds to Δp , which should be found. Substitution the numerical values into the right part of the above equation ($T = 298 \text{ K}$, $R = 82 \text{ cm}^3 \text{ atm K}^{-1} \text{ mol}^{-1}$) gives $\Delta p \sim 1700 \text{ atm}$.

6-3. Isokinetic relationship means that $\Delta H^\ddagger = T\Delta S^\ddagger + \text{const}$. After rearrangement $\Delta H^\ddagger - T\Delta S^\ddagger = \Delta G^\ddagger = \text{const}$, i.e. free energy of activation (and therefore rate constants) is constant within the series.

6-4. The rate expression is given by

$$v = k_1[M][\text{ROOH}] + k_2[\text{MOH}][\text{ROOH}] + k_3[M][\text{ROO}^-] + k_4[\text{MOH}][\text{ROO}^-]$$

$$M_t = [M] + [\text{MOH}]; K_{a1} = \frac{[\text{MOH}][\text{H}^+]}{[M]},$$

$$\text{ROOH}_t = [\text{ROOH}] + [\text{ROO}^-]; K_{a2} = \frac{[\text{ROO}^-][\text{H}^+]}{[\text{ROOH}]}$$

After finding equilibrium concentrations of all four participants followed by substitution into the expression for v , one obtains

$$v = \frac{k_1[\text{H}^+]^2 + k_2K_{a1}[\text{H}^+] + k_3K_{a2}[\text{H}^+] + k_4K_{a1}K_{a2}}{[\text{H}^+]^2 + K_{a1}[\text{H}^+] + K_{a2}[\text{H}^+] + K_{a1}K_{a2}}$$

Kinetically indistinguishable are the k_2 and k_3 pathways.

7-1. Mass balance: $\text{MeCHO}_t \approx [\text{MeCHO}]$ (aldehyde is difficult to deprotonate).

$$v = k_2[\text{MeCHO}][\text{H}_2\text{CCHO}].$$

SSA:

$$0 = k_1[\text{MeCHO}][\text{OH}^-] - [\text{H}_2\text{CCHO}](k_{-1} + k_2[\text{MeCHO}]).$$

Therefore

$$[\text{H}_2\text{CCHO}] = k_2[\text{MeCHO}][\text{OH}^-]/(k_{-1} + k_2[\text{MeCHO}]).$$

Correspondingly

$$v = k_1k_2[\text{MeCHO}]^2[\text{OH}^-]/(k_{-1} + k_2[\text{MeCHO}]).$$

This is eq 7.2.1 with $k = k_1k_2/k_{-1}$, if $k_{-1} \gg k_2[\text{MeCHO}]$.

7-2. A) If the last step is fast, the mass balance equation is $\text{Co}_t = [\text{A}] + [\text{B}]$ (A and B are $[\text{Co}(\text{NH}_3)_5\text{Cl}]^{2+}$ and $[\text{Co}(\text{NH}_3)_4(\text{NH}_2)\text{Cl}]^+$, respectively). SSA for B is

$$0 = k_1[\text{A}][\text{OH}^-] - (k_{-1} + k_2)[\text{B}]$$

Correspondingly

$$[\text{B}] = \frac{k_1[\text{OH}^-]}{k_{-1} + k_2 + k_1[\text{OH}^-]} \text{Co}_t$$

Finally

$$k_{\text{obs}} = \frac{k_1k_2[\text{OH}^-]}{k_{-1} + k_2 + k_1[\text{OH}^-]}$$

because $v = k_2[\text{B}]$.

B) If the last step (k_3) is not fast, the mass balance is $\text{Co}_t = [\text{A}] + [\text{B}] + [\text{C}]$ ($\text{C} = [\text{Co}(\text{NH}_3)_4(\text{NH}_2)]^{2+}$). SSA should be applied for both B and C:

$$0 = k_1[\text{A}][\text{OH}^-] + k_{-2}[\text{C}][\text{Cl}^-] - (k_{-1} + k_2)[\text{B}]$$

and

$$0 = k_2[\text{B}] - [\text{C}](k_{-2}[\text{Cl}^-] + k_3)$$

The rate in this case is $v = k_3[\text{C}]$. There are three equations with three unknowns. This allows to find the expression for the steady-state

concentration of C. Substitution of thus found C into the equation for v gives

$$k_{\text{obs}} = \frac{k_1 k_2 k_3 [\text{OH}^-]}{k_1(k_2 + k_3)[\text{OH}^-] + k_1 k_{-2} [\text{OH}^-][\text{Cl}^-] + k_{-1} k_{-2} [\text{Cl}^-] + (k_{-1} + k_2) k_3}$$

7-3. A) $\text{BH} \rightleftharpoons \text{B}^- + \text{H}^+$ (K_a); $\text{B}_t = \text{BH} + \text{B}^-$; $[\text{B}^-] = K_a \text{B}_t / ([\text{H}^+] + K_a)$. SSA with respect to intermediate **7.1**:

$$0 = (k_1[\text{S}][\text{B}^-] - (k_{-1} + k_2)[\text{7.1}])$$

$\text{S}_t = [\text{S}] + [\text{7.1}]$, but since $[\text{7.1}]$ is very low, $\text{S}_t \sim [\text{S}]$ and $[\text{7.1}] = \frac{k_1}{k_{-1} + k_2} \text{S}_t [\text{B}^-] = \frac{k_1}{k_{-1} + k_2} \times \frac{K_a}{[\text{H}^+] + K_a} \text{S}_t \text{B}_t$. Correspondingly

$$k_{\text{obs}} = \frac{k_1 k_2}{k_{-1} + k_2} \times \frac{K_a}{[\text{H}^+] + K_a} \text{B}_t$$

7-4. Example of a general acid catalysis with H_2PO_4^- as a reactive species.

7-5. Rate $\sim [\text{OH}^-]^{-1}$.

8-3. $c_{\text{red}}/c_{\text{ox}} = 0.01$.

8-4. Let us find the conditions when the first derivative is zero. Rearrangement of eq 8.3.1 gives

$$\frac{\lambda}{4} \left(1 + \frac{2\Delta G}{\lambda} + \frac{\Delta G^2}{\lambda^2} \right) = \frac{\lambda}{4} + \frac{\Delta G}{2} + \frac{\Delta G^2}{4\lambda}$$

After differentiation with respect to ΔG gives

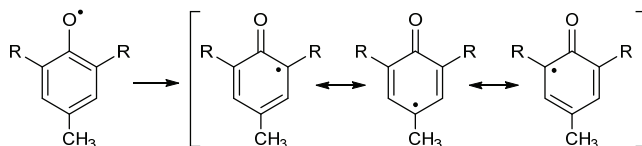
$$0 = \frac{1}{2} + \frac{\Delta G}{2\lambda}$$

And finally, $\lambda = -\Delta G$.

9-1. Inverse rate dependence in $[\text{Co}^{\text{II}}]$.

9-3. The last step in Scheme 9.4.6 should not be fast; rates of steps 2 and 3 should be comparable.

9-4.



9-5. Radical species are potentially carcinogenic.

11-5. Fe-N, Fe-S and Fe-O, respectively.

14-1. Dissociative - S_N1 ; associative S_N2 .

14-4. *S*-Character of the rate versus [Glucose] dependence, which is emphasized in the inset, is indicative of the allosteric regulation of the enzymatic activity by glucose.

14-5. Retention which is due to two inversions.

LECTURE 1.

KEY DEFINITIONS

1.1. A Reaction Mechanism. What Is It?

The most gorgeous in chemistry is almost certainly the understanding of mechanisms of chemical reactions. After finding a novel chemical transformation or synthesizing a new unique compound, the next question that arises inevitably is: "How? How does this reaction occur? Why and how are old bonds cleaved and new bonds are formed?" Apparently, there are certain approaches to study reaction mechanisms. Our ultimate goal is to understand and remember two important issues. First, one should have a clear perception what is the mechanism of a chemical reaction and, second, what methods should be applied for its elucidation in order to claim with confidence that the mechanism of a particular reaction is more or less reliably established.

There are two key definitions.

Definition 1. A mechanism of any chemical reaction is a series of its elementary steps.

Definition 2. A step is referred to as elementary (concerted or synchronous), if it *does not* involve any intermediate.

They define the exact essence of a concept of a *chemical mechanism*. There are two levels of understanding a mechanism. They referred to as *stoichiometric* and *intimate* mechanisms. Note that a stoichiometric mechanism is not synonym of a stoichiometric equation. A stoichiometric mechanism is just a sequence of its elementary steps without detailing the nature of bonds that are cleaved and formed, the nature of orbitals involved, stereochemical features, etc. If these issues are known, one may speak about the intimate mechanism. Consider the electrophilic bromination of ethene. This is an Ad_E (addition

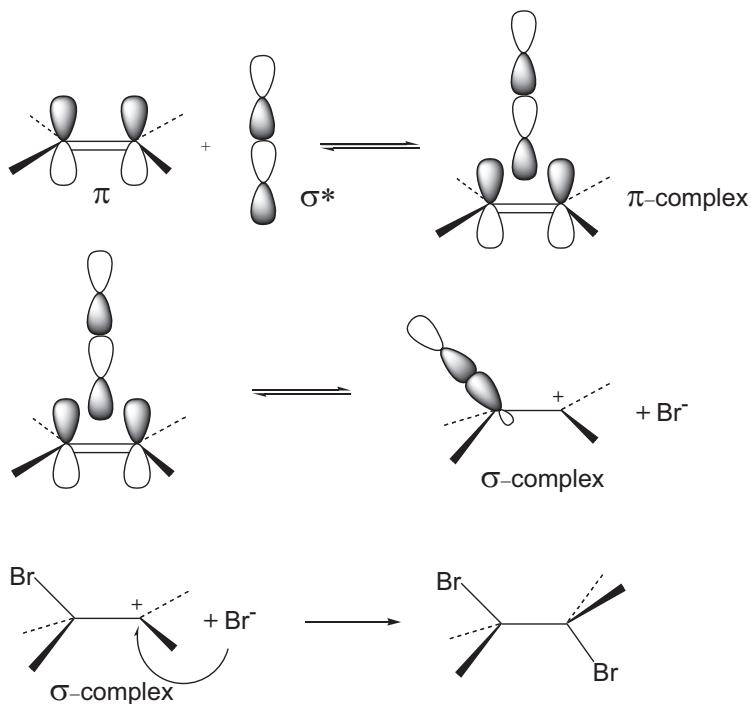
electrophilic) process. Its stoichiometric *equation* (not stoichiometric mechanism!) is given by eq 1.1.1.



The stoichiometric *mechanism* of reaction 1.1.1 consists of three steps:



The intimate mechanism of reaction 1.1.1 specifies key molecular orbitals involved and adds stereochemical details:



The information required for establishing a reaction mechanism is the following:

- 1) A full spectrum of kinetic data for a particular reaction (rate law, absolute values of rate constants and activation parameters, isotope effects, effects of substituents, field or medium effects, etc.).
- 2) Stereochemical information, if appropriate. For example, the retention or inversion of configuration at the sp^3 -hybridized carbon, stereochemical reaction course, etc.).
- 3) Molecular or electronic structure of reacting molecules and products.

The goal of the present *practical* course is to learn the basics of chemical and enzymatic kinetics and to acquire comprehensive tools for elucidating mechanisms of chemical and enzymatic reactions in **solution**.

1.2. Rates of Chemical Reactions and the Mass Law

A **rate (or velocity) of chemical reaction** (v) is a change of moles of a reagent (or a product) per time t referred to a volume V . Rates are always *positive* values. For a simple reaction $A \rightarrow B$ this means:

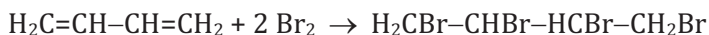
$$v = -\frac{1}{V} \frac{da}{dt} = \frac{1}{V} \frac{db}{dt} \quad (1.2.1)$$

Here a and b are moles of reagent and product, respectively. A solution volume V stays approximately unchanged during the reaction course and this allows one to operate with molar concentrations, since

$$v = -\frac{1}{V} \frac{da}{dt} = -\frac{d\left(\frac{a}{V}\right)}{dt} = -\frac{dc_a}{dt} = -\frac{d[A]}{dt} \quad (1.2.2)$$

Rates of reactions in solution are commonly measured in $\{\text{M s}^{-1}\}$ or $\{\text{mol L}^{-1} \text{s}^{-1}\}$.

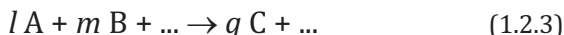
For reactions involving two or more components, which react in a stoichiometric ratio other than 1:1, for example:



the rate expression should be corrected in accordance with the corresponding stoichiometric coefficients:

$$v = -\frac{d[\text{C}_4\text{H}_6]}{dt} = -\frac{1}{2}\frac{d[\text{Br}_2]}{dt} = \frac{d[\text{C}_4\text{H}_6\text{Br}_4]}{dt}$$

For the most general case



The expression for the rate is

$$v = -\frac{1}{l}\frac{d[A]}{dt} = -\frac{1}{m}\frac{d[B]}{dt} = \frac{1}{q}\frac{d[C]}{dt}$$

The rate of chemical reaction is defined. The main law of chemical kinetics known as the **mass law** can now be introduced. According to the mass law, the rate of reaction 1.2.3 follows eq 1.2.4.

$$v = k[A]^{n_A}[B]^{n_B} \dots [?]^{n_{?}} \quad (1.2.4)$$

In other words, **the rate of a chemical reaction** is directly proportional to the product of concentrations of all reagents taken power n_i , which is a *reaction order* with respect to a particular reagent (order in a reagent). The rate constant k can be associated with (in fact, equals to) the reaction rate when concentrations of all reagents equal 1 M. A sum of orders in all reagents is the overall (kinetic) reaction order:

$$\Sigma n_i = \text{overall reaction order}$$

Orders in a particular reagent (and hence overall orders) are usually small **real** numbers (whole numbers, fractions, positive and negative). It is important to see the difference between closely related notions such as *reaction order* and *molecularity*. Molecularity is a reaction order applied to an elementary step. Since an elementary reaction step involves a transformation of one molecule or a collision of two molecules, it becomes clear why molecularity is given by a **natural** number. Reactions with the molecularity of 1 and 2 are often referred to as uni- (mono-) and bimolecular, respectively.

It is vital to remember that reaction orders do not match stoichiometric coefficients of the corresponding balanced equations. The stoichiometric coefficients are derived using a paper and a pen.

Reaction orders are obtained experimentally. Consider reaction 1.2.5 between decaborane $B_{10}H_{14}$ and alcohols:



The stoichiometric coefficient at ROH of 30 should be compared with the reaction kinetic order of 1 found experimentally. Correspondingly, the experimentally determined rate expression for reaction 1.2.5 is given by:¹

$$v = k[B_{10}H_{14}][ROH]$$

1.3. Transition State Theory (Activated Complex)

A comprehensive treatment of kinetic data is based on the concept of the transition state, activated complex (**AC**), or absolute rates. A pseudo-thermodynamic treatment of reacting species, A and B in particular, is used. Its essential postulates look obvious:

- A transformation of molecules A and B into C ($A + B \rightarrow C$) requires an “equilibrium” formation of the transition state (or activated complex) AB^\ddagger , all thermodynamic laws being applicable to this equilibrium



- The rate of chemical reaction is proportional to the concentration of **AC**:

$$v \sim [AB^\ddagger]$$

- According to Eyring, the coefficient between the rate and the concentration of **AC** is the frequency factor $\frac{\bar{k}T}{h}$:

$$v = \frac{\bar{k}T}{h} [AB^\ddagger] \quad (1.3.2)$$

Here

¹ Beachell HC, Meeker TR, *JACS*, **78**, 1796 (1956).

- \bar{k} is the Boltzmann constant ($1.381 \times 10^{-23} \text{ J K}^{-1}$);
- h is the Planck constant ($6.626 \times 10^{-34} \text{ J s}$);
- $\frac{\bar{k}}{h} = 2.08 \times 10^{10} \text{ K}^{-1} \text{ s}^{-1}$; $\ln\left(\frac{\bar{k}}{h}\right) = 23.758$;
- T is the temperature ($273.15 \text{ K} = 0 \text{ }^\circ\text{C}$).

Substitution of the numerical values of the Boltzmann and Planck constants gives the frequency factor $\frac{\bar{k}T}{h}$ of $5.693 \times 10^{12} \text{ s}^{-1}$ at $0 \text{ }^\circ\text{C}$. The physico-chemical meaning of the factor is a frequency of conversion of **AC** into reaction products, which is thus always one and the same, i.e. independent on the nature of **AC**.

The consequences of eq 1.3.2 follow. Consider process 1.3.1 as a simple equilibrium, which is characterized by the equilibrium constant K^\ddagger .

$$K^\ddagger = \frac{[\text{AB}^\ddagger]}{[\text{A}][\text{B}]} \quad \text{or} \quad [\text{AB}^\ddagger] = K^\ddagger [\text{A}][\text{B}] \quad (1.3.3)$$

Substitution of the expression for $[\text{AB}^\ddagger]$ into 1.3.2 affords the rate equation as a function of concentrations of reagents A and B:

$$v = \frac{\bar{k}T}{h} K^\ddagger [\text{A}][\text{B}] \quad (1.3.4)$$

Equation 1.3.4 illustrates a relation between experimentally obtained kinetic information and a composition of the transition state. Confirmed only experimentally, concentrations in eq 1.3.4 reflect type and number of molecules that assemble the transition state. The reaction rate depends on concentrations of those reagents, which create **AC**. Equation 1.3.4 shows in particular that **AC** is made of one molecule A and one molecule B, since the reaction orders in both reagents equal 1. The overall reaction order equals 2, and the expression for the second-order rate constant k_2 is given by eq 1.3.5.

$$v = \frac{\bar{k}T}{h} K^\ddagger [\text{A}][\text{B}] = k_2 [\text{A}][\text{B}]; \quad k_2 = \frac{\bar{k}T}{h} K^\ddagger \quad (1.3.5)$$

Let us show how k_2 depends on the temperature. The equilibrium constant for a chemical equilibrium at a constant pressure is related to

a change in the Gibbs free energy ΔG° . By definition, the Gibbs free energy is

$$G = E + PV - TS = H - TS$$

The thermodynamic function G is used since reactions are usually run at constant temperature and pressure. This condition (constant T and P) should hold in the course of collecting kinetic data. Since for any equilibrium $\Delta G^\circ = -RT \ln K^\circ$, it follows

$$\Delta G^\ddagger = \Delta H^\ddagger - T\Delta S^\ddagger = -RT \ln K^\ddagger$$

or

$$K^\ddagger = e^{-\frac{\Delta H^\ddagger}{RT}} e^{\frac{\Delta S^\ddagger}{R}} \quad (1.3.6)$$

Here R is the gas constant (8.314 J K⁻¹ mol⁻¹, or 1.987 cal K⁻¹ mol⁻¹, or 0.08205 L atm K⁻¹ mol⁻¹). Finally,

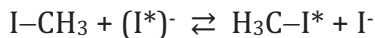
$$k_2 = \frac{\bar{k}T}{h} e^{-\frac{\Delta G^\ddagger}{RT}} = \frac{\bar{k}T}{h} e^{-\frac{\Delta H^\ddagger}{RT}} e^{\frac{\Delta S^\ddagger}{R}} \quad (1.3.7)$$

Parameters ΔH^\ddagger and ΔS^\ddagger in eq 1.3.7 are the *enthalpy* and *entropy*, respectively, of activation or formation of **AC**. Found experimentally, they are important characteristics for establishing mechanisms of chemical reactions. Equation 1.3.7 is often referred to as the fundamental equation of the transition state theory.

1.4. Transition State Is By Now Not Initial State But It Is Not Product Yet!

If the pseudo-thermodynamic approach is applied for characterizing the reactivity, the required key information is the energy difference between the initial and transition states. A common relation is $\Delta G^\ddagger > 0$, i.e. the transition state energy is higher than the energy of the initial state. This implies that for a reaction to occur, molecule/s must gain extra energy needed for breaking chemical bonds. In the thirties, this concept found theoretical support for ideal reactions of the type A + BC

$\rightleftharpoons \text{AB} + \text{C}$. Examples of such reactions in solution are the classical $\text{S}_{\text{N}}2$ bimolecular nucleophilic substitutions:



Such systems were used for construction of illustrative three-dimensional profiles of the potential energy (Fig. 1.4.1). Along the x axis is the $r(\text{BC})$ distance, along y is the $r(\text{AB})$ distance, along z is the energy of the system. A pathway of the lowest energy from the initial state $\text{A} + \text{BC}$ to the final state $\text{AB} + \text{C}$ is the **reaction coordinate**. A graph viewing the energy along the reaction coordinate is the reaction **energy profile**. The transition state is located at a saddle point on the potential energy surface. This is the lowest energy maximum. Obviously, a particle with a maximal energy cannot be stable. That is why it is unwise to ascribe properties of a real molecule to an activated complex. In contrast to an intermediate species, a transition state cannot be registered by any analytical technique. If somebody succeeded to "characterize" the transition state for the $\text{A} \rightarrow \text{B}$ reaction, this means most likely that it is a two-step process $\text{A} \rightarrow \text{C} \rightarrow \text{B}$ and the characterized species is an unstable high energy intermediate C rather than the transition state A^\ddagger . Energy profiles are also shown as two-dimensional plots (Fig. 1.4.2).

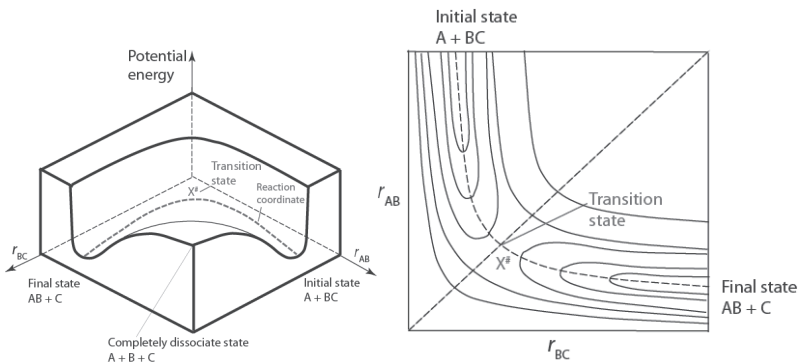


Figure 1.4.1. 3D energy profile for reaction $\text{A} + \text{BC} \rightleftharpoons \text{AB} + \text{C}$ (left); its simplified 2D version is shown on the right. Transition state X^\ddagger is located in the saddle point.

It is impossible to measure the energy along the entire reaction coordinate. The energy difference between the initial and transition states can only be obtained experimentally. To calculate this energy

using eq 1.3.7, one should determine the rate constant for forward reaction. If it is possible to determine a rate constant for the reverse reaction, one can calculate the relative energy of the final state. The final state energy can also be calculated from the equilibrium constant for a reaction such as $A + BC \rightleftharpoons AB + C$ using the equation $\Delta G^\circ = -RT \ln K^\circ$ (Fig. 1.4.2).

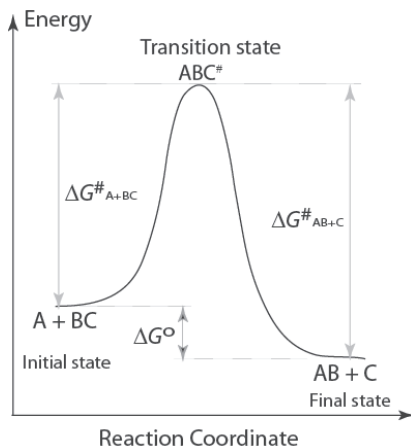


Figure 1.4.2. 2D energy profile for reaction $A + BC \rightleftharpoons AB + C$.

1.5. Transition States and Their Formulations

One can judge about a reaction mechanism knowing the composition of the transition state. The rate law such as in eq 1.2.4 provides the required information. It is easy to interpret the mechanism when the reaction orders in reagents A, B, etc. are small natural numbers (0; 1, rarely 2), when the reaction order is identical to the molecularity. Imagine that a reaction order in B equals not 1 as in eq 1.3.5 but zero. This means that the transition state of the reaction $A + B \rightarrow C$ is made of reagent A only and reagent B is not included in AC . This case is realized for the S_N1 reactions. It should also be mentioned that fractional, high, and negative reaction orders are encountered rather often; they are indicative of multistep reactions. Such cases require extra information and will be considered later.

Transition states may be *early* and *late*, *reagent-like* and *product-like* (Fig. 1.5.1). Early and reagent-like transition states are closer to

reagents on the reaction coordinate. They remind of starting reagents rather than of products. The opposite is true for the late and product-like transition states. In associative reactions, the bond making dominates in the transition state. The bond breaking dominates in the transition states of dissociative reactions.

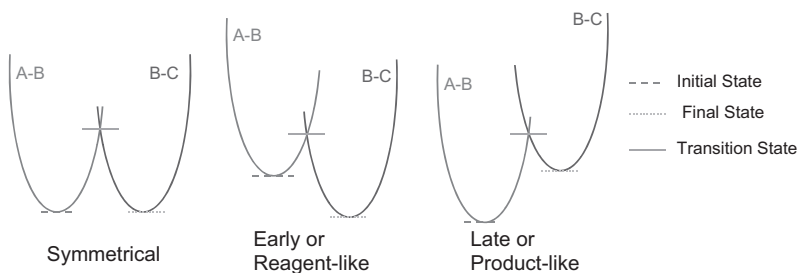


Figure 1.5.1. Types of transition states for reaction $AB + C \rightarrow A + BC$.

1.6. Diffusion and Collision Theory

There is a rhetorical question. Is it necessary to stir or shake a homogeneous non-viscous solution of compounds A and B for ensuring faster reaction between the reagents? The answer must be negative, since the reaction cannot occur faster than the rate of diffusion of molecules A to B and the stirring does not diminish diffusion time. That is why the rate of second-order reactions has the upper limit controlled by diffusion.

The second-order rate constant for a homogeneous reaction cannot be higher than 10^9 - $10^{10} \text{ M}^{-1} \text{ s}^{-1}$.

Let us make sure that this is the case. The rate of linear diffusion, i.e. a number of molecules N , which cross the surface $s \text{ \{cm}^2\}$ in 1 s, is determined by the first Fick's law:

$$\frac{dN}{dt} = -Ds \frac{dn_r}{dr} \quad (1.6.1)$$

Here D is the diffusion coefficient $\{\text{cm}^2 \text{ s}^{-1}\}$ and dn_r/dr is the concentration gradient. We will solve this differential equation for the

steady-state diffusion using the centro-symmetric function. A number of species in a given volume is

$$n_r = A + \frac{B}{r}$$

The parameters A and B are found from the limiting conditions. Let at the infinite r ($r \rightarrow \infty$) the number of species in a given volume be zero, but at $r = r_0$ the number $n_r = n$ (Fig. 1.6.1). When $r \rightarrow \infty$, $n_r = 0$. Therefore $A = 0$ and $B = nr_0$. Hence

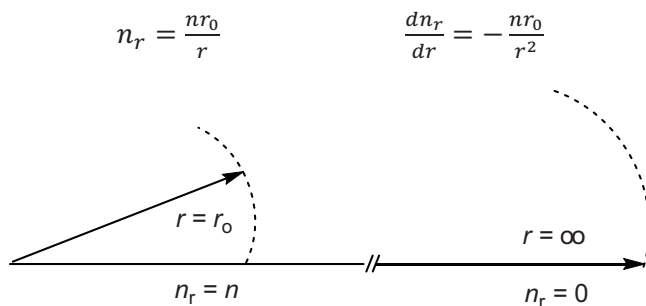


Figure 1.6.1. Evaluation of parameters A and B .

A number of species N that cross a spherical surface of $4\pi r^2$ in 1 second is

$$N = 4\pi D n r_0 \quad (1.6.2)$$

Let the species be now reacting molecules A and B of radii r_A and r_B , respectively. A number of molecules A , which after 1 s reach a spherical surface with a diameter $(r_A + r_B)$, will equal $4\pi D_A (r_A + r_B) n_A$. This quantity can be associated with the number of collisions of all molecules A with one molecule B , if r_A and r_B are the radii of A and B , respectively.

$$Z_A = 4\pi D_A (r_A + r_B) n_A$$

The collision number with all molecules B will be:

$$Z_{AB} = 4\pi D_A (r_A + r_B) n_A n_B$$

Application of the same approach to species B , which diffuse independently of species A , affords:

$$Z_{BA} = 4\pi D_B(r_A + r_B)n_A n_B$$

Total number of *double collisions* is obviously a sum of Z_{AB} and Z_{BA} .

$$Z = 4\pi(D_A + D_B)(r_A + r_B)n_A n_B$$

The expression for Z helps to estimate the upper limit for the bimolecular rate constant k_2 on the assumption that each collision results in a chemical reaction. Let us set that $r_A = r_B = r$ and $D_A = D_B = D$. By definition $k_2 = Z/(n_A n_B)$ and, if expressed in $\text{M}^{-1} \text{s}^{-1}$, the equation for the second-order rate constant appears as

$$k_2 = \frac{16\pi N_A}{1000} D r \quad (1.6.3)$$

Here N_A is the Avogadro number ($6.022 \times 10^{23} \text{ mol}^{-1}$). Substitution of the numerical values of $r \approx 5 \times 10^{-8} \text{ cm}$ and $D \approx 10^{-5} \text{ cm}^2 \text{ s}^{-1}$ gives k_2 of $1.5 \times 10^{10} \text{ M}^{-1} \text{ s}^{-1}$. Second-order rate constants cannot largely exceed this value. Representative examples of diffusion-controlled processes are shown in Table 1.1.

Table 1.1. Second-order rate constants for protonation of some anions in water at 25 °C.

Anion	$10^{-10} \times k_2 / \text{M}^{-1} \text{s}^{-1}$
OH^-	14
MeCOO^-	5.1
PhCOO^-	3.7

Rate constants for diffusion-controlled reactions are temperature dependent. The diffusion coefficient for spherical particles of radius r is inversely proportional to the viscosity of solution ($\eta = 8.94 \times 10^{-3} \text{ g cm}^{-1} \text{ s}^{-1}$ at 25 °C in water) and is given by the Stokes-Einstein equation

$$D = \frac{\bar{k}T}{6\pi\eta r} \quad (1.6.4)$$

Viscosity η depends exponentially on temperature according to the empirical law

$$\eta = b e^{\frac{B}{RT}} \quad (1.6.5)$$

Here b и B are constants (B is often called the activation energy of diffusion). The equation obtained after substitution of equation 1.6.5 into the Stokes-Einstein equation 1.6.4 and then the expression for D into 1.6.3 demonstrates the dependence of a rate constant for the diffusion-controlled reaction on the activation energy of diffusion

$$k_2 = \frac{2.66 N_A \bar{k} T}{1000 b} e^{-\frac{B}{RT}} \quad (1.6.6)$$

Equation 1.6.6 indicates that B can be considered as the enthalpy of activation for a diffusion-controlled process. At 25 °C in water the numerical value of B is ca. 16 kJ mol⁻¹. Important conclusion is that if one obtains rather low values of the enthalpy of activation for a heterogeneous reaction, it should first be tested whether or not this is a diffusion-controlled reaction. If so, stirring must increase the rate.

1.7. Arrhenius Equation

This is a tribute to the history of chemical kinetics. Chemists do not use often nowadays Arrhenius eq 1.7.1 because the transition state theory equation (1.3.7) is preferred.

$$k = A e^{-\frac{E_A}{RT}} \quad (1.7.1)$$

Nevertheless, the Arrhenius equation is worth considering. Let us show how it can be derived by the example of reversible reaction 1.7.2.



The equilibrium occurs when the rates of forward and reverse reactions are the same, i.e.

$$k_1[A][B] = k_{-1}[C][D]$$

and

$$\frac{k_1}{k_{-1}} = \frac{[C][D]}{[A][B]} = K_1 \quad (1.7.3)$$

Since $\Delta G^\circ = \Delta H^\circ - T\Delta S^\circ = -RT\ln K_1$, after dividing by T and differentiation we arrive to the van't Hoff's equation

$$\Delta H^0 = RT^2 \left(\frac{d\ln K_1}{dT} \right)_p \quad (1.7.4)$$

Substitution of eq 1.7.3 into eq 1.7.4 gives the expression for the enthalpy of reaction

$$\Delta H^0 = RT^2 \left(\frac{d\ln k_1}{dT} \right)_p - RT^2 \left(\frac{d\ln k_{-1}}{dT} \right)_p \quad (1.7.5)$$

The right side terms of eq 1.7.5 are referred to as the activation energies for the forward and reverse steps of reaction 1.7.2. Therefore

$$\Delta H^\circ = E_{A,1} - E_{A,-1}$$

Here by definition

$$E_A = RT^2 \left(\frac{d\ln k}{dT} \right)_p \quad (1.7.6)$$

Integration gives Arrhenius equation 1.7.1. Integration constant A is known as a *pre-exponential factor* and has the same units as the rate constant k . One may say that A equals the rate constant at zero activation energy.

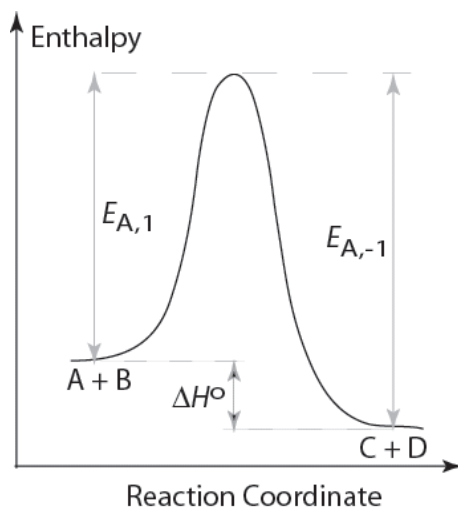


Figure 1.7.1. Enthalpy change along the reaction coordinate for reaction 1.7.2 illustrating the Arrhenius approach.

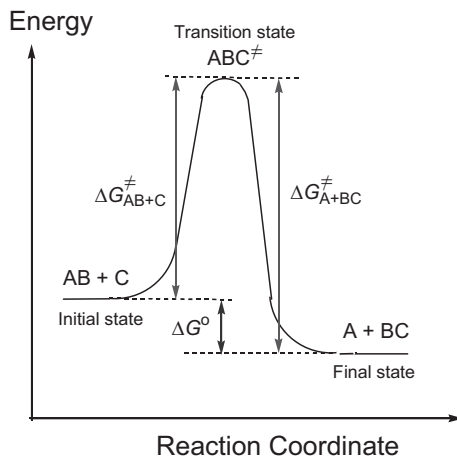
Equation 1.7.1 emphasizes exponential dependence of a rate constant on the temperature. Higher the activation energy, which is measured in kcal mol^{-1} or kJ mol^{-1} , more sensitive the reaction rate to the temperature. It is worth remembering simple relations between “energy” and “factor”. In particular, a decrease in the activation energy by $1.4 \text{ kcal mol}^{-1}$ (5.85 kJ mol^{-1}) provides a ten-fold increase in the rate. If the activation energy equals 5, 10, and 20 kcal mol^{-1} , the reaction rate will increase by a factor of 12.3, 140, and 2.1×10^4 , respectively, on raising the temperature from 273 to 373 K.

Problems

1-1. Choose a chemical reaction (organic, inorganic, bioinorganic, etc.), the mechanism of which is rather familiar to you. Write:

1. its stoichiometric equation;
2. its stoichiometric mechanism;
3. its intimate mechanism. Indicate participating orbitals. Comment on the stereochemistry, if applicable.

1-2. Suggest a formula for calculating ΔG^\ddagger_{AB+C} from the corresponding rate constant (Figure). How to calculate the free energy of activation ΔG^\ddagger_{A+BC} for the reverse reaction, if the equilibrium constant is available for reaction $AB + C \rightleftharpoons A + BC$?



1-3. Consider the kinetic scheme for reaction $A + B \rightarrow C$ in solution, which involves an intermediate A_1 :



Comment on feasibility of this stoichiometric mechanism as shown from the standpoint of *diffusion limitations*. Take into account that the experimental rate law is $v = k_{\text{obs}}[A][B]$, $k_{\text{obs}} = 1 \times 10^6 \text{ M}^{-1} \text{ s}^{-1}$, and the equilibrium constant $K = [A_1]/[A] = 1 \times 10^{-20}$. (Hint: make sure first that $k_{\text{obs}} = kK$, since $v = k[A_1][B]$).

1-4. Find the relation between the Arrhenius activation energy E_A and the enthalpy of activation ΔH^\ddagger . (Hint: play with the relation $k(\text{Arrhenius}) = k(\text{transition state})$, k is a rate constant).

1-5. Show that a decrease in the activation energy by $1.4 \text{ kcal mol}^{-1}$ (5.85 kJ mol^{-1}) provides a ten-fold increase in a rate constant if the pre-exponential factor stays the same.

1-6. Show that if the activation energy equals 5, 10, and 20 kcal mol^{-1} , the reaction rate will increase by a factor of 12.3, 140, and 2.1×10^4 ,

respectively, on raising the temperature from 273 to 373 K, the pre-exponential factor being the same.

1-7. Suggest a relation between diffusion coefficient and molecular weight. Approximate a molecule by a spherical particle.

1-8. Consider reaction 1.2.5 and the corresponding rate equation. Identify reaction orders in each reagent and the overall reaction order.

LECTURE 2.

KINETICS OF SIMPLE REACTIONS

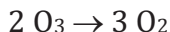
2.1. Irreversible First-Order Reactions

Rather unexpectedly, it is not easy to find true irreversible first order reactions that occur in solution. A few processes that take place in condensed media and in a gas phase are shown below.

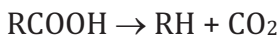
1) Decomposition of nitrogen(V) pentoxide in solution and the gas phase



2) Decomposition of ozone



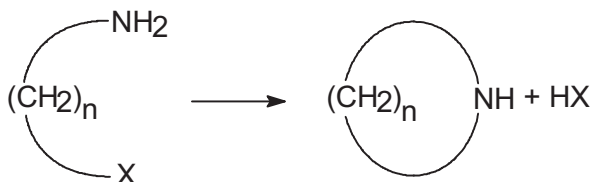
3) Decarboxylation of carboxylic acids



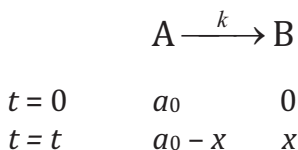
4) Elimination of CS₂ in xanthic acids



5) Various intramolecular reactions



For all these reactions the rate law is simple, *i.e.* $v = k[A]$. Our goal is to calculate the rate constant k from the time dependence of either reagent or product concentration. For a first order irreversible reaction



(at time $t = 0$ concentrations of A and B equal a_0 and 0, whereas at time $t = t$ the concentrations are $a_0 - x$ and x , respectively). The corresponding differential equation is

$$-\frac{dA}{dt} = \frac{dB}{dt} = -\frac{da}{dt} = -\frac{d(a_0 - x)}{dt} = k(a_0 - x)$$

Here a is a current concentration of A. This equation can be rewritten for convenient integration

$$\frac{d(a_0 - x)}{(a_0 - x)} = -kdt$$

Integration gives

$$\ln(a_0 - x) = c - kt$$

The boundary condition ($x = 0$ at $t = 0$) provides $c = \ln a_0$. Therefore

$$\ln(a_0 - x) = \ln a_0 - kt \quad (2.1.1)$$

$$\ln \frac{(a_0 - x)}{a_0} = -kt \quad \text{or} \quad \ln \frac{a_0}{(a_0 - x)} = kt \quad (2.1.2)$$

And

$$a = a_0 - x = a_0 e^{-kt} \quad (2.1.3)$$

or

$$x = b = a_0(1 - e^{-kt}) \quad (2.1.4)$$

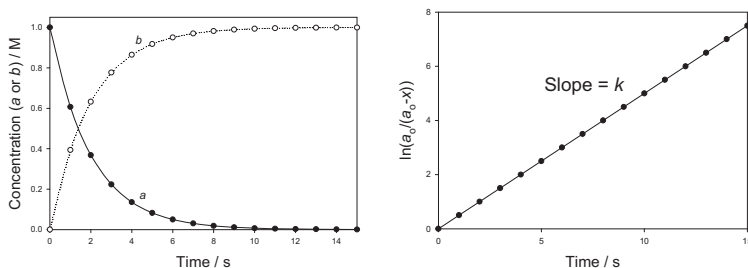


Figure 2.1.1 (left). Kinetics of a first-order reaction; $a_0 = 1 \text{ M}$; $k = 0.5 \text{ s}^{-1}$.

Figure 2.1.2 (right) Example for calculation of a first-order rate constant k .

Figure 2.1.1 shows how current concentrations of a and b depend on time. Equations 2.1.1 and 2.1.2 suggest possible procedures for calculating first-order rate constants k , which are expressed in s^{-1} . Equation 2.1.2 is particularly valuable for chemists, since it shows that for calculation of k one must know a parameter which is just **proportional** to the concentration of a or b , such as absorbance, conductivity, intensity of an NMR signal, etc.

An important characteristic of a first-order reaction is the **half-life**¹ (half-time) of A. It is time during which half of A reacts, i.e. such t when $x = a_0/2$. It comes from eq 2.1.2 that

$$t_{1/2} = \frac{\ln 2}{k} = \frac{0.693}{k} \quad (2.1.5)$$

Importantly, $t_{1/2}$ is independent of the concentration of A for first-order reactions and depends only on the rate constant k . If a linear dependence between, for example, $\ln[a_0/(a_0-x)]$ and time holds for 2-3 half-lives, it is a "satisfactory" first-order; if for 5 and more half-lives, this is a reliable first-order process. However, a linear dependence observed in a matter of 1-2 half-lives may not indicate that the reaction order equals 1! Figures 2.1.3 and 2.1.4 should make these points very clear. Figure 2.3.1 shows theoretical kinetic curves for zero-, first-, and second-order reactions when A is transformed into B, $[A]_t = 1 \text{ M}$, and the corresponding rate constants equal 0.2 M s^{-1} , 0.2 s^{-1} , and $0.2 \text{ M}^{-1} \text{ s}^{-1}$, respectively. Figure 2.1.4 demonstrates attempted linearization of the

¹ Cf. with life-time, which is inverse first-order rate constant.

three curves using a first-order approach (eq 2.1.1). As seen, the zero- and second-order curves are far from being linear. However, their curvature is much less obvious, if one analyzes the data collected within one or two half-lives (in less than 5 min in this case).

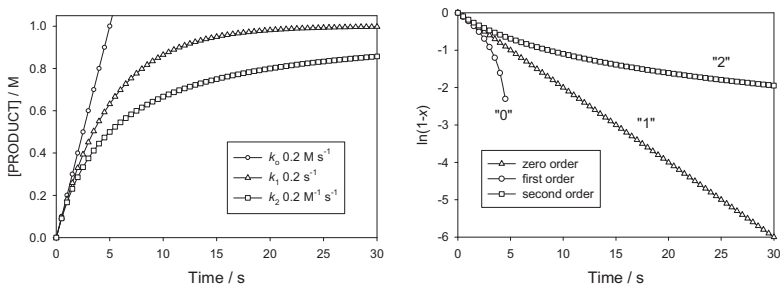


Figure 2.1.3 (left). Theoretical kinetic curves for zero-, first- and second-order reactions at $[A]_t = 1 \text{ M}$.

Figure 2.1.4 (right) Attempted linearization of three curves in Fig. 2.1.3 using the first-order routine (eq 2.1.1).

If first-order dependence is reliably established and the kinetic data is collected by measuring a change in absorbance, a first-order rate constant k is often calculated by the computer fitting of the absorbance (A) versus time (t) data to the equation

$$A = A_\infty - (A_\infty - A_0)e^{-kt} \quad (2.1.6)$$

Here A_0 and A_∞ are absorbances at time $t = 0$ and $t = \infty$, respectively.

First-order rate constants can be calculated from initial rates which are the slopes at $t = 0$ of either of the curves in Fig. 2.1.1. In fact

$$v = -\frac{d(a_0 - x)}{dt} = k(a_0 - x)$$

When the conversion of A is lower 10%, $a_0 \gg x$. Therefore

$$v_0 = -\frac{da_0}{dt} = ka_0$$

Initial rates v_0 should be measured at different a_0 . At least a 10-fold concentration range should be covered. A slope of linear plot of v_0 versus a_0 equals k .

2.2. Reversible First-Order Reactions

The elementary reaction to be considered is:



Examples include the mutarotation of *D*-glucose (interconversion between its α and β anomers) and the *cis* \rightarrow *trans* isomerization of azobenzene. Let at $t = 0$ the concentration of [A] be a_0 and [B] = 0 for simplicity. At $t = t$ we have [A] = $(a_0 - x)$ and [B] = x . The differential equation appears as:

$$-\frac{d(a_0 - x)}{dt} = k_1(a_0 - x) - k_{-1}x = k_1a_0 - x(k_1 + k_{-1})$$

If $\alpha = (k_1 + k_{-1})$

$$-\frac{1}{\alpha} \frac{d(a_0k_1 - \alpha x)}{dt} = dt$$

Integration leads to

$$-\frac{1}{\alpha} \ln(a_0k_1 - \alpha x) = t + c$$

Since $x = 0$ at $t = 0$, $c = -\frac{1}{\alpha} \ln(a_0k_1)$. Substitution and rearrangement give the final expression for x as a function of time.

$$x = \frac{a_0k_1}{k_1 + k_{-1}} (1 - e^{-(k_1 + k_{-1})t}) \quad (2.2.1)$$

At infinite time ($t \rightarrow \infty$), x is the equilibrium concentration of product B:

$$x_{\text{eq}} = (k_1a_0)/(k_1 + k_{-1}).$$

Therefore

$$x = x_{\text{eq}}(1 - e^{-(k_1+k_{-1})t}) \quad (2.2.2)$$

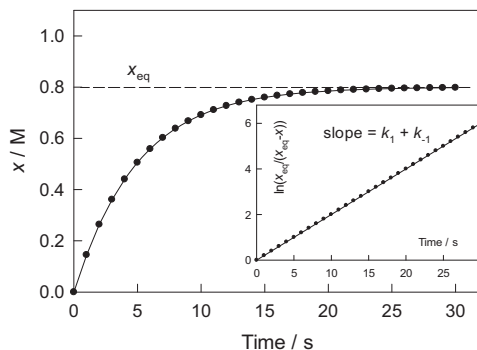
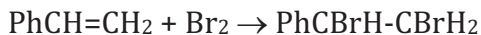


Figure 2.2.1. Kinetic analysis of a reversible first-order reaction ($a_0 = 1$ M, $x_{\text{eq}} = 0.8$ M).

Equation 2.2.2 shows that kinetic analysis of irreversible and reversible first-order reactions is similar (Fig. 2.2.1). A peculiarity of the reversible case is that the slope equals the **sum** of the forward and reverse rate constants $k_1 + k_{-1}$. For calculation of the individual rate constants k_1 and k_{-1} , it is necessary to determine independently the equilibrium constant $K = k_1/k_{-1}$. Two equations (the slope = $k_1 + k_{-1}$ and $K = k_1/k_{-1}$) allow calculating k_1 and k_{-1} .

2.2.1. Pseudo-first-order reactions

Integration of first-order reactions is simple. Therefore, it is preferable to deal with such reactions. True first-order reactions are however limited. Fortunately, it is possible to “create” such artificially. Consider the bromination of styrene



for which the following kinetic equation holds

$$v = k_2[\text{PhCH}=\text{CH}_2][\text{Br}_2]$$

If the concentration of one reagent is by many times higher than that of the other, ($[\text{PhCH}=\text{CH}_2] \gg [\text{Br}_2]$ in particular) we can assume that the

concentration of styrene remains unchanged during the reaction and therefore constant. Consequently

$$v = k_{\text{obs}}[\text{Br}_2]$$

Here $k_{\text{obs}} = k_2[\text{PhCH}=\text{CH}_2]$ is a ***pseudo-first-order rate constant***. What was done? The second-order reaction was artificially transformed into a pseudo-first-order process.

Pseudo-first-order approximation is applicable when the concentration of one of reagents is at least *10-times* higher than that of the other. It is better to keep higher excess, but this is difficult to achieve experimentally. The intrinsic second-order rate constant k_2 is calculated from the series of k_{obs} obtained at different concentrations of reagent X which is in excess. The slope of linear plot k_{obs} against $[\text{X}]$ gives k_2 (Fig. 2.2.2).

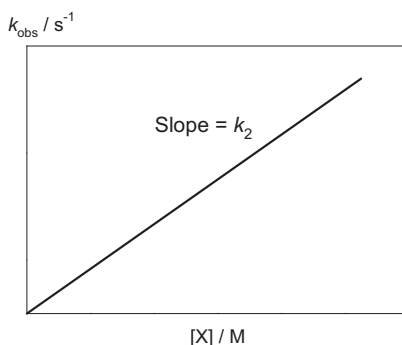


Figure 2.2.2. Calculation of the second-order rate constant from k_{obs} measured at various $[\text{X}]$.

More challenging are reversible reactions of the type



When X_t is in excess compared to A_t (total concentrations of X and A), i.e. under pseudo-first-order conditions, the expression for k_{obs} is given by

$$k_{\text{obs}} = k_1[\text{X}] + k_{-1},$$

provided the reaction is first order in X. Thus, a plot of k_{obs} vs. $[X]$ is a straight line with the slope and intercept of k_1 and k_{-1} , respectively. The equilibrium constant K equals k_1/k_{-1} . It also can be calculated from the same set of data that is required for obtaining observed pseudo-first-order rate constants. Let one measures an absorbance change D by uv-vis spectroscopy due to conversion of A into B (X does not absorb). The absorbance $D = \epsilon_A[A] + \epsilon_B[B]$ (ϵ_A and ϵ_B are extinction coefficients² of A and B, respectively). The mass balance equation is $A_t = [A] + [B]$. Hence $D = \epsilon_A(A_t - [B]) + \epsilon_B[B] = D_0 + \Delta\epsilon[B]$, here $D_0 = \epsilon_A A_t$, viz. absorbance of A at $X_t=0$, and $\Delta\epsilon = \epsilon_B - \epsilon_A$. By definition $K = [B]/([A]X_t)$. Substitution using the mass-balance equation gives

$$[B] = \frac{KX_t}{1+KX_t} A_t \quad (2.2.3)$$

Therefore

$$\frac{D - D_0}{\Delta\epsilon} = \frac{KX_t}{1 + KX_t} A_t$$

Finally

$$\frac{A_t}{D - D_0} = \frac{1}{\Delta\epsilon K} X_t^{-1} + \frac{1}{\Delta\epsilon}$$

The equilibrium constants K can be calculated from the slope $(\Delta\epsilon K)^{-1}$ and intercept $(\Delta\epsilon)^{-1}$ of a linear plot $A_t(D - D_0)^{-1}$ versus X_t^{-1} .^{3,4}

Equation (2.2.3) is very common in biochemistry. Imagine that A is protein which reversibly binds a ligand $X = L$ taken in excess to form a 1:1 associate $B = \{A, L\}$. Equation 2.2.3 can be rewritten as

$$[\{A, L\}] + [\{A, L\}]K[L] = K[L]A_t$$

² Measured in $M^{-1} \text{ cm}^{-1}$.

³ Problem 2-5 will reveal additional features of a $A + X \rightleftharpoons B$ reaction.

⁴ There is even easier approach. The change in absorbance A with X_t equals

$$A = \frac{A_0 + A_\infty KX_t}{1 + KX_t} \quad (2.2.1.1)$$

Hence $(A - A_0)/(A_\infty - A) = KX_t$. The slope of the linear plot equals K .

After dividing both sides by $[L]A_t$ and rearrangement

$$\frac{[\{A, L\}]}{A_t} \times \frac{1}{[L]} = K - K \frac{[\{A, L\}]}{A_t}$$

Note that K here is the association constant ($K_a = \frac{[\{A, L\}]}{[A][L]}$) measured in M^{-1} . The dissociation constant K_d , the inverse of K_a , is measured in M . When K_d is used, the latter equation appears as

$$\frac{[\{A, L\}]}{A_t} \times \frac{1}{[L]} = \frac{1}{K_d} - \frac{1}{K_d} \frac{[\{A, L\}]}{A_t}$$

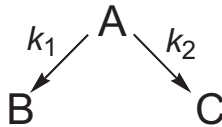
or

$$\frac{\alpha}{[L]} = \frac{1}{K_d} - \frac{\alpha}{K_d} \quad (2.2.4)$$

Biochemists associate $\alpha = \frac{[\{A, L\}]}{A_t}$ with a ratio of concentrations of the protein with bound ligand $\{A, L\}$ and the total protein concentration A_t . Then eq 2.2.4 is the Scatchard equation.

2.3. Parallel First-Order Reactions

Consider a case with two parallel first-order reactions:



At time $t = t$ x moles of A will transform into products B and C . Then

$$-\frac{d(a_0 - x)}{dt} = k_1(a_0 - x) + k_2(a_0 - x) = (k_1 + k_2)(a_0 - x)$$

Remembering that $x = 0$ when $t = 0$, integration leads to the expression for consumption of A :

$$a_0 - x = a_0 e^{-(k_1 + k_2)t} \quad \text{and} \quad x = a_0(1 - e^{-(k_1 + k_2)t})$$

The slope of the plot $\ln[a_0/(a_0 - x)]$ against t is the sum of the rate constants $k_1 + k_2$, i.e. $k_{\text{obs}} = k_1 + k_2$. To obtain individual rate constants k_1 and k_2 , one should measure relative amounts of B and C formed after any period of time:

$$db/dt = k_1(a_0 - x) \quad \text{and} \quad dc/dt = k_2(a_0 - x)$$

$$db/dc = k_1/k_2$$

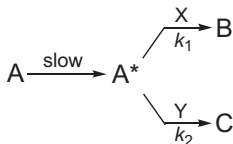
Or using increments instead of differentials

$$\Delta b/\Delta c = k_1/k_2$$

Since $k_{\text{obs}} = k_1 + k_2$, the individual rate constants are easy to calculate.

Make sure that if one follows the formation of B or C, the calculated rate constant k_{obs} is $k_1 + k_2$. Also, if reagent A gives i products, the integration of any of these will result in $k_{\text{obs}} = \sum k_i$.

This concept of parallel reactions is useful for characterizing relative reactivities of short-lived reactive intermediates. For example, let an intermediate A^* be rapidly reacting with molecules X and Y:

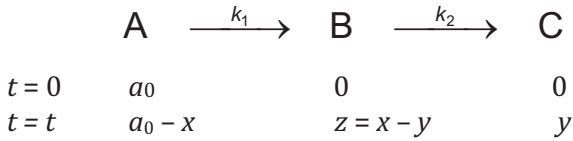


Then $db/dt = k_1[A^*][X]$ and $dc/dt = k_2[A^*][Y]$. Hence, $\Delta b/\Delta c = k_1[X]/k_2[Y]$ and finally

$$\frac{k_1}{k_2} = \frac{\Delta b[Y]}{\Delta c[X]}$$

2.4. Consecutive Irreversible First-Order Reactions

In the most general case:



Let at $t = 0$ concentration of A be a_0 , $[B] = 0$ and $[C] = 0$. Let at $t = t$ concentration of A be $(a_0 - x)$ and $[C] = y$; then $[B] = z = x - y$. Consumption of A is governed just by the rate constant k_1 :

$$a_0 - x = a_0 e^{-k_1 t} \quad (2.4.1)$$

The differential equation for B appears in the form:

$$\frac{dz}{dt} = k_1(a_0 - x) - k_2 z$$

or taking into account equation 2.4.1

$$\frac{dz}{dt} + k_2 z = k_1 a_0 e^{-k_1 t} \quad (2.4.2)$$

Differential equation such as 2.4.2 was elegantly solved by Euler.⁵ He multiplied its both sides by $e^{k_2 t}$

$$e^{k_2 t} \times \frac{dz}{dt} + k_2 z \times e^{k_2 t} = k_1 a_0 e^{(k_2 - k_1)t} \quad (2.4.3)$$

and noticed that the left side of eq 2.4.3 is a derivative of $ze^{k_2 t}$ by t .

$$\frac{d}{dt} (ze^{k_2 t}) = k_1 a_0 e^{(k_2 - k_1)t} \quad (2.4.4)$$

Integration of 2.4.4 on the condition $z = 0$ at $t = 0$ affords

$$ze^{k_2 t} = \frac{a_0 k_1}{k_2 - k_1} (e^{(k_2 - k_1)t} - 1)$$

Finally,

⁵ *Leonhard Euler* (pronounced Oiler) (1707–1783) was a Swiss mathematician and physicist. He is considered to be the preeminent mathematician of the 18th century and one of the greatest of all time.

$$z = \frac{a_0 k_1}{k_1 - k_2} (e^{-k_2 t} - e^{-k_1 t}) \quad (2.4.5)$$

Since $z = x - y$, therefore $y = x - z$. As a result

$$y = a_0 - a_0 e^{-k_1 t} - z = a_0 \left(1 + \frac{k_2}{k_1 - k_2} e^{-k_1 t} - \frac{k_1}{k_1 - k_2} e^{-k_2 t} \right) \quad (2.4.6)$$

Let us perform a standard analysis of current concentrations of A, B, and C. Figure 2.4.1 shows how these vary with time at arbitrary chosen rate constants k_1 and k_2 . It is important to remember the following.

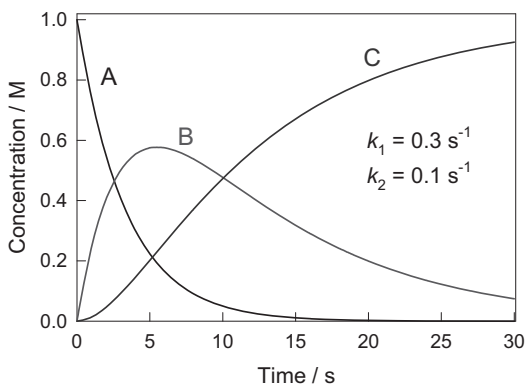


Figure 2.4.1. Concentration profiles for A, B, and C for an arbitrary pair of rate constants k_1 and k_2 (0.3 and 0.1 s^{-1} , respectively).

- i) A disappears exponentially (eq 2.4.1).
- ii) Concentration of B reaches maximum at time t . In fact

$$\frac{dz}{dt} = \frac{k_1 a_0}{k_1 - k_2} (-k_2 e^{-k_2 t} + k_1 e^{-k_1 t})$$

At maximum, the derivative $\frac{dz}{dt}$ equals zero. Hence

$$e^{(k_1 - k_2)t} = \frac{k_1}{k_2}, \quad (k_1 - k_2)t = \ln\left(\frac{k_1}{k_2}\right)$$

Finally

$$t = \frac{\ln k_1 - \ln k_2}{k_1 - k_2} \quad (2.4.7)$$

The state when $\frac{dz}{dt} = 0$ is referred to as the **steady-state**. Here (at time t) the rates of formation and further conversion of the intermediate B are the same.

iii) The concentration profile for C has the point of inflection⁶:

$$0 = \frac{d^2y}{dt^2} = a_0 \left(\frac{k_1^2 k_2}{k_1 - k_2} e^{-k_1 t} - \frac{k_2^2 k_1}{k_1 - k_2} e^{-k_2 t} \right)$$

Therefore again

$$t = \frac{\ln k_1 - \ln k_2}{k_1 - k_2}$$

In other words, the inflection point is observed at the steady-state!

iv) Let us follow the concentration of C when $k_1 \ll k_2$. It comes from eq 2.4.6 that

$$y \approx a_0 \left(1 + \frac{k_2}{-k_2} e^{-k_1 t} + \frac{k_1}{k_2} e^{-k_2 t} \right) = (1 - e^{-k_1 t})$$

This means that the overall reaction rate is determined by the rate constant for the slowest (**rate-limiting** or **rate-determining**) step. If, in contrast, $k_1 \gg k_2$ one arrives to:

$$y \approx a_0 (1 - e^{-k_2 t})$$

As before, the slowest step determines the rate of the overall process. This rule holds always: *the overall reaction rate is determined by the slowest step.*

If $k_1 \ll k_2$, intermediate B is formed in very low concentrations (Fig. 2.4.2A). The steady-state (better quasi-steady-state) happens early and holds within a rather long period of time. As a result, linearization of

⁶ At this point the second derivative $\frac{d^2y}{dt^2}$ equals zero.

the concentration profiles of both A and C using a first-order approach gives the rate constant k_1 .

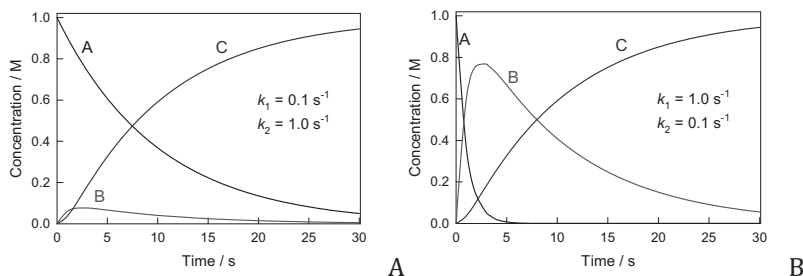
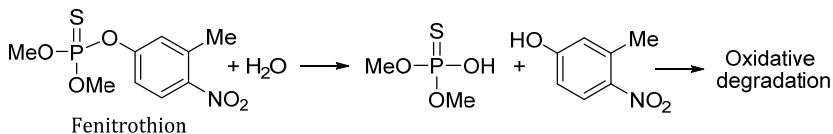


Figure 2.4.2. Consecutive 1st-order reactions. **A:** $k_1 \ll k_2$; **B:** $k_1 \gg k_2$. Note that C profiles are the same in accordance with a concept of the rate-limiting step.

If $k_1 \gg k_2$, large amount of intermediate B is formed rapidly followed by slower conversion with the rate constant k_2 . The steady-state takes place also fast but its duration is momentary (Fig. 2.4.2B). Conversion of A is driven by the rate constant k_1 ; whereas consumption of rapidly formed B and accumulation of C is driven by the rate constant k_2 .

An example of a consecutive first-order reaction (in fact, pseudo-first-order) is a Fe^{III}-TAML-catalyzed oxidation of the pesticide fenitrothion by H₂O₂ (Scheme 2.4.1). 3-Methyl-4-nitrophenolate is first formed and then is oxidized.⁷



Scheme 2.4.1. Fe^{III}-TAML-catalyzed oxidation of fenitrothion by H₂O₂.

⁷ Chanda A, et al, *JACS*, **2006**, *128*, 12058.

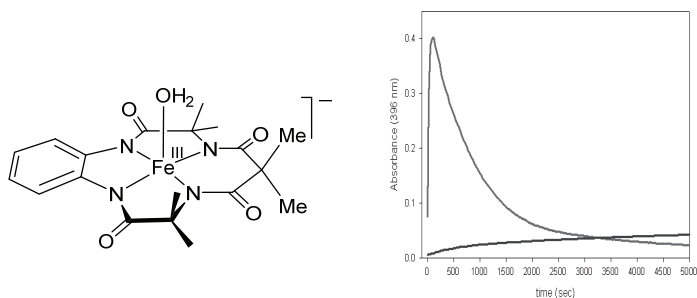


Figure 2.4.3. Structure of Fe^{III}-TAML activator of H₂O₂ (TAML = tetraamido macrocyclic ligand) and kinetics of the catalyzed degradation of fenitrothion featuring intermediate formation of 3-methyl-4-nitrophenolate (top line). Bottom line is a slower accumulation of the phenolate without the catalyst.

How to calculate k_1 and k_2 ? One may use a computer software such as SigmaPlot, Origin, Mathematica, etc:

$$B = \frac{k_1 a_0}{k_1 - k_2} (e^{-k_2 t} - e^{-k_1 t})$$

$$f = a * [\exp(-b * x) + * \exp(-c * x)]; \text{ fit } f \text{ to } y$$

$$C = a_0 \left(1 + \frac{k_2}{k_1 - k_2} e^{-k_1 t} - \frac{k_1}{k_1 - k_2} e^{-k_2 t} \right) = \alpha_1 + \alpha_2 e^{-k_1 t} - \alpha_3 e^{-k_2 t}$$

$$f = y_0 + a * \exp(-b * x) + c * \exp(-d * x); \text{ fit } f \text{ to } y$$

In conclusion, the kinetics of one-step irreversible first-order reaction is described by one exponent. A two-step irreversible reaction is described by two exponents. An n -step reaction will be described by a function with n exponential terms.

2.5. Second-Order Reactions: Simplest Cases

As always



and at $t = 0$ concentrations of A and B equal a_0 and b_0 , respectively. At time t the concentration of C is x ; those of A and B are $a_0 - x$ and $b_0 - x$, respectively.

A differential equation for disappearance of A:

$$-\frac{d(a_0 - x)}{dt} = k(a_0 - x)(b_0 - x)$$

Hence

$$\frac{dx}{(a_0 - x)(b_0 - x)} = kdt \quad (2.5.1)$$

For solving this equation, its left side should be rewritten as a sum of two easy-to-integrate terms with the coefficients y and z

$$\frac{1}{(a_0 - x)(b_0 - x)} = \frac{y}{(a_0 - x)} + \frac{z}{(b_0 - x)} \quad (2.5.2)$$

Since $yb_0 - yx + a_0z - xz = 1$, y and z are found by solving the system of two equations

$$yb_0 + a_0z = 1$$

$$-yx - xz = 0$$

Hence

$$y = \frac{1}{(b_0 - a_0)} \quad \text{and} \quad z = \frac{1}{(a_0 - b_0)}$$

Combining the found expressions for y and z with equations 2.5.1 and 2.5.2 gives the equation ready for integration

$$\frac{d(a_0 - x)}{(a_0 - x)} - \frac{d(b_0 - x)}{(b_0 - x)} = k(a_0 - b_0)dt$$

Therefore

$$\ln(a_0 - x) - \ln(b_0 - x) = k(a_0 - b_0)t + c$$

The boundary condition is $t = 0$ $x = 0$, and $c = \ln a_0 - \ln b_0$. Finally

$$\frac{1}{(a_0 - b_0)} \ln \frac{(a_0 - x)b_0}{(b_0 - x)a_0} = kt \quad (2.5.3)$$

If $a_0 \gg b_0$, equation 2.5.3 transforms into

$$\ln \frac{b_0}{(b_0 - x)} = ka_0t \quad \text{with} \quad k_{\text{obs}} = ka_0$$

thus showing the pseudo-first-order case!

Equation 2.5.3 is occasionally used because it is more convenient to perform measurements under the pseudo-first-order conditions. Equation 2.5.3 is used when, for example, a reaction is fast, and it is vital to slow it down by decreasing the concentrations of both reagents. Particularly, if $a_0 = b_0$, the differential equation is

$$-\frac{d(a_0-x)}{dt} = k(a_0 - x)^2 \qquad -\frac{d(a_0-x)}{(a_0-x)^2} = kdt$$

Hence

$$1/(a_0 - x) = kt + c \qquad \text{with} \quad c = 1/a_0$$

Finally

$$\frac{1}{(a_0-x)} - \frac{1}{a_0} = kt \qquad (2.5.4)$$

or

$$(a_0 - x) = \frac{a_0}{1+a_0kt} \qquad \text{and} \qquad x = \frac{a_0^2kt}{1+a_0kt}$$

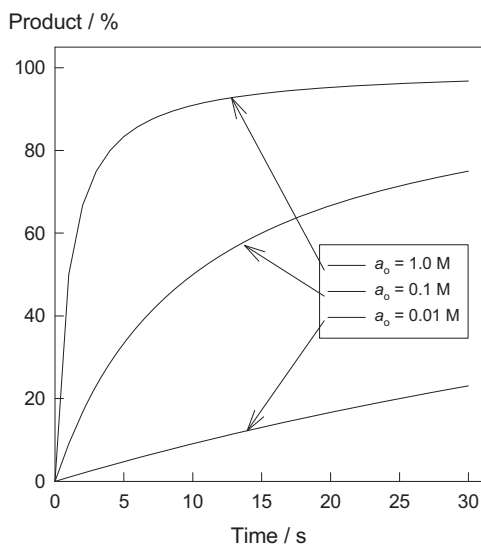
Equation 2.5.4 shows that the half-life of the second-order reaction $t_{1/2}$ **does depend** on the concentration of a_0 . Since $t = t_{1/2}$ when $x = \frac{1}{2}a_0$, one arrives to

$$t_{1/2} = 1/(a_0k)$$

In other words the “second-order” half-life $t_{1/2}$ is inversely proportional to the total concentration of reagents. Figure 2.5.1 shows the kinetics of consumption of reagent A at its different concentrations ranging from 0.01 to 1 M, the second-order rate constant being constant. Table 2.5.1 emphasizes the key difference between $t_{1/2}$ for first- and second order reactions in terms of their dependence on reagent concentrations.

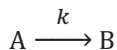
Table 2.5.1. Half-life $t_{1/2}$ for first- and second reactions.

	First order	Second order
$t_{1/2}$	$\frac{\ln 2}{k_1}$	$\frac{1}{a_0 k_2}$
Comment	Concentration independent	Concentration dependent

**Figure 2.5.1.** Kinetics of the second-order conversion of reagent A at different initial concentrations of A and $k_2 = 1.0 \text{ M}^{-1} \text{ s}^{-1}$.

2.6. Zero-Order Reactions

These are when the reaction rate does not change with time as reaction proceeds (Fig. 2.6.1).



Therefore

$$-d(a_0 - x)/dt = k; \quad dx/dt = k$$

$$x = kt + c,$$

Here $c = 0$ since at $t = 0$ $x = 0$. Finally

$$k = x/t$$

The rate constant, which is measured in M s^{-1} , is easy to calculate, since it is just a slope of a linear plot.

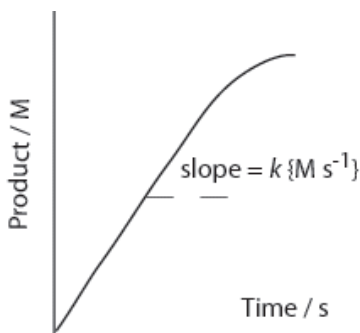


Figure 2.6.1. Typical kinetic curve of a zero-order reaction.

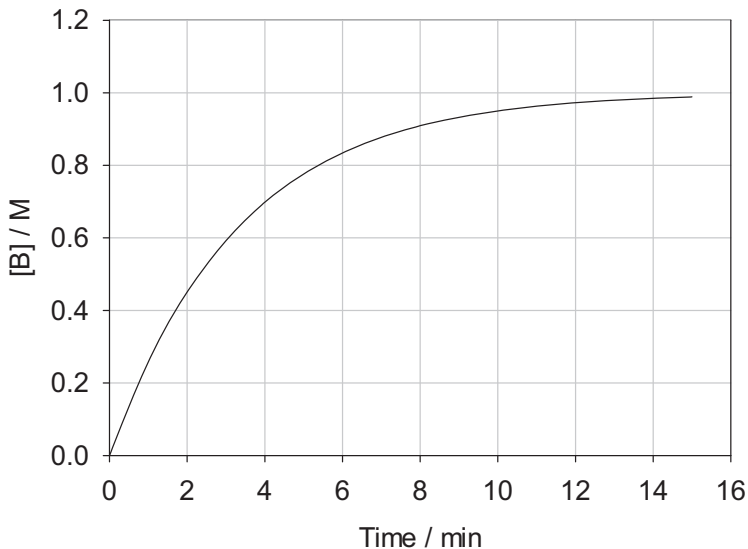
Problems

2-1. Imagine you follow a first-order reaction by measuring the absorbance change created by reagent A and product B. Show that if you plot $\ln\{(A_0 - A_\infty)/(A_t - A_\infty)\}$ against time t (A_t is absorbance at time t), the slope equals k even though both A and B absorb light at this wavelength.

2-2. Below is a kinetic curve for the irreversible formation of product B from compound A ($A \rightarrow B$ reaction). Assume that conversion of A is complete. Using any available graphical software or a graph paper linearize the curve applying a first-order treatment. Also:

- 1) calculate a first-order rate constant;

- 2) calculate $\tau_{1/2}$ and comment on a “purity” of this curve as a first-order reaction.



- 2-3.** Derive the expression such as 2.2.1 for reversible first-order reaction



for the case when at $t = 0$, $[A] = a_0$ and $[B] = b_0$.

- 2-4.** Based on the solution of Problem 2-3 derive the expressions for a_{eq} and b_{eq} . Make sure that the ratio $[b_{eq}]/[a_{eq}] = K$ in fact equals k_1/k_{-1} .

2-5. Dependence of k_{obs} on the concentration of X, which is in a large excess, can reveal a first-order in X with the intercept, i.e. the k_{obs} versus $[X]$ plot may not pass through the origin affording $k_{obs} = k_0 + k_2[X]$. For the reaction

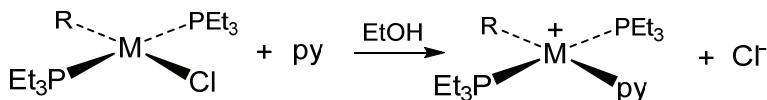


This may indicate:

1. The reaction is in fact reversible $A + X \rightleftharpoons B (K)$;

2. The reaction is irreversible and has two parallel pathways a) and b), for example: a) $A \rightarrow A^*$ (k'); $A^* + X \rightarrow B$ (fast); b) $A + X \rightarrow B$ (k'').

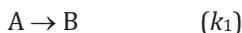
How to discriminate mechanisms 1. and 2.? Note that such chemistry is often encountered in ligand substitution reactions involving 16 electron square-planar transition metal complexes (Pd^{II} , Pt^{II} ; py = pyridine):



2-6. Equations 2.4.5 и 2.4.6 are invalid when $k_1 = k_2 = k$. Show that in this case:

1. $z = a_0kte^{-kt}$;
2. $y = a_0(1 - e^{-kt} - kte^{-kt})$
3. the steady-state occurs at $t = 1/k$.

2-7. Consider the reaction $A \rightarrow B$ with two parallel pathways, which are first and second order in A:



Find the expression for the dependence of current concentration of A [i.e. (a_0-x)] versus time. Suggest a routine for independent determination of the rate constants k_1 and k_2 .

2-8. Derive eq 2.1.6.

2-9. Derive eq 2.2.1.1.

2-10. Prove that if one measures an increase in concentration of product B (k_1), which is formed together with C (k_2) in a parallel manner from starting material A (see first scheme in Section 2.3), the observed first-order rate constant k_{obs} equals (k_1+k_2) . Make sure that similar result will be obtained if one measures just C.

2-11. Prove that for consecutive irreversible first-order reactions the rate of formation of B equals the rate of its disappearance at the steady state.

2-12. Using eq 2.5.3, derive the expression for x as a function of time. Prove that if:

- 1) $a_0 > b_0, x \rightarrow b_0$ when $t \rightarrow \infty$;
- 2) $a_0 < b_0, x \rightarrow a_0$ when $t \rightarrow \infty$.

LECTURE 3.

FROM SIMPLE REACTIONS TO MORE COMPLICATED KINETIC SCHEMES

3.1. The Steady-State Approximation (SSA)

The steady-state approximation is a powerful tool for an easy access without integration to kinetic equations for multistep reactions. The steady state was defined in Section 2.4 by the example of consecutive first-order irreversible reactions $A \rightarrow B$ (k_1); $B \rightarrow C$ (k_2). At the steady-state $d[B]/dt = 0$ and the rates of consumption of A and formation of C are equal. The steady-state approximation assumes that the steady state occurs during the entire reaction course, not in a single point. This condition holds nicely when the concentration of intermediate B is low. Figure 2.4.2A (Lecture 2) shows that the rates of consumption of A and the formation of C are practically identical within the entire timescale and driven by the rate constant k_1 . Let us reach the same conclusion using SSA.

$$0 \approx d[B]/dt = d[A]/dt - d[C]/dt = k_1[A] - k_2[B] \approx 0 \quad (3.1.1)$$

We will solve this equation with respect to [B] and derive the rate expression for the formation of C. The steady-state concentration of intermediate B is

$$[B]_{ss} = k_1[A]/k_2$$

The rate of formation of final product C ($k_2[B]_{ss}$) is determined by the rate constant k_1 , since

$$d[C]/dt = k_1[A]k_2/k_2 = k_1[A]$$

Thus, there is further evidence that when the condition $k_1 \ll k_2$ holds for consecutive first-order reactions the overall rate is determined by

the rate constant of the slowest step. The steady-state approximation affords a kinetically correct result without integration.

In other limiting case, i.e. when $k_1 \gg k_2$ (Fig. 2.4.2B, Lecture 2) the rates of consumption of A and formation of C are not equal and the steady-state approximation $d[B]/dt = 0$ holds within a limited time interval. However, SSA can still be used for evaluating the rate-limiting step. The concentrations of A and B may be comparable at the steady-state and *the mass balance equation* should be applied

$$A_t = [A] + [B] \quad (3.1.2)$$

Here A_t is total, but $[A]$ and $[B]$ are current concentrations. SSA is now applied to the concentration of B. By analogy with equation 3.1.1:

$$0 \approx d[B]/dt = k_1(A_t - [B]_{ss}) - k_2[B]_{ss}; \quad [B]_{ss} = k_1 A_t / (k_1 + k_2)$$

Since $k_1 \gg k_2$

$$\frac{d[C]}{dt} = \frac{k_1 A_t}{k_1 + k_2} k_2 = k_2 A_t$$

The rate expression obtained agrees with the result reached by other means without any assumption! It is surprising, but this is a fact. The SSA is one of the less strict rules of chemical kinetics, which nevertheless leads to correct results!

It is worth giving a qualitative explanation why equation 3.1.1 is valid. When the steady state condition holds, we subtract two rather large quantities, viz. $d[A]/dt$ and $d[C]/dt$ (Fig. 2.4.2), and therefore the difference is often close to zero. But the most important is that the difference is much smaller than both $d[A]/dt$ and $d[C]/dt$!

The steady state approximation is absolutely crucial for kinetic analysis of multistep reactions. It allows avoiding integration. Kinetic equations thus obtained are chemically transparent and easy to interpret. Let us support these statements by considering Scheme 3.1.1.



Scheme 3.1.1. Mechanism with an intermediate C.

Let $A_t \gg B_t$. We will derive a rate law for the formation of product D that corresponds to the stoichiometric mechanism in Scheme 3.1.1 by applying SSA with respect to the intermediate C

$$0 = d[C]/dt = k_1[A][B] - [C](k_{-1} + k_2),$$

The rate expression $d[D]/dt$ is

$$\frac{d[D]}{dt} = k_2[C] = \frac{k_1 k_2 [A][B]}{k_{-1} + k_2}$$

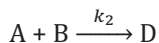
Since $A_t \gg B_t$

$$k_{\text{obs}} = \frac{k_1 k_2 A_t}{k_{-1} + k_2}$$

The case when $k_{-1} \gg k_2$ is referred to as a reaction with *pre-equilibrium*. This means that the transformation of intermediate C into final product D is preceded by a rapidly established equilibrium driven by the equilibrium constant $K_1 = k_1/k_{-1}$. It is important to note that the equilibrium in Scheme 3.1.1 is strongly shifted to the left, i.e. the concentration of intermediate C is very low:

$$k_{\text{obs}} = \frac{k_1 k_2}{k_{-1} + k_2} A_t \approx \frac{k_1}{k_{-1}} k_2 A_t = K_1 k_2 A_t \quad (3.1.3)$$

This case is kinetically indistinguishable from a simple second-order reaction



The reason is that the observed second-order rate constant for the reaction with pre-equilibrium equals $K_1 k_2$. It is worth looking at Scheme 3.1.1 alternatively. Let the first step be a rapidly established equilibrium and there are no limitations on concentration of

intermediate C. That means that the mass balance equation with respect to B (why?) should be taken into account.

$$B_t = [B] + [C]$$

The equilibrium constant K_1 is then given by:

$$K_1 = \frac{[C]}{A_t(B_t - [C])} \quad \text{and} \quad [C] = \frac{K_1 A_t B_t}{1 + K_1 A_t}$$

Here $[C]$ is the equilibrium concentration of C. An expression for the observed pseudo-first-order rate constant obtained without SSA is

$$k_{\text{obs}} = \frac{k_2 K_1 A_t}{1 + K_1 A_t} \quad (3.1.4)$$

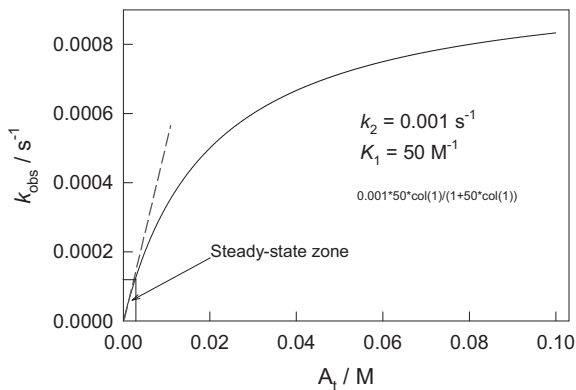


Figure 3.1.1. Dependence of k_{obs} on A_t according to eq 3.1.4. A dashed line shows that k_{obs} is a linear function of A at low concentrations of A .

Comparison of equation 3.1.3 obtained using SSA with equation 3.1.4, which was derived assuming a rapidly established equilibrium, indicates that the latter transforms into the former when $1 \gg K_1 A_t$, i.e. when the equilibrium driven by K_1 is strongly shifted to the left. In other words when the concentration of the intermediate is very low! Figure 3.1.1 is a graphical illustration of the rate law 3.1.4. A rectangle indicates a “steady-state zone” where k_{obs} is directly proportional to the concentration of A .

Equation similar to 3.1.4 for Scheme 3.1.1 can formally be obtained using SSA. In this case the concentration of C is meaningful and therefore $B_t = [B] + [C]$. Then

$$0 = k_1 A_t (B_t - [C]) - [C](k_{-1} + k_2) = k_1 A_t B_t - [C](k_{-1} + k_2 + k_1 A_t)$$

The steady-state concentration of C equals

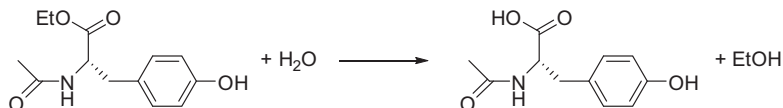
$$[C] = \frac{k_1 A_t B_t}{k_{-1} + k_2 + k_1 A_t}$$

Finally

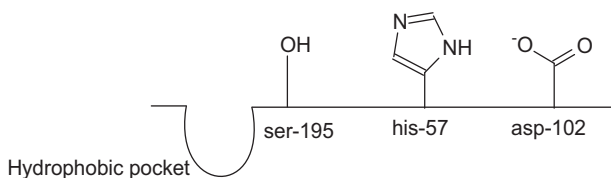
$$\frac{d[D]}{dt} = \frac{k_1 k_2 A_t B_t}{k_{-1} + k_2 + k_1 A_t} \quad \text{and} \quad k_{\text{obs}} = \frac{k_1 k_2 A_t}{k_{-1} + k_2 + k_1 A_t}$$

3.2. The Michaelis-Menten Equation and Its Numerous Analogs

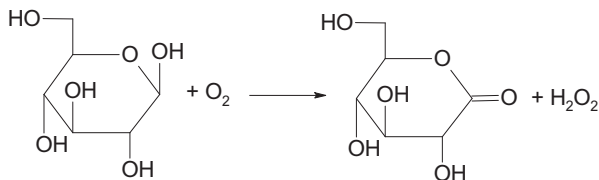
Enzyme-catalyzed reactions have an interesting feature. Their rates increase first with increasing a concentration of a reacting molecule (substrate), the transformation of which is catalyzed, and then level off. This trend is commonly independent of the enzyme nature and is manifested for a rather simple 25 kDa proteolytic enzyme α -chymotrypsin, which catalyzes, for example, the hydrolysis of *N*-acetyl-*L*-tyrosine ethyl ester (ATEE):



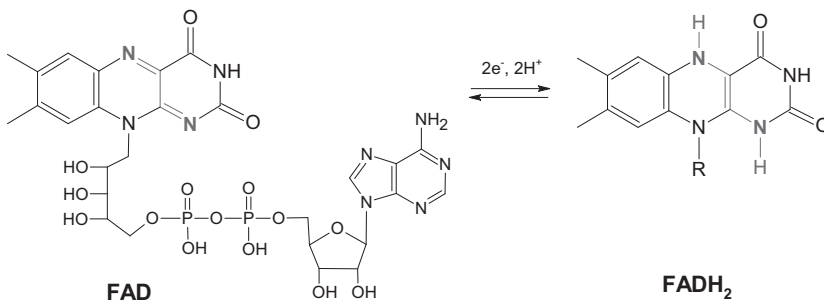
The active site of α -chymotrypsin consists of a hydrophobic pocket and the amino acid residues ser-195, his-57, and asp-102.



Glucose oxidase is a more sophisticated 155 KDa oxidoreductase, which is a two-substrate enzyme. The enzyme catalyzes the oxidation of β -*D*-glucose into γ -*D*-gluconolactone by dioxygen:



The active site of glucose oxidase has flavin adenine dinucleotide (FAD), which actually oxidizes *D*-glucose to transform into FADH₂, which is then reoxidized back by O₂. Rates of both enzymatic reactions will level off at relatively high concentrations of ATEE and *D*-glucose. Other details about glucose oxidase are in Lecture 12.



To account for this phenomenon, consider a formal scheme, where S is a substrate that transforms into product P in the presence of enzyme E via the reactive intermediate ES (enzyme-substrate complex).



Scheme 3.2.1. General Michaelis-Menten mechanism.

Let us apply SSA with respect to intermediate ES considering the mass balance. If $S_t \gg E_t$, one obtains:

$$E_t = [\text{E}] + [\text{ES}]; \quad [\text{E}] = E_t - [\text{ES}]$$

and

$$0 = k_1 S_t (E_t - [ES]) - [ES] (k_{-1} + k_2)$$

Hence

$$k_1 E_t S_t = [ES] (k_{-1} + k_2)$$

The steady-state concentration of ES is

$$[ES] = \frac{k_1 E_t S_t}{k_{-1} + k_2 + k_1 S_t}$$

The rate of enzymatic reaction equals

$$v = -\frac{d[S]}{dt} = \frac{k_1 k_2 E_t S_t}{k_{-1} + k_2 + k_1 S_t} \quad (3.2.1)$$

The dependence of v on S_t is identical to that in Fig. 3.1.1.

Equations of type 3.2.1 are frequently referred to as the Michaelis type equation. Their general feature is that the rate depends hyperbolically on S_t . It can be rewritten as equation 3.2.2. In the beginning of the 20th century Mr. Michaelis and Mrs. Menton introduced equation 3.2.2 that describes the kinetics of simple enzymatic reactions.

$$v = -\frac{d[S]}{dt} = \frac{k_1 k_2 E_t S_t}{k_{-1} + k_2 + k_1 S_t} = \frac{k_2 E_t S_t}{\frac{k_{-1} + k_2}{k_1} + S_t} = \frac{V_M S_t}{K_M + S_t} \quad (3.2.2)$$

Here $V_M = k_2 E_t$ is the maximal reaction rate (k_2 is usually defined as a catalytic rate constant k_{cat}) and $K_M = (k_{-1} + k_2)/k_1$ is the Michaelis constant. When $K_M = S_t$, the rate is half of its maximal value. Make sure that this is the case.

Both parameters V_M and K_M can be calculated directly from the dependence of v on the concentration of S_t , eq 3.2.2. One should plot v^{-1} against S_t^{-1} (*Lineweaver-Burk plot*). The intercept and the slope equal V_M^{-1} and K_M/V_M , respectively.

Consider now not necessarily enzymatic case when ligand L binds to A fast and reversibly ($L_t \gg A_t$) and both forms, i.e. A and AL, give product P, i.e.



Scheme 3.2.2. Binding of ligand L to reactant A to form two reactive species.

It is easy to show that the expression for k_{obs} in excess of L is:¹

$$k_{\text{obs}} = \frac{k + k_1 K [L]}{1 + K [L]}$$

At $[L] = 0$, i.e. in the absence of ligand L (Scheme 3.2.2), $k_{\text{obs}} = k$. If the reagent is “saturated” by the ligand, i.e. when $[L] \rightarrow \infty$, $k_{\text{obs}} = k_1$. This is the case when L has converted all reagent A into the AL form. The k_{obs} vs $[L]$ profiles are hyperbolic (Fig. 3.2.1) that that in Fig. 3.1.1. The former function can be ascending or descending depending on the relation between k and k_1 . When $k > k_1$, k_{obs} decreases and when $k < k_1$, in contrast, increases.

¹ $A_t = [A] + [AL]$; $K = [AL]/(A_t - [AL])$; $[AL] = K L_t A_t / (1 + K L_t)$; $[A] = A_t / (1 + K L_t)$;
 $d[P]/dt = k[A] + k_1[AL] = (k + k_1 K L_t) A_t / (1 + K L_t)$; $k_{\text{obs}} = (k + k_1 K L_t) / (1 + K L_t)$.

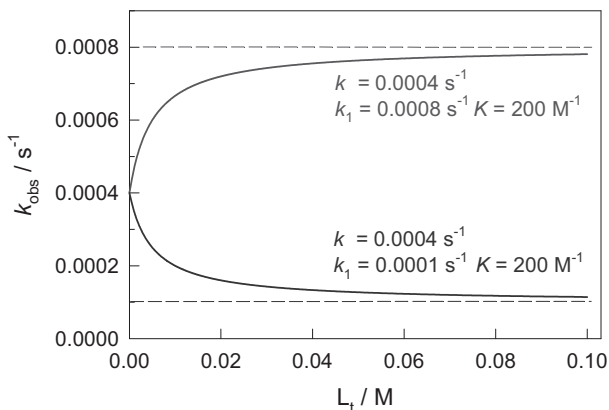


Figure 3.2.1. Dependencies of k_{obs} vs $[L]$ in case of Scheme 3.2.2.

3.2.1. Integration of the Michaelis-Menten Equation

In principle, the parameters of the Michaelis-Menten equation could be calculated in a single experiment by following a substrate conversion as a function of time. In fact, eq 3.2.2 could be rewritten as

$$-(K_M + [S])d[S] = V_M[S]dt \quad \text{or} \quad \left(\frac{K_M}{[S]} + 1\right)d[S] = -V_M dt$$

Integration gives

$$K_M \ln[S] + [S] = -V_M t + c$$

Since at time $t = 0$ $[S] = [S_0]$ (boundary condition), $c = K_M \ln[S_0] + [S_0]$. Finally

$$\frac{1}{t}([S_0] - [S]) = V_M - \frac{K_M}{t} \ln \frac{[S_0]}{[S]} \quad (3.2.3)$$

Thus, the plot of $\frac{[S_0] - [S]}{t}$ vs. $\frac{1}{t} \ln \frac{[S_0]}{[S]}$ should be a straight line with the intercept and slope of V_M and $-K_M$, respectively (Fig. 3.2.3). Though looks attractive, application of eq 3.2.2 is rather limited because V_M and K_M should be constant, i.e. an enzyme should not denature during the kinetic experiment.

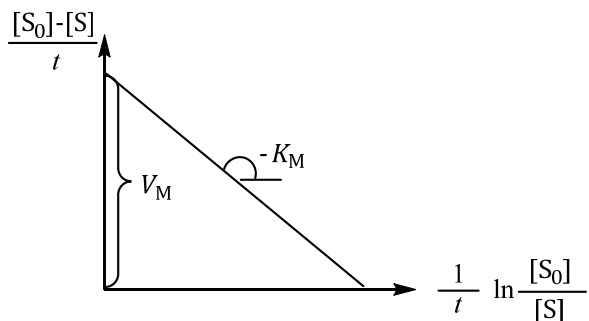


Figure 3.2.2. Linearization of integrated Michaelis-Menten equation 3.2.3.

3.2.2. Michaelis-Menten versus Henri Controversy

Let us imagine that the enzyme-substrate complex ES does not collapse into the reaction product P but the latter is formed in a bimolecular process between E and S. Such scenario presented in Scheme 3.2.3 is referred to as the Henri mechanism.



Scheme 3.2.3. The Henri mechanism of enzymatic catalysis.

When $S_t \gg E_t$, the mass balance equation is $E_t = [E] + [ES]$. The key equilibrium is $[E][S]/[ES] = k_{-1}/k_1 = K_s$ and therefore

$$v = -\frac{d[S]}{dt} = \frac{k_2 K_s E_t S_t}{K_s + S_t} \quad (3.2.4)$$

Thus, eqs 3.2.2 and 3.2.4 predict identical hyperbolic dependences of the reaction rates on substrate concentration under the steady-state conditions. Mechanistically diverse Schemes 3.2.1 and 3.2.3 were differentiated by following the dynamics of product P formation at earlier stages of an enzymatic reaction when the substrate concentration is assumed to be constant. Key differences between the Michaelis-Menten and Henri mechanisms are presented in Fig. 3.2.3. In a qualitative sense the reason for the different behavior during the pre-steady state is simple. In the Michaelis-Menten scheme, the

product formation will reach its maximum rate only when the enzyme-substrate complex ES attains its maximum concentration. However, the maximum rate in the Henri scheme is observed at the very beginning when concentrations of free enzyme and substrate are the highest. The rate of reaction will decrease to its steady-state level after the formation of unreactive ES.

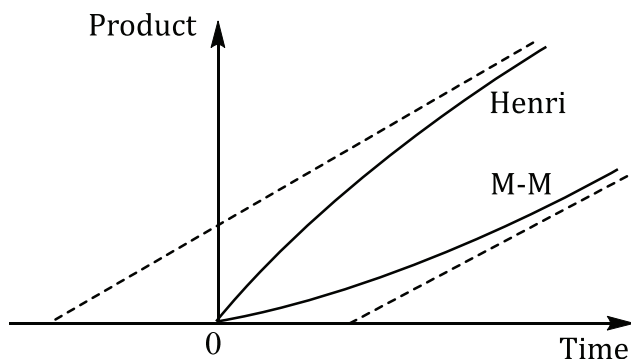


Figure 3.2.3. Pre-steady-state kinetics of product accumulation via Henri and Michaelis-Menten (M-M) mechanisms (Schemes 3.2.3 and 3.2.1, respectively). Dashed lines are asymptotic to the respective steady states (eqs 3.2.2 and 3.2.4, respectively).²

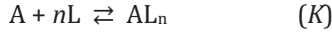
3.2.3. Hill Equation

Equation 3.2.5 is known as Hill equation. Applied to rate of enzymatic reaction, it emphasizes that n molecules of substrate S should bind to enzyme E to form a reactive complex, which then collapses to product P and E. When $n = 1$, eq 3.2.5 is the Michaelis-Menten equation 3.2.2. Binding of n S to E tunes the enzyme to the highest catalytic activity, which is much lower when a number of bound molecules S is less than n .

$$v = \frac{V_M S_t^n}{k' + S_t^n} \quad (3.2.5)$$

² Viale RO, *J Theor Biol*, **1970**, 27, 377.

Here k' and n are the Hill constant and the Hill coefficient, respectively. Equations similar to 3.2.5 are used for analysis of binding of molecules to biological objects. Consider the following equilibrium:



Since

$$K = \frac{[AL_n]}{[A][L]^n} \quad \text{and} \quad A_t = [A] + [AL_n]$$

one obtains

$$\frac{[AL_n]}{A_t} = \alpha = \frac{K[L]^n}{1+K[L]^n} \quad (3.2.6)$$

Here α is the fraction of AL_n molecules. Therefore

$$\log \frac{\alpha}{1-\alpha} = n \log [L] + \log K \quad (3.2.7)$$

or

$$\log \frac{\alpha}{1-\alpha} = n \log [L] - \log K_D \quad (3.2.8)$$

if K_D is the dissociation constant $K_D = [A][L]^n/[AL_n]$. When α is known at different concentrations of L , eq 3.2.8 is used for calculating n and K_D .

Figure 3.2.4 illustrates main features of the Hill equation 3.2.5. The graph was computed in the range of substrate concentrations 0.01–1.00 M using the following arbitrary values: $V_M = 10^{-3} \text{ M s}^{-1}$, $k' = 0.1 \text{ M}$ and $n = 3$. This is a *S*-shaped (or sigmoid) curve. The rate of enzymatic reaction is very low at the lowest concentrations of S but it increases sharply at higher concentrations and finally levels off.

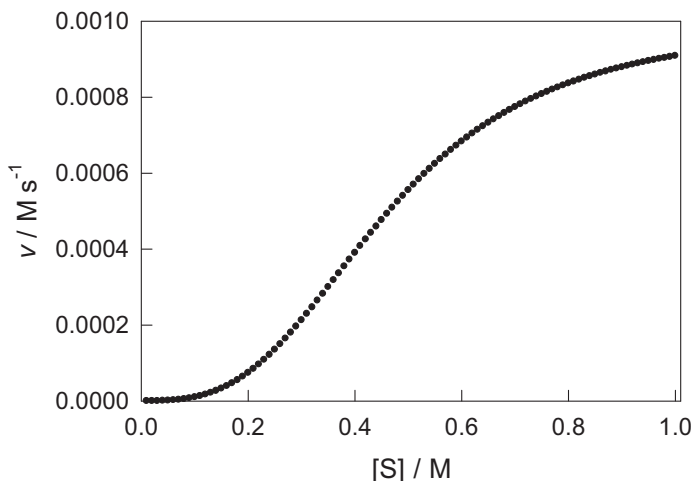


Figure 3.2.4. Hill equation 3.2.5 at work: reaction rate versus substrate concentration when $V_M = 10^{-3} \text{ M s}^{-1}$, $k' = 0.1 \text{ M}$ and $n = 3$; see text for details.

If $\alpha = v/V_M$, eq 3.2.5 can be re-written as often used eq 3.2.9.

$$\log \frac{\alpha}{1-\alpha} = n \log [S] - \log k' \quad (3.2.9)$$

The Hill equation is used for illustration the concept of allosteric regulation of enzymatic activity, which is an increase in the activity as a result of binding of additional molecule/s, which could be substrate/s, to the enzyme at a site/s other than its active site.

3.3. pH-Dependent Reactions

Common effectors are hydrogen ions. Both forms of a molecule involved in the acid-base equilibrium, viz. free and protonated, are reactive, i.e. Scheme 3.3.1 is operative:



Scheme 3.3.1. Reaction mechanism when both forms of a molecule involved in the acid-base equilibrium, viz. free and protonated, are reactive.

Make sure that the expression for k_{obs} appears as:³

$$k_{\text{obs}} = \frac{k_{\text{AH}}[\text{H}^+] + k_{\text{A}}K_a}{K_a + [\text{H}^+]} \quad (3.3.1)$$

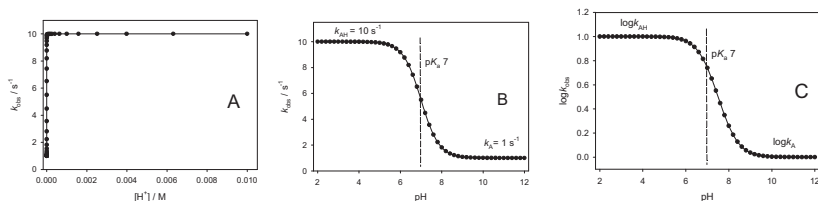


Figure 3.3.1. Different presentations of the dependence of k_{obs} on the concentration of H^+ or pH in terms of eq 3.3.1. See text for details.

Consider limiting situations. If pH is low (acidic media), the concentration of H^+ is high and eq 3.3.1 simplifies to $k_{\text{obs}} = k_{\text{AH}}$ since the reagent exists as AH^+ under such conditions (fully protonated). If pH is high, $k_{\text{obs}} = k_{\text{A}}$ since it exists as a conjugate base A at low concentrations of H^+ . Naturally, k_{obs} is a function of pH ^{4,5} and Fig. 3.3.1 illustrates presentations of dependencies of k_{obs} on acidity, which were simulated for $k_{\text{A}} = 1 \text{ s}^{-1}$, $k_{\text{AH}} = 10 \text{ s}^{-1}$, $\text{p}K_a = 7$. Figure 3.3.1A, which is similar to Fig. 3.1.1, is much less informative than Fig. 3.3.1B where two non-zero plateaus show the existence of two active species. The

³ $A_t = [\text{A}] + [\text{AH}^+]$; $K_a = \frac{[\text{A}][\text{H}^+]}{[\text{AH}^+]}$; $[\text{A}] = \frac{K_a A_t}{([\text{H}^+] + K_a)}$; $[\text{AH}^+] = \frac{[\text{H}^+] A_t}{([\text{H}^+] + K_a)}$; $d[\text{P}]/dt = k_{\text{A}}[\text{A}] + k_{\text{AH}}[\text{AH}^+] = (k_{\text{A}}K_a + k_{\text{AH}}[\text{H}^+])A_t/([\text{H}^+] + K_a)$; $k_{\text{obs}} = (k_{\text{A}}K_a + k_{\text{AH}}[\text{H}^+])/([\text{H}^+] + K_a)$.

⁴ A simple problem. There is a case when mechanism in Scheme 3.3.1 holds but k_{obs} is nevertheless independent of pH. When?

⁵ Suggest a purely algebraic solution of the above problem.

midpoint equals pK_a .⁶ Figure 3.3.1C is also more informative than 3.3.1A, but the midpoint is not pK_a in this case! It is often possible to measure one of the two rate constants, viz. k_{AH} or k_A , at low and high pH, respectively. If so, determination of two remaining parameters of eq 3.3.1 is easy. If k_A is known, it could be subtracted from both sides of eq 3.3.1

$$k_{\text{obs}} - k_A = \frac{k_{AH}[H^+] - k_A[H^+]}{K_a + [H^+]}$$

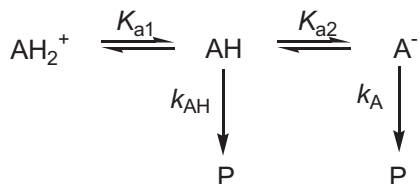
Therefore

$$\frac{1}{k_{\text{obs}} - k_A} = \frac{K_a + [H^+]}{[H^+]\Delta k} = \frac{K_a}{[H^+]\Delta k} + \frac{1}{\Delta k}$$

Here $\Delta k = k_{AH} - k_A$. Thus, the plot $(k_{\text{obs}} - k_A)^{-1}$ versus $[H^+]^{-1}$ is a straight line, the slope and intercept of which allow calculating k_{AH} and K_a . Naturally, if one obtains a plot such as in Fig. 3.3.1, all three parameters k_A , k_{AH} , and K_a can be found by the computer fitting of the experimental data to eq 3.3.1.

The most trivial case of Scheme 3.3.1 is when $k_A = 0$ and $K_a \gg [H^+]$, i.e. only AH^+ form is reactive. It is easy to see that $k_{\text{obs}} = k_{AH}K_a^{-1}[H^+]$. This case is kinetically indistinguishable from the case when A reacts just with H^+ in a bimolecular fashion.

Now we will analyze a case with two acid-base equilibria and two rate constants (Scheme 3.3.2; protons are omitted for clarity).



Scheme 3.3.2. One molecule, two acid-base equilibria, two reactive species (AH and A⁻); protons are omitted for clarity.

⁶ A simple problem. What is the physico-chemical meaning of pK_a ? What condition does hold when $pH = pK_a$?

How does k_{obs} depend on $[\text{H}^+]$ in this case? The mass balance and the acid-base equilibria are as follows

$$A_t = [\text{AH}_2^+] + [\text{AH}] + [\text{A}^-]; \quad K_{a1} = \frac{[\text{AH}][\text{H}^+]}{[\text{A}_2^+]}; \quad K_{a2} = \frac{[\text{A}^-][\text{H}^+]}{[\text{AH}]}$$

There are three equations and three unknown equilibrium concentrations. Our task is to find equilibrium concentrations of reactive species, i.e. of AH and A⁻. Substitution into the mass balance equation affords

$$A_t = [\text{AH}] \left(\frac{[\text{H}^+]}{K_{a1}} + 1 \right) + [\text{A}^-] = [\text{AH}] \left(\frac{[\text{H}^+]}{K_{a1}} + 1 + \frac{K_{a2}}{[\text{H}^+]} \right)$$

Equilibrium concentrations are

$$[\text{A}^-] = A_t \left(\frac{K_{a1}K_{a2}}{[\text{H}^+]^2 + K_{a1}[\text{H}^+] + K_{a1}K_{a2}} \right);$$

$$[\text{AH}] = A_t \left(\frac{K_{a1}[\text{H}^+]}{[\text{H}^+]^2 + K_{a1}[\text{H}^+] + K_{a1}K_{a2}} \right)$$

Since $d[\text{P}]/dt = k_{\text{AH}}[\text{AH}] + k_{\text{A}}[\text{A}^-]$

$$k_{\text{obs}} = \frac{k_{\text{AH}}K_{a1}[\text{H}^+] + k_{\text{A}}K_{a1}K_{a2}}{[\text{H}^+]^2 + K_{a1}[\text{H}^+] + K_{a1}K_{a2}} \quad (3.3.2)^7$$

The limiting cases follow. When $[\text{H}^+] \rightarrow 0$, $k_{\text{obs}} = k_{\text{A}}$. If $[\text{H}^+] \rightarrow \infty$, $k_{\text{obs}} = k_{\text{AH}}K_{a1}/[\text{H}^+]$.

Figure 3.3.2 shows possible dependencies of k_{obs} on the acidity, which correspond to eq 3.3.2. The first graph $\{k_{\text{obs}} \text{ vs. } [\text{H}^+]\}$ contains minor information (cf. with Fig. 3.3.1A). Figure 3.3.2B $\{k_{\text{obs}} \text{ vs. pH}\}$ is more useful; the number of inflection points corresponds to the number of ionogenic groups involved (two in this case), but the total number of plateau corresponds to the *total* number of species involved. Figure 3.3.2C has two non-zero plateaus, which indicate the number of *reactive* species.

⁷ How will eq 3.3.2 change, if AH_2^+ is also reactive ($k_{\text{AH}_2} \neq 0$)?

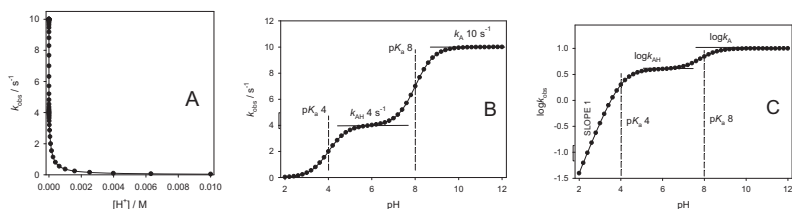


Figure 3.3.2. Different presentations of the dependence of k_{obs} on the concentration of H^+ or pH in terms of eq 3.3.2.

The left part of the curve in Fig. 3.3.3C is characterized by the slope of +1, since here

$$k_{\text{obs}} = k_{\text{AH}}K_{\text{a1}}/[\text{H}^+] \quad \text{and} \quad \log k_{\text{obs}} = \text{const} + \text{pH}$$

Equation 3.3.2 is rather general and accounts for various pH-profiles of rate constants. A so-called “bell-shaped” profile typically encountered in enzymatic reactions⁸ occurs when $k_{\text{A}} = 0$. Note that $\text{p}K_{\text{a1}}$ and $\text{p}K_{\text{a2}}$ of the corresponding groups can be obtained using the so-called tangent routine provided the values of $\text{p}K_{\text{a1}}$ and $\text{p}K_{\text{a2}}$ are not too close to each other (see Fig. 3.3.3).

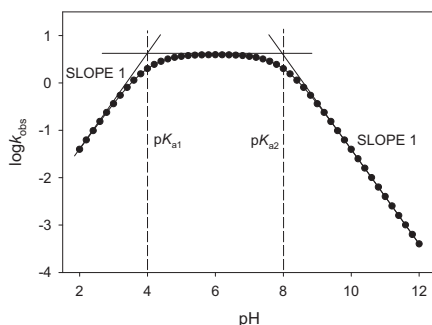
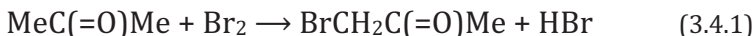


Figure 3.3.3. The tangent routine for obtaining $\text{p}K_{\text{a}}$ of inogenic groups.

⁸ In enzymatic reactions, both k_{cat} and K_{M} depend on pH. Therefore, it is worth studying their dependences on pH independently, i.e. one should first find k_{cat} (or V_{M}) and K_{M} at different pH. Effects of pH on k_{cat} are interpreted identically to those on k_{obs} described in detail in Section 3.3.

3.4. Autocatalytic (Product-Catalyzed) Reactions

Autocatalysis accompanies, for example, the bromination of acetone in the presence of acids



Reaction 3.4.1 accelerates because protons released speed it up according to the experimental rate law 3.4.2.

$$v = k[\text{acetone}][\text{H}^+] \quad (3.4.2)$$

Note that the reaction rate does not depend on $[\text{Br}_2]$.⁹ Consider a variation of product concentration with time. If the initial concentrations of acetone and protons are a_0 and c_0 , respectively, the differential equation is

$$-d(a_0 - x)/dt = k(a_0 - x)(c_0 + x) \quad (3.4.3)$$

Its solution is identical to that described for the second-order reactions in Section 2.5. Using similar approach one arrives to

$$\begin{aligned} \frac{dx}{(a_0 - x)(c_0 + x)} &= -\frac{1}{a_0 + c_0} \times \frac{d(a_0 - x)}{a_0 - x} + \frac{1}{a_0 + c_0} \times \frac{d(c_0 + x)}{c_0 + x} = kdt \\ -\ln(a_0 - x) + \ln(c_0 + x) &= (a_0 + c_0)kt + q \end{aligned}$$

The boundary condition is $x = 0$ at $t = 0$. Then

$$q = -\ln a_0 + \ln c_0$$

Therefore

$$\ln \frac{a_0(c_0 + x)}{c_0(a_0 - x)} = (a_0 + c_0)kt$$

Finally

$$x = \frac{a_0(1 - e^{-(a_0 + c_0)kt})}{1 + \frac{a_0}{c_0}e^{-(a_0 + c_0)kt}} \quad (3.4.4)$$

⁹A simple problem. Does the transition state contain bromine?

Figure 3.4.1 shows that this function has an inflection point. It reminds of, for example, accumulation of the final product C in a consecutive first-order reaction (Fig. 2.4.1). These cases are easy to discriminate. One must just run the reaction in excess of C with respect to A ($C_t \gg A_t$).

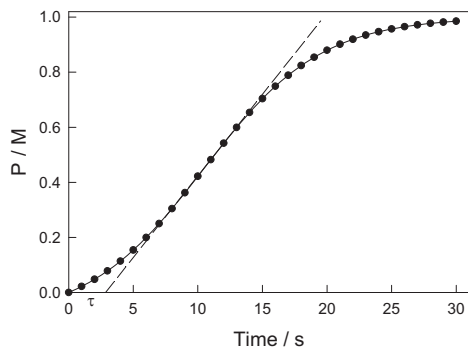


Figure 3.4.1. Autocatalysis described by kinetic equation 3.4.4: accumulation of a hypothetical reaction product at k $0.2 \text{ M}^{-1} \text{ s}^{-1}$, a_0 1 and c_0 0.1 M .

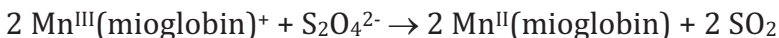
Autocatalysis is also revealed by adding reaction products to the reagents. The induction period τ (intercept of the tangent at the inflection point with axis x , Fig. 3.4.1) should decrease, if autocatalysis occurs.

In conclusion, let us look again at the bromination of acetone (eq 3.4.1) and the corresponding rate expression 3.4.2. Catalysis by protons is due to the fact that the overall reaction rate is limited by the acid-catalyzed ketone enolization, whereas halogenation occurs fast (that is why the overall rate is independent of both the concentration and the nature of dihalogen).

3.5. Mechanistic Interpretation of Rate Laws¹⁰

1. The concentration dependences in the rate law establish the elemental composition of the transition state and its charge:

¹⁰ Section 3.5 is an adapted compilation from: Espenson JH, *Chemical Kinetics and Reaction Mechanisms*; 2 ed.; McGraw-Hill, NY, 1995, p. 127.

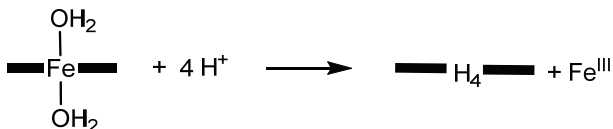


$$v = [\text{Mn}^{\text{III}}(\text{mioglobin})^+][\text{S}_2\text{O}_4^{2-}]^{1/2}$$

Reversible homolysis of hydrosulfite (dithionite) to form $\text{SO}_2^{\cdot-}$ precedes the electron transfer.

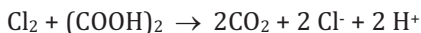
2. Rule 1 is true when applied to the predominant species in solution. Therefore, knowledge of the reagent speciation is essential.

3. The number of positive terms in the rate law is the number of parallel pathways. The acid induced demetalation of Fe^{III} -TAMLs (Fig. 2.4.3) is an example.¹¹



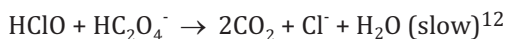
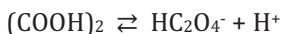
$$k_{\text{obs}} = k^*_1[\text{H}^+] + k^*_3[\text{H}^+]^3$$

4. Species whose concentrations appear in single-term denominators are produced in step(s) prior to the rate-limiting step.



$$\frac{d[\text{CO}_2]}{dt} = \frac{k[\text{Cl}_2][(\text{COOH})_2]}{[\text{H}^+]^2[\text{Cl}^-]}$$

The reversible steps are the formation of hypochlorous acid and dissociation of oxalic acid:



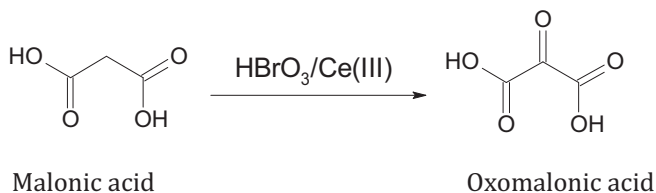
¹¹ Ghosh A, et al, *JACS*, **2003**, *125*, 12378.

¹² Other representative example is the Wacker synthesis of acetaldehyde from ethane $\text{H}_2\text{C}=\text{CH}_2 + \frac{1}{2}\text{O}_2 \rightarrow \text{H}_3\text{CCHO}$ catalyzed by the square-planar Pd^{II}

5. A summation of terms in denominator implies successive steps. Examples are the catalysis by Fe^{III}-TAMLs (Fig. 2.4.3) and by horseradish peroxidase which are mechanistically related. If problem 3-6 is solved correctly, the denominator should contain three terms that correspond to the steps driven by the rate constants k_1 , k_2 , and k_3 .
6. Rapid reactions may follow the rate-limiting step; any step before a fast step should be considered as irreversible.

3.6. Belousov-Zhabotinsky Oscillating Reactions

Reactions are referred to as oscillating when the concentration of one or several reagents varies periodically. The Belousov-Zhabotinsky¹³ reaction itself is the oxidation of citric or malonic acid by bromate in the presence of cerium ions under acidic conditions.

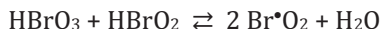


complex $[\text{PdCl}_4]^{2-}$. The rate expression for the dominant pathway is $v = k[\text{Pd}^{\text{II}}][\text{H}_2\text{C}=\text{CH}_2]/([\text{Cl}^-]^2[\text{H}^+])$. Inverse second order in Cl⁻ is due to a reversible dissociation of two chloro ligands.

¹³ The reaction was found by Boris Pavlovich Belousov (1893-1970). Maybe the first interest in chemistry arose in Boris mind when he together with his elder brother tried to make a bomb to kill the Czar. In 1905 there was the first Russian revolution. The Belousov's family was arrested, soon released, but forced to go out of Russia. They moved to Switzerland. There Boris devoted himself to science. He got his chemical education in Zurich. With the beginning of World War I he returned back with great desire to help Russia. But he was not admitted to the army because of health problems. He came to a military laboratory of the famous chemist Professor Ipatiev. In the beginning of 1950-th Belousov wrote a manuscript about the oscillating reaction. The paper was sent to journals twice and rejected due to the referee comments "it is impossible". Why impossible? Obviously because chemical reactions should go to the thermodynamic equilibrium. These should go to the equilibrium smoothly. This was his tragedy; he decided to leave science forever. Publication: *Ref. Radiats. Med.* 1958: 145(1959)–Сборник рефератов по радиационной медицине (Russian).

Reaction occurs until all malonic acid is oxidized by bromate into oxomalonic acid. Concentrations of Ce^{III} and Ce^{IV} (or complexes of Fe^{II} and Fe^{III}) vary with time in an oscillating manner (Fig. 3.6.1). Changes in color (oscillations) occur due to different colors of oxidized and reduced forms of metal species, i.e. colorless/yellow $Ce^{III/IV}$ or blue/red $[Fe(phen)_3]^{2+/3+}$. Consider main steps which provide oscillations.

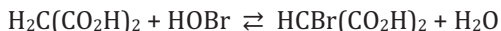
1. Branched chain reaction between the oxidant $HBrO_3$ (bromic acid) and the autocatalyst $HBrO_2$ (bromous acid) which results in the catalyst oxidation, viz. Ce^{III} or Fe^{II} :



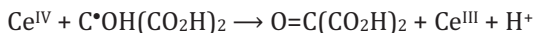
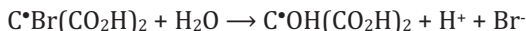
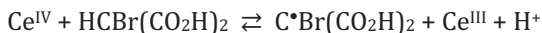
2. Inhibition of the oxidation with termination of the branched chain and formation of a powerful oxidant ($HBrO$):



3. Bromination of the reductant (malonic acid):



4. Reduction of the oxidized catalyst, formation of the inhibitor (Br^-) and final product (oxomalonic acid):



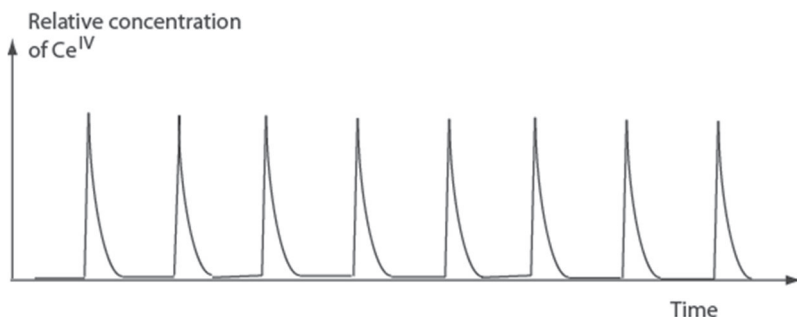


Figure 3.6.1. Oscillations of concentration of Ce^{IV} in a Belousov-Zhabotinsky oscillating reaction.

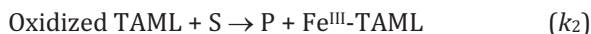
Problems

3-1. Derive the expression for k_{obs} for a stoichiometric mechanism (shown in the Scheme) of conversion of A into product P in the presence of a ligand L. Assume that L is in large excess relative to A. Use SSA and the mass balance equation for A. Analyze the limiting cases, i.e. when the concentration of L is very low and very high.



Scheme

3-2. Catalysis by Fe^{III} -TAML activators of hydrogen peroxide (see Fig. 2.4.3) in oxidation of organic compounds (S) into products (P) agrees with the following stoichiometric mechanism:



1. Derive the equation for the rate of consumption of substrate S. Apply SSA with respect to Oxidized TAML under the conditions $[\text{H}_2\text{O}_2]_t > S_t \gg [\text{Fe}^{\text{III}}\text{-TAML}]_t$.

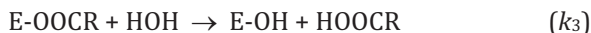
2. Draw dependencies of the reaction rate on concentrations of H_2O_2 and S. Suggest a procedure for calculation of rate constants k_1 and k_2 on assumption that $k_{-1} \sim 0$.

3-3. Analyze the Michaelis-Menten scheme of enzymatic catalysis assuming that the formation of ES is a rapidly established equilibrium described by the equilibrium constant $K_s = [\text{E}][\text{S}]/[\text{ES}]$. Derive a kinetic equation for the product formation. Perform comparative analysis of the equation derived and the Michaelis-Menten equation obtained using the SSA approximation.

When $K_s = K_M$?

What it may mean from a chemical point of view?

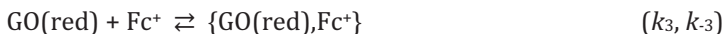
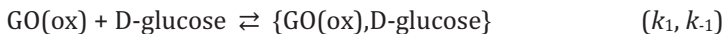
3-4. The actual mechanism of catalysis by α -chymotrypsin involves the reversible binding of ATEE to the hydrophobic cavity of the enzyme, the formation of the so-called acyl enzyme involving ser-195 followed by the deacylation step under the action of water. The latter step affords the acid and regenerates the active enzyme:



Applying the SSA with respect to $\{\text{E-OH,RCOOR}'\}$ and E-OOCR, derive the rate equation for the formation of HOOCR. Assume that the enzyme is in deficiency.

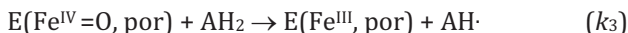
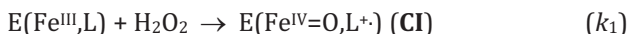
3-5. Catalysis by glucose oxidase (GO) is a typical example of the so-called “ping-pong” mechanism which generally consists of two independent “symmetrical half-reactions”. The first is the oxidation of glucose by the resting state (oxidized) of glucose oxidase $[\text{GO}(\text{ox})]$ to afford the reduced enzyme $\text{GO}(\text{red})$ and the gluconolactone. The second is the reoxidation of the reduced enzyme $\text{GO}(\text{red})$ by either dioxygen (in nature) or a corresponding electron acceptor, for example, the ferricenium cation Fc^+ (Scheme). By applying the steady-state approximation with respect to all intermediates involved in the Scheme, taking into account the mass balance equation with respect to

all forms of GO ($[D\text{-glucose}] > [Fc^+] \gg [GO]$), derive the expression for the steady-state rate of formation of ferrocene (Fc).¹⁴



Scheme

3-6. Derive the steady-state rate expression for catalysis by horseradish peroxidase (E) shown below. Assume that you follow the formation of AH^\bullet and the enzyme is in deficiency. Apply the steady-state approximation to Compound I (**CI**) and Compound II (**CII**).



3-7. Consider eq 3.3.2. When $k_A = 0$, pK_{a1} and pK_{a2} can be obtained using the so-called tangent routine (see Fig. 3.3.3). Confirm this statement. Prove that intersection of the horizontal line in Fig. 3.3.3 two other lines corresponds to pK_{a1} and pK_{a2} .

3-8. As opposed to Fig. 3.3.3 (Problem 3-7), suggest a reaction scheme which corresponds to the “inverted bell” (flip graph in Fig. 3.3.3 vertically). Derive and analyze the corresponding expression for k_{obs} .

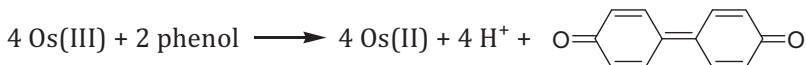
3-9. Show that if $[C]_0 \gg [A]_0$ eq 3.4.4 turns to the equation for a first-order reaction. Explain physico-chemical reasons for that.

¹⁴ Answer: $v = \frac{k_2 k_4 E_t G_l Fc_t^+}{k_4 K_M^{G_l} Fc_t^+ + k_2 K_M^{Fc} G_l + (k_2 + k_4) G_l Fc_t^+}$; $K_M^{Fc} = \frac{k_4 + k_{-3}}{k_3}$ and $K_M^{G_l} = \frac{k_2 + k_{-1}}{k_1}$.

3-10 (bonus; needs efforts). Find the relations between τ , k , a_0 and c_0 for the autocatalytic reaction. First find the time that corresponds to the inflection point.

3-11 (optional). Belousov-Zhabotinsky reaction. Make yourself. *Solution A:* 80 mL water, 6 g NaBrO_3 , 2.4 mL conc. H_2SO_4 . *Solution B:* 2.5 g malonic acid, 25 mL water. *Solution C:* 0.05 g 1,10-phenanthroline, 0.1 g iron(II) ammonium sulfate·6 H_2O , 10 mL water. Mix together: 18 mL Solution A, 13 mL water, 3 mL Solution B, and 1 mL Solution C. This gives a solution that is mostly red but flashes blue at 17-19 s intervals at 25 °C for approximately one hour and 15 min, if stirred continuously.

3-12. Outer-sphere oxidation of phenol into biphenoquinone by $\text{Os}(\text{phen})_3^{3+}$ in aqueous medium follows the stoichiometric equation:

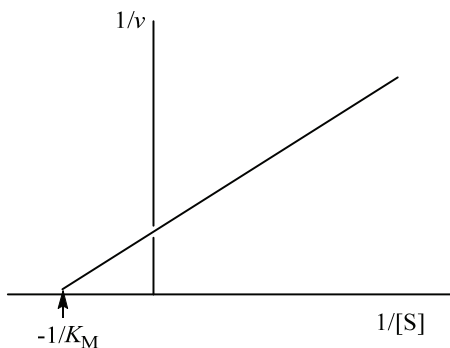


The experimentally determined rate law is unusual

$$-\frac{d[\text{Os(III)}]}{dt} = \frac{k[\text{Os(III)}]^2[\text{phenol}]^2}{[\text{Os(II)}]^2[\text{H}^+]^2}$$

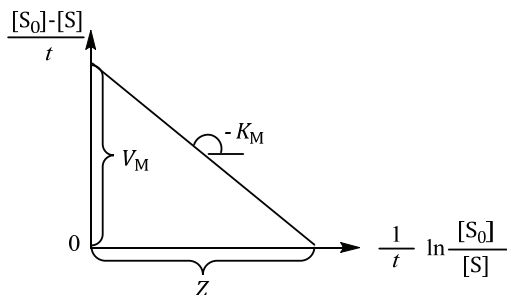
Suggest a stoichiometric mechanism.

3-13. The parameters of the Michaelis-Menten equation can be found using the Lineweaver-Burk linearization of the experimental data. Prove that for the extension of the straight line to cross the x -axis gives the negative inverse K_M (see graph).



3-14. Prove that the Michaelis-Menten equation becomes linear when rate v is plotted against $v/[S]$ (Eadie-Hofstee routine). What is the meaning of the slope and intercept in this case?

3-15. Analyze eq 3.2.3 in more detail and find analytical expression for Z (x at zero y).

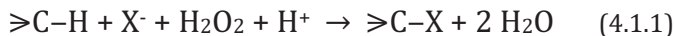


LECTURE 4.

INHIBITION IN CHEMISTRY AND ENZYMOLOGY

4.1. Substrate Inhibition

Haloperoxidases catalyze chlorination or bromination of C–H bonds in the presence of Cl^- or Br^- (X^-) and hydrogen peroxide H_2O_2 (eq 4.1.1).



Formally, haloperoxidases are three substrate enzymes. Rates of halogenation of monochlorodimedon (S) catalyzed by chloroperoxidase increase first with increasing concentrations of both Br^- and H_2O_2 , reach maxima and then decline as it is shown in Fig. 4.1.1.¹ Both substrates Br^- and H_2O_2 inhibit the enzymatic reaction at higher loadings revealing the case of substrate inhibition.

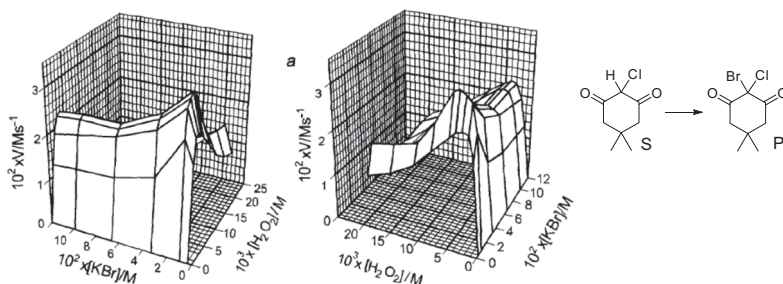


Figure 4.1.1. 3D plots showing initial rates of bromination of monochlorodimedon (S) catalyzed by heme chloroperoxidase as functions of concentrations of Br^- and H_2O_2 at pH 2.75, 25 °C, $[\text{E}] 10^{-8} \text{ M}$, $[\text{S}] 10^{-4} \text{ M}$.² S and P are structures of substrate and product, respectively.

¹ See Sections 5.1.1 and 11.2.7 for additional information about heme chloroperoxidase.

² Shevelkova AN, et al, *FEBS Lett*, **1996**, *383*, 259.

The stoichiometric mechanism of substrate inhibition for the simplest one substrate process $S \rightarrow P$ catalyzed by E is as follows (watch the "enzymological" approach with $K_s = [E][S]/[ES]$, etc):



If ES_2 is unreactive, the rate expression is given by eq 4.1.2³

$$\frac{d[P]}{dt} = \frac{k_{cat}[E][S]}{K_s + [S] + \frac{[S]^2}{K_{2s}}} \quad (4.1.2)$$

An idealized example of substrate inhibition is shown in Fig. 4.1.2. A typical Michaelis-Menten kinetics is observed in the absence of inhibition, i.e. when $K_{2s} \rightarrow \infty$ (Fig. 4.1.2a), though, when present, there is a maximum on the rate versus $[S]$ profile (Fig. 4.1.2b). At low $[S]$, the two curves are close, i.e. the system is insensitive to substrate inhibition and therefore the values of k_{cat} and K_s could be found.

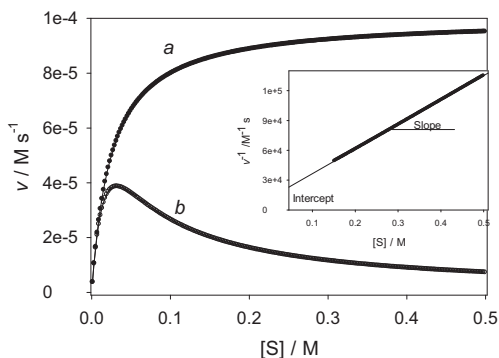


Figure 4.1.2. Theoretical plots for the rate of simple enzymatic reaction without (a) and with substrate inhibition (b) calculated using $k_{cat} = 100 \text{ s}^{-1}$, $K_s = 0.025 \text{ M}$ (a) plus $K_{2s} = 0.04 \text{ M}$ (b).

³ $E_t = [E] + [ES] + [ES_2]$; $K_s = [E][S]/[ES]$; $K_{2s} = [ES][S]/[ES_2]$; $E_t = [ES]\{K_s/[S] + 1 + [S]/K_{2s}\}$ and hence $[ES] = E_t[S]/\{K_s + [S] + [S]^2/K_{2s}\}$; $v = k_{cat}[ES]$. Substitution of the expression for $[ES]$ into the equation for v affords eq 4.1.2.

The value of K_{2s} can be estimated using the data such as in Fig. 4.1.2b collected at higher $[S]$ when the reaction rate decreases with increasing $[S]$ ($> ca.$ 0.15 M in this case). A double inverse form of eq 4.1.2 is eq 4.1.3.

$$\frac{dt}{d[P]} = \frac{K_S}{k_{cat}[E][S]} + \frac{1}{k_{cat}[E]} + \frac{[S]}{k[E]K_{2S}} \quad (4.1.3)$$

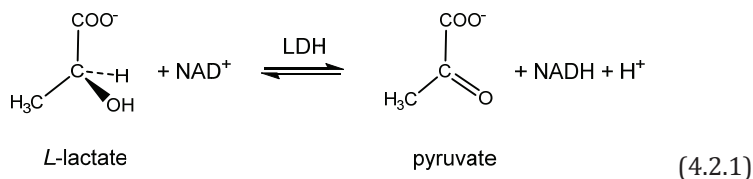
At high $[S]$ the term $K_S/k_{cat}[E][S]$ becomes negligible and therefore

$$\frac{dt}{d[P]} \approx \frac{1}{k_{cat}[E]} + \frac{[S]}{k_{cat}[E]K_{2S}} \quad (4.1.4)$$

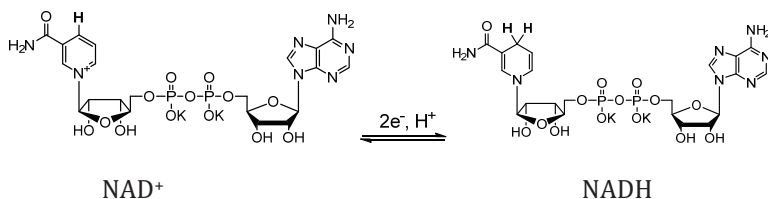
Thus, the inverse rate should be a linear function of $[S]$ as shown in inset to Fig. 4.1.2. The intercept and the slope of the straight line equal $1/(k_{cat}[E])$ and $1/(k_{cat}[E]K_{2s})$, respectively, and therefore $K_{2s} = \text{intercept/slope}$.

4.2. Competitive Inhibition

Enzyme lactate dehydrogenase (LDH) catalyzes interconversions of *L*-lactate and pyruvate in both directions (eq 4.2.1).



The oxidative process (*L*-lactate \rightarrow pyruvate) requires oxidation equivalents delivered by the NAD^+ cofactor (nicotinamide adenine dinucleotide oxidized) shown in Scheme 4.2.1. The reverse reductive process (pyruvate \rightarrow *L*-lactate) occurs in the presence of NADH (nicotinamide adenine dinucleotide reduced).



Scheme 4.2.1. Cofactors NAD^+ and NADH , which deliver oxidative and reductive equivalents, respectively. Cofactors are usually low molecular weight compounds which are essential for catalytic activity of redox enzymes (oxidoreductases); they are not bound covalently to enzymes and diffuse freely in solution.

The activity of LDH is compromised by numerous organic and inorganic compounds including ruthenium(II) complexes **4.1** and **4.2**.

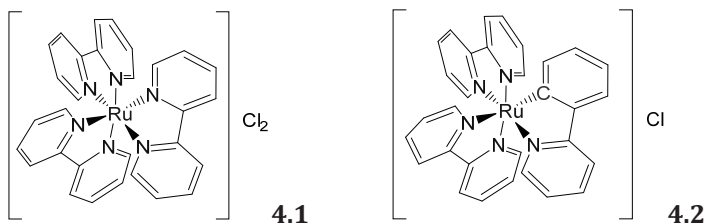


Figure 4.2.1a shows how rates of the enzymatic LDH-catalyzed reduction of pyruvate by NADH as a function of $[\text{NADH}]$ diminish with increasing the concentration of **4.1** in solution. The type of inhibition could be established using the corresponding Lineweaver-Burk plots (inverse rate vs. inverse $[\text{S}]$), which in this case are shown in Fig. 4.2.1b.

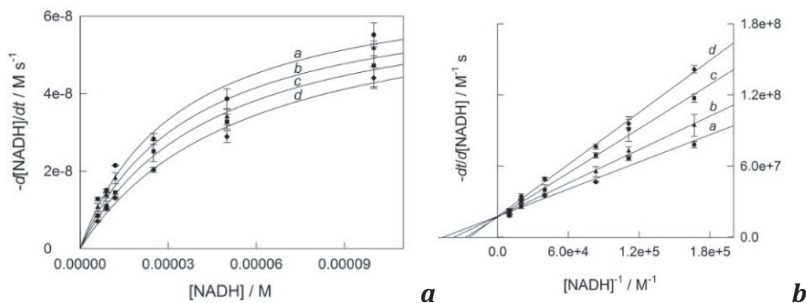


Figure 4.2.1. (a) Steady-state rates of LDH_{rm}-catalyzed reduction of pyruvate by NADH as a function of [NADH] in the presence of $(0.5\text{--}2.0)\times 10^{-4}$ M **4.1** at pH 7.5 and 37 °C; [LDH_{rm}] 1×10^{-10} M, [pyruvate] 1.2×10^{-3} M. (b) Lineweaver-Burk plots of the data in (a). LDH_{rm} is lactate dehydrogenase from rabbit muscle.⁴

The straight lines in Fig. 4.2.1b intercept the y-axis in one point indicating that the maximal rates V_M (see eq 3.2.2) are unaffected by **4.1**. Effective Michaelis constants $K_{M,\text{eff}}$, in contrast, are larger at higher loadings of **4.1**. This manifests in smaller negative intercepts on the x-axis, which equal $(-1/K_{M,\text{eff}})$.⁵ These two observations indicate that inhibitor I (*i*) does not change the catalytic activity of enzyme (V_M or k_{cat}) but (*ii*) competes with a substrate S for the binding to enzyme. Features *i* and *ii* are quantifiable in terms of Scheme 4.2.2, the key feature of which is the competition between substrate S and inhibitor I for binding to enzyme E.



Scheme 4.2.2. Formal mechanism of competitive inhibition.

In fact, when $S_t, I_t \gg E_t$, the mass balance equation is $E_t = [E] + [ES] + [EI]$. Using the "enzymological" language, $K_s = [E][S]/[ES]$ and $K_I = [E][I]/[EI]$. Therefore

⁴ Data are from Rico-Bautista H, et al, *J Inorg Biochem*, **2016**, 163, 28.

⁵ See problem 3-13.

$$[\text{ES}] = \frac{[\text{S}]K_i}{K_s K_i + [\text{S}]K_i + K_s [\text{I}]} = \frac{[\text{S}]K_i}{K_s (K_i + [\text{I}]) + [\text{S}]K_i}$$

Since $v = k_{\text{cat}}[\text{ES}]$, the final equation for the rate is given by eq 4.2.2

$$v = \frac{k_{\text{cat}} E_t [\text{S}]}{K_s \frac{K_i + [\text{I}]}{K_i} + [\text{S}]} = \frac{V_M [\text{S}]}{K_{M,\text{eff}} + [\text{S}]} \quad (4.2.2)$$

with

$$K_{M,\text{eff}} = K_s \frac{K_i + [\text{I}]}{K_i} = K_s + \frac{K_s}{K_i} [\text{I}] \quad (4.2.3)$$

Equations 4.2.2 and 4.2.3 agree with experimental observations in Fig. 4.2.1b, i.e. in case of competitive inhibition V_M is unaffected by inhibitor but the effective Michaelis constant $K_{M,\text{eff}}$ increases with increasing $[\text{I}]$ as predicted by eq 4.2.3. The plot $K_{M,\text{eff}}$ vs. $[\text{I}]$ should be a straight line with the intercept and slope of K_s and $K_s K_i^{-1}$, respectively. The intercept over the slope equals K_i . Such plot is shown in Fig. 4.2.2 using the data in Fig. 4.2.1. The calculated value of K_i equals 2.2×10^{-4} M. It could be compared with K_s of 2.2×10^{-5} M for NADH to reveal that the effective affinity of NADH toward LDH is by order of magnitude higher than that of complex **4.1**.

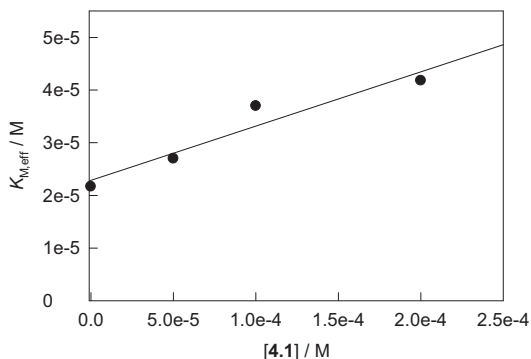


Figure 4.2.2. Effective Michaelis-Menten constants versus concentration of **4.1** for LDH_{rm}-catalyzed reduction of pyruvate by NADH. Conditions are as in Fig. 4.2.1.

4.3. Noncompetitive Inhibition

The case when inhibitor decreases V_M leaving K_M unchanged is referred to as a *noncompetitive* inhibition. The case is presented in Fig. 4.3.1 by the example of reductive reaction 4.2.1 (pyruvate \rightarrow L-lactate) retarded by complex 4.2. The diagnostic double inverse plot in Fig. 4.3.1b has a common intercept on the x -axis (unaffected K_M) and the values of V_M decrease as the inhibitor concentration grows.

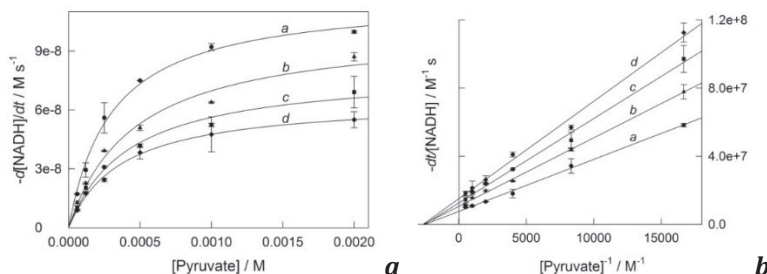


Figure 4.3.1. (a) Steady-state rates of LDH_{rm}-catalyzed reduction of pyruvate by NADH as a function of pyruvate concentration at different concentrations of 4.2 (0, 0.5×10^{-4} , 1.0×10^{-4} , and 2.0×10^{-4} M from a to d, respectively) at pH 7.5 and 37 °C; [LDH_{rm}] 1×10^{-10} M, [NADH] 1.2×10^{-4} M. (b) Lineweaver-Burk plots of the data in (a).

The term noncompetitive implies that substrate and inhibitor do not compete with each other for the binding to enzyme, i.e. each binds to the enzyme independently of its "opponent" and therefore Scheme 4.3.1 contains an extra step compared to Scheme 4.2.2 for the competitive inhibition.



Scheme 4.3.1. Formal mechanism of noncompetitive inhibition.

The rate equation corresponding to Scheme 4.3.1 when $S_t, I_t \gg E_t$ is derived as follows. The mass balance equation is $E_t = [E] + [ES] + [EI] + [ESI]$. In the "enzymological" terms, $K_s = [E][S]/[ES]$, $K_i = [E][I]/[EI]$ and $K_i' = [ES][I]/[ESI]$. Hence

$$E_t = [ES] \left\{ \frac{K_s}{[S]} + 1 + \frac{K_s}{[S]} \times \frac{[I]}{K_i} + \frac{[I]}{K_i'} \right\}$$

$$[ES] = E_t \frac{[S]K_i K_i'}{K_s K_i' (K_i + [I]) + [S]K_i (K_i' + [I])}$$

A common assumption $K_i \approx K_i'$ reflects the fact that inhibitor binds to enzyme independently of substrate, i.e. the substrate binding does not affect the affinity of enzyme to the inhibitor and vice versa. This simplifies the latter expression to eq 4.3.1.

$$[ES] = \frac{\frac{K_i}{K_i + [I]} E_t [S]}{K_s + [S]} \quad (4.3.1)$$

Finally

$$v = \frac{k_{\text{cat}} \frac{K_i}{K_i + [I]} E_t [S]}{K_s + [S]} \quad (4.3.2)$$

Correspondingly

$$V_{M,\text{eff}} = V_M \frac{K_i}{K_i + [I]} \quad (4.3.3)$$

Thus, $V_{M,\text{eff}}$ in the case of noncompetitive inhibition should decrease hyperbolically with increasing $[I]$ but inverse $V_{M,\text{eff}}$ is a linear function of $[I]$:

$$\frac{1}{V_{M,\text{eff}}} = \frac{1}{V_M} + \frac{[I]}{V_M K_i} \quad (4.3.4)$$

Such plot (inverse $V_{M,\text{eff}}$ vs $[I]$) is shown in Fig. 4.3.2. The intercept and the slope equal V_M^{-1} and $(V_M K_i)^{-1}$, respectively, and $K_i = \text{intercept/slope} = 2.0 \times 10^{-4} \text{ M}$ in this case.

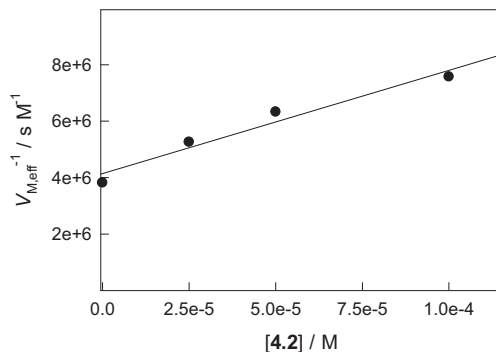


Figure 4.3.2. Inverse effective maximal rates versus concentration of **4.2** for LDH_{rm}-catalyzed reduction of pyruvate by NADH. Conditions are as in Fig. 4.3.1.

Practical biochemists operate with the values of $i_{0.5}$ measured in M which are inhibitor concentrations needed for 50% inhibition of enzymatic activity. The noncompetitive inhibition is the only scenario when $i_{0.5}$ is identical to K_i (work on problem 4-4). For all other types of inhibition $i_{0.5}$ is an effective characteristic which is not directly related to the inhibition constant K_i .

4.4. Uncompetitive and Mixed Inhibition

The case when an inhibitor decreases both V_M and K_M in the same manner is referred to as a *uncompetitive* inhibition. It is presented in Fig. 4.4.1a. As the inhibitor concentration increases, both V_M and K_M decrease which is emphasized in the Lineweaver-Burk plot in Fig. 4.4.1b. There is a set of parallel lines for different inhibitor loadings.

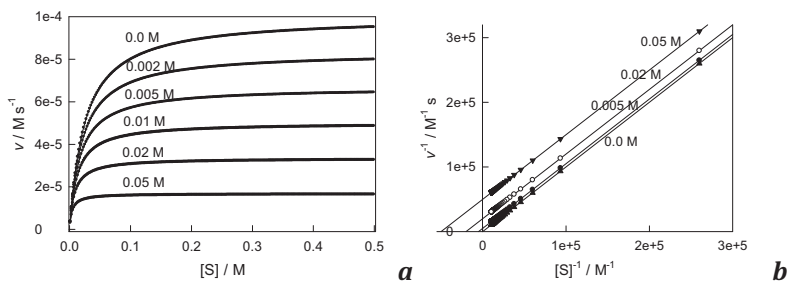
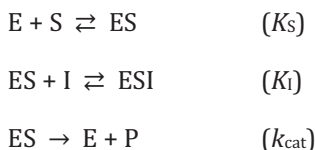


Figure 4.4.1. (a) Simulated rate versus $[S]$ profiles for a one substrate enzymatic reaction with uncompetitive inhibition using $k = 100 \text{ s}^{-1}$, $K_s = 0.025 \text{ M}$ and $K_i = 0.01 \text{ M}$ at different inhibitor concentrations. (b) Corresponding double inverse plot.

Mechanistically the case of uncompetitive inhibition is uncommon because it necessitates that inhibitor binds only to enzyme-substrate complex ES and does not bind to free enzyme E (Scheme 4.4.1).



Scheme 4.4.1. Formal mechanism of uncompetitive inhibition.

The rate equation consistent with Scheme 4.4.1 when $S_t, I_t \gg E_t$ is derived as before. The mass balance equation is $E_t = [E] + [ES] + [ESI]$. In the "enzymological" terms, $K_s = [E][S]/[ES]$ and $K_i = [ES][I]/[ESI]$. Hence

$$\begin{aligned}
 E_t &= [ES] \left\{ \frac{K_s}{[S]} + 1 + \frac{[I]}{K_i} \right\} \\
 [ES] &= E_t \frac{[S]K_i}{K_s K_i + [S]K_i + [S][I]} = E_t \frac{[S] \frac{K_i}{K_i + [I]}}{K_s \frac{K_i}{K_i + [I]} + [S]}
 \end{aligned}$$

Therefore

$$v = k_{\text{cat}}[\text{ES}] = \frac{k_{\text{cat}} \frac{K_i}{K_i + [\text{I}]} E_t [\text{S}]}{K_s \frac{K_i}{K_i + [\text{I}]} + [\text{S}]}$$

Finally

$$V_{\text{M,eff}} = V_{\text{M}} \frac{K_i}{K_i + [\text{I}]} \quad \text{and} \quad K_{\text{M,eff}} = K_s \frac{K_i}{K_i + [\text{I}]}$$

Note that the ratios $V_{\text{M,eff}}/K_{\text{M,eff}} = V_{\text{M}}/K_s$ or $k_{\text{cat,eff}}/K_{\text{M,eff}} = k_{\text{cat}}/K_s$ are insensitive to the presence of inhibitor I. Uncompetitive inhibition is the only case where this is observed. Table 4.1 summarizes major features of the three inhibition mechanisms considered in Lecture 4 and makes this point clear because the $V_{\text{M,eff}}/K_{\text{M,eff}}$ ratios for both competitive and noncompetitive inhibitions are functions of [I].

Table 4.1. Features of competitive, noncompetitive and uncompetitive inhibition.

Inhibition Mechanism	$V_{\text{M,eff}}$	$K_{\text{M,eff}}$
Competitive	V_{M}	$K_s \frac{K_i + [\text{I}]}{K_i}$
Noncompetitive	$V_{\text{M}} \frac{K_i}{K_i + [\text{I}]}$	K_s
Uncompetitive	$V_{\text{M}} \frac{K_i}{K_i + [\text{I}]}$	$K_s \frac{K_i}{K_i + [\text{I}]}$

Rather often an enzymatic inhibition cannot be classified as competitive, noncompetitive or uncompetitive. These cases are referred to as a mixed inhibition. An example of such is presented in Fig. 4.4.2. Lineweaver-Burk lines for the LDH_{rm}-catalyzed oxidation of L-lactate by NAD⁺ (eq 4.2.1) in the presence of inhibitor 4.1 are not parallel and do not cross either x- or y-axis in a common point.

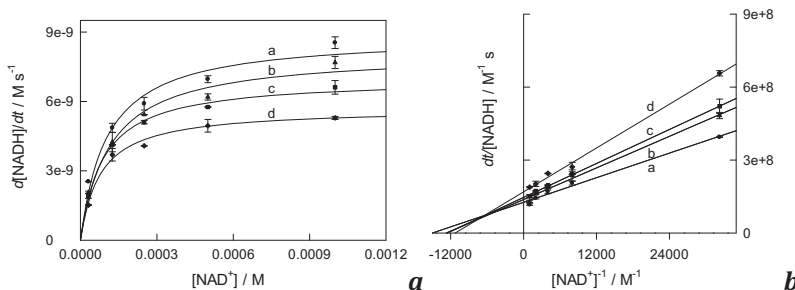


Figure 4.4.2. Mixed inhibition: **(a)** Steady-state rates of LDH_{rm}-catalyzed oxidation of *L*-lactate by NAD⁺ as a function of NAD⁺ concentration in the presence of $(0.5\text{--}2.0)\times 10^{-4}$ M **4.1** at pH 7.5 and 37 °C; [LDH_{rm}] 4×10^{-10} M, [lactate] 0.1 M. **(b)** Lineweaver-Burk plots of the data in **(a)**.

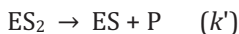
Problems

4-1. Substrate may also bind to enzyme somewhere away from its active site to form ES' which is catalytically inactive, i.e.



Derive the equation for the rate as a function of [S] when $S_t \gg E_t$.

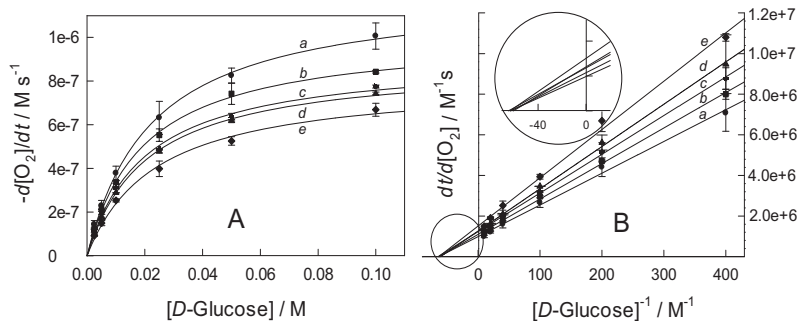
4-2. Derive and analyze the rate equation for substrate inhibition when ES₂ is also reactive, i.e. when the step



is not negligible. Will the rate drop on increasing [S] when $k' > k$?

4-3. The data for the glucose oxidase-catalyzed oxidation of *D*-glucose by O₂ are shown below. Determine the type of inhibition by increasing

concentrations of **4.2** (0, 0.001, 0.004, 0.009, and 0.016 M from *a* to *e*, respectively).⁶



4-4. Practical biochemists operate with the values of $i_{0.5}$ measured in M which are inhibitor concentrations for 50% inhibition of enzymatic activity. Prove that in the case of noncompetitive inhibition $i_{0.5} = K_i$.

4-5. Suggest Eadie-Hofstee plots (v vs $v/[S]$) for competitive, noncompetitive and uncompetitive inhibition at $[I] = 0$, $[I] > 0$ and $[I] \gg 0$.

⁶ Díaz ROS, et al, *J Biol Inorg Chem (JBIC)*, **2013**, *18*, 547.

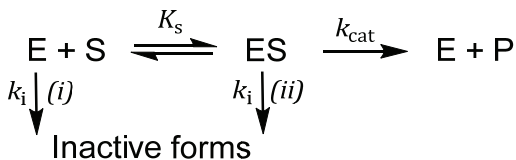
LECTURE 5.

IRREVERSIBLE INACTIVATION OF CATALYSTS IN CHEMISTRY AND ENZYMOLOGY

5.1. Enzymology

Enzymes likewise other proteins undergo irreversible inactivation due to various phenomena including (1) aggregation; (2) thiol-disulfide exchange; (3) alterations in the primary structure, e.g. chemical modification of functional groups; (4) cleavage of S-S bonds; (5) dissociation of the prosthetic group from the active site of the enzyme; (6) dissociation of oligomeric proteins into subunits; and (7) conformational changes in the macromolecule.¹

In terms of the Michaelis-Menten formalism, the loss of enzymatic activity driven by the first-order rate constant k_i (rate constant of *inactivation*) may occur as a result of inactivation of (i) the resting state of enzyme E, (ii) the enzyme-substrate complex ES or both (Scheme 5.1.1).



Scheme 5.1.1. Mechanistic options for irreversible inactivation of enzymes in terms of the Michaelis-Menten formalism.

Pathway (i) is arguably more common because specific substrates may stabilize enzymes within ES intermediates. These two (i) and (ii) scenarios will be examined independently.

¹ Mozhaev VV, Martinek K, *Enzyme Microbiol Technol*, **1982**, 4, 299.

5.1.1. Case (i): Resting State Inactivation

Consider Scheme 5.1.1 with the nonexistent (ii) pathway when $S_t \gg E_t$. Let x be a current time-dependent *total* concentration of the active enzyme, which decreases with time due to inactivation. At any time

$$x = [E] + [ES]$$

Due to the inactivation via pathway (i)

$$-\frac{dx}{dt} = k_i[E] = k_i(x - [ES]) \quad (5.1.1)$$

The rate of product formation equals the negative rate of substrate conversion:

$$\frac{d[P]}{dt} = \left(-\frac{d[S]}{dt}\right) = k_{\text{cat}}[ES] = \frac{k_{\text{cat}}}{K_S}[E][S] = \left(\frac{k_{\text{cat}}}{K_S}(x - [ES])[S]\right) \quad (5.1.2)$$

After dividing eq 5.1.1 by parenthesized part of eq 5.1.2, one arrives to eq 5.1.3, which is ready for integration.

$$\frac{dx}{d[S]} = \frac{k_i K_S}{k_{\text{cat}}[S]} \quad \text{or} \quad dx = \frac{k_i K_S}{k_{\text{cat}}[S]} d[S] \quad (5.1.3)$$

When inactivation is complete, the enzyme concentration changes from E_t to zero, whereas the substrate concentration varies from S_t to S_∞ . Therefore

$$\int_{E_t}^0 dx = \int_{S_t}^{S_\infty} \frac{k_i K_S}{k_{\text{cat}}[S]} d[S]$$

Finally

$$\ln \frac{S_t}{S_\infty} = \frac{k_{\text{cat}} E_t}{K_S k_i} \quad (5.1.4)$$

Equation 5.1.4 shows that the rate constant of inactivation k_i can be effortlessly calculated after measuring the amount of unreacted substrate S_∞ , which is left untouched after the complete inactivation of enzyme. Of course, k_{cat} and K_S should be obtained first by measuring initial rates of the enzymatic reaction.

The data needed for calculating k_i are shown in Fig. 5.1.1 by the example of catalysis by heme chloroperoxidase (see also Sections 4.1 and 11.2.7). Kinetic data for the bromination of the monochlorodimedon substrate were obtained at fixed $[\text{Br}^-]$ and different $[\text{H}_2\text{O}_2]$. The substrate consumption is virtually complete in the presence of 3-6 mM H_2O_2 . Starting with $[\text{H}_2\text{O}_2] = 7$ mM and above, the reaction does not go to completion and the kinetic curves level off. The degree of conversion decreases with increasing $[\text{H}_2\text{O}_2]$ due to the H_2O_2 -induced inactivation of the enzyme because addition of a new aliquot of the chloroperoxidase enzyme restarts the reaction (Fig. 5.1.1). The effect is observed after the third, fourth, etc., additions of the enzyme till complete consumption of the substrate.

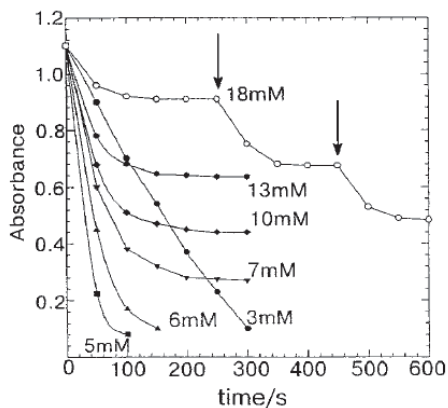


Figure 5.1.1. Kinetics of chloroperoxidase-catalyzed bromination of monochlorodimedon (0.1 mM) at different concentrations of H_2O_2 ; $[\text{KBr}]$ 0.01 M, $[\text{E}]$ 10^{-8} M, pH 2.75, 25 °C. Arrows indicate additions of new portions of the enzyme after its inactivation during previous cycle.²

Equation 5.1.4 was used for calculating k_i because the k_{cat} and K_S values were available. As anticipated, k_i appeared to be an ascending function of $[\text{H}_2\text{O}_2]$ in a form $k_i = a[\text{H}_2\text{O}_2]/(b+[\text{H}_2\text{O}_2])$. High loadings of H_2O_2 increased k_i , which resulted of lower degrees of substrate conversions at higher $[\text{H}_2\text{O}_2]$.

² Shevelkova AN, Ryabov AD, *Biochem Mol Biol Int*, **1996**, 39, 665.

5.1.2. Case (ii): Inactivation of Enzyme-Substrate Complex

Consider now Scheme 5.1.1 with the nonexistent (*i*) pathway using similar designations. This time eq 5.1.1 should be replaced by

$$-\frac{dx}{dt} = k_i[\text{ES}]$$

and

$$\frac{d[\text{P}]}{dt} = \left(-\frac{d[\text{S}]}{dt}\right) = k_{\text{cat}}[\text{ES}]$$

Correspondingly

$$\frac{dx}{d[\text{S}]} = \frac{k_i}{k_{\text{cat}}} \quad \text{and} \quad \int_{E_t}^0 dx = \frac{k_i}{k_{\text{cat}}} \int_{S_t}^{S_\infty} d[\text{S}]$$

After integration

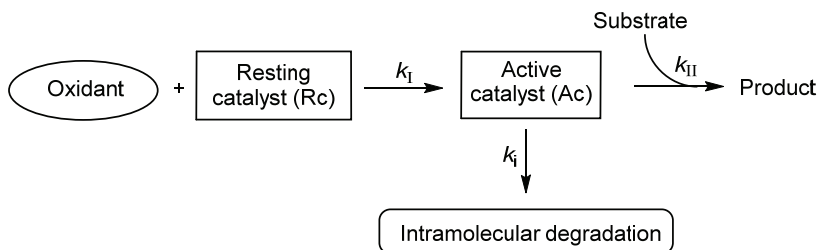
$$S_t - S_\infty = \frac{k_{\text{cat}}E_t}{k_i} \quad (5.1.5)$$

Equation 5.1.5 differs from eq 5.1.4. The former does not contain K_S reflecting the fact that it is the enzyme-substrate complex itself that undergoes inactivation. Correspondingly, just k_{cat} needs to be known for calculating k_i from the $S_t - S_\infty$ difference.

5.2. Chemistry

Resting states (Rc) of low-molecular weight synthetic catalysts are usually sufficiently resistant to degradation under reaction conditions. Problems start to emerge when catalysts catalyze, for example, oxidations by powerful oxidants, which are not sufficiently reactive under noncatalytic conditions (Scheme 5.2.1).³

³ Chanda A, et al, *Chem - Eur J*, **2006**, *12*, 9336.



Scheme 5.2.1. Catalytic steps and the step leading to inactivation of the active form of an oxidation catalyst involved in a two-substrate process.

Active catalyst (Ac), which is produced from an oxidant and a catalyst in the resting state, may target its oxidative power at itself with the first-order rate constant k_i . It is easier to calculate k_i when $k_I \gg k_{II}$,⁴ i.e. when AC is formed rapidly and quantitatively in the presence of an oxidant. In this case

$$-\frac{d[S]}{dt} = k_{II}[S][Ac]$$

Since $[Ac]$ decreases exponentially due to first-order inactivation ($[Ac] = C_t \times e^{-k_i t}$; C_t is the total catalyst concentration)

$$-\frac{d(S_t - x)}{dt} = k_{II}(S_t - x)C_t e^{-k_i t} \quad (5.2.1)$$

Here x is the concentration of *converted* substrate at time t . Integration of eq 5.2.1 using the boundary conditions $x = x_\infty$ when $t = \infty$ and rearrangement lead to eq 5.2.2.

$$\ln \left[\ln \left(\frac{S_t - x}{S_t - x_\infty} \right) \right] = \ln \left(\frac{k_{II}}{k_i} C_t \right) - k_i t \quad (5.2.2)$$

Thus, the linear plot $\ln[\ln(S_t - x)/(S_t - x_\infty)]$ versus time t should have a slope of $-k_i$ and an intercept of $\ln(k_{II}C_t/k_i)$, which allow to obtain k_i and k_{II} .

The solution of eq 5.2.1 using the boundary condition $x = 0$ at $t = 0$ leads to eq. 5.2.3 which at $t \rightarrow \infty$ becomes eq 5.2.4.

⁴ See Problem 5-1.

$$\ln \frac{S_t}{S_t - x} = \frac{k_{II}}{k_I} C_t (1 - e^{-k_I t}) \quad (5.2.3)$$

$$\ln \frac{S_t}{S_t - x_\infty} = \frac{k_{II}}{k_I} C_t \quad (5.2.4)$$

Since $(S_t - x_\infty) = S_\infty$ (unreacted substrate after complete inactivation of catalysts), equation 5.2.4 is comparable with eq 5.1.4 taking into consideration that the k_{cat}/K_S ratio in eq 5.1.4 corresponds to the second-order rate constant for the reaction between E and S. Equation 5.2.4 allows effortless estimation of k_I from S_∞ provided the rate constant k_{II} is known.

If a reaction is followed by uv-vis spectroscopy by measuring substrate consumption and S is the only absorbing species at a given wavelength, it is convenient to replace concentrations S by directly measured absorbances A:

$$\ln \left[\ln \left(\frac{A}{A_\infty} \right) \right] = \ln \left(\frac{k_{II}}{k_I} C_t \right) - k_I t \quad (5.2.5)$$

Here A and A_∞ are absorbances at time t and ∞ , respectively. If the double logarithm of the ratio A/A_∞ is plotted against time, the slope of the straight line equals $-k_I$. The rate constant k_{II} can be calculated from the intercept which equals $\ln(k_{II}C_t/k_I)$. A linearization of four kinetic traces of Fig. 5.2.1 in terms of eq 5.2.5 is demonstrated in the Inset. All four straight lines have similar slopes that are equal to k_I . It should be mentioned that A is not the measured absorbance A_m at time t but the difference $A = A_m - A_{m,\infty}$. Correspondingly, $A_\infty = A_m(t=0) - A_{m,\infty}$. Note that in Fig. 5.2.1 $A_\infty = x_\infty$.

When the condition $k_I \gg k_{II}$ (Scheme 5.2.1) does not hold, the evaluation of k_I from product versus time profiles using formulas similar to 5.2.5 becomes impossible because the system of differential equations corresponding to Scheme 5.2.1 does not have analytical solution.⁵ Luckily, under such conditions eq 5.2.4 still holds in excess of [oxidant] over [substrate] and therefore k_I could be found provided k_{II} is known.

⁵ Emelianenko M, et al, *J Math Chem*, **2014**, 52, 1460.

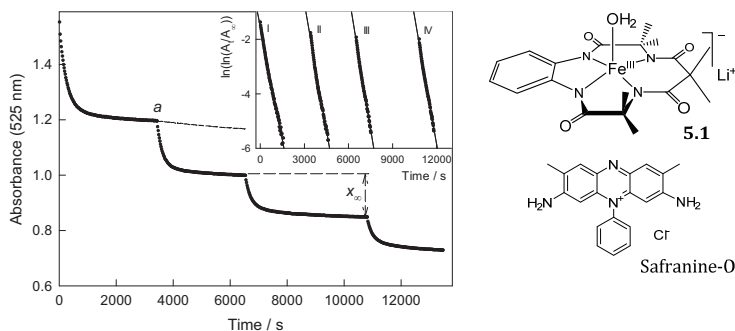
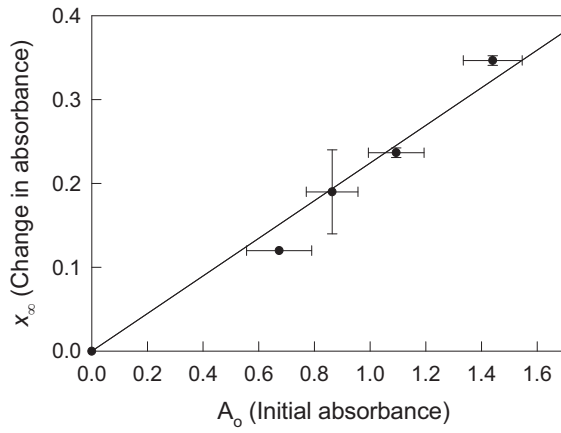


Figure 5.2.1. Kinetics of **5.1**-catalyzed bleaching of Safranin-O (4.3×10^{-5} M) by 0.012 M H_2O_2 . Initial concentration of **5.1** (7.5×10^{-8} M); aliquots of the same amount of **5.1** were added after complete inactivation of the catalyst giving rise to the stepped dependence. The dashed line demonstrates that addition of 0.012 M H_2O_2 does not resume the catalytic bleaching. **Inset** shows linearization of the data obtained after each addition of **5.1** in terms of eq 5.2.5. Conditions: pH 11, 25 °C.

Problems

5-1. Strictly speaking, the relation $k_1 \gg k_{II}$ is not sufficient and the condition $k_1[\text{oxidant}] \gg k_{II}[\text{substrate}]$ should hold to ensure rapid and quantitative formation of the active catalysts Ac (Scheme 5.2.1). Prove the latter statement.

5-2. Careful inspection of the data in Fig. 5.2.1 indicates that the total amount of the bleached dye (x_∞) after adding a new aliquot of catalyst **5.1** is not constant and gradually decreases after each new addition. Prove that there should be a linear dependence between x_∞ and A_0 (initial absorbance) or substrate concentration S_0 at a time of addition of catalyst as it shown in the graph below.



LECTURE 6.

BASIC TOOLS OF CHEMICAL KINETICS

6.1. Kinetic Isotope Effects

Many reactions involve a transfer of hydrogen atom/s or ion/s between participating fragments. To confirm or rule out that a hydrogen transfer occurs in the slowest step, a corresponding deuterium-labeled compound should be prepared and the rate constants $k(\text{H})$ and $k(\text{D})$ for the protium and deuterium molecules, respectively, be compared. The ratio $k(\text{H})/k(\text{D})$ is the *kinetic isotope effect* (KIE). If KIE equals 1, there is likely no hydrogen transfer in the rate-limiting step. If $k(\text{H})/k(\text{D}) > 1$, there is a certain probability that hydrogen is transferred in the rate-limiting step. The probability increases as far as KIE becomes larger than unity. KIA is usually not higher than 7. This estimate comes from the transition state theory. The ground state, which is convenient to associate with the C–H bond to be cleaved, should not be the absolute energy minimum but rather a *quantum zero-energy state* which equals $\frac{1}{2}h\nu$ (here ν is the stretching frequency of the bond to be cleaved; the harmonic oscillator approximation) (Fig. 6.1.1). For the C–H and C–D bonds the corresponding frequencies are in the ranges of 2800–3300 and 2000–2200 cm^{-1} , respectively. Therefore, the C–D bond energy is

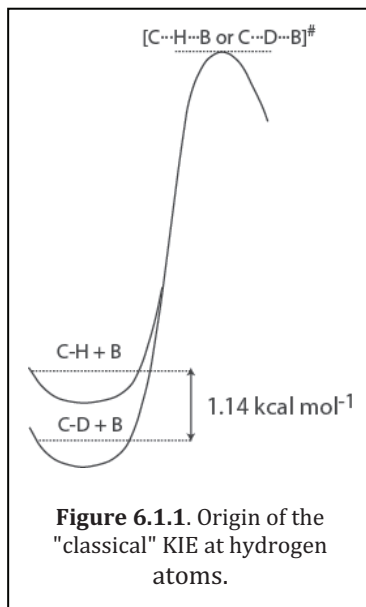


Figure 6.1.1. Origin of the "classical" KIE at hydrogen atoms.

lower and the energy gap is

$$\frac{1}{2}hv_{\text{C-H}} - \frac{1}{2}hv_{\text{C-D}} = \frac{1}{2}(2900 - 2100) = 400 \text{ cm}^{-1} = 1.14 \text{ kcal mol}^{-1}$$

Going from *energies* to *rates* ($e^{-E/RT}$), one obtains the rate difference of a factor of 6.9 at 25 °C. Such an interpretation of KIE is a rough approximation, since it is assumed that the transition state energies are the same for C–H and C–D bonds. It is argued though that the stretching frequency in the transition state becomes the reaction coordinate.

In the most general case for any X–Y bond, the ratio of stretching frequencies is inversely proportional to the square root of the reduced masses ($\mu = m_1m_2/(m_1+m_2)$):

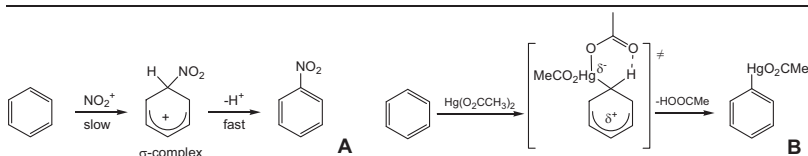
$$\frac{\nu_1}{\nu_2} = \sqrt{\frac{\mu_2}{\mu_1}}$$

The maximal KIE effect will obviously be observed for the pair protium-tritium. KIEs are possible for other isotopes, for example, ^{16}O and ^{18}O . It should however be noted that if the O–H bond is cleaved, the KIE is only 1.01. Therefore, its estimation from experimentally measured rate constants is hardly possible.

When H/D KIE differs from 1 only slightly (1.0 ± 0.2), it is referred to as a *secondary* kinetic isotope effect. This may result from the following.

- Contribution of the H–X bond cleavage into the transition state is minimal.
- The H–X bond is not cleaved at all in the transition state; the substitution of H by D results mostly in the electronic effects, since deuterium, although weak, but stronger electron donor compared to protium.

An example is electrophilic ($\text{S}_{\text{E}}2$) nitration of arenes by $\text{HNO}_3/\text{H}_2\text{SO}_4$, for which KIE is close to 1. In this case, the formation of σ -complex is rate-limiting but the dissociation of proton is fast (Scheme 6.1.1A).



Scheme 6.1.1. S_E2 reactions with different rate-limiting steps: nitration (A) and mercuration (B).

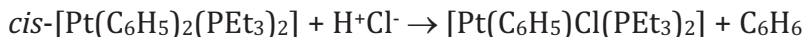
If H/D KIE is higher than *ca.* 1.5, this is a *primary* kinetic isotope effect and the H–X bond is in fact cleaved in the rate-limiting step. Metalation of arenes, for example by Hg(O₂CCH₃)₂ (Scheme 6.1.1B), is more concerted in nature and KIE ~ 5.

KIEs are sometime estimated in competitive experiments using mixtures of H- and D-containing substrates (Section 2.3). It should be realized that if even KIE > 1, it does not inevitably mean that the H–X bond is cleaved in the rate-limiting step.

Incorporation of deuterium in solvent molecules may affect rates of pH-dependent chemical reactions, since it is known that the acidity decreases approximately 3-fold in D₂O. The explanation can be found in Fig. 6.1.1, i.e. as a result of a lower energy of the ground state. pH measurements in D₂O solutions require a correction

$$\text{pD} = \text{pH}(\text{measured}) + 0.4$$

If proton itself or as a part of solvent is involved in a chemical transformation (*the solvent isotope effect* in the latter case), the observed KIE's are similar to those for the cleavage of H–X bonds. For example, the protonolysis of Pt–C bonds in complexes of Pt^{II}:



is exemplified by $k(\text{H}^+)/k(\text{D}^+) \approx 6$,¹ but the solvent KIE $k(\text{MeOH})/k(\text{MeOD})$ in reaction 4.1.1 equals 11.0.²

¹ Romeo R, et al, *Inorg Chem*, **1978**, *17*, 2813.

² Hutton WC, Crowell TI, *JACS*, **1978**, *100*, 6904.



There are cases when $\text{KIE} < 1$ (inverse KIE; bonds formed are much stronger than bonds cleaved) and when $\text{KIE} \gg 7$. For instance, for the deprotonation of 2-nitropropane by 2,6-dimethylpyridine the ratio $k_{\text{H}}/k_{\text{D}} = 19.5$ at 25 °C in aqueous solution.³ Noticeably, for the sterically unhindered pyridine molecule the KIE is practically normal (9.9). Higher KIE are usually associated with a tunneling of proton through a potential barrier. One of the conclusions of the quantum theory is that the probability of tunneling diminishes strongly with an increase in the molecular weight of a molecule. Therefore, the tunneling of deuterium is less probable than that of protium. It should also be mentioned that the tunneling for larger molecules is usually observed at very low temperatures. The tunneling manifests itself in independence of the reaction rate on temperature. Molecules do not require extra energy for penetrating through an activation barrier.

6.2. Linear Free Energy Relationships (LFER)

“Bald” theory reads:⁴

- The changes in the value of ΔG^\ddagger for any reaction involving X which are produced by a series of changes in R are linearly related to the changes in ΔG° for the same reaction:

$$\Delta G_i^\ddagger = \alpha \Delta G_i^\circ + \beta$$

Here subscript i refers to reaction i ;

- The changes in the value of ΔG^\ddagger or of ΔG° for one reaction involving a reacting group X_1 produced by a series of changes in R are linearly related to the changes in the corresponding values for another reaction involving X_1 and also to those for a reaction involving a different group X_2 :

$$\Delta G_i^\ddagger = \alpha \Delta G_j^\circ + \beta \quad \text{or} \quad \Delta G_i^\ddagger = \alpha \Delta G_j^\ddagger + \beta$$

Here subscripts i and j refer to different reactions. Sounds great but nothing is clear yet. Is not it? The messages are the following.

³ Bell RP, Goodall DM, *Proc Roy Soc*, **1966**, 294, 273.

⁴ Hammett LP, *Physical organic chemistry; reaction rates, equilibria, and mechanisms*, McGraw-Hill, NY, **1970**, p. 349.

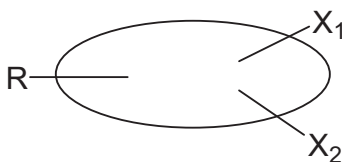
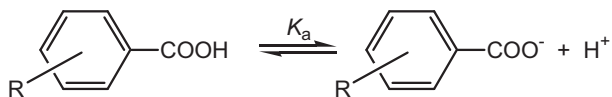


Figure 6.2.1. Imaginary molecule with two reacting centers X_1 and X_2 plus a center with variable groups R .

Look at the imaginary molecule in Fig. 6.2.1 that has two reacting centers X_1 and X_2 plus a center with variable groups R . The first postulate claims that for one and the same reaction involving X_1 the rate and equilibrium constants measured for different R should correlate. The second postulate claims that the same is true for different reactions involving the same center X_1 , as well as for reactions involving different centers X_1 and X_2 . It should be remembered that the energy equivalents of rate and equilibrium constants should be used in LFER, i.e. their logarithms or ΔG^\ddagger and ΔG° .

6.2.1. Hammett and Taft Equations

As a standard scale for reactions involving arenes, Hammett introduced the dissociation constants for substituted benzoic acids:



Each substituent R at position 4 or 3 is characterized by its σ constant, which is easy to calculate

$$\sigma_i = \text{p}K_a^\circ - \text{p}K_a^i$$

Here symbol $^\circ$ refers to the standard compound, viz. benzoic acid ($R = \text{H}$). Thus generated σ values (Table 6.2.1) do characterize electronic properties of substituents R in the aromatic series. Electron-donating and electron-withdrawing groups are characterized by small *negative* and *positive* numbers, respectively. The entire scale covers basically the range of from -1 to $+1$.

Table 6.2.1. Examples of the Hammett σ constants.⁵

R	3-Substituent	4-Substituent	
	σ_m	σ_p	σ^+
<i>t</i> -Bu	-0.10	-0.20	-0.26
Me	-0.07	-0.17	-0.31
S-	-0.36	-1.21	-2.62
NMe ₂	-0.1	-0.63	-1.7
OMe	+0.12	-0.27	-0.78
OH	+0.12	-0.37	-0.92
COOMe	+0.39	+0.31	+0.49
F	+0.34	+0.06	-0.07
Br	+0.39	+0.23	+0.15
Cl	+0.37	+0.23	+0.11
CF ₃	+0.43	+0.54	+0.61
CN	+0.56	+0.66	+0.66
NO ₂	+0.71	+0.78	+0.79

Parameters σ^+ were calculated from the kinetic data for the solvolysis of 4-substituted cumyl chlorides $\text{RC}_6\text{H}_4\text{CClMe}_2$. They reflect the mesomeric effect that contributes to the stabilization of charges developed in the transition state:



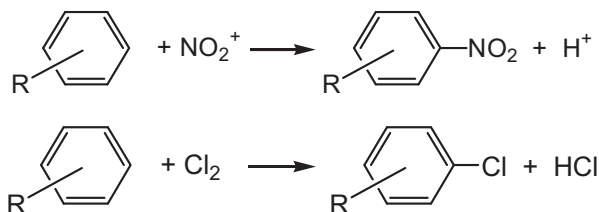
Thus, electronic properties of substituents σ are defined. Consider chemical reactions involving a center X of an aromatic molecule using eq 6.2.1, the **Hammett** equation.

$$\log k = \log k_0 + \rho\sigma \quad \text{or} \quad \log \frac{k}{k_0} = \rho\sigma \quad (6.2.1)$$

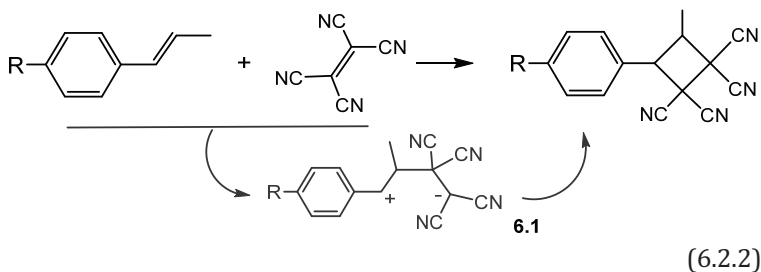
The rate constant k_0 corresponds to a reaction when $\text{R} = \text{H}$. Parameter σ characterizes substituent R; parameter ρ characterizes a particular chemical reaction. Both sign (+ or -) and absolute value of ρ contain important mechanistic information.

⁵ Hansch C, et al, *Chem Rev*, **1991**, *91*, 165.

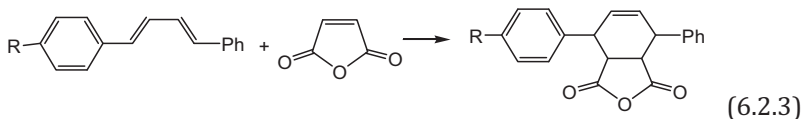
A *sign* of ρ indicates the electronic nature, i.e. nucleophilic or electrophilic, of the reactive center X. In other words it is an indicator of either nucleophilic or electrophilic attack of an incoming molecule at X. Consider the classical electrophilic aromatic substitutions, viz. nitration of arenes in acetic anhydride and chlorination by Cl_2 in glacial acetic acid.⁶ The ρ value in both cases is negative (-6.5 and -11.1 , respectively, against σ^+) reflecting the fact that electron-donating groups R speed up the substitution and that the incoming species are electrophilic in nature. Correspondingly, arenes themselves behave as nucleophiles in these reactions.



The *absolute value* of ρ indicates a degree of development of charge in the transition state. The ρ value is usually less than 1 for concerted reactions, which do not have charged intermediates. Multistep reactions with charged intermediates have notably higher absolute values of ρ , which however do not exceed 10-12 (cf. with the electrophilic reactions mentioned above). The Hammett equation is a sensitive indicator of whether a reaction is concerted or not. Consider the data for illustrative reactions 6.2.2 and 6.2.3.



⁶ Okamoto Y, Brown HC, *J Org Chem*, **1957**, *22*, 485.



Interaction of alkenes with tetracyanoethene is a formal [2,2] cycloaddition which is symmetry forbidden as a concerted process.⁷ Therefore, it should involve zwitter-ion intermediate **6.1**. As a result of a considerable charge development, a slope of the Hammett plot ρ equals -7.1 .⁸ Reaction 6.2.3 involving 1,4-diphenyl-1,3-butadiene derivatives and maleic anhydride, in contrast, is concerted, since the [4,2] cycloaddition is symmetry allowed.⁷ Correspondingly, the value of ρ drops to -0.62 .⁶

The Hammett equation does not work when the reactive site X and substituent R are *ortho* to each other. Steric effects do interfere with electronic effects. The Hammett plots may have breaks. A first reason to consider is a change of the rate-limiting step on going from electron-rich to electron-poorer molecules.

The Taft equation is an equivalent of the Hammett equation applied to aliphatic compounds. The corresponding substituent parameters are calculated from the dissociation constants of acetic acid derivatives XCH_2COOH ; K_a° is the dissociation constant for acetic acid:

$$\sigma = 0.262 \times \log(K_a/K_a^\circ)$$

6.2.2. Brønsted Equation

The Brønsted equation ties rate constants of reactions catalyzed by acids or bases with their $\text{p}K_a$ values:

$$\log k = \alpha \text{p}K_a + \beta$$

Here α is often referred to as the Brønsted coefficient, which is usually between 0 and 1. This reflects the fact that no more than one proton can be moved in the elementary step.

⁷ A small extra problem. Why?

⁸ Uosaki Y, et al, *Bull Chem Soc Japan*, **1981**, *54*, 3681.

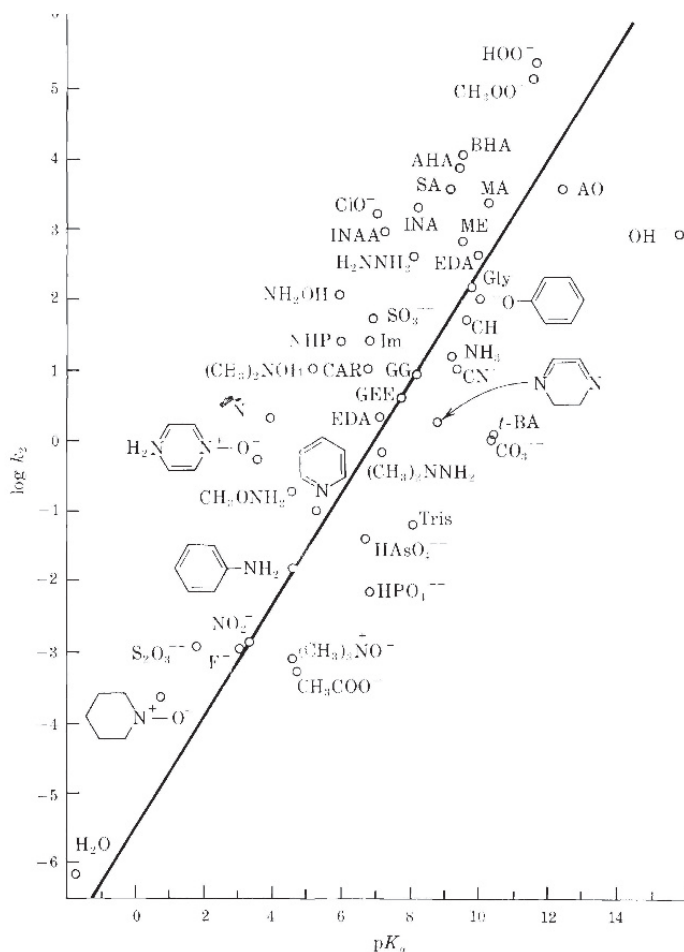
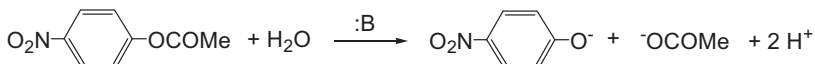


Figure 6.2.1. Second-order rate constants k_2 for the catalyzed hydrolysis of 4-nitrophenylacetate plotted against pK_a of the catalytic species at 25 °C. Abbreviations: BHA, *n*-butyrolhydroxamate; AHA, acetohydroxamate; INA, isonitrosoacetone; SA, salicylaldoxime; MA, mercaptoacetate; ME, mercaptoethanol; AO acetone oxime; GLY, glycine; INAA, isonitrosoacetylacetone; EDA, ethylenediamine (free base and monocation); NHP, *N*-hydroxyphthalimide; IM, imidazole; CH, chloral hydrate anion (at 30 °C); CAR, carnosine; GG, glycylglycine; GEE, glycine ethyl ester; acid; *t*-BA, *t*-butylamine. Reprinted with permission. Copyright 1960 American Chemical Society.

The best ever example of the Brønsted dependence is presented in Fig. 6.2.1,⁹ which shows the second-order rate constants k_2 for the hydrolysis of 4-nitrophenylacetate catalyzed by free (deprotonated) bases $:B$ as a function of their pK_a 's. As seen, there is a linear dependence between $\log k_2$ and pK_a .



The importance of the Brønsted equation will become more obvious later, when catalytic reactions involving acids and bases will be considered in Lecture 7.

6.2.3. Solvent and Medium Effects on Rates of Chemical Reactions. Empirical Approaches and Separation of the Ground and Transition State Effects

There are several tools for analysis of medium effects on reaction rates. Many are based on the transition state theory without neglecting the fact that the activities $a = \gamma c$, not concentrations c (γ is activity coefficient), should be used in eq 1.3.3:

$$K^\ddagger = \frac{a^\ddagger}{a_A a_B} = \frac{c^\ddagger}{c_A c_B} \times \frac{\gamma^\ddagger}{\gamma_A \gamma_B}$$

Therefore

$$c^\ddagger = K^\ddagger c_A c_B \frac{\gamma_A \gamma_B}{\gamma^\ddagger}$$

Substitution of c^\ddagger into eq 1.3.2 gives

$$v = \frac{\bar{k}T}{h} K^\ddagger c_A c_B \frac{\gamma_A \gamma_B}{\gamma^\ddagger}$$

⁹ Jencks WP, Carriuolo J, *JACS*, **1960**, *82*, 1778; Jencks WP, *Catalysis in Chemistry and Enzymology*, McGraw-Hill, 1969, p 91.

The rate constant is expressed as

$$k = \frac{\bar{k}T}{h} K^\ddagger \frac{\gamma_A \gamma_B}{\gamma^\ddagger} = k_0 \frac{\gamma_A \gamma_B}{\gamma^\ddagger} \quad (6.2.4)$$

Here k_0 is the rate constant when activity coefficients equal 1. Thus, effectors influence rates because they affect the activity coefficients γ . In particular, the effect of the ionic strength ($\mu = \frac{1}{2} \sum c_i Z_i^2$) on the activity coefficient of the ion i , the charge of which is Z_i , is given by the Debye-Hückel equation

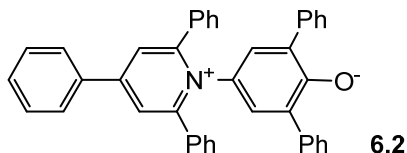
$$-\ln \gamma_i = \frac{Z_i^2 a \sqrt{\mu}}{1 + b \sqrt{\mu}}$$

Substitution of γ_i into eq 6.2.4 taking into account that a charge of the transition state is the sum of charges of A and B leads to eq 6.2.5.

$$\ln k = \ln k_0 + \frac{2Z_B Z_A a \sqrt{\mu}}{1 + b \sqrt{\mu}} \approx \ln k_0 + 2Z_B Z_A a \sqrt{\mu} \quad (6.2.5)$$

It shows that an increase in the ionic strength speeds up a reaction between similarly charged ions and slows down a reaction between oppositely charged ions.

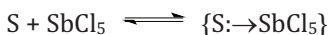
Electrostatic models have been used for describing the effects of the dielectric constant (ϵ) on reaction rates. Such concepts predict linear plots between $\ln k$ and $1/\epsilon$ or the Kirkwood function $(\epsilon-1)/(2\epsilon+1)$. However, satisfactory linearity is only observed for binary mixtures of variable composition. If different *pure* solvents are used, correlations are usually poor. Therefore, a series of empiric solvent parameters were suggested, which could be useful for analysis of reaction rates. These approaches are based on LFER. Let us consider some of these parameters.



Dimroth Parameter E_T .¹⁰ It characterizes the medium polarity or, better to say, its ability to stabilize either charged intermediates or transition states. Expressed in kcal mol⁻¹, E_T is related to the energy of the charge-transfer band in the electronic spectrum of 2,6-diphenyl-4-(2,4,6-triphenyl-1-pyridinium)phenolate, **6.2**.

$$E_T \{\text{kcal/mole}\} = 2.59 \times 10^{-3} \times \nu \{\text{cm}^{-1}\}$$

Gutmann Donor Numbers DN .¹¹ This parameter characterizes the ability of solvents to donate the unshared pair of electrons. It is defined as a negative enthalpy (kcal mol⁻¹) of the adduct formation between a solvent molecule S and SbCl₅:



Donor Numbers are used for the interpretation of solvent effects on reactions involving metal centers (electrophiles), since complexation of metal centers with solvents strongly affect the reactivity.

The parameter Z introduced by Kosover and π^* introduced later by Kamlet and Taft¹² should also be mentioned. Both parameters have much in common with E_T . Application of π^* is obviously preferred since it was determined for very many solvents. In contrast to other parameters, it is dimensionless. By definition, π^* equals zero for *n*-heptane (-0.08) and 1.00 for dimethylsulfoxide.

Rate constants are usually correlated with the solvent parameters using the following equations

$$\log k = a_0 + a_1 A_1 \quad \text{or} \quad \log k = a_0 + a_1 A_1 + a_2 A_2$$

Here A_1 and A_2 are the empirical parameters and a_1 and a_2 are the coefficients the meaning of which is similar to the Hammett coefficient ρ .

¹⁰ Dimroth K, et al, *Ann Chem*, **1963**, 661, 1.

¹¹ Gutmann V, *Coord Chem Rev*, **1976**, 18, 225.

¹² Kamlet MJ; et al, *JCS Perkin II*, **1979**, 337; Kamlet M, et al, *J Org Chem*, **1983**, 48, 2877.

Solvation of the Ground and Transition States. Strictly speaking, studies of solvent effects on *rates* of chemical reactions may be insufficient for characterizing the transition state. The reason is that this information refers to the *difference* in energy of transition and ground states. More important is the energy of the transition state in different solvents. The absolute transition state energy cannot be calculated in principle. But it is feasible to calculate the relative energy level of the transition state (relative to a standard solvent) as:¹³

$$\delta\mu^\ddagger = \delta\Delta G^\ddagger + \sum\Delta\mu_j^\circ$$

Here $\delta\mu^\ddagger$ is the relative energy of the transition state, $\delta\Delta G^\ddagger = (\Delta G^\ddagger - \Delta G^\ddagger_0)$ the difference between the free energies of activation in a given and a standard solvent, and $\Delta\mu_j^\circ$ is the Gibbs free energy of transfer of reagent *j* from standard into given solvent (summation involves all participating reagents). Figure 6.2.2 illustrates the approach described. The Gibbs free energies of transfer are essential for calculating $\delta\mu^\ddagger$. The easiest routine to obtain these is simply to measure the solubility *S* of all reagents involved in the standard and given solvents. The Gibbs function is then:

$$\Delta\mu_j^\circ = RT \ln(S_0/S)$$

Here *S*₀ is the solubility of reagent in a standard solvent. Calculated values of $\delta\mu^\ddagger$ are then correlated with the empiric solvent parameters.

¹³ Blandamer MJ, Burgess J, *Coord Chem Rev*, **1980**, 31, 93.

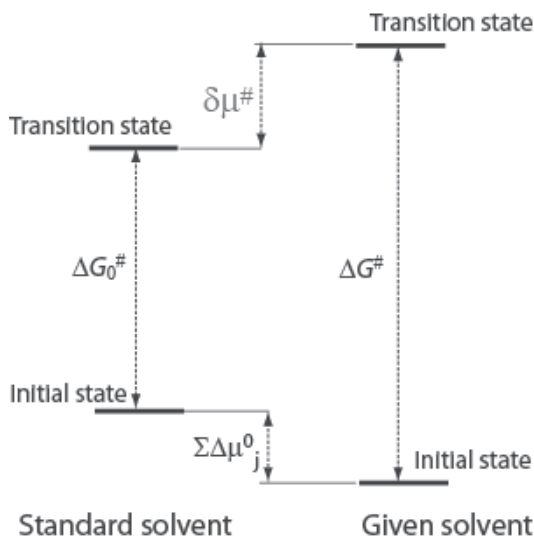


Figure 6.2.2. Illustration of the principle of separation of initial and transition states.

6.3. Activation Parameters and Mechanisms

6.3.1. Enthalpy and Entropy of Activation

How to determine the activation parameters, viz. the enthalpy and entropy of activation? Let us divide eq 1.3.7 by T and take the logarithm of the ratio. One obtains

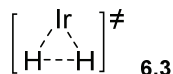
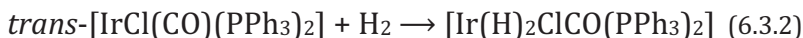
$$\ln \frac{k}{T} = \ln \frac{\bar{k}}{h} - \frac{\Delta H^\ddagger}{RT} + \frac{\Delta S^\ddagger}{R} \quad (6.3.1)$$

To calculate the enthalpy of activation ΔH^\ddagger , it is required to measure the rate constants at different temperatures at least in the range of 15-20 degrees and plot $\ln(k/T)$ versus T^{-1} . The slope gives $\Delta H^\ddagger/R$. The entropy of activation can be calculated from the intercept, which equals $(\ln \frac{\bar{k}}{h} + \frac{\Delta S^\ddagger}{R})$. The absence of linearity in the $\ln(k/T)$ versus T^{-1} plot may be indicative of a change of the rate-limiting step in temperature range used. It should be remembered that although it is sufficient to use k_{obs} for calculating ΔH^\ddagger , it is not true for ΔS^\ddagger and it is

necessary to operate with true individual (intrinsic) rate constants. Otherwise the values of ΔS^\ddagger are meaningless.

Values of the enthalpy and entropy of activation (ΔH^\ddagger and ΔS^\ddagger), which refer to the individual rate constants, report on the nature of rate-limiting step. In particular, if ΔH^\ddagger equals:

- 5 kcal mol⁻¹ or less (20 kJ mol⁻¹), it is wisely to consider possible diffusion control, especially for heterogeneous reactions;
- 20 kcal mol⁻¹ or more (80 kJ mol⁻¹), a cleavage of a bond in the transition state is likely (dissociative mechanisms of activation);
- intermediate values are observed when bond formation dominates in the transition state or bond cleavage is compensated by formation of a new bond. An example is an oxidative addition at iridium(I):



The reaction follows first-order kinetics in both reagents with ΔH^\ddagger 10.8 kcal mol⁻¹ in benzene.¹⁴ Three-centered transition state **6.3** was postulated.

As known, the entropy characterizes a degree of disorder of a thermodynamic system. This property is useful for analysis of the entropy of activation ΔS^\ddagger . In particular, if ΔS^\ddagger is:

- close to zero (± 5 cal mol⁻¹ K⁻¹ (eu, entropy units) or ± 20 J mol⁻¹ K⁻¹): this is a feature of unimolecular transformation;
- values around -20 eu or -80 J mol⁻¹ K⁻¹ are typical of bimolecular transition states, in which one molecule is “lost” during the formation of transition state thus providing entropy loss. For the second-order reaction 6.3.2, for example, the entropy of activation equals -23 eu;

¹⁴ Chock P B, Halpern J, *JACS*, **1966**, *88*, 3511.

- if the entropy of activation is even more negative, this is a highly ordered or highly structured transition state. In such, a rigid orientation of all species involved results in significant decrease in degrees of freedom and, hence, entropy.

The *isokinetic* dependence is a linear plot of ΔH^\ddagger against ΔS^\ddagger either for the same process with structurally similar reagents or for one and the same reagent/s under different conditions. The slope is referred to as the isokinetic temperature (T_{iso}).¹⁵ Isokinetic plots are often used as evidence for a common mechanism in the entire series.

6.3.2. Volume of Activation as a Mechanistic Indicator

By definition the Gibbs free energy $G \equiv U + pV - TS$. Also $\Delta G = -RT \ln K$ for a reversible reaction. Then the expression for a partial derivative is

$$\frac{\partial \ln K}{\partial p} = -\frac{\Delta V}{RT}$$

Here ΔV is the *volume molar change*, which is the difference between partial molar volumes of all products V_P and reagents V_R :

$$\Delta V = \sum V_P - \sum V_R$$

The ΔV is measurable for a chemical reaction between A and B in solution using an instrument shown in Fig. 6.3.1 (Carlsberg dilatometer).

¹⁵ Make sure that the rate constants are the same in the series of reagents or reactions when $T = T_{\text{iso}}$.

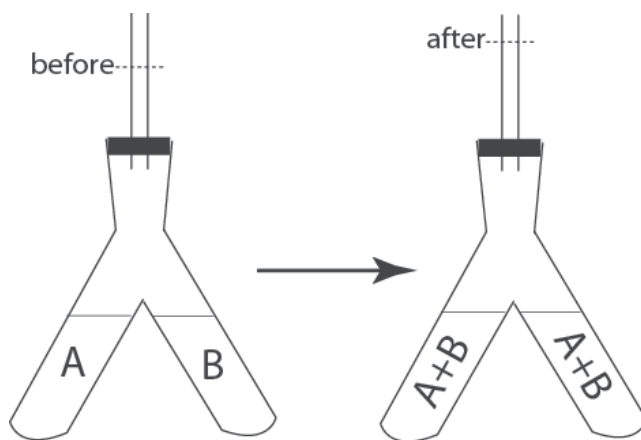


Figure 6.3.1. Carlsberg dilatometer. Compounds A and B are dissolved in solvent X immiscible with solvent Y. Solvent Y is above solutions of A and B in X. A and B react after mixing and the volume change is registered by a dilatometer.

Similar treatment of reaction rates in terms of the transition state theory gives a relation between rate constants and pressure¹⁶

$$\frac{\partial \ln k}{\partial p} = - \frac{\Delta V^\ddagger}{RT}$$

Here $\Delta V^\ddagger = V^\ddagger - \sum V_{R_i}$, and V^\ddagger {cm³ mol⁻¹} is a partial molar volume of the transition state. The activation volume is actually a sum of two terms, i.e. of ΔV^\ddagger_1 which arises from volume changes of reagents themselves and ΔV^\ddagger_2 , which is a result of changes in solvation of reacting species in the transition state.

¹⁶ Van Eldik R, et al, *Adv Inorg Chem*, **2000**, 49, 1.

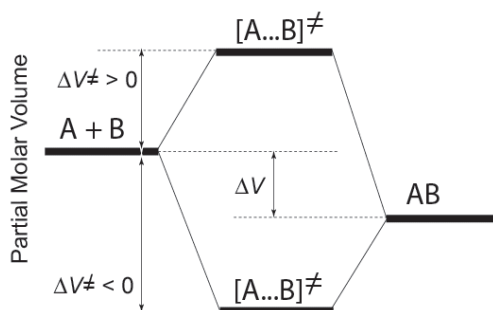


Figure 6.3.2. Volume profiles with positive and negative volumes of activation.

If under higher pressure (up to 1500 atm) a reaction runs faster, the activation volume is negative and an associative mechanism is operative. In contrast, if a reaction is slowed down by applying pressure, the volume of activation is positive and a dissociative mechanism is operative. Examples of the volume profiles of chemical reactions are shown in Fig. 6.3.2. Types of mechanisms, which are deduced from studies of the pressure effects, are in Fig. 6.3.3. Volumes of activation usually correlate with the corresponding entropies of activation.

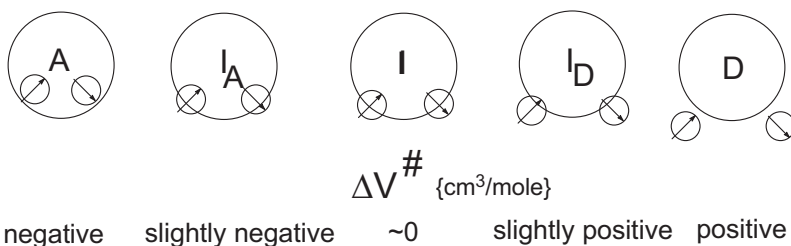
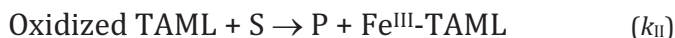


Figure 6.3.3. Mechanisms of chemical reactions and their relation to volumes of activation: A – associative, I_A – associative interchange, I – interchange, I_D – dissociative interchange, D – dissociative mechanism. Small circles indicate incoming (↗) and leaving (↘) group/ligand. In limiting A mechanism the rate-limiting binding of incoming group occurs first followed by fast departure of leaving group. In D case incoming group adds after the rate-limiting dissociation of leaving group. Mechanism I involves concerted bond-making and bond-breaking (cf. S_N2 reactions). I_d and I_a are intermediate cases.

Problems

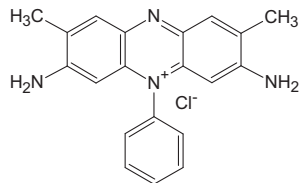
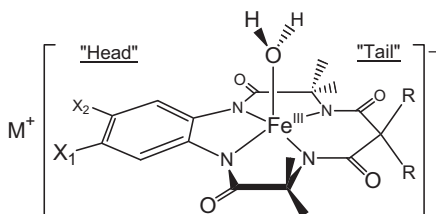
6-1. The oxidative catalysis by the Fe^{III}-TAML activators of H₂O₂ occurs in accordance with the following scheme (Problem 3-2):



In addition to this, Oxidized TAML is involved in suicidal inactivation, which results in complete loss of the catalytic activity:



The rate constants k_{11} for Safranin O (commercial dye) as a substrate and k_i were found at different temperatures at pH 11. Using the data in the Table calculate the corresponding activation parameters ΔH^\ddagger and ΔS^\ddagger .



Safranin O

1	X ₁	X ₂	R
a	Cl	Cl	Et
b	H	H	Me
c	H	H	Cyclopropyl
d	Cl	Cl	F

Table: Rate constants (k_i and k_{II}) calculated for different **1**.

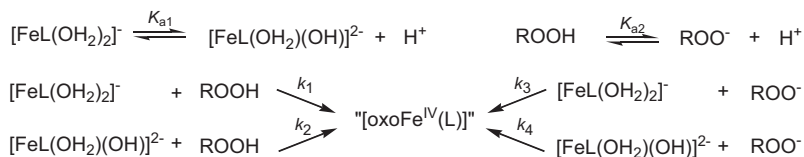
Complex	T / °C	$10^3 \times k_i / \text{s}^{-1}$	$10^{-4} \times k_{II} / \text{M}^{-1} \text{s}^{-1}$
1a	13	0.44±0.05	0.24±0.3
	25	1.5±0.1	0.7±0.1
	42	5.7±0.6	1.2±0.1
	60	33±3	3.6±0.4
1b	13	1.9±0.2	0.9±0.1
	25	3.4±0.3	1.1±0.1
	42	5.2±0.5	1.5±0.2
	60	12±1	3.1±0.3
1c	13	2.5±0.3	0.99±1.1
	25	6.2±0.4	1.9±0.2
	42	11±1	3.6±0.7
	60	18±2	5.6±0.6
1d	13	4.8±0.5	6.3±0.6
	25	13±1	10±2
	42	20±2	14±1
	60	45±2	23±3

6-2. Estimate the pressure change required for increasing the rate constant two-fold when the activation volume $\Delta V^\ddagger = -10 \text{ cm}^3 \text{ mol}^{-1}$ at 25 °C. Use $R = 0.082 \text{ L atm K}^{-1} \text{ mol}^{-1}$.

6-3. Provided the isokinetic relationship between ΔH^\ddagger and ΔS^\ddagger does hold, prove that the speed of all reactions in the series is constant at the temperature known as the isokinetic temperature (T_{iso}).

6-4. Fe^{III} -TAML activators of peroxides shown in Fig. 2.4.3 undergo rapid hydrolysis of chloride in solution and exist in water as diaqua octahedral species $[\text{Fe}^{\text{III}}\text{L}(\text{OH}_2)_2]^-$ ($\text{L}^4 = \text{TAML}^4^-$). One axial aqua ligand undergoes deprotonation and this is essential for understanding the mechanism of reaction of Fe^{III} -TAMLs with peroxides in water to afford an oxo derivative of Fe^{IV} (Scheme).

- a) Based on the Scheme, derive the rate expression for the second-order rate constant k_1 (the reaction is first-order both in Fe^{III} -TAML and peroxide) that would show its dependence on pH. Indicate kinetically indistinguishable pathways.

**Scheme**

- b) For Fe^{III}-TAMLs shown below the calculated rate constants are summarized in the Table. Make the Hammett plots for the rate constants k_2 and k_3 . Calculate the values of ρ . Assume that each substituent delivers electronic effects at Fe^{III} via two channels, viz meta and para (see structure **1**).

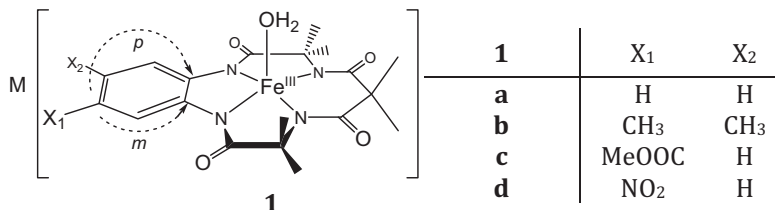


Table. Rate constants (in M⁻¹ s⁻¹) and pK_a values for the reactions between **1** and ^tBuOOH as indicated in Scheme in 0.01 M phosphate buffer at 25 °C.

Complex	k_1	$10^{-3} \times k_2$	$10^{-3} \times k_3$	k_4	pK _{a1}	pK _{a2}
1a	10±0.2	1.3±0.2	83±3	15±1	10.8±0.1	12.6±0.2
1b	10.0±0.5	1.1±0.03	28±4	38±2	11.0±0.3	12.4±0.1
1c	30±1.5	0.95±0.03	380±4	35±3	9.9±0.1	12.5±0.2
1d	10±0.3	1.25±0.05	620±0.7	15±1	9.9±0.2	12.6±0.4

LECTURE 7.

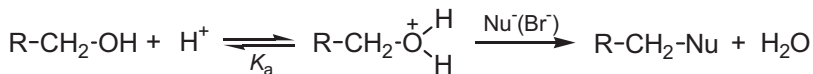
CATALYSIS

7.1. Specific Acid Catalysis (Catalysis by Proton)

Specific acid catalysis is the catalysis by proton H^+ . Proton is a very small particle of a high charge density. It may strongly affect electronic properties of any molecule and hence influence its reactivity. Consider some mechanisms of increasing reactivity by proton.

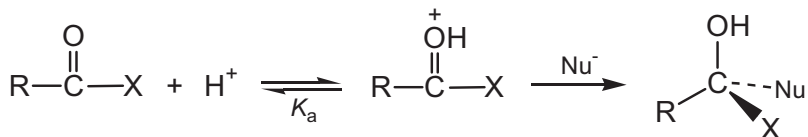
- *Creating a good leaving group*

Alcohols are insufficiently reactive in S_N2 reactions because hydroxyl is a poor leaving group. Alcohols are weak bases (pK_a of methanol is ca. -2) and hence the OH group is protonated in strongly acidic media. As a result, a good leaving group, water, is generated and a nucleophile is capable of replacing it:

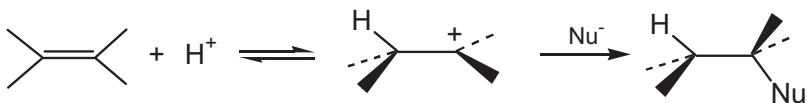


- *Increasing electrophilicity of the carbonyl carbon*

The carbonyl oxygen in esters, aldehydes, and ketones is even less basic than the alcohol oxygen (pK_a from -5 to -8). But even these centers accept proton. This facilitates nucleophilic attack at the sp^2 carbonyl carbon:

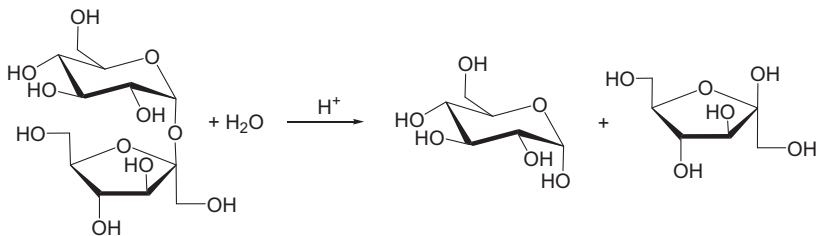


- *Generating electrophilic centers in unsaturated π -systems*



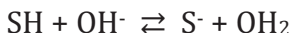
Catalysis by proton is also observed, for example, in:¹

- hydrolysis of esters (*t*-butyl acetate);
- esterification of alcohols with sulfuric acid;
- lactonization of γ -hydroxybutyric acid; hydrolysis of acetals, ketals, and glucosides;
- hydrolysis of epoxides;
- hydrolysis of acetic anhydride;
- dehydration of tertiary alcohols;
- pinacol rearrangement ($R_2C(OH)CR_2OH \rightarrow R_3C-C(=O)R$);
- Beckman rearrangement ($>C=N-OH \rightarrow -C(=O)-NH-$);
- hydration of alkenes;
- hydrolysis (inversion) of sucrose which is characterized by the inverse KIE $k(D^+)/k(H^+) = 1.89$ at 18.7 °C (a feature of specific acid catalysis):



7.2. Specific Base Catalysis (Catalysis by Hydroxide)

This is catalysis by the hydroxide ion OH^- . It is less frequent than catalysis by proton and usually occurs due to creation of carboanionic reactive centers:



¹ Bender ML, et al, *The Bioorganic Chemistry of Enzymatic Catalysis*, 1984, J Wiley & Sons, NY.

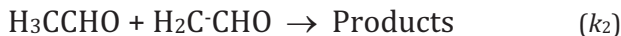
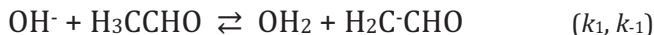
The specific base mechanism is operative in a series of organic reactions such as Claisen,² Michael,³ Perkin,⁴ and aldol additions. The alkaline hydrolysis of esters is also catalyzed by hydroxide. Consider the aldol addition as an example.



It is known that this reaction (i) follows second- and first-order kinetics in aldehyde and hydroxide, respectively:

$$v = k[\text{H}_3\text{CCHO}]^2[\text{OH}^-] \quad (7.2.1)$$

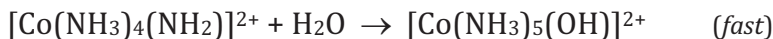
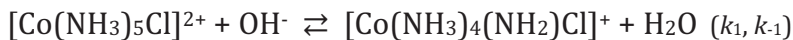
(ii) If the reaction is run in D_2O , deuterium is incorporated into the aldehyde. The mechanism that corresponds to these observations is the following:



An example of catalysis by hydroxide in inorganic chemistry is the so-called *conjugate-base* mechanism of hydrolysis of ammine transition metal complexes.



The substitution reactions start with reversible deprotonation of NH_3 ligand by hydroxide. The reactive conjugate base intermediate is thus formed followed by the rate-limiting dissociation of chloride:



² $\text{PhCHO} + \text{MeCHO} \rightarrow [\text{PhCH}(\text{OH})\text{CH}_2\text{CHO}] \rightarrow \text{PhCH}=\text{CHCHO} \quad (\text{NaOH})$

³ $\text{PhCH}=\text{CHCOPh} + \text{H}_2\text{C}(\text{COOEt})_2 \rightarrow \text{PhCH}\{\text{CH}(\text{COOEt})_2\}\text{CH}_2\text{COPh} \quad (\text{piperidine})$

⁴ $\text{PhCHO} + (\text{MeCO})_2\text{O} \rightarrow \text{PhCH}=\text{CHCOOH} \quad (\text{KOAc})$

7.3. General Acid-Base and Nucleophilic Catalysis

Let us imagine the case when at a constant pH a reaction rate grows with a concentration of buffer component/s (Fig. 7.3.1). Reasons for that are either nucleophilic or general acid-base catalysis. General acid catalysis implies a participation of any *proton donor* (AH) in the catalytic cycle. General base catalysis involves a *donor of unshared pair of electrons* (A^- , for example). Both AH and A^- are components of a buffer solution.



Concentrations of either AH (general acid) or A^- (general base) are proportional to the total buffer concentration. The rate constant k' (Fig. 7.3.1) depends on pH, since the ratio $[AH]/[A^-]$ is a function of pH. If the general acid catalysis occurs, the catalytic activity decreases with increasing pH, since the concentration of proton donor AH drops. If the reverse case is realized, i.e. an increase in pH accelerates the reaction, the actual catalyst is base A^- . The latter can be either nucleophilic or general base catalyst. These two types of catalytic mechanisms look, at a first glance, very similar, but nevertheless have a crucial difference. Discrimination between the general base and nucleophilic mechanisms is not easy. Consider their features by the example of ester hydrolysis.

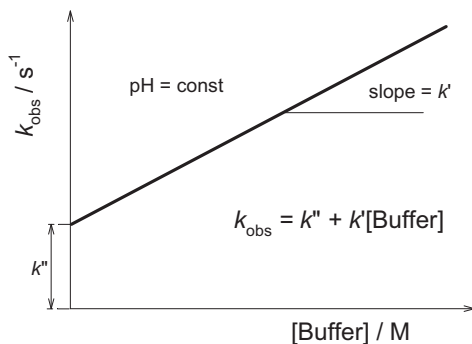
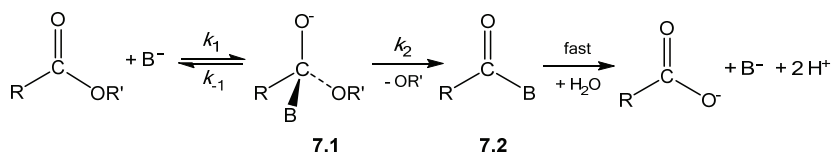


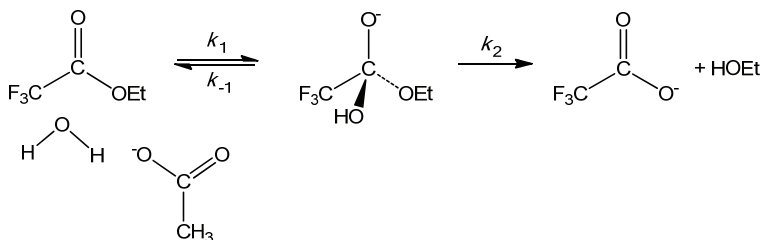
Figure 7.3.1. An example showing how the rate constant may depend on the buffer concentration.

Nucleophilic catalysis involves a direct attack of a nucleophile (base B^-) at the ester carbonyl carbon to form the so-called tetrahedral intermediate **7.1**, the key species in catalytic hydrolysis of esters and amides (Scheme 7.3.1). Then the leaving group $R'O^-$ dissociates from intermediate **7.1** and the acylated base **7.2** is attacked by the nucleophilic water molecule to afford carboxylate and a free catalyst B^- .



Scheme 7.3.1. Ester hydrolysis: nucleophilic mechanism.

The general base catalysis is realized when the nucleophilic catalysis is principally impossible. For example, the hydrolysis of ethyl trifluoroacetate catalyzed by acetate cannot follow the nucleophilic mechanism because of a huge difference in basicity of ethoxide ($pK_a \sim 16$) and acetate ($pK_a \sim 5$), and hence acetate is unable to replace ethoxide. On the other hand, hydroxide ($pK_a \sim 16$) is capable of substituting ethoxide and therefore the role of the general base (acetate) is to polarize the incoming water molecule and make it similar to hydroxide (Scheme 7.3.2). A polarization of water by a general base does not, of course, afford free hydroxide, but does increase its nucleophilicity substantially.⁵



Scheme 7.3.2. Ester hydrolysis: general base mechanism.

⁵ Notions *nucleophilicity* and *basicity* are similar, but not identical. The former is more general. The latter characterizes nucleophilicity with respect to proton only!

Nucleophilic and general base catalysis is difficult to distinguish kinetically. In fact, the expression for k_{obs} in the former case is given by:

$$k_{\text{obs}} = \frac{k_1 k_2}{k_{-1} + k_2} \times \frac{K_a}{K_a + [\text{H}^+]} \times B_t \quad (7.3.1)$$

Here K_a is a dissociation constant of the conjugate acid of base B and B_t is the total concentration of the base. The corresponding rate expression for a general base mechanism involves the rate constant k_1 , which formally corresponds to the trimolecular step where the third species is a water molecule:

$$k_{\text{obs}} = \frac{k_1 [\text{H}_2\text{O}] k_2}{k_{-1} + k_2} \times \frac{K_a}{K_a + [\text{H}^+]} \times B_t \quad (7.3.2)$$

Equations 7.3.1 and 7.3.2 are similar. Nevertheless, there are ways to prove or rule out the involvement of water (this is the main formal difference between nucleophilic and general base mechanisms of ester hydrolysis):

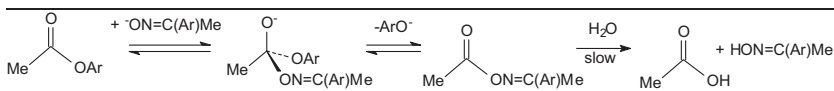
- In certain instances, it is possible to detect an acylated nucleophile by spectral means and thus to prove the nucleophilic mechanism.
- Solvent kinetic isotope effect ($k(\text{H}_2\text{O})/k(\text{D}_2\text{O}) > 2$) supports the general base mechanism.
- Large and negative entropy of activation for k_1 ($-140 \text{ kJ mol}^{-1} \text{ K}^{-1}$ and lower) agrees with an ordered transition state typical of the general base mechanism.
- If $\text{p}K_a$ of a conjugate base of a leaving group is much higher than that of an incoming nucleophile, the nucleophilic mechanism is highly improbable and the general base mechanism seems to operate.
- The Brønsted plot as a perfect straight line supports a general base mechanism. Nucleophilic pathways are more sensitive to steric effects and the data is more scattered because of interference of the steric effects.

It should be emphasized that the true (not effective or observed) rate constants should be used in the Brønsted plots. In terms of eq 7.3.1 and 7.3.2 these are

$$\frac{k_{\text{obs}}}{B_t} = \frac{k_1 k_2}{k_{-1} + k_2} \quad \text{or} \quad \frac{k_{\text{obs}}}{B_t} = \frac{k_1 [\text{H}_2\text{O}] k_2}{k_{-1} + k_2} \quad (7.3.3)$$

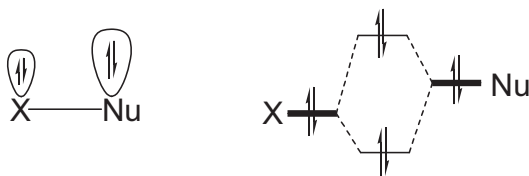
These are the cases when bases are fully deprotonated. Equations 7.3.3 emphasize the meaning of the Brønsted plots by showing that the nucleophilicity of a base toward the carbonyl carbon driven by the rate constant k_1 is correlated with the basicity of this base (K_a is a measure of basicity).

For simplicity, it was assumed that the hydrolysis of acylated nucleophile **7.2** in Scheme 7.3.1 occurs fast. This is not a rule. Deacylation may be slow as in the aryl oxime-catalyzed hydrolysis of *p*-nitrophenyl acetate. The $\text{p}K_a$ of hydroxy groups of aryl oximes are in the range 11-12 (cf. with $\text{p}K_a$ of *p*-nitrophenol). The nucleophilic mechanism with slower deacylation of acetyl oximes is shown below.



This step can however be speeded up so much that it is not limiting any more (note a role of metals in hydrolytic reactions; electrophilic catalysis).

α -Effect as a reason for enhanced reactivity. Positive deviations (higher rates) on the Brønsted plots may result from the so-called α -effect, i.e. increased activity of a nucleophilic center with an adjacent atom with a pair of unshared electrons. As a result, the corresponding orbitals may interact giving two new populated orbitals, Scheme 7.3.3. Consequently, the energy of HOMO increases; the rate should increase correspondingly.

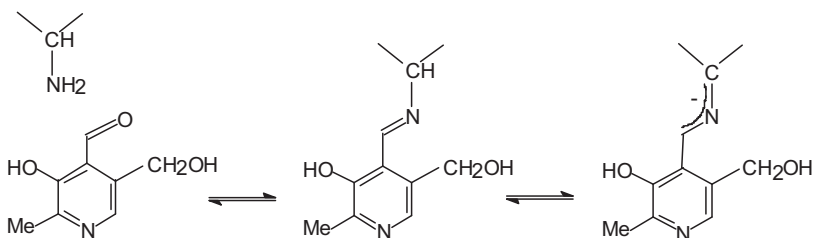


Scheme 7.3.3. Illustration of the origin of α -effect.

General acid catalysis, i.e. the catalysis by any proton donor, occurs in the following processes.

- Proton transfer to carbon (cleavage of C–Hg bond; aromatic hydrogen exchange; hydration of 4-methoxy- α -methylstyrene).
- Proton transfer to or from carbon (acetone iodination, keto-enol transformation).
- Addition to carbonyl and carboxylic groups (Schiff base formation, esterification, hydrolysis of amides, etc).

In conclusion, we have considered examples of nucleophilic (covalent) catalysis where it is difficult to distinguish it from the general base mechanism. There are though examples where the nucleophilic catalysis is more obvious. Such is the catalysis by pyridoxal (vitamin B₆), which is crucial in racemization and transformation of amino acids. It involves the formation of aldimines as key intermediates (Scheme 7.3.4).



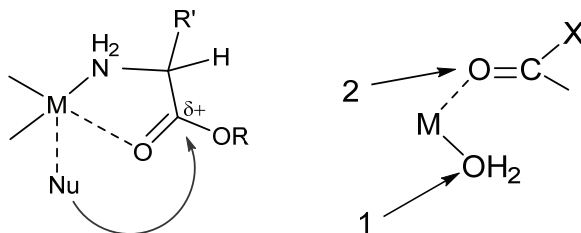
Scheme 7.3.4. Nucleophilic catalysis by vitamin B₆ of racemization of amino acids.

7.4. Electrophilic Catalysis

Catalysts are electrophilic molecules, i.e. such that have an empty LUMO orbital of the corresponding energy. Such are practically all metal cations, since they are usually electron deficient. From this point of view catalysis by metal ions, their derivatives, and Lewis acids, for example, has similarities with the catalysis by proton. First instances of the electrophilic catalysis are encountered in the course of organic chemistry. These are the electrophilic Friedel-Crafts alkylation of arenes (why this is less true for acylation?), electrophilic bromination of benzene which involves pathways with high (>1) reaction orders in dihalogen. This is also the electrophilic Hg^{II}-catalyzed aqutation of ethyne to acetaldehyde. The metal complex catalysis that has evolved several decades ago is also electrophilic

catalysis. Many unique reactions occur in the presence of transition metal complexes but these cannot be considered here. We will analyze the transition metal-catalyzed hydrolysis of esters and amides. Its importance is dictated by the fact that metal ions are constituents of the active sites of a number of hydrolytic enzymes (carboxypeptidase, urease, etc.) There are three accepted mechanism of catalysis by metals in biological and related systems. A metal center can be responsible for:

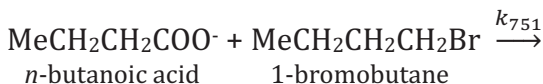
- Increasing the acidity of the coordinated water (type "1" in Scheme 7.4.1). As a result, a strong nucleophile is generated under neutral conditions.
- Metal acts as a Lewis acid and thus increases an effective positive charge at the carbonyl carbon (type "2").
- Combination of mechanisms "1" and "2".



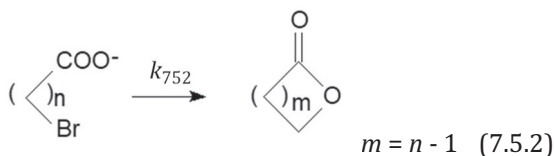
Scheme 7.4.1. Catalysis by metal ions.

7.5. Proximal Catalysis

Consider related nucleophilic substitution reactions 7.5.1 and 7.5.2. The intermolecular process 7.5.1 affords the ester.



The intramolecular processes 7.5.2 afford lactones.



We will be interested in the ratio of the rate constants for reactions 7.5.1 and 7.5.2. Note that these rate constants are measured in $\text{M}^{-1} \text{s}^{-1}$ and s^{-1} as for the second- and first-order reactions, respectively. Nevertheless, the ratio k_{752}/k_{751} , referred to as the *effective molarity* (EM), is of interest.⁶ EM is measured in M and has a definite meaning. It is such concentration of one of the two “intermolecular” reagent (B, for example), at which the rates of the corresponding intra- and intermolecular processes at the same [A] are identical! In fact, similar rates of reactions 7.5.1 and 7.5.2 imply that

$$v = k_{751}[A][B] = k_{752}[A]$$

Therefore

$$[B] = k_{752}/k_{751}.$$

Let us look how EMs, in this case the ratio of the rate constants k_{752}/k_{751} , depend on the number of methylene groups n in $\text{Br}(\text{CH}_2)_n\text{COO}^-$ (Fig. 7.5.1). The highest EM or, in other words, the maximal rate increase on going from inter- to intramolecular process is realized when $n = 3$, i.e. when the most thermodynamically favorable five-membered lactone is formed. Further increase in n leads to a decrease in EM. The dependence disappears when $n > 10$ because two reactive terminals of the molecule “forget” and do not “recognize” each other. The minimum that corresponds to the nine-membered lactone is most likely due to the formation of unfavorable medium cycle.

The concept of effective molarities was used as a tool to account for high reactivity of enzymes. Anticipated EM or a customary rate increase on going from an inter- to intramolecular process in H_2O is considered to be 55 M. The estimate is based on the assumption that the volume of reactive groups involved is close to the volume of water.

⁶ Galli C, et al, *JACS*, **1977**, 99, 2591.

But the concentration of water in pure water is 55 M. This reactivity gain is achieved by locating one reactive center in a close proximity to another. The backbone, to which reactive centers are attached, plays an enormous role. It may both rule out any intramolecular interaction as in the case of 4-bromomethylbenzoate and bring about accelerations as high as 10^8 M!

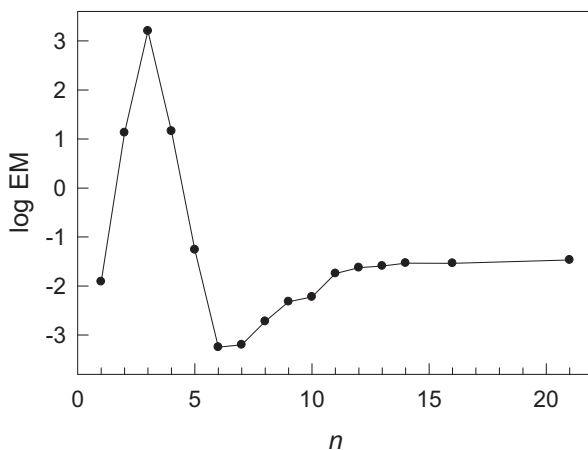


Figure 7.5.1. Effect of the number of CH_2 groups on the relative rates of reactions 7.5.1 and 7.5.2.

7.6. Micellar Catalysis

A micelle is an aggregate of surfactant molecules dispersed in liquid. In a typical spherical micelle in water the hydrophilic "head" regions are in contact with water molecules, sequestering the hydrophobic tails in the micelle center (Fig. 7.6.1). Micelles are formed when the concentration of surfactant is above the critical micelle concentration (cmc) and the temperature of the system exceeds the critical micelle temperature (Krafft temperature).

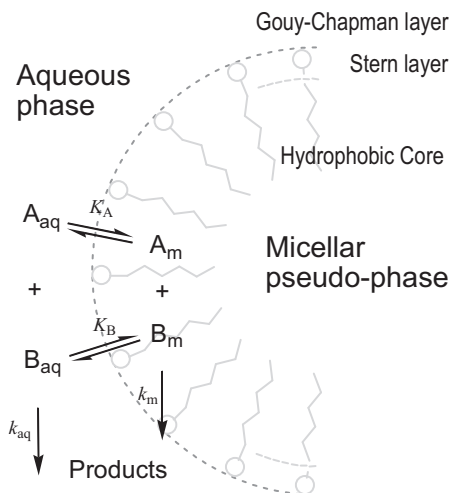


Figure 7.6.1. Reacting species A and B in the presence of micelles. Subscripts “aq” and “m” indicate location of reagents in either the aqueous phase or the micellar pseudo-phase. A fragment of a spherical micelle is shown in gray.

Chemical reactivity is affected by micelles. Micelles speed up and retard chemical reactions. There are several concepts for quantifying micellar effects. We consider the *pseudo-phase model*.⁷ Micelles are viewed as a pseudo-phase. Any reagent is distributed between micellar and aqueous phases:

$$[A_m]/[A_{aq}] = P_A$$

P_A is the partition coefficient of A between the micellar pseudo-phase and the aqueous phase. The total concentration of A in the system

$$A_t = [A_m]CV + [A_{aq}](1 - CV) \quad \text{or} \quad A_t/[A_{aq}] = 1 + (P_A - 1)CV$$

Here $C = [\text{surfactant}] - \text{cmc}$; $V \cong 0.36 \text{ M}^{-1}$ is the molar volume of micelles. Thus, CV and $(1 - CV)$ are the volume fractions of micellar and aqueous phases, respectively. As it will be shown below, it is convenient to use the relation $K_A = (P_A - 1)V$. K_A is measured in M^{-1} and has a meaning of the binding constant of A to micelle (Fig. 7.6.1).

⁷ Berezin IV, et al, *Usp Khim*, **1973**, 42, 1729.

The pseudo-phase model assumes that a unimolecular reaction of A or a bimolecular reaction between A and B may occur simultaneously in the aqueous phase v_{aq} and micellar pseudo-phase v_{m} , the rate constants being k_{aq} and k_{m} , respectively.

$$v = v_{\text{m}}CV + v_{\text{aq}}(1 - CV) \quad (7.6.1)$$

Equation 7.6.1 holds for both first- and second-order reactions. Taking into account all equations mentioned above and after combination, one obtains the general expression for a second-order rate constant

$$k = \frac{k_{\text{m}}P_{\text{A}}P_{\text{B}}CV + k_{\text{aq}}(1 - CV)}{(1 + K_{\text{A}}C)(1 + K_{\text{B}}C)}$$

which appears as eq 7.6.2 for dilute surfactant solutions ($1 \gg CV$)

$$k = \frac{k_{\text{m}}P_{\text{A}}P_{\text{B}}CV + k_{\text{aq}}}{(1 + K_{\text{A}}C)(1 + K_{\text{B}}C)} \quad (7.6.2)$$

Equation 7.6.2 is particularly important because it accounts for acceleration and retardation of chemical reactions in the presence of micelles. A key factor here is how strong reagents A and B interact with (bind to) micelles.

Case 1. Reagents A and B do not bind to micelles (K_{A} and K_{B} are very low; $1 \gg KC$). Equation 7.6.2 becomes $k = k_{\text{m}}P_{\text{A}}P_{\text{B}}CV + k_{\text{aq}}$. Since k_{m} is rarely higher than k_{aq} , the reaction rate is not affected by micelles ($k_{\text{m}}P_{\text{A}}P_{\text{B}}CV < k_{\text{aq}}$).

Case 2. Reagent A is strongly bound to micelles and B does not bind to micelles ($1 \gg K_{\text{B}}C$). Equation 7.6.2 becomes

$$k = \frac{k_{\text{m}}P_{\text{A}}P_{\text{B}}CV + k_{\text{aq}}}{1 + K_{\text{A}}C}$$

As it was mentioned above, k_{m} is rarely higher than k_{aq} . The rate of reaction will be hyperbolically inhibited by micelles.

Case 3. Reagents A and B bind strongly to micelles. Acceleration by micelles is possible when $k_{\text{m}} > 0$ because both reagents are concentrated in the micellar pseudo-phase. Equation 7.6.2 suggests

that the rate constant k should increase first with increasing C , reach maximum at $C \sim (K_A K_B)^{-1/2}$, and then decline.

Such example is shown in Fig. 7.6.2 for the interaction between Fe^{III} -TAML activator (see Fig. 2.4.3) with *tert*-butylhydroperoxide. The acceleration by the positively charged CTAB surfactant occurs due to concentrating the two reagents in the micellar pseudo-phase where they presumably localized in the Stern layer (Fig. 7.6.1). Interestingly, only the positively charged surfactant causes acceleration; neutral and negatively charged surfactants retard the reaction.⁸

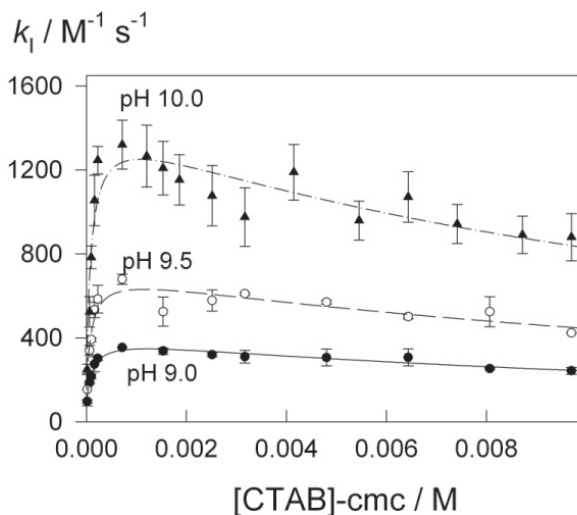


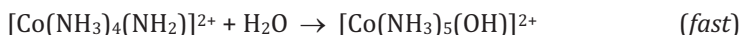
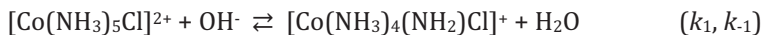
Figure 7.6.2. Second-order rate constant k_1 for the reaction of Fe^{III} -TAML activator (Fig. 2.4.3) with *tert*-butylhydroperoxide against the concentration of CTAB (cetyltrimethylammoniumbromide) at 25 °C and pH 9.0, 9.5, and 10.0.

⁸ Banerjee D, et al, *Chem - Eur J*, **2009**, 15, 10199.

Problems

7-1. By deriving the rate expression show that eq 7.2.1 corresponds to this mechanism under certain conditions. Define these conditions.

7-2. Show that if the last step is fast, the rate expression for



is given by $k_{\text{obs}} = k_1 k_2 [\text{OH}^-] / (k_1 [\text{OH}^-] + k_2 + k_{-1})$. Show that the reaction rate should depend on the concentration of added chloride, if the second step is reversible (k_2, k_{-2}) and the last step is not fast but characterized by the rate constant k_3 .

7-3. Applying the steady-state approximation to the tetrahedral intermediates, prove eqs 7.3.1 and 7.3.2. Assume that their steady-state concentrations are negligible.

7-4. The Fe^{III} -TAMLs are subject to the catalyzed demetalation by the phosphate buffer components at pH 4–9 (see Section 3.5). Typical data are presented in the Figure. Based on the results shown conclude on the nature of catalysis realized in this case. Note that $k_{1,\text{eff}}$ are second order rate constants obtained as slopes of linear plots in (A).

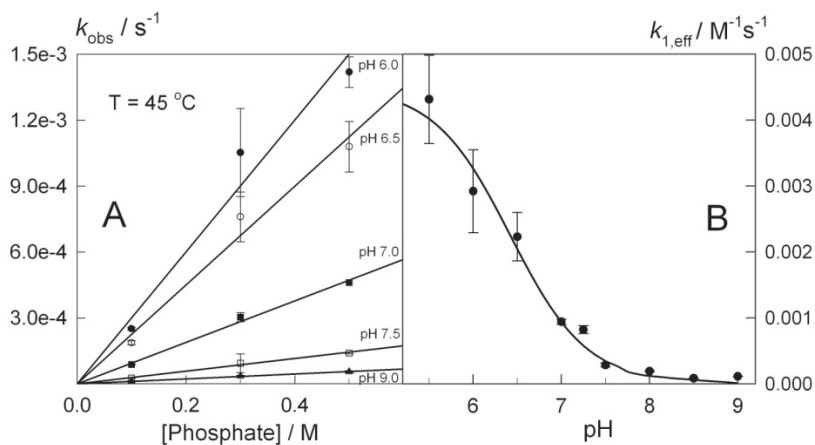


Figure. (A) Pseudo-first-order rate constants for demetalation of Fe^{III} -TAML versus phosphate concentration at different pHs and $45\text{ }^{\circ}\text{C}$. (B) Corresponding second-order rate constants $k_{1,\text{eff}}$ for demetalation of Fe^{III} -TAML as a function of pH.⁹ Reprinted with permission. Copyright 2008 American Chemical Society.

7-5. Conversion of A into B is subject of the specific acid catalysis. How will the rate of this process depend on the concentration of hydroxide anions? Prove your statement.

⁹ Polshin V, et al, *J Am Chem Soc*, **2008**, *130*, 4497.

LECTURE 8.

ELECTRON TRANSFER

8.1. Introduction

8.1.1. Reduction Potentials and Nernst Equation

The fundamental property of all chemical units is accepting (reduction) and releasing electrons (oxidation). Reduction potentials E° (Table 8.1.1) characterize quantitatively their abilities to be reduced or oxidized. The reduction potential is a feature of a hypothetical half-reaction between a particular oxidized species referred to as Ox and the electron/s to form a reduced species Red (eq 8.1.1). Formally, the second reagent is an electron, a reference pseudo-reagent that allows to compare a relative ability of different species to accept electrons.



Consider eq 8.1.1 as an equilibrium. The concentration ratio $c_{\text{red}}/c_{\text{ox}}$ should formally depend on the concentration of electrons in solution. This is impossible to hold. A substitute is a working electrode — a conducting material that may have excess or deficit of electrons depending on the electrode potential applied. If the potential is negative, the electrode has excess of electrons, if positive — there is a deficit of electrons. Zero potential corresponds to the pair H^+ and H_2 at $c_{\text{red}}/c_{\text{ox}} = 1$. Generally, the case $c_{\text{red}}/c_{\text{ox}} = 1$ is realized at a certain electrode potential, which is a standard reduction potential E° for a given half-reaction 8.1.1.

There is a similarity between the ability of species to undergo protonation/deprotonation and reduction/oxidation. The former is driven by $\text{p}K_{\text{a}}$ and the latter is driven by E° . The difference is that $\text{p}K_{\text{a}}$ and E° deal with protons and electrons, respectively. In fact, if the

solution pH is below pK_a , a protonated form dominates, but if the electrode potential is below E° (high supply of electrons), a reduced species Red is in excess. If the potential is higher than E° (low supply of electrons), an oxidized species Ox dominates.

Table 8.1.1. Standard reduction potentials E° for selected half-reactions in water at 25 °C versus normal hydrogen electrode (NHE).¹

Ox	Red	n	E° / V
Li ⁺	Li	1	-3.04
Na ⁺	Na	1	-2.71
Mg ²⁺	Mg	2	-2.38
Zn ²⁺	Zn	2	-0.76
Fe ²⁺	Fe	2	-0.41
Ni ²⁺	Ni	2	-0.23
Sn ²⁺	Sn	2	-0.14
Pb ²⁺	Pb	2	-0.13
Fe ³⁺	Fe	3	-0.04
2H ⁺	H ₂	2	0.00
Sn ⁴⁺	Sn ²⁺	2	0.15
Cu ²⁺	Cu ⁺	1	0.16
Cu ²⁺	Cu	2	0.34
I ₂ (s)	2 I ⁻	2	0.54
Fe ³⁺	Fe ²⁺	1	0.77
Ag ⁺	Ag	1	0.80
Hg ²⁺	Hg	2	0.85
ClO ⁻ + H ₂ O	Cl ⁻ + 2 OH ⁻	2	0.90
NO ₃ ⁻ + 4 H ⁺	NO + 2 H ₂ O	3	0.96
Br ₂	2 Br ⁻	2	1.07
O ₂ + 4 H ⁺	4 H ₂ O	4	1.23
Cr ₂ O ₇ ²⁻ + 14 H ⁺	2 Cr ³⁺ + 7 H ₂ O	6	1.33
Cl ₂	2 Cl ⁻	2	1.36
MnO ₄ ⁻ + 8 H ⁺	Mn ²⁺ + 4 H ₂ O	5	1.49
F ₂	2 F ⁻	2	2.87

The quantitative relation between concentrations of Red and Ox, the electrode potential E , and standard reduction potential E° is given by

¹ *CRC Handbook of Chemistry and Physics, 2014-2015*, 95th Ed.

the Nernst equation 8.1.2. It shows in particular that if $n = 1$ (1 electron is moved), the ratio $c_{\text{red}}/c_{\text{ox}} = 10$ holds when the electrode potential is lower by 0.059 V than the standard potential.²

$$E(\text{Volt}) = E^0 - \frac{RT}{nF} \ln \frac{c_{\text{red}}}{c_{\text{ox}}} = E^0 - \frac{0.059}{n} \log \frac{c_{\text{red}}}{c_{\text{ox}}} \quad (8.1.2)$$

The reduction potential is related to the ability of species to behave as either reducing or oxidizing agent. If E^0 is significantly negative like those of alkali metals, it is a reductant. Metallic Li or Na are known for that. Positive values of E^0 are typical of oxidants such as the fluorine gas F_2 .

8.1.2. Cyclic Voltammetry

It is an advantageous technique for measuring reduction potentials. A commonly used three electrode cell shown in Fig. 8.1.1 contains a working electrode, the potential of which is varied, a reference electrode,³ and an auxiliary electrode.

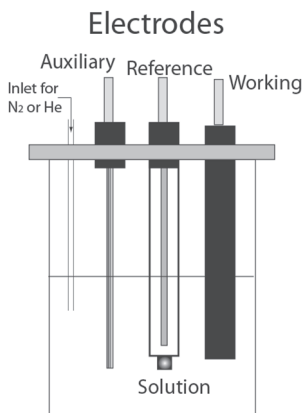


Figure 8.1.1. Three electrode cell used for recording cyclic voltammograms. See text for details.

² This will occur when the electron transfer occurs very fast in the absence of other limitations (see below). This is the so-called Nernstian electrode behavior of Red and Ox counterparts at an electrode.

³ Customarily used: saturated calomel electrode (SCE, Hg/Hg_2Cl_2), silver chloride ($Ag/AgCl$) electrode, normal hydrogen electrode (NHE, H_2/H^+).

The setup is made such that the potential between the working and reference electrodes is varied and the current (faradaic, i.e. due to reduction or oxidation) between the working and auxiliary electrodes is measured. The working electrode potential is changed with time in a cycling manner as shown on top of Fig. 8.1.2. The corresponding current change as a function of applied potential is in the bottom of Fig. 8.1.2.

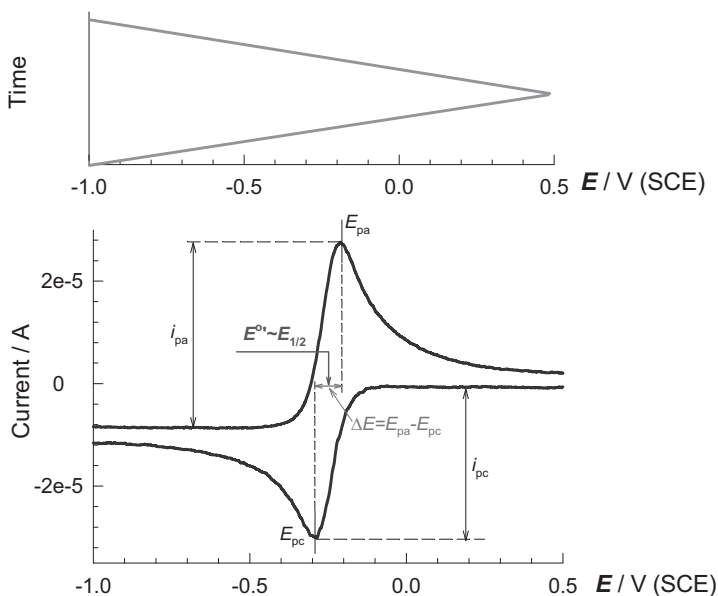


Figure 8.1.2. *Top:* linear relation between the potential applied to the working electrode and time. *Bottom:* the corresponding voltammogram for a species that behaves fully reversible at an electrode. SCE is saturated calomel electrode. See text for details.

A starting potential of the working electrode is customary much lower (as in Fig. 8.1.2) or higher than E^0 of a given redox couple. When the electrode potential approaches E^0 , the oxidation of Red begins and the current starts to rise. At a certain period of time most of Red at the electrode surface is converted into Ox and the current does not grow further. Diffusion brings new portions of Red to the electrode surface but the current descends nevertheless. Then the potential scan is reverted (at 0.5 V in Fig. 8.1.2) and Ox accumulated in the proximity of

electrode surface (not in the bulk!) is reduced back to form Red. Formal ($E^{0'}$)⁴ reduction potential is exactly between anodic (E_{pa}) and cathodic (E_{pc}) peaks. Identity of anodic and cathodic currents (i_{pa} and i_{pc}), independence of E_{pa} and E_{pc} of the scan rate, and 59 mV between E_{pa} and E_{pc} ($\Delta E = E_{pa} - E_{pc}$) indicates a movement of one electron and the Nernstian (or fully reversible) behavior at the electrode (Red and Ox are formed very fast after primary electron transfer). A representative example of the reversible behavior is shown in Fig. 8.1.3. If the peak separation ΔE equals 30 mV, two electrons are moved.

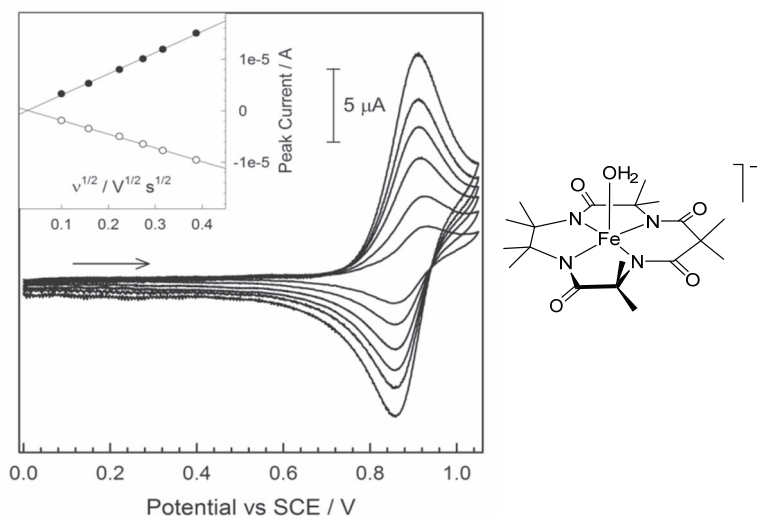


Figure 8.1.3. Cyclic voltammograms of the TAML activator shown on the right at scan rates 10, 25, 50, 75, 100 and 150 mV s^{-1} at pH 2. Inset shows anodic and cathodic peak currents vs square root of scan rate. Conditions: 2 mM TAML, 0.1 M NaClO_4 , 25°C, glassy carbon working, SCE reference and Pt wire counter electrode.⁵ Reprinted with permission. Copyright 2016 American Chemical Society.

The Randles-Ševčík equation 8.1.3 makes cyclic voltammetry a particularly attractive technique because the current is a linear

⁴ The reduction potential that applies under specified set of conditions (pH, ionic strength, etc.).

⁵ Mills MR, et al, *JACS*, **2016**, *138*, 13866.

function of concentration and square root of both diffusion coefficient and scan rate.

$$i_p = 2.69 \times 10^5 n^3/2 AD^{1/2} v^{1/2} c_0 \quad (8.1.3)$$

Here i_p is a peak current (A), n – number of electrons moved (eq mol⁻¹), A – electrode surface (cm²), D – diffusion coefficient (cm² s⁻¹), v – scan rate (V s⁻¹), c_0 – concentrations of Red or Ox (mol cm⁻³).

Quasi-reversible electrode behavior is when the anodic and cathodic peaks are separated by more than 60 mV, the difference between the peaks increases progressively with increasing scan rates, and anodic and cathodic peak currents may not be similar. Such is shown in Fig. 8.1.4 by the example of a TAML iron(III) complex.⁶ The difference $\Delta E = E_{pa} - E_{pc}$ increases noticeably as the scan rates grows from 10 to 200 mV s⁻¹.

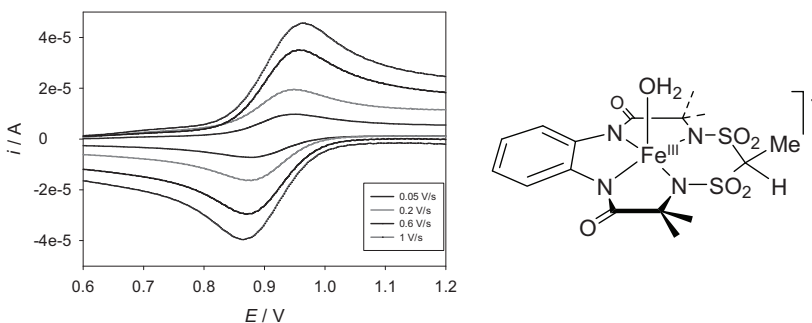


Figure 8.1.4. Cyclic voltammograms of TAML complex at different scan rates. Conditions: MeCN (0.1 M $(n\text{-Bu})_4\text{NPF}_6$; glassy carbon electrode, 30 °C. Potentials are against Ag/AgCl reference electrode.

Irreversible behavior at an electrode (an example is shown in Fig. 8.1.5) is such when only either anodic or cathodic feature shows up on cyclic voltammograms. There are numerous reasons for irreversibility. Here we will consider two cases when it is due a reaction that follows an electrochemical step referred to an *EC* mechanism (Electrochemical step is followed by Chemical step). Let us assume that electrochemical oxidation of A gives B, which rearranges into electrochemically *inactive* form C.

⁶ Somasundar Y, et al, *Chem – Eur J*, **2020**, *26*, 14738.

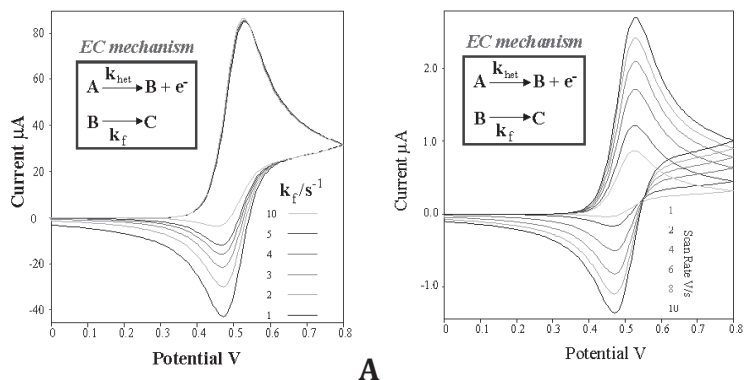


Figure 8.1.5. Examples of irreversible electrode behavior encountered due to the EC mechanism. See text for details.⁷

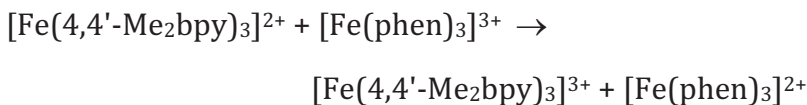
Case A predicts cyclic voltammograms obtained at a fixed scan rate. The rate constants k_f for conversion of B to C vary. When k_f is the smallest, B does not convert into C within the time of scan, the concentration of B does not drop, and the cathodic feature is well defined — the behavior is close to reversible. When k_f is high, B vanishes very fast, there is nothing to reduce during the reverse scan, the cathodic current is small, and the cyan voltammogram is a feature of irreversible process. Similar situation (Fig. 8.1.5B) projects by varying scan rate at fixed k_f . When a scan rate is high, B has not enough time to convert to C. Therefore most of B is reduced back into A at the electrode. Low scan rate gives time for B to rearrange into C and thus to create, as above, a nothing-to-reduce case.⁸

8.2. Inner- and Outer-Sphere Electron Transfer

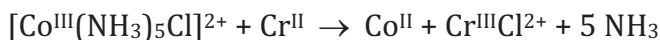
The net result of both processes is identical. Electron will migrate from one species to another. Consider an electron transfer (ET) reaction that occurs during a collision of two rigid spheres (billiard balls) as in the example:

⁷<http://www.downloads.imune.net/journals/2008%20Special%20Issue%20on%20Voltammetry/pdf/A%20Cyclic%20Voltammetry%20Primer.pdf>

⁸ Why is the peak current lower in this case?



It occurs without changing the ligand environment of both partners and without chemical binding between the partners. Such process is referred to as *outer-sphere* ET. If ET is preceded by the formation of a chemical adduct between the partners, it is the *inner-sphere* electron transfer. For example, the reaction



involves the chloro-bridged intermediate $\text{Co}^{\text{III}}\text{-Cl-Cr}^{\text{II}}$. The second-order rate constants k_{12} of outer-sphere ET can be predicted theoretically. Examples are in Table 8.2. An impressive match between calculated and experimental rate constants is due to the electron transfer theory, which was pioneered by Rudolf A. Marcus (Noble Prize in Chemistry 1992).

Table 8.2.1. Comparison of calculated and experimental rate constants k_{12} for outer-sphere electron transfer.

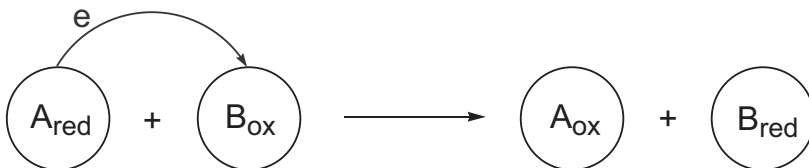
Reaction	$k_{12} / \text{M}^{-1} \text{s}^{-1}$	
	observed	calculated
$[\text{IrCl}_6]^{2-} + [\text{W}(\text{CN})_8]^{4-}$	6.1×10^7	6.1×10^7
$[\text{IrCl}_6]^{2-} + [\text{Fe}(\text{CN})_6]^{4-}$	3.8×10^5	7×10^5
$[\text{IrCl}_6]^{2-} + [\text{Mo}(\text{CN})_8]^{4-}$	1.9×10^6	9×10^5
$[\text{Fe}(\text{CN})_6]^{3-} + [\text{W}(\text{CN})_8]^{4-}$	4.3×10^4	6.3×10^4
$[\text{Co}(\text{terpy})_2]^{2+} + [\text{Co}(\text{bpy})_3]^{3+}$	6.4	3.2
$[\text{Fe}(\text{phen})_3]^{2+} + \text{MnO}_4^-$	6×10^3	4×10^3

8.3. Marcus Electron Transfer Theory⁹

We shall consider the most general principles of the Marcus concept. This will nevertheless allow us to use its potential in full. It should first be mentioned that the concept is based on the transition state theory. The factors that affect the rate of ET from molecule A to

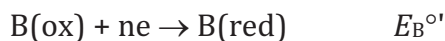
⁹ Marcus RA, *Angew Chem, Int Ed Eng*, **1993**, 32, 1111.

molecule B and hence the second-order rate constant or the free energy of activation ΔG^\ddagger of electron transfer are the following.



- *Thermodynamics of ET, i.e. a change of the free energy of reaction ΔG .*

This change is estimated from the standard or formal reduction potentials of the participants. The half-reaction for each participant is given by:



ET from A to B will be thermodynamically favorable, if $E_B^{\circ'} > E_A^{\circ'}$, i.e. if the oxidizing power of B (its reduction potential) is higher than that of A. The difference between the standard (formal) reduction potentials of A and B is the reaction *driving force* $\Delta E = E_B^{\circ'} - E_A^{\circ'}$. It is directly related to the free energy change ΔG° :

$$\Delta G^\circ = -nF \times \Delta E = -RT \ln K$$

Here $F = eN_A$ is the Faraday constant (96,485.3 C mol⁻¹, 96.5 kJ V⁻¹ mol⁻¹) and n is the number of electrons transferred.

- *Reorganization term λ , which is introduced to account for differences in size and solvation of oxidized and reduced species (A and B).*

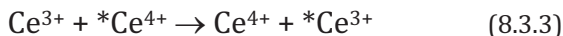
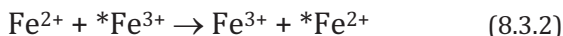
The reorganization term is a sum of solvational (λ_o) and vibrational (λ_i) components:

$$\lambda = \lambda_o + \lambda_i$$

It can roughly be said that the solvational correction is needed to compensate different solvation of the oxidized and reduced forms. The vibrational term compensates differences in bond lengths. The final expression for a change in the free energy of activation is given by eq 8.3.1.

$$\Delta G^\ddagger = \frac{\lambda}{4} \left(1 + \frac{\Delta G^0}{\lambda} \right)^2 \quad (8.3.1)$$

The important consequences of the main equation are associated with the so-called self-exchange reactions such as 8.3.2 and 8.3.3.



The self-exchange rate constants k_{11} were determined for many redox pairs and they are helpful for predicting the reactivity based on the Marcus equation for the cross-reaction 8.3.4, i.e. between A and B such as $\text{Fe}^{2+} + \text{Ce}^{4+} \rightarrow \text{Fe}^{3+} + \text{Ce}^{3+}$.

$$k_{12} = (k_{11}k_{22}K_{12}f_{12})^{1/2} \quad (8.3.4)$$

Here k_{11} and k_{22} are the self-exchange rate constants for the redox partners A and B, K_{12} is the equilibrium constant, and f_{12} is a known function of k_{11} , k_{22} , and K_{12} ; f_{12} is usually close to unity particularly when $E_B^{\circ'} \sim E_A^{\circ'}$. Equation 8.3.4 holds when the reorganization term for the cross-reaction (between A and B) equals $\lambda_{12} \sim \frac{1}{2}(\lambda_{11} + \lambda_{22})$, where λ_{11} and λ_{22} are the reorganization terms for the corresponding self-exchange reactions. Equation 8.3.4 is used for:

- Prediction of rate constants for cross-reactions (k_{12}).
- Calculation of self-exchange rate constants (k_{11} and k_{22}).
- Estimation of equilibrium constant K_{12} and reduction potentials.

Table 8.3.1. Reduction potentials (vs SCE) and self-exchange rate constants k_{11} for selected inorganic and organometallic complexes in water at 25 °C.¹⁰

Entry	Complex	$E /$ mV	$k_{11} /$ M^{-1} s^{-1}	Conditions
1	[Ru(bpy) ₃] ^{3+/2+}	1025	1.2×10^9	1.0 M HClO ₄
2	[Ru(phen) ₃] ^{3+/2+}	1025	1.2×10^9	1.0 M HClO ₄
3	[Ru(CN) ₆] ^{3-/4-}	685	8.3×10^3	0.1 M NaClO ₄
4	[Ru(NH ₃) ₆] ^{3+/2+}	-345	8.2×10^2	μ 0.013, D ₂ O
5	[Ru(en) ₃] ^{3+/2+}	-455	$< 2 \times 10^2$	μ 0.1 M
6	[Fe(phen) ₃] ^{3+/2+}	825	1.3×10^7 a)	D ₂ O/D ₂ SO ₄ , $\mu \sim$ 0.4 M
7	[Fe(CN) ₆] ^{3-/4-}	185	2.4×10^2 b)	μ 0.2 M
8			1.5×10^4	
9	Ferrocene/ferricenium (FcH/FcH ⁺)	270	5.7×10^6	1:1 v/v <i>n</i> - PrOH/H ₂ O 0.05 M Ba(ClO ₄) ₂
10	[FcCH ₂ N+Me ₃] ^{0/+}	385	1.2×10^7	pD 5, 0.1 M NaBF ₄
11	[Os(bpy) ₃] ^{3+/2+}	600	$> 10^9$	$\mu > 0.9$ M
12	[Co(phen) ₃] ^{3+/2+}	175	40	0.1 M KNO ₃
13	"		0.35	μ 0.11 M
14	[Co(bpy) ₃] ^{3+/2+}	125	17	0.1 M KNO ₃
15	[Co(en) ₃] ^{3+/2+}	-425	3.4×10^{-5}	0.2 M KCl
16	[Co(NH ₃) ₆] ^{3+/2+}	-185	$\sim 10^{-7}$	-
17	[Co(sep)] ^{3+/2+ c)}	-524	5	0.2 M NaCl
18	[Co([9]aneS ₃) ₂] ^{3+/2+ d)}	-655	9.5×10^4	μ 0.1 M

a) at 3 °C; b) 100 times lower than usually reported due to the K⁺ effect; c) sep = sepulhrate (1,3,6,8,10,13,16,19-octazaabicyclo[6.6.6]eicosane); d) ([9]aneS₃) = 1,4,7-trithiacyclononane.

Table 8.3.1 lists the self-exchange rate constants for selected inorganic and organometallic molecules. The k_{11} values depend crucially on the nature of (i) metal center (cf. entries 1 & 14) and (ii) ligand/s (cf.

¹⁰ Ryabov AD, *Adv Inorg Chem*, **2004**, 55, 201.

entries 1 & 4). Higher the rigidity of ligand shell, larger the self-exchange rate constants.

8.4. Important Predictions

If, as generally assumed, the reorganization term λ is nearly the same in a series of related reactions but the reaction driving force increases, it follows from eq 8.3.1 that ΔG^\ddagger decrease first (ET rates increase) while ΔG° increases from certain value till $\Delta G^\circ = -\lambda$. But when $-\Delta G^\circ > \lambda$, the free energy of activation ΔG^\ddagger begins to increase and the ET rate decreases (Fig. 8.4.1). The region where rates increase with increasing the driving force is the normal region. The normal region is followed by the inverted region. The maximum is observed when $-\Delta G^\circ = \lambda$. Marcus predicted first the inverted region theoretically. The experimental evidence has been collected later.

Figure 8.4.2 is a visualization of how an increase in the driving force results in rate retardation. A significant decrease in the potential energy of products P creates a new higher lying barrier at the other side of the potential energy curve of the initial state R.

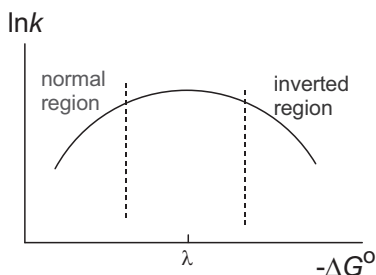


Figure 8.4.1. Normal and inverted regions for ET reactions.

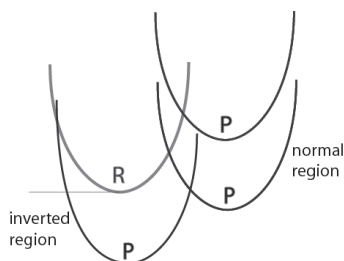


Figure 8.4.2. Illustration of the origin of inverted region.

Problems

8-1. The working electrode is polarized at $E = -1$ V. Assuming the Nernstian behavior, indicate the dominating species of Mg, Pb, and Hg using the data in Table 8.1.1.

8-2. Finish the stoichiometric equations for reactions summarized below. Using the data in Table 8.3.1 calculate the corresponding driving force and equilibrium constant in water at 25 °C. There is no reduction potential for $[\text{Fe}(\text{bpy})_3]^{3+}$ in Table 8.3. Use the data for $[\text{Fe}(\text{phen})_3]^{3+}$. Why can such assumption be made?

1. $[\text{Co}(\text{phen})_3]^{2+} + [\text{Os}(\text{bpy})_3]^{3+}$
2. $[\text{Fe}(\text{CN})_6]^{4-} + [\text{Fe}(\text{bpy})_3]^{3+}$
3. Ferrocene + $[\text{Ru}(\text{bpy})_3]^{3+}$

8-3. Using the Nernst equation 8.1.2 suggest what to expect for the ratio $C_{\text{red}}/C_{\text{ox}}$ when the electrode potential is higher by 0.06 V than the corresponding formal potential and it is known that $n = 2$ (2 electrons are moved).

8-4. Prove that eq 8.3.1 accounts for minimum in ΔG^\ddagger when $-\Delta G^\circ = \lambda$.

LECTURE 9.

OXIDATIONS BY METAL IONS

9.1. Metal Ions as One-Electron Oxidants:

Co^{III}, Ce^{IV}, Fe^{III}, V^V, Mn^{III} and Ag^I

Oxidizing properties of metal cations in aqueous solutions are commonly observed under very acidic conditions when they are cationic aqua species $[M(H_2O)_n]^{m+}$. Coordinated water starts to deprotonate at higher pH to form aqua/hydroxo metal complexes $[M(OH)(H_2O)_{n-1}]^{(m-1)+}$, which are less oxidizing than the parent aqua complexes. Therefore, pK_a of the first ionization (eq 9.1.1) is an important property of metal oxidants.

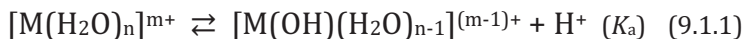


Table 9.1.1 summarizes reduction potentials and pK_a 's of selected metal ions which are commonly used as 1e oxidants.

Table 9.1.1. Reduction potentials, pK_a 's and other relevant properties of metal ions used as 1e oxidants under acidic conditions.

Metal ion	E / V vs NHE (conditions)	pK_a	Key properties/comments
Co ^{III a)}	1.9 (4 M HClO ₄)	2.7	$[Co(H_2O)]^{3+} + [Co(OH)]^{2+} \rightleftharpoons [Co-O-Co]^{4+} + H^+$
Ce ^{IV}	1.7 V (1 M HClO ₄) 1.4 V (0.5 M H ₂ SO ₄)	-1	

V ^V	~ 1 V		$\text{VO}_2^+ + 2 \text{H}^+ \rightleftharpoons \text{VO}^{2+} + \text{H}_2\text{O}$ $\text{VO}_2^+ + \text{H}^+ + \text{H}_2\text{O} \rightleftharpoons \text{V}(\text{OH})_3^{2+}$ $[\text{V}(\text{OH}_2)_6]^{2+}$ (violet); $[\text{V}(\text{OH}_2)_6]^{3+}$ (dark blue); VO^{2+} (bright blue); V ^V (yellow)
Mn ^{III}	~1.56 V	~-0.4	$\text{Mn}^{\text{III}} + \text{e} \rightarrow \text{Mn}^{\text{II}}$ Unstable: $2 \text{Mn}^{\text{III}} \rightleftharpoons \text{Mn}^{\text{II}} + \text{MnO}_2$ Stable is $[\text{Mn}^{\text{III}}(\text{OAc})_3] \times 2\text{H}_2\text{O}$ ^{b)}
Fe ^{III}	~0.77 V	3.0 6.3	$[\text{Fe}(\text{OH}_2)]^{3+} \rightleftharpoons [\text{Fe}(\text{OH})]^{2+} + \text{H}^+$ $[\text{Fe}(\text{OH})(\text{OH}_2)]^{2+} \rightleftharpoons [\text{Fe}(\text{OH})_2]^{2+} + \text{H}^+$
Ag ^{II}	~2 V		$\text{Ag}^{\text{II}} + \text{e} \rightarrow \text{Ag}^{\text{I}}$
	~0.8 V		$\text{Ag}^{\text{I}} + \text{e} \rightarrow \text{Ag}^0$

a) Generated by electrolysis. b) Obtained by oxidation of $[\text{Mn}^{\text{II}}(\text{OAc})_2]$ with KMnO_4 in glacial acetic acid. Actually it is $[\text{Mn}_3\text{O}(\text{OAc})_6](\text{OAc})$, an oxo-centered cation. Oxidizes **water** to O_2 .

Cerium(IV) is commercially available as $(\text{NH}_4)_2[\text{Ce}(\text{NO}_3)_6]$ and therefore it is most commonly used. Manganese(III) is very unstable. It is included in Table 9.1.1 due to its unique ability to oxidize water, the feature that will be considered in Lecture 13. Silver(II) is the strongest oxidant in Table 9.1.1. Remarkably, the product of its 1e oxidation, i.e. silver(I), is also an oxidant with the reduction potential of 0.8 V.

9.2. KMnO_4 and $\text{K}_2\text{Cr}_2\text{O}_7$

Potassium permanganate KMnO_4 and chromate $\text{K}_2\text{Cr}_2\text{O}_7$ are standard oxidants and therefore their properties should also be considered along with those of metal ions included in Table 9.1.1.

Table 9.2.1. Reduction potentials of KMnO_4 and $\text{K}_2\text{Cr}_2\text{O}_7$ (vs NHE) for different half-reactions which reflect acidity of the medium.

Metal	Half-reaction	E / V
Mn^{VII}	$\text{MnO}_4^- + 8 \text{H}^+ + 5 \text{e} \rightarrow \text{Mn}^{\text{II}} + 4 \text{H}_2\text{O}$	1.49
	$\text{MnO}_4^- + 2 \text{H}_2\text{O} + 3 \text{e} \rightarrow \text{MnO}_2 + 4 \text{OH}^-$	0.588
	$\text{MnO}_4^- + \text{e} \rightarrow \text{MnO}_4^{2-}$	0.56
Cr^{VI}	$\text{Cr}_2\text{O}_7^{2-} + 14 \text{H}^+ + 6 \text{e} \rightarrow 2 \text{Cr}^{\text{III}} + 7 \text{H}_2\text{O}$	1.33 V
Cr^{III}	$\text{Cr}^{\text{III}} + \text{e} \rightarrow \text{Cr}^{\text{II}}$	-0.41 V

Like bare metal oxidants, potassium permanganate is a strong oxidizing agent under acidic conditions when Mn^{VII} is reduced to Mn^{II} (Table 9.2.1). Its reduction under neutral and basic media to Mn^{IV} dioxide and manganate MnO_4^{2-} , respectively, occurs with the reduction potentials by almost 1 V lower, i.e. the oxidizing power of permanganate is strongly compromised. Yellow-orange potassium dichromate $\text{K}_2\text{Cr}_2\text{O}_7$ behaves similarly. The greenish reduction product formed under acidic conditions, chromium(III), has no oxidizing power. Instead, the reduction potential of -0.41 V indicates that Cr^{II} is a reducing agent.

9.3. Key Reduction Potentials of O_2 and H_2O_2

Dioxygen and hydrogen peroxide are primary oxidants in Nature. Their redox properties are collected in Table 9.3.1. The former is a strong oxidant in acidic media when O_2 is reduced to water by four electrons. Dioxygen as two electron oxidant, when O_2 is reduced to H_2O_2 , is noticeably less aggressive. The reduction potential of hydrogen peroxide is even higher than that of O_2 . It is still a reasonable oxidant under strongly basic conditions when H_2O_2 is deprotonated ($\text{p}K_{\text{a}} \sim 11.2\text{--}11.6$) though the corresponding reduction potential is by 0.5 V lower. Note that under certain basic conditions H_2O_2 is a reducing agent—the property operated by Nature in catalase enzymes, which catalyze disproportionation of hydrogen peroxide into O_2 and H_2O (Lecture 11).

Table 9.3.1. Reduction potentials of O₂ and H₂O₂ for different half-reactions which reflect acidity of the medium.

Oxidant	Half-reaction	<i>E</i> / V vs NHE
O ₂	O ₂ + 4 H ⁺ + 4e → 2 H ₂ O	1.229
	O ₂ + 2 H ₂ O + 4e → 4 OH ⁻	0.401 ^{a)}
	O ₂ + 2 H ⁺ + 2e → H ₂ O ₂	0.682
H ₂ O ₂	H ₂ O ₂ + 2 H ⁺ + 2e → 2 H ₂ O	1.33
	HO ₂ ⁻ + H ₂ O + 2e → 3 OH ⁻	0.807
	O ₂ + 2 H ₂ O + 2e → H ₂ O ₂ + 2 OH ⁻	-0.146

a) Potential of the Clark electrode used for electrochemical monitoring of O₂ content in aqueous media.

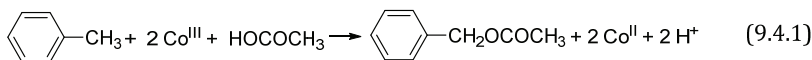
9.4. Oxidation of Hydrocarbons by "Hard" Metal Oxidants

Oxidizing metal cations in Table 9.1.1 such as Co^{III}, Mn^{III} and Ce^{IV} are hard acids in terms of the concept of hard and soft acids and bases introduced by Ralph Pearson.¹ The term hard metal oxidants is convenient and broadly used. It cuts off permanganate, dichromate and other similar molecules from the list of oxidants because these anions are soft bases. Mechanisms of oxidation of hydrocarbons (alkylaromatics, benzene, alkanes) by hard oxidants are similar but differ from those by soft oxidants.

9.4.1. Oxidation of Toluene by Co^{III} in Acetic Acid at 90-100 °C

Cobalt(III) oxidizes toluene into benzyl acetate in ca. 100% yield in acetic acid according to eq 9.4.1. The reaction goes smoothly in the absence of O₂, the presence of which changes products dramatically. Benzaldehyde and benzoic acid dominate in O₂-containing media but products of deeper oxidation are sometime formed.

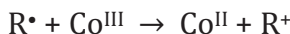
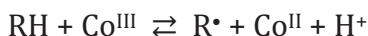
¹ Pearson R, *J Chem Ed*, **1968**, *45*, 581.



When dioxygen is excluded, the rate law for reaction 9.4.1 is given by eq 9.4.2.

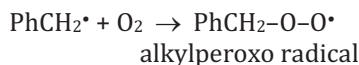
$$v = \frac{k[\text{RH}][\text{Co}^{\text{III}}]^2}{[\text{Co}^{\text{II}}]} \quad (9.4.2)$$

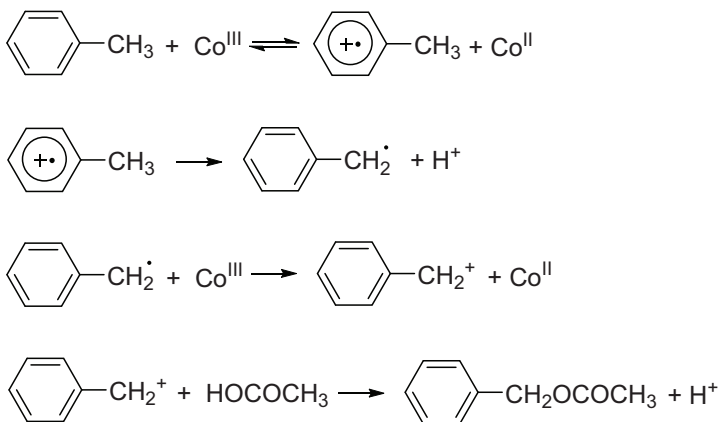
Equation 9.4.2 is consistent with the following stoichiometric mechanism:



The oxidation starts with an electron abstraction by Co^{III} ; a free radical produced is further oxidized by the second Co^{III} ion into the cation R^+ . The process is concluded by the rapid recombination of the former with the acetate anion. The mechanism is detailed in Scheme 9.4.1. One-electron transfer gives the toluene radical-cation which transforms into benzylic radical after dissociation of proton. The reactivity of arenes correlates with their ionization potentials and the formation of radical-cations was proven by spectroscopic techniques (uv-vis, EPR). Lifetimes of radical-cations are different; there are long-lived and short-lived species.

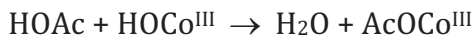
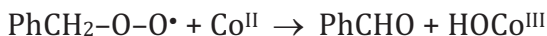
Dioxygen affects the oxidation products drastically. Benzaldehyde and benzoic acid form because Co^{III} and O_2 compete for the intermediate benzyl radical PhCH_2^\bullet . The competition ends up in a triumphant victory of O_2 because the rate constants for its bimolecular reactions with carbon-centered radicals to form alkylperoxo radicals approach the diffusion-controlled limit ($k > 10^9 \text{ M}^{-1} \text{ s}^{-1}$):



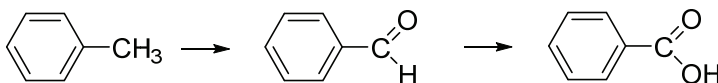


Scheme 9.4.1. Intimate mechanism of oxidation of toluene by Co^{III} in O_2 free systems.

Benzylperoxy radical is reduced by Co^{II} to form benzaldehyde:

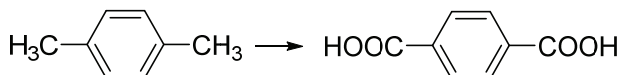


Aldehydes, which are less reactive than alkylaromatics due to the electron-withdrawing formyl group, can further be oxidized into carboxylic acids (Scheme 9.4.2). Higher concentrations of Co^{III} and lower pressures of O_2 favor the formation of aldehydes.

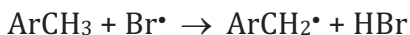


Scheme 9.4.2. Conversion of toluene to benzaldehyde and benzoic acid in the presence of O_2 .

Halides Cl^- and Br^- provide synergistic effects by enhancing rates of oxidation of alkylaromatics by Co^{III} and Mn^{III} . *para*-Xylene, for example, is cleanly oxidized into terephthalic acid at 60°C :

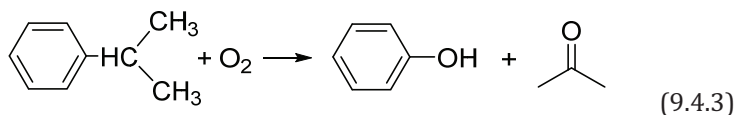


Under these conditions, the mechanism is principally different and involves the oxidation of halides by Co^{III} . Halide radicals abstract hydrogens from sp^3 carbons as it occurs during thermal or photo-induced oxidation of alkanes by Cl_2 and Br_2 :

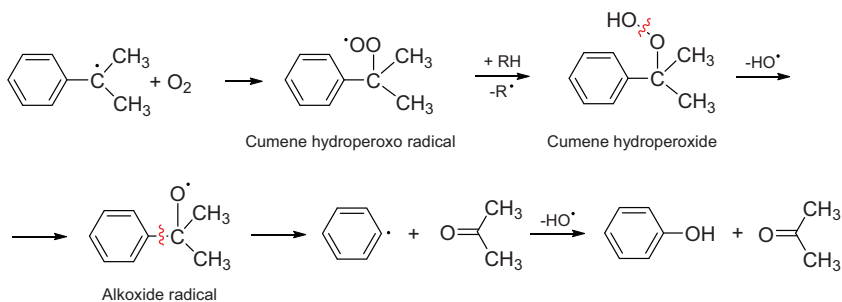


9.4.2. Green Oxidation of Isopropylbenzene to Phenol and Acetone

It is generally assumed that free radical, O_2 involved oxidations are not selective, end up in a variety of products and therefore cannot be considered as environmentally benign. This generality does not however concern the oxidation of isopropylbenzene (cumene), which affords phenol and acetone, both valuable organic materials, without formation of by-products (eq 9.4.3).



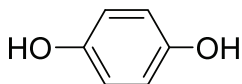
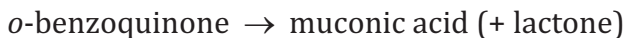
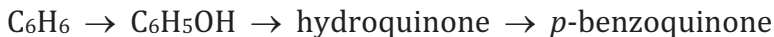
Tertiary carbon of isopropylbenzene has the most reactive C-H bond with the lowest dissociation energy. The corresponding carbon-centered radical is therefore produced effortlessly by a hydrogen abstractor. The radical reacts fast with O_2 to form the cumene hydroperoxo radical (Scheme 9.4.3). The latter finds a hydrogen donor RH and converts into isopropylbenzene (cumene) hydroperoxide. Alkyl hydroperoxides are the species responsible for the cleavage of C-C bonds. It is a general process and therefore the mechanism in Scheme 9.4.3 is worth attention. The O-O bond in alkyl hydroperoxides has a low dissociation energy (see Section 9.4.5) and is a subject of a homolytic cleavage with a dissociation of the hydroxo radical. It is the alkoxide radical within which C-C bonds are homolytically cleaved to afford a carbonyl compound and a carbon-centered radical, in this case acetone and phenyl radical, respectively. Phenol is a product of recombination of phenyl and hydroxo radicals.



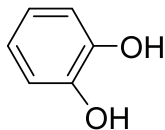
Scheme 9.4.3. Mechanism of green oxidation of isopropylbenzene to phenol and acetone.

9.4.3. Oxidation of Benzene

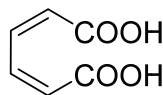
Benzene is more difficult to oxidize than alkyl aromatic compounds because it does not have aliphatic sp^3 C–H bonds. Cobalt(III) oxidizes benzene slowly in aqueous $HClO_4$ breaking the aromatic ring when Mn^{III} is unreactive. There are two major pathways, phenol being a primary product in both of them:



hydroquinone



catechol

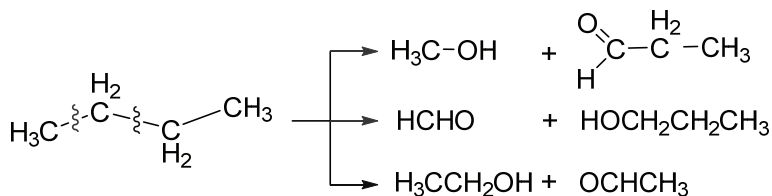


cis,cis-muconic acid

9.4.4. Autoxidation of Alkanes

The term autoxidation sounds slightly mysterious though it is just the oxidation of alkanes by dioxygen. Autoxidation is a free radical process leading to fragmentation of hydrocarbon chains and formation of

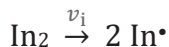
various oxygen-containing products. Rates of autoxidation are determined by the speed of formation of carbon-centered radicals (initiation) and therefore the reaction conditions play an important role. *n*-Butane, for example, will be oxidized at elevated temperatures into a mixture of all possible alcohols and aldehydes formed after cleavages of C–C bonds (Scheme 9.4.4). Aldehydes produced could further be oxidized into the corresponding carboxylic acids (see below).



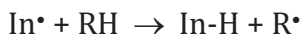
Scheme 9.4.4. Primary products of autoxidation of *n*-butane.

The autoxidation mechanism (Scheme 9.4.5) involves initiation, propagation and termination. Autoxidation rates are determined by all three steps, particularly by rates or rate constants of the slowest steps indicated above arrows in red. Initiation, which generates free radical species In^\bullet , usually occurs thermally or photochemically. Therefore, autoxidation reactions are slower at lower temperatures and in the dark. Hydrogen abstraction from hydrocarbon by In^\bullet is much faster than initiation and therefore it does not contribute to the overall rate.

Initiation

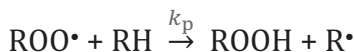


(In_2 – initiator; v_i – rate of initiation)



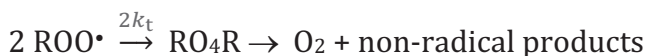
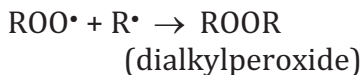
Propagation





(alkylhydroperoxides primary products)

Termination



Scheme 9.4.5. Mechanisms of unbranched autoxidation of hydrocarbons, an example of a chain reaction.

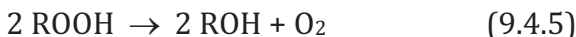
Propagation starts with trapping a carbon-centered radical by O_2 to form an alkylperoxide radical. The trapping occurs with diffusion-controlled rates and therefore does not affect the rate. Abstraction of hydrogen from RH by an alkylperoxide radical is slower and the rate constant k_p contributes to the overall rate. Termination takes place due to free radical recombination, which may involve either different ($\text{ROO}\cdot$ and $\text{R}\cdot$) or identical ($\text{ROO}\cdot$) radicals, were just a "homoleptic" process affects the rates.

General rate law for unbranched autoxidation is given by eq 9.4.4, which involves characteristics of slower steps in Scheme 9.4.5.

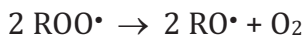
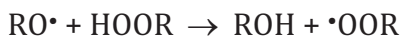
$$-\frac{d[\text{RH}]}{dt} = -\frac{[\text{O}_2]}{dt} = k_p[\text{RH}] \sqrt{\frac{v_i}{2k_t}} \quad (9.4.4)$$

Equation 9.4.4 shows that the autoxidation rate should be a linear function of hydrocarbon concentration, directly proportional to a square root of the initiation rate and inversely proportional to the square root of the termination rate constant k_t .

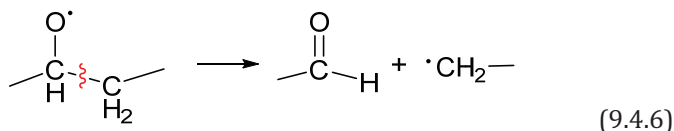
Primary products of autoxidation, alkylhydroperoxides, transform slowly to alcohols (eq 9.4.5).



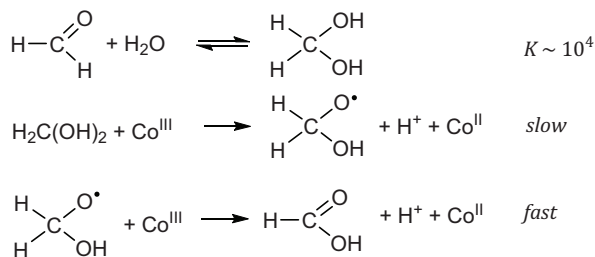
The mechanism of this process includes homolysis of the O–O bond of alkylhydroperoxides to form an *alkoxide* radical (cf. with the mechanism in Scheme 9.4.3):



Note that the O–O homolysis gives two free radicals and both of them may abstract hydrogen from hydrocarbon RH. In such a case autoxidation turns into a branched chain reaction. The C–C bond cleavage is an indicator of the *branched* free radical mechanism. It should be emphasized again that the O–O homolysis initiates a cleavage or fragmentation of hydrocarbon chains (eq 9.4.6). The alkyl radical produced reacts with HO• to form an alcohol.



Alcohols generated via eq 9.4.5 are oxidized further into aldehydes/ketones. Final products, carboxylic acids, are formed from aldehydes. For example, oxidation of *n*-butane at 180 °C, 60 bar O₂, Co^{III}(OAc)₃ in HOAc gives acetic acid as a major product together formic acid, acetone, acetaldehyde, methanol and esters as by-products. Metal oxidants M^{III} are involved in conversion of aldehydes into carboxylic acids through hydrated forms of aldehydes (Scheme 9.4.6).



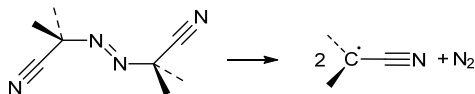
Scheme 9.4.6. Mechanism of oxidation of aldehydes into carboxylic acids by metal oxidants.

9.4.5. Initiators and Antioxidants

Undesired autoxidation may occur spontaneously, i.e. without adding initiators, heating, or irradiation. Oxidation and fragmentation of nutrient fats is one of such processes: butter turns rancid on storing. Initiators facilitate both autoxidation and free-radical polymerization.

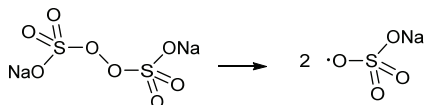
Table 9.4.1. Initiators of free radical processes.

Initiator	Bond dissociation energy / kcal mol ⁻¹
Hydrogen peroxide, HO–OH	48
<i>t</i> -Butylhydroperoxide, ^t BuO–OH	42
<i>t</i> -Butylperoxide, ^t BuO–OBu ^t	37
Benzoylperoxide, C ₆ H ₅ OCO–OCOC ₆ H ₅	30
Acetylperoxide, CH ₃ OCO–OCOCH ₃	30–32
α,α′-Azodiisobutyronitrile (AIBN)	30

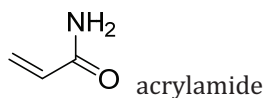


Sodium persulfate, Na₂S₂O₈

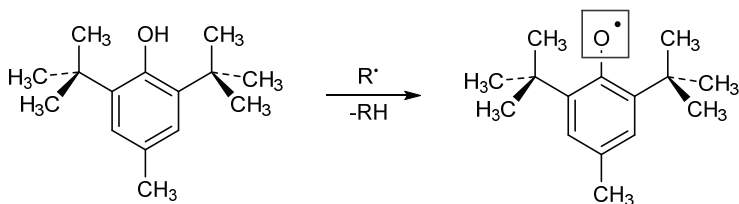
Photochemical initiation (*hν*)



Therefore, it is worth looking at these compounds in some detail. Generally, initiators should contain a bond with a low dissociation energy which undergoes a facile homolytic cleavage. Examples in Table 9.4.1 show that such are hydrogen peroxide, organic peroxides and hydroperoxides, i.e. molecules with the O–O bond. Dissociation energies of all peroxides are below 50 kcal mol^{-1} , 2–3 times lower than dissociation energies of sp^3 C–H bonds. The initiation produces oxygen-centered radicals. Initiation by α,α' -azodiisobutyronitrile (AIBN), which is widely used in polymer chemistry, occurs due to a labile N=N linkage. A carbon-centered radical is produced on thermolysis alongside with dinitrogen. Water soluble sodium persulfate is popular among biochemists for the preparation of polyacrylamide gels used for protein electrophoresis. Its homolysis under mild irradiation does not usually denature biomolecules.

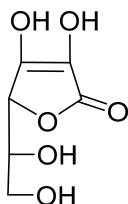


Nutrient fats are protected from autoxidation by antioxidants, which trap and deactivate free radicals capable of hydrogen abstraction. Such are, for example, phenolic compounds and ascorbic acid (vitamin C). 2,6-Di-*tert*-butyl-4-methylphenol is a commonly used food additive. Its phenolic unit is sterically protected by two bulky *t*-butyl radicals. Phenolic hydrogen of the antioxidant deactivates an aggressive radical R^\bullet converting it to RH but the oxygen-centered radical formed is significantly less aggressive partially due to a radical delocalization over the aromatic ring.



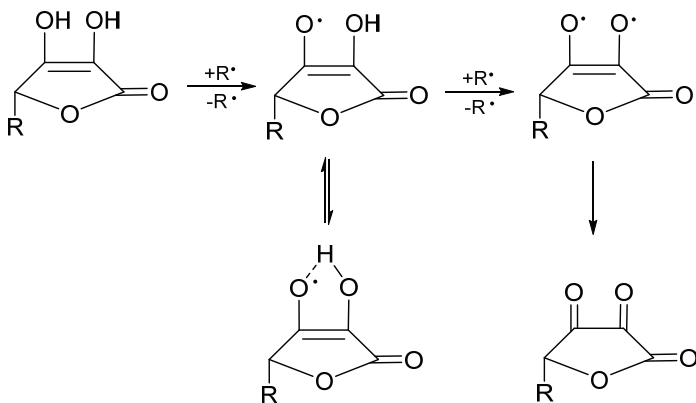
2,6-Di-*tert*-butyl-4-methylphenol

Ascorbic acid (γ -lactone of 2,3-dehydro-*L*-gulonic acid) is a natural antioxidant. The mechanism of its antioxidant action is shown in Scheme 9.4.7.



Ascorbic acid

An aggressive radical R^\bullet abstracts hydrogen from OH group at position 2 or 3 to form a radical stabilized by the internal hydrogen bond. The latter reacts with the second radical R^\bullet to produce ascorbic acid biradical, which rearranges rapidly into γ -lactone of 2,3-diketogulonic acid.



Scheme 9.4.7. Mechanism of antioxidant action of ascorbic acid (vitamin C).

Problems

9-1. Consider rate law 9.4.2. Indicate the evidence for the reversibility of the first step of the corresponding stoichiometric mechanism. Prove that the stoichiometric mechanism below is consistent with eq 9.4.2.

9-2. Make sure that the units of the left side of eq 9.4.4 correspond to the units of its right side.

9-3. Prove that the mechanism in Scheme 9.4.6 is consistent with a first reaction order in Co^{III} . How should Scheme 9.4.6 be modified to observe a second kinetic order in Co^{III} ?

9-4. Draw resonance structures of the phenolic radical produced from 6-di-*tert*-butyl-4-methylphenol showing delocalization (and deactivation) of unpaired electron.

9-5. Consider the mechanism of antioxidant action of ascorbic acid in Scheme 9.4.7. What type of potential threat may one expect from the intermediate formation of the H-bond stabilized radical?

Additional Reading

Benson D. *Mechanisms of Oxidation by Metal Ions*, Elsevier, NY, 1975.

LECTURE 10.

FENTON CHEMISTRY AND OTHER OXIDATIONS BY HYDROGEN PEROXIDE

10.1. Fenton oxidations

10.1.1. Introduction to Fenton Oxidations

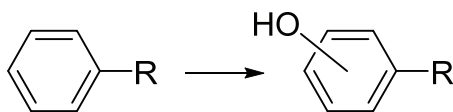
In 1894, Fenton described iron(II)-catalyzed oxidations by hydrogen peroxide.¹ Since then a $\text{Fe}^{\text{II}}\text{-H}_2\text{O}_2$ mixture has been referred to as the Fenton system and corresponding oxidations as Fenton oxidations. The meaning of the Fenton chemistry is much broader nowadays and perhaps could be formulated as free radical, metal-catalyzed oxidations by peroxides.

10.1.2. Scope of Fenton Oxidations: *t*-Butanol

The diversity of products which could be obtained from *tert*-butanol in the Fenton system is illustrated in Scheme 10.1.1.² In the absence of additives, i.e. in the presence of only Fe^{II} and H_2O_2 under acidic conditions, the alcohol is oxidized rather selectively into 2,5-dimethyl-2,5-dihydroxyhexane as a result of the oxidative coupling and the carbon chain doubles. Metal ions, copper(II) for example, direct the Fenton process to diols with the same number of carbons and 2,3-dihydroxy-2-methylpropane becomes the major product of oxidation of *tert*-butanol. Carbon monoxide allows adding just one carbon atom to make 3-hydroxy-3-methylbutanoic acid, the yield of which is however low due to simultaneous formation of the oxidative coupling product.

¹ Fenton HJH, *J Chem Soc*, **1894**, 65, 899.

² Walling C, *Acc Chem Res*, **1975**, 8, 125.



10.1.4. Generally Accepted Fenton Mechanism

Main steps of the Fenton mechanism are shown in Scheme 10.1.2. It is presented as suggested by Walling² and represents the most popular, generally accepted version. Other mechanistic variants of the Fenton chemistry exist also and such will be mentioned later. The events in Scheme 10.1.2 occur at ambient conditions (25 °C) and at pH < 7. The principal Fenton step F.1 is one electron reduction of hydrogen peroxide by a metal ion (Fe^{II} in Scheme 10.1.2). It results in a cleavage of the O–O bond and formation of the hydroxyl radical which is responsible for all further transformations. Note that the principal step is rather slow — the second-order rate constant k_1 is just 76 M⁻¹ s⁻¹.

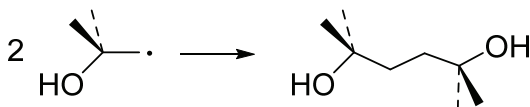
Step #	Elementary step	Rate constant	Value (M ⁻¹ s ⁻¹)
F.1	Fe ^{II} + H ₂ O ₂ → Fe ^{III} + HO ⁻ + HO [•]	k_1	76
F.2	Fe ^{II} + HO [•] → Fe ^{III} + HO ⁻	k_2	3 × 10 ⁸
F.3i	R _i H + HO [•] → R _i [•] + H ₂ O	k_{3i}	10 ⁷ – 10 ⁸
F.3j	R _j H + HO [•] → R _j [•] + H ₂ O	k_{3j}	
F.3k	R _k H + HO [•] → R _k [•] + H ₂ O	k_{3k}	
F.4	R _i [•] + M ⁿ → P + M ⁽ⁿ⁻¹⁾ "oxidation"	k_4 (M ⁿ = Fe ^{III} , Cu ^{II})	
F.5	2 R _j [•] → R _j -R _j "dimerization"	k_5	
F.6	R _k [•] + M ^{II} → R _k -H + M ^{III} "reduction"	k_6 (M = Fe)	

Scheme 10.1.2. Major steps of generally accepted Fenton mechanism.

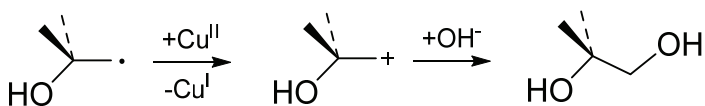
Next key steps F.2 and F.3 in Scheme 10.1.2 all involve hydroxyl radical HO^\bullet and therefore are much faster. The corresponding rate constants approach the limit controlled by diffusion. Carbon-centered radicals R^\bullet generated via steps F.3 give rise to different products, the nature of which is determined by additives in reaction mixtures. One-electron metal oxidants (Fe^{III} , Cu^{II}) launch oxidative pathways F.4. One-electron reducing agents such as Fe^{II} are responsible for reductive pathways F.6. Dimerization F.5 usually occurs in the absence of additional reagents.

10.1.5. Mechanisms of Major Pathways

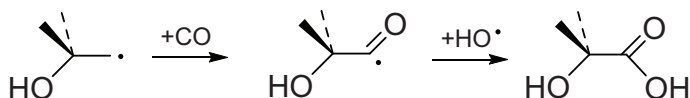
Dimerization of alkyl radicals represents the simplest concerted process, which involves the recombination of two radicals resulting in doubling the overall length of a hydrocarbon chain (of *tert*-butanol in this example).



Oxidation with diol formation occurs due to oxidation of alkyl radical by a 1e metal oxidant to form a carbocation which reacts then with hydroxide affording a final product. The length of hydrocarbon chain does not change.

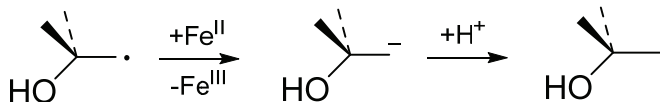


Carboxylation happens due to the trapping of alkyl radical by carbon monoxide. This step affords a carbonyl centered radical capable of adding hydroxyl radical to produce a carboxylic acid. The length of hydrocarbon chain increases by one carbon.



"Zero reaction", i.e. radical reduction, is initiated by 1e reducing agents such as Fe^{II} , which convert radicals into the corresponding carbanions.

Protonation of the latter accounts for regeneration of the starting hydrocarbon:

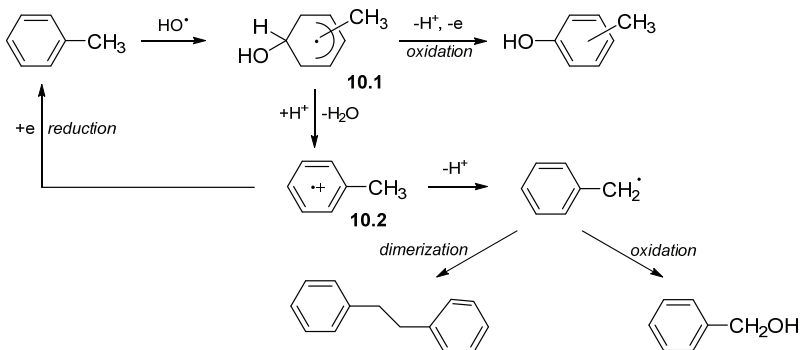


10.1.6. Mechanistic Pathways of Arenes

Low yields of hydroxylation products of arenes are accounted for several, sometime competing pathways. They are shown in Scheme 10.1.3 by the example of toluene. There is a major difference between reaction pathways of alkanes and arenes. The hydroxyl radical adds to arenes to produce the arene-centered radical **10.1**. Note that the aromaticity is lost due to $sp^2 \rightarrow sp^3$ rehybridization of the carbon which accepts $\text{HO}\cdot$ radical. Methylphenol, the hydroxylation product, is produced as a result of 1e oxidation of **10.1**, which is associated with the proton loss. Similar processes are often referred to as a proton-coupled electron transfer.³

Hydroxy group of radical **10.1** may undergo protonation creating a better leaving group, i.e. water. Its dissociation leads to radical-cation **10.2**, which is involved in two competing reactions. The 1e reduction regenerates starting toluene. Dissociation of the methyl group proton affords the benzylic radical, which may undergo either oxidation to form benzylic alcohol or dimerization affording 1,2-diphenylethane.

³ Costentin C, et al, *Acc Chem Res*, **2010**, *43*, 1019.



Scheme 10.1.3. Mechanistic pathways of Fenton oxidation of toluene.

10.1.7. Competing Reactions of HO^\bullet

Hydroxyl radical HO^\bullet is a very reactive species and therefore it is not surprising that it reacts with species other than hydrocarbons RH . In the Fenton systems, such is hydrogen peroxide which reacts with HO^\bullet via eq 10.1.2 to form the hydroperoxo radical HOO^\bullet :



Step 10.1.2 is fast; the corresponding second-order rate constant is in the range of $(1.2\text{--}4.5) \times 10^7 \text{ M}^{-1} \text{ s}^{-1}$.

Recombination of hydroxyl radicals to form hydrogen peroxide (eq 10.1.3) is an extra competing pathway, which diverts HO^\bullet from target substrates RH . The corresponding second-order rate constant equals $5.3 \times 10^9 \text{ M}^{-1} \text{ s}^{-1}$.



10.1.8. Relative Reactivity of Aliphatic C–H Bonds

Reactivity of different aliphatic C–H bonds toward hydroxyl radical varies significantly. This fact explains why different classes of organic compounds behave differently in the Fenton systems. Table 10.1.1 compares the rate constants k_3 for selected organic compounds with respect to k_2 (both rate constants are defined in Scheme 10.1.2).

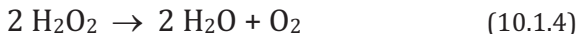
Table 10.1.1. Relative reactivity of aliphatic C–H bonds. Values of k_3 are normalized, i.e. given with respect to a single reacting C–H bond.

Compound	$\frac{k_3(\text{RH} + \text{HO}^\bullet \rightarrow \text{R}^\bullet + \text{H}_2\text{O})}{k_2(\text{Fe}^{\text{II}} + \text{HO}^\bullet \rightarrow \text{Fe}^{\text{III}} + \text{HO}^-)}$
H_3COH	4.0
$(\text{H}_3\text{C})_2\text{CHCH}_2\text{OH}$	1.4
$(\text{H}_3\text{C})_3\text{COH}$	1.9
$(\text{H}_3\text{C})_2\text{C}=\text{O}$	0.32
$\text{H}_3\text{CCO}_2\text{H}$	0.09

The k_3/k_2 ratios in Table 10.1.1 show different reactivities of aliphatic C–H bonds toward hydroxyl radical HO^\bullet . The difference may be as high as a factor of 40. Clearly, carbonyl groups decrease the speed of hydrogen abstraction as acetone and acetic acid are noticeably less reactive than methanol and *tert*-butanol.

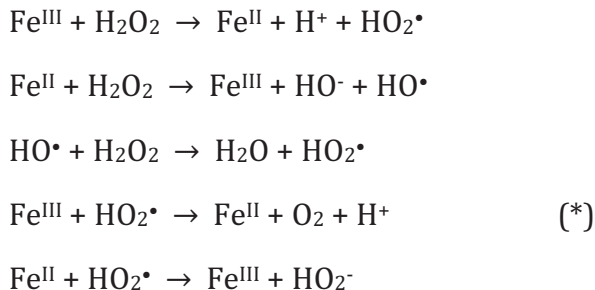
10.1.9 Catalase Activity in Fenton Systems

Catalase, catalase-like or catalatic activity is a property of a catalyst to speed up the disproportionation of hydrogen peroxide into dioxygen and water (eq 10.1.4).



In Nature, reaction 10.1.4 is efficiently catalyzed by catalase, an iron(III) heme enzyme, which will be briefly considered in Lecture 11. In the Fenton systems, iron(III) is produced, *inter alia*, from iron(II) and H_2O_2 (Scheme 10.1.2) and therefore the catalatic activity is an anticipated phenomenon. The sequence of events that accounts for disproportionation of H_2O_2 is shown in Scheme 10.1.4. The process starts with the interaction between Fe^{III} and H_2O_2 . In contrast to

biological systems where iron(III) is oxidized into higher valent forms, there is an iron reduction accompanied by generation of the hydroperoxo radical HO_2^\bullet . Dioxygen is produced when HO_2^\bullet is further oxidized by Fe^{III} (step (*) in Scheme 10.1.4).



Scheme 10.1.4. Mechanism of H_2O_2 disproportionation in Fenton systems.

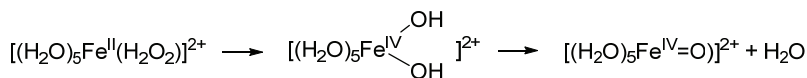
10.1.10. Alternative Mechanistic Views on Fenton Systems

The mechanistic portrayal of Fenton systems presented above is undoubtedly the most popular within the scientific community. However, it is still much debated and therefore alternative mechanistic variants are worth considering. One of such was proposed by Sawyer and coworkers.⁴ Their key mechanistic postulates were the following. The Fenton systems do not produce: (i) free HO^\bullet radicals; (ii) free carbon-centered radicals; (iii) aryl adducts HO-Ar^\bullet such as **10.1** in Scheme 10.1.3. The first piece of evidence was based on the fact that the pulse radiolysis, the method of generation of HO^\bullet radicals in water without involvement of Fe^{II} and H_2O_2 , gives slightly different end-products compared to those obtained in the Fenton systems. It was suggested that iron(II) complexes react with H_2O_2 to form active intermediates with the coordinated hydrogen peroxide HO_2^- of the type $[\text{Fe}^{\text{II}}(\text{OOH})(\text{ligand}/\text{s})]$ which react further with hydrocarbons RH . The second piece of evidence included theoretical results, which predicted the oxidation of Fe^{II} by H_2O_2 to form an iron(IV)oxo reactive intermediate, which was originally proposed in 1932:

⁴ Sawyer DT, et al, *Acc Chem Res*, **1996**, 29, 409.



The mechanism of this reaction could involve coordination of H_2O_2 to iron(II), heterolysis of the O–O bond, flow of two electrons from Fe^{II} and dissociation of the aqua ligand:



Scheme 10.5. Mechanism of formation of iron(IV)oxo species.

Iron(IV)oxo species were in fact generated from $[\text{Fe}(\text{H}_2\text{O})_6]^{2+}$ and ozone⁵ and its reactivity in oxidation of selected substrates was also tested. The conclusion was the following: the oxidation of selected substrates with $[(\text{H}_2\text{O})_5\text{Fe}^{\text{IV}}(\text{=O})]^{2+}$ yields unique products that are different from those generated in the Fenton reaction or derived from HO^\bullet radicals.

10.2. Heterolytic Oxidations by H_2O_2

10.2.1. Oxidations Catalyzed by Carboxylic Acids

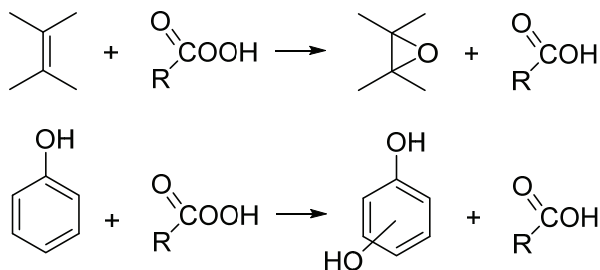
There are numerous examples of oxidations by H_2O_2 or by organic peroxides ROOH which do not involve radical intermediates. Such processes are referred to as heterolytic oxidations by peroxides and occur when two important conditions hold.

- Radicals HO^\bullet are not generated (there are no 1e reducing agents to initiate step F.1 in Scheme 10.1.2).
- The electrophilicity of the peroxide oxygen is strongly enhanced, for example, by carboxylic acids or, in other words, peroxides convert carboxylic acids into more electrophilic peroxy acids:



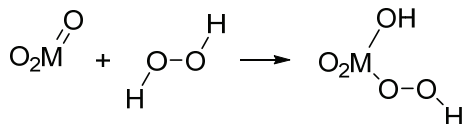
Examples of heterolytic oxidations include conversions of alkenes into epoxides and hydroxylation of phenols.

⁵ Pestovsky O, et al, *Angew Chem, Int Ed*, **2005**,*44*, 6871.



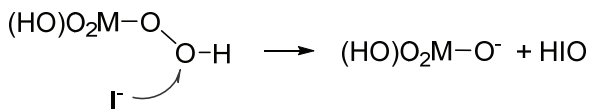
10.2.2. Oxidations Catalyzed by Metal Oxides

Metal oxides MO_3 (Mo, W), V_2O_5 , SeO_3 catalyze heterolytic oxidations of hydrocarbons by H_2O_2 in some way similar to the catalysis by *meta*-chlorobenzoic acid (*mCBA*).

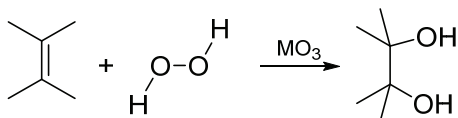


If $\text{M} = \text{S}$, the oxidant is known as persulfuric or Caro's acid. It is a key ingredient of the commercial oxidizing agent *oxone* (potassium peroxy-monosulfate, KHSO_5). Oxone converts amines into nitroso compounds, which rearrange into oximes ($\text{RCH}_2\text{NH}_2 \rightarrow \text{RCH}_2\text{N}=\text{O} \rightarrow \text{RCH}=\text{NOH}$).

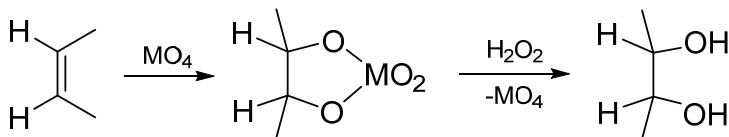
When $\text{M} = \text{Mo}$ and W , these are permolybdic and pertungstic acids, respectively. The compounds oxidize iodide into hypoiodite via "redox" nucleophilic substitution:



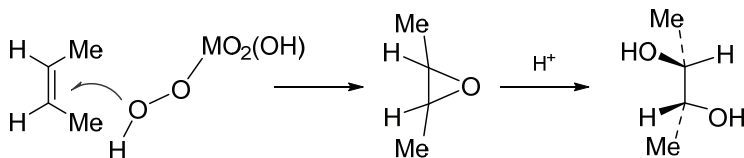
Metal oxides MO_3 catalyze oxidations of alkenes into vicinal diols:



The same net result is achieved when alkenes are oxidized by H_2O_2 in the presence of tetrahedral metal tetraoxo species OsO_4 , RuO_4 , MnO_4^- . The mechanisms of these reactions are fundamentally different:



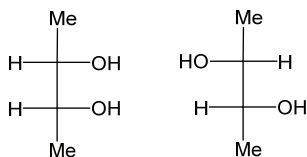
Mechanistic dissimilarity was established using *cis*-butene-2 which affords different stereochemical products, viz. *threo* and *erythro* glycols, in reactions catalyzed by MO_3 and MO_4 species, respectively.^{6,7}



10.2.3. Baeyer-Villiger Oxidation (Ketones into Esters)

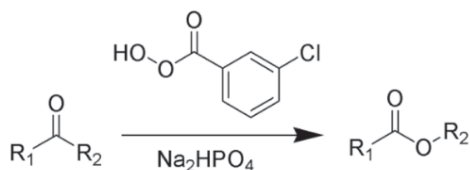
Conversion of ketones into esters by peroxy acids (usually by *meta*-chloroperoxy benzoic acid, *mCPBA*) or hydrogen peroxide is a Baeyer-Villiger oxidation.⁸

⁶ Fischer projections of *erythrose* (left) and *threose* (right), viz. stereoisomers of tetrose.

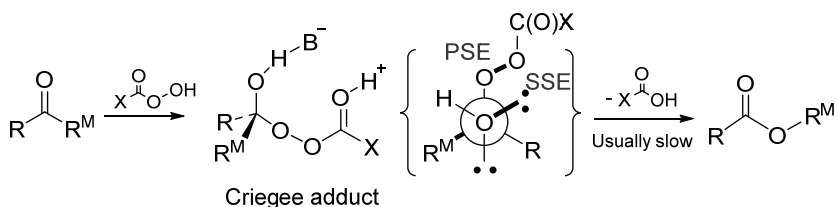


⁷ Suggest a type of acid catalysis.

⁸ Baeyer A, Villiger V, *Ber Dtsch Chem Ges*, **1899**, 32, 3625.

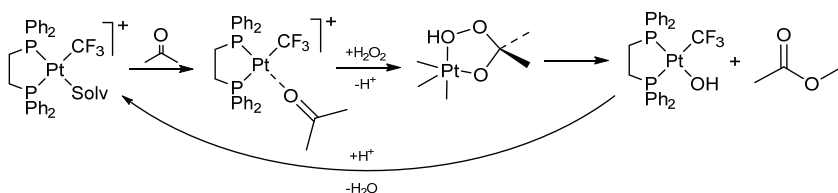


Mechanism as proposed by Criegee is presented in Scheme 10.2.1.⁹ R^M is the migrating group. R^M needs to be antiperiplanar to the O–O bond of the leaving group (primary stereoelectronic effect, PSE) and antiperiplanar to a lone pair of the hydroxyl group (secondary stereoelectronic effect, SSE).



Scheme 10.2.1. Mechanism of Bayer-Villiger oxidation involving the Criegee intermediate. For details, see text.

Baeyer-Villiger reactions are also catalyzed by metal complexes. The mechanism of oxidation of acetone by H_2O_2 in the presence of $[(dppe)Pt(CF_3)]^+$ is shown in Scheme 10.2.2. Acetone coordinates first Pt^{II} as a result of substitution of a solvent molecule. Then, addition of H_2O_2 to the $Pt-O$ bond gives a five-membered cyclic intermediate which collapses into methyl acetate, the final oxidation product.

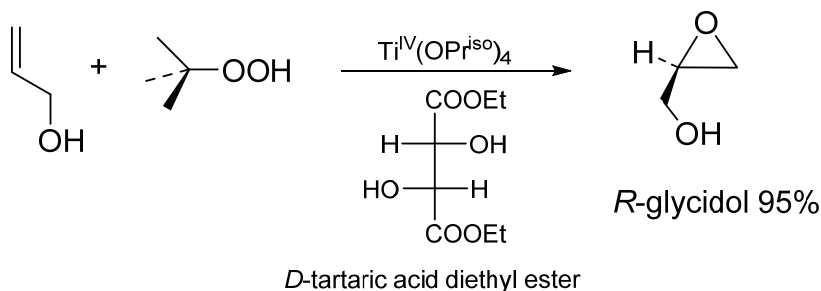


Scheme 10.2.2. Mechanism of platinum(II)-catalyzed Bayer-Villiger oxidation of acetone.

⁹ ten Brink G-J, et al, *Chem Rev*, **2004** *104*, 4105.

10.2.4. Sharpless Asymmetric Oxidation

In 2001 K. Barry Sharpless was awarded, among others, with the Nobel Prize in Chemistry for his works on asymmetric oxidation of prochiral molecules. A representative example in Scheme 10.2.3 shows asymmetric oxidation of allyl alcohol by *tert*-butylperoxide catalyzed by homoleptic tetrakis alkoxide complex of titanium(IV). The reaction was run in CH₂Cl₂ as a solvent at 25 °C in the presence diethyl ester of *D*-tartaric acid used as an asymmetric inductor and resulted in 95% yield of *R*-glycidol.



Scheme 10.2.3. Asymmetric oxidation of allylic alcohol into *R*-glycidol.

Problems

10-1. Formulate conditions which are the most favorable for running the Fenton chemistry.

10-2. Define dimerization, oxidation and reduction pathways in the Fenton oxidations. Specify conditions under which the pathways mentioned above occur.

10-3. What should be usually done for switching from the Fenton chemistry to radical-free heterolytic oxidations by hydrogen peroxide?

10-4. Specify key pathways that make different the reactivity behavior of alkanes and arenes in the Fenton systems.

10-5. What are primary and secondary stereoelectronic effects (PSE and SSE, respectively) in the mechanism of the Baeyer-Villiger reaction suggested by Criegee ?

LECTURE 11.

BIOOXIDATION: PEROXIDASES, CYTOCHROMES P450 AND CATALASES

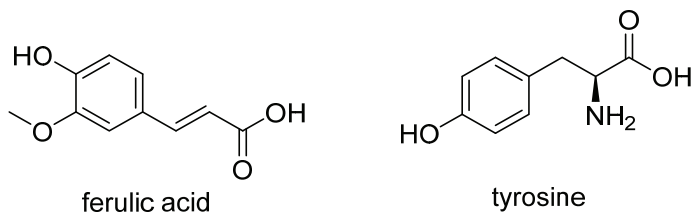
11.1. Horseradish Peroxidase (HRP)

11.1.1. Introduction

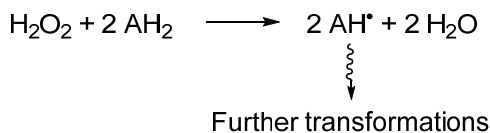
Peroxidases are enzymes that catalyze oxidation of a variety of targets by hydrogen peroxide.¹ Names of particular peroxidases may specify either their particular substrates, to which peroxidases are the most specific, or sources, from which they are isolated. The former, for example, are ascorbate and lignin peroxidases. The latter are turnip and horseradish peroxidases (HRP). Active sites of peroxidases are variable as well as the mechanisms of catalysis. Heme peroxidases including HRP incorporate iron(III) complex of protoporphyrin IX. Their mechanisms of catalysis have a number of similarities and therefore just one, horseradish peroxidase, is selected here for a systematic analysis.

Substrates of HRP are aromatic amines, phenols, indoles, sulfonates, which are usually oxidized into oligomers or polymers. HRP is thus an enzyme with a broad substrate specificity. Its role in nature is still disputable. The enzyme could be (*i*) responsible for decomposition of H₂O₂ in plants or (*ii*) involved in chemical transformations because the oxidative coupling of phenol derivatives such as ferulic acid or tyrosine could lead to polymeric compounds which contribute to healing of wounds.

¹ Dunford HB, *Heme Peroxidases*, Wiley, NY, 1999.



Because of a broad substrate specificity, the stoichiometry of catalysis by HRP is convenient to present as in Scheme 11.1.1. Two oxidation equivalents of H_2O_2 are initially distributed between two substrate molecules AH_2 (donors of electrons). Each AH_2 substrate undergoes one electron oxidation first to give an AH^\bullet radical which is then rapidly oxidized into final products.



Scheme 11.1.1. Stoichiometry of catalysis by horseradish peroxidase (HRP).

11.1.2. Composition of HRP (Isoenzyme C)

The composition of horseradish peroxidase based on an X-ray structural investigation is presented in Fig. 11.1.1. Its polypeptide chain is shown as a ribbon and heme, the essential element of the active site, is emphasized using a stick model.

The essential compositional elements of HRP are the following.

- There is a single polypeptide chain with 308 amino acid residues.
- There are four S–S bridges involving cysteine residues 11-91, 44-49, 97-301, and 177-209, which contribute essentially to the stabilization of the protein tertiary structure.
- HRP is a glycoprotein with 8 carbohydrate chains attached to aspartic acid residues.
- Heme, an iron(III) complexed to protoporphyrin IX (Fig. 11.1.1), is a key component of the active site. It is a *prosthetic* group because heme is tightly bound to the protein via a coordinative Fe–N bond involving a histidine residue.
- The molecular mass of HRP is ca. 44,000 Da.

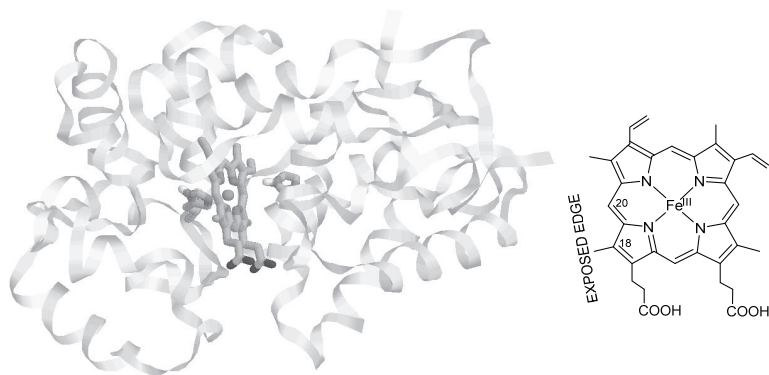


Figure 11.1.1. Structure of HRP (left) and heme, the key component of its active site (right). See text for details.²

- Horseradish peroxidase consists of seven isoenzymes (A1, A2, A3, B, C, D, and E) which differ mainly in the isoelectric point³ (pI) values.
- The most common is isoenzyme C with $pI \sim 7$.

Heme is firmly bound to the apoenzyme⁴ via coordinative Fe–N bond (Fig. 11.1.2). The donor nitrogen atom is a part of the His170 residue, which is referred to as a proximal histidine. In the resting state, the coordination number of iron(III) at pH ca. 10 and below is five. Under basic conditions, iron(III) coordinates hydroxide ion to form a six-coordinate species (Fig. 11.1.2). Equal amounts of five- and six-coordinate iron is observed at pH around 11 and therefore this value is the effective pK_a .

² Ryabov AD, *Adv Inorg Chem*, **2004**, 55, 201.

³ Value of pH at which the overall charge of a molecule is zero.

⁴ An enzyme with dissociated active site.

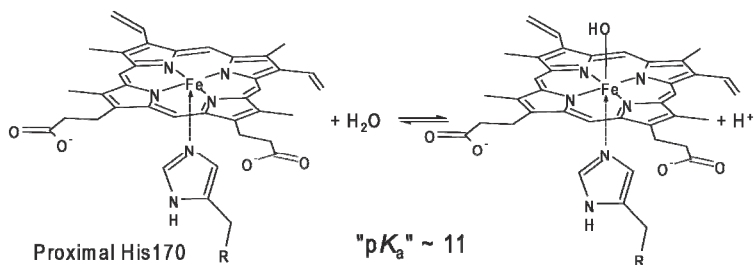
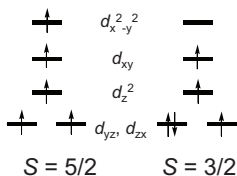


Figure 11.1.2. Reversible transition from 5- to 6-coordinated heme of HRP under basic conditions with effective pK_a around 11.

The spin state of iron(III) in the resting state is mixed. There are $S = 5/2$ and $S = 3/2$ species as in the diagram below.



The stoichiometric mechanism of catalysis by HRP is shown in Fig. 11.1.3. The resting state of HRP reacts with H₂O₂ to form the so-called Compound I which is by two oxidation equivalents above the resting state. Compound I is reduced by one electron by an electron donor AH₂ and transforms into Compound II which is by one oxidation equivalent above the resting state. Compound II also undergoes one electron reduction by AH₂ with a regeneration of the resting state. One electron oxidation of AH₂ by both Compound I and II give radical species AH• which are rapidly oxidized into final products.

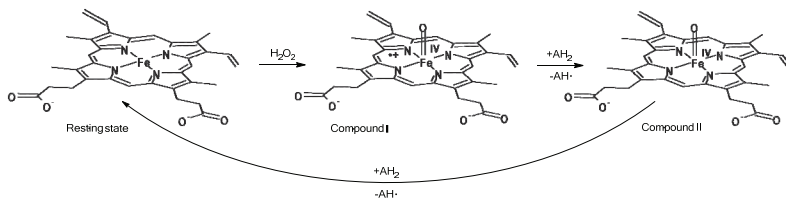
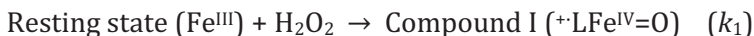


Figure 11.1.3. Stoichiometric mechanism of catalysis by of HRP. See text for details.

Compound I is an iron(IV)oxo species, which accounts for one oxidation equivalent above the iron(III) resting state. The second oxidation equivalent in the form of a radical-cation is delocalized around the aromatic porphyrin ring. There is a true double oxygen-iron oxoferryl $\text{Fe}^{\text{IV}}=\text{O}$ bond of 1.64 Å as measured by the EXAFS spectroscopy. Formal reduction potentials E° between Compounds I and II ($E^{\circ}(\text{CI/CII})$) and Compound II and the resting state $E^{\circ}(\text{CII/HRP})$ both equal ca. 0.9 V (vs NHE) though reactivities of Compounds I and II vary noticeably.

11.1.3. Kinetics and Mechanism of HRP

It is kinetically convenient to rewrite the mechanism in Fig. 11.1.3 as a sequence of elementary steps (Scheme 11.1.1).



Scheme 11.1.1. A kinetic version of HRP mechanism.

The corresponding rate expression for the steady-state oxidation of AH_2 when concentrations of AH_2 and H_2O_2 are much higher than $[\text{HRP}]$ is equation 11.1.1 (see Lecture 3, problem 3-6).

$$-\frac{d[\text{AH}_2]}{dt} = \frac{2k_1k_2k_3[\text{H}_2\text{O}_2][\text{AH}_2][\text{HRP}]}{k_1(k_2 + k_3)[\text{H}_2\text{O}_2] + k_2k_3[\text{AH}_2]} \quad (11.1.1)$$

Compound I is usually by a factor of ca. 100 more reactive than Compound II ($k_2 \sim 100k_3$) and therefore eq 11.1.1 simplifies to eq 11.1.2 because $(k_2 + k_3) \approx k_2$.

$$-\frac{d[\text{AH}_2]}{dt} = \frac{2k_1k_3[\text{H}_2\text{O}_2][\text{AH}_2][\text{HRP}]}{k_1[\text{H}_2\text{O}_2] + k_3[\text{AH}_2]} \quad (11.1.2)$$

The latter shows that (i) the steady-state of oxidation of AH_2 does not depend on k_2 , i.e. the reactivity of Compound I; (ii) eq 11.1.2 predicts ascending hyperbolic dependencies of reaction rates on concentrations

of both AH_2 and H_2O_2 . These are the Michaelis type dependencies which are often associated with the formation of enzyme-substrate complexes (see Lecture 3). Note that eq 11.1.2. for HRP was derived without assuming the formation of enzyme-substrate intermediates.

Experimental data in Fig. 11.1.4 for the peroxidase-catalyzed oxidation of Ru^{II} cyclometalated complex $[\text{Ru}(\text{2-phy})(\text{phen})_2]\text{PF}_6$ by H_2O_2 (eq 11.1.3) obtained by uv-vis spectroscopy validate eq 11.1.2 by revealing ascending hyperbolic growths of the rate of $\text{Ru}^{\text{II}} \rightarrow \text{Ru}^{\text{III}}$ conversion with increasing of concentrations of both H_2O_2 and Ru^{II} .

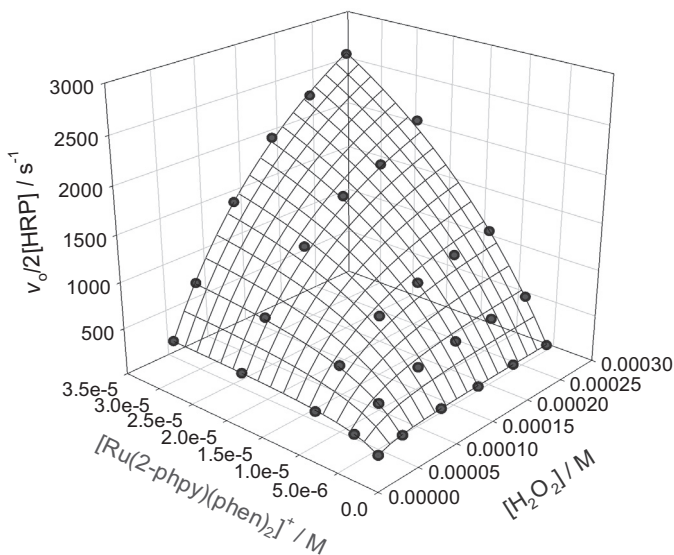
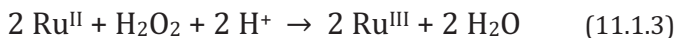
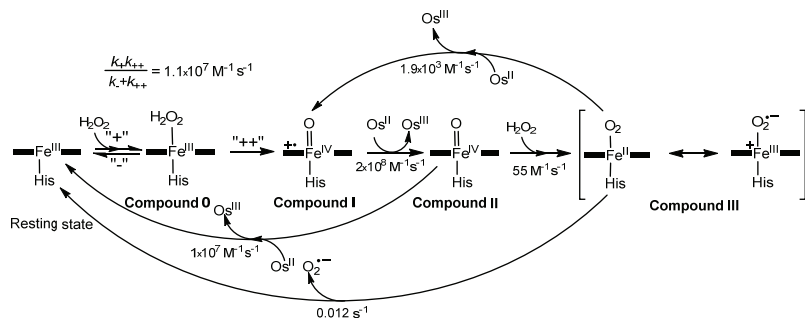


Figure 11.1.4. 3D plot showing steady-state rate of the HRP-catalyzed oxidation of Ru^{II} complex (1,10-phenanthroline analogue of **4.2**) by H_2O_2 against $[\text{H}_2\text{O}_2]$ and $[\text{Ru}^{\text{II}}]$ at $[\text{HRP}] 5 \times 10^{-11} \text{ M}$, pH 6.7, 2% MeOH, 25 °C.⁵ Reprinted with permission. Copyright 2001 American Chemical Society.

The mechanism of catalysis by HRP involving Compound I and Compound II intermediates (Fig. 11.1.3 and Scheme 11.1.1) accounts for nicely basic kinetic features of this enzymatic reaction. However, it

⁵ Ryabov AD, et al, *Inorg Chem*, **2001**, *40*, 6529.

is incomplete because the experts operate frequently with Compounds 0 and III in addition to Compounds I and II. The detailed mechanism of catalysis by HRP with intermediate Compounds 0 and III is presented in Scheme 11.1.2.



Scheme 11.1.2. Detailed mechanism of catalysis by horseradish peroxidase involving Compounds 0, I, II, and III; the donor of electrons Os^{II} is osmium(II) complex $\text{cis-}[\text{Os}^{\text{II}}(\text{bpy})_2\text{pyCl}]^+$. Numbers are the corresponding rate constants.⁶

Compound 0 is a postulated intermediate in which H_2O_2 is reversibly (k_+ , k_-) coordinated to iron(III) of the resting state to form an octahedral species. It transforms to Compound I with the rate constant k_{++} . Thus, the experimentally measured rate constant $k_1 = k_+ k_{++} / (k_+ + k_-)$. The value of k_1 for HRP equals $1.1 \times 10^7 \text{ M}^{-1} \text{ s}^{-1}$ under the optimal conditions, i.e. HRP is very efficient in activating the H_2O_2 molecule. The donor of electrons in Scheme 11.1.2 is a one electron reducing Os^{II} complex and therefore it reduces cleanly and rapidly Compound I to Compound II. The latter is also rapidly reduced by Os^{II} to the resting state. Compound II may much slower react with H_2O_2 to produce Compound III, which might be viewed either as iron(II) complex with coordinated dioxygen O_2 or iron(III) complex with coordinated superoxide $\text{O}_2^{\cdot-}$. Slow dissociation of the latter from Compound III leads to the resting state of the enzyme. Rate constants were measured for the majority of steps in Scheme 11.1.2. Note that $k_1 \gg k_2$ though the reduction potentials $E^\circ(\text{CI/CII})$ and $E^\circ(\text{CII/HRP})$ are practically identical. To understand this effect, one should look at the position of heme within the protein globule (Fig. 11.1.1). Heme is deeply embedded in the protein; iron(III) and the $\text{Fe}^{\text{IV}}=\text{O}$ unit of Compounds I and II are not exposed to the

⁶ Dequaire M, et al, *JACS*, **2002**, *124*, 240.

enzyme surface. Donors of electrons cannot approach $\text{Fe}^{\text{IV}}=\text{O}$. The heme itself is embedded such that one of its edges is exposed to the surface and electron donors come close to it easily. The second oxidation equivalent of Compound I is localized (or better to say delocalized) at the aromatic porphyrin ligand. Thus, the electron transfer distance is much lower than in the case of Compound II where the electron should travel from AH_2 to the $\text{Fe}^{\text{IV}}=\text{O}$ unit, which sits deep within the protein globule.

11.1.4. How to Measure Reactivities of Compounds I and II?

It was mentioned above that kinetic studies of HRP-catalyzed oxidation of electron donors AH_2 by H_2O_2 under the steady state conditions do not allow to access k_2 because of the condition $k_2 \gg k_3$. As a result, reaction rates follow eq 11.1.2 which does not contain k_2 . Fortunately, uv-vis spectra of the resting state, Compounds I and II of HRP are (i) all different and (ii) the corresponding, known as Soret bands are so intense in the visible region that they are not usually obscured by excess of AH_2 (Fig. 11.1.5). Thus, reactivities of the resting state (RS), Compounds I and II (CI and CII, respectively) are measurable directly in single turnover experiments. Note that the above $\text{RS} \rightarrow \text{CI} \rightarrow \text{CII}$ series of events resemble the case of consecutive reactions $\text{A} \rightarrow \text{B} \rightarrow \text{C}$ analysed in detail in Lecture 2. Certain rules should be applied in order to measure the corresponding pseudo-first order rate constants correctly. This refers to steps $\text{RS} \rightarrow \text{CI}$, $\text{CI} \rightarrow \text{CII}$ and $\text{CII} \rightarrow \text{RS}$. In particular, the reactivity of Compound I should be measured at 411 nm which is the isosbestic point between the HRP resting state and Compound II because kinetic data will not be affected at all, if Compound II will further be converted to RS. Similarly, the reactivity of Compound II should be measured 427 nm which is the isosbestic point between RS and CI.

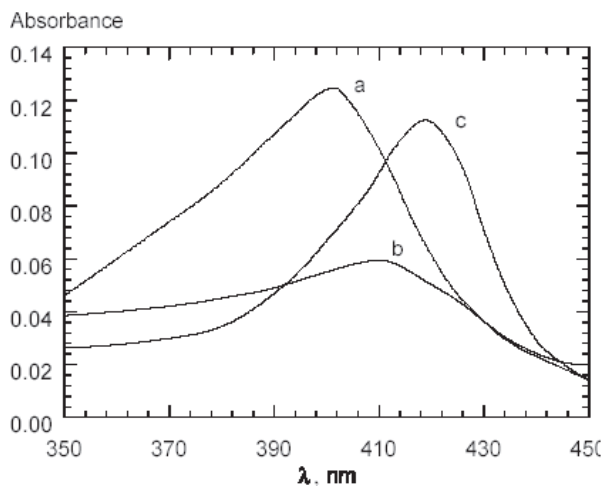


Figure 11.1.5. The *Soret* spectra of native (resting state) HRP (a), Compounds I (b) and II (c); [HRP] = 1.2×10^{-6} M, pH 6.0, 25 °C. Compound I was obtained upon addition of 1.2×10^{-6} M H_2O_2 followed by addition of 1.2×10^{-6} M $\text{K}_4[\text{Fe}(\text{CN})_6]$ to obtain Compound II. From ref. 7.

Another aspect of single turnover experiments with enzymes to be taken into account is that enzymatic reactions are usually too fast to be measured by conventional spectroscopy and therefore methods of rapid kinetics should be applied. Such, for example, is a stopped-flow technique. Its simplest two-syringe version is presented in Fig. 11.1.6.

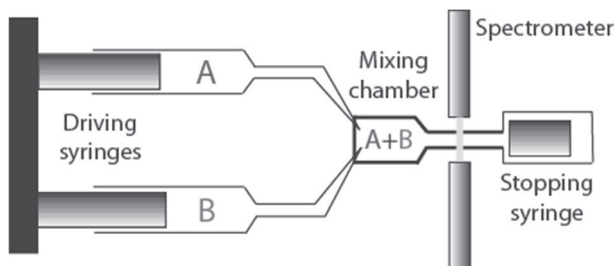


Figure 11.1.6. Basic principles of the stopped-flow technique.

Two reacting solutions A and B are rapidly mixed in a mixing chamber by two driving syringes and a reaction starts. Spectral changes are registered by a rapid scan diode array spectrometer. A dead time of

such instruments is around 10^{-3} s. As an example of application of a stopped-flow technique to the HRP catalysis, consider the catalyzed 1e oxidation of ferrocenes FcR into ferricenium cations FcR^+ by H_2O_2 (eq 11.1.4 and Fig. 11.1.7).



Ferrocenes are yellow orange; ferricenium cations are deep blue. The oxidation is accompanied by spectral changes as in Fig. 11.1.7 and steady-state kinetics is easy to monitor by conventional uv-vis spectroscopy for calculation of the rate constants k_3 using eq 11.1.2.

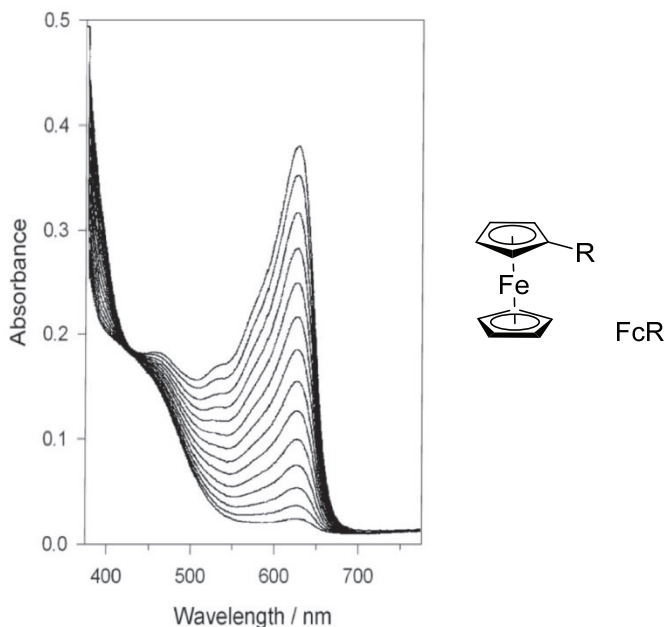


Figure 11.1.7. A growth of absorbance due to oxidation of ferrocene (FcR , $\text{R} = \text{H}$) into ferricenium ion (FcR^+) in aqueous medium.

Single turnover measurements using a stopped-flow technique allow to measure k_2 and k_3 for substituted ferrocenes by monitoring conversions of HRP Compounds I and II, respectively, as it is described above. The rate constants obtained using stopped-flow technique (k_2

and k_3) and conventional spectroscopy (k_3') are compared in Table 11.1.1. Two conclusions should be made. First, the rate constants k_3 and k_3' obtained for two-water soluble ferrocenes are close. Second, there is a typical of HRP higher reactivity of Compound I compared to that of Compound II — the gap is a factor of 100.

Table 11.1.1. Second-order rate constants for the oxidation of ferrocenes by HRP Compounds I (k_2) and II (k_3) (pH 6.0, 25 °C) and for their HRP-catalyzed steady-state oxidation (k_3') ($[H_2O_2] = 2.4 \times 10^{-4}$ M, pH 6, 25 °C).⁷

Substrate	Stopped-flow		Steady-state
	k_2 ($M^{-1} s^{-1}$)	k_3 ($M^{-1} s^{-1}$)	k_3' ($M^{-1} s^{-1}$)
FcCOOH	$(100 \pm 4) \times 10^4$	$(112 \pm 8) \times 10^2$	$(89 \pm 3) \times 10^2$
FcCH ₂ NMe ₂	$(26.8 \pm 0.9) \times 10^4$	$(25.4 \pm 0.7) \times 10^2$	$(23.9 \pm 0.6) \times 10^2$

11.1.5. Intimate Mechanism of Activation of H₂O₂ by HRP

The HRP story will be concluded by the intimate mechanism of heterolytic activation of H₂O₂. Not just iron(III) of heme will now be involved but the key amino acid residues of the protein as well. These functionalities combined contribute to a super-efficient catalytic machine (Fig. 11.1.8) which cleaves H₂O₂ with a rate constant higher than $10^7 M^{-1} s^{-1}$.

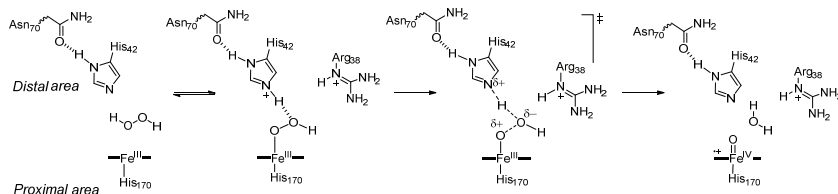


Figure 11.1.8. Intimate mechanism of H₂O₂ activation by horseradish peroxidase. See text for details.

⁷ Goral VN, Ryabov AD, *Biochem Mol Biol Int*, **1998**, *45*, 61.

Hydrogen peroxide approaches iron(III) of heme from the *distal* area. Proton of H₂O₂ moves to histidine 42; the Fe–O^αO^βH bond is formed and the entire unit is stabilized by a hydrogen bond involving protonated histidine 42 and the β oxygen of the coordinated peroxide anion. The heterolytic cleavage of the peroxide O–O bond, which happens next, is assisted by arginine 38. Compound I is produced after a formal departure of a water molecule, which is always a good leaving group.

Table 11.1.2. Rate constants k_1 for the formation of Compound I from H₂O₂ and selected peroxidases or catalases in water.⁸

Entry	Enzyme with peroxidatic or catalatic activity	pH (T / °C)	$k_1 / \text{M}^{-1} \text{s}^{-1}$
1	Pea cytosolic ascorbate peroxidase	7.8 (20)	8.0×10^7
2	Yeast cytochrome <i>c</i> peroxidase	6.1 (25)	3.4×10^7
3	Yeast cytochrome <i>c</i> peroxidase	6.1 (25)	1.4×10^7
4	Horseradish peroxidase	4.7 (25)	1.7×10^7
5	Myeloperoxidase (<i>H. sapiens</i>)	7.0 (25)	2.3×10^7
6	Manganese peroxidase (<i>P. chrysosporium</i>)	4.5 (28)	2.0×10^6
7	Soybean cytosolic ascorbate peroxidase	7.0 (20)	3.3×10^7
8	Chloroperoxidase (<i>Caldariomyces fumago</i>)	4.7 (25)	2.4×10^6
9	Hog thyroid peroxidase	7.5 (20)	7.8×10^6
10	Turnip peroxidase P7	3.5 (25)	1.6×10^6
11	Lignin peroxidase H8 (<i>P. chrysosporium</i>)	3.5 (25)	5.4×10^5
12	Catalase (Horse erythrocyte)	6.7 (25)	3×10^7
13	Catalase (Beef liver)	7.0 (25)	5.6×10^6
14	Microperoxidase-8	5.0 (25)	680
15	Hemin	10 (25)	~1

Nature awarded peroxidases (other than HRP) and catalases with the ability to activate H₂O₂ very fast. Representative examples are in Table 11.1.2. Heme units without or with a minimalistic number of amino acid residues (hemin and microperoxidase-8, entries 15 and 14,

⁸ Ghosh A, et al, *JACS*, **2008**, *130*, 15116.

respectively) activate H_2O_2 by orders of magnitude slower than proteins emphasizing the importance of heme microenvironment of in catalysis.

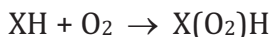
11.2. Cytochromes P450: Functions and Biological Role

11.2.1. General Features

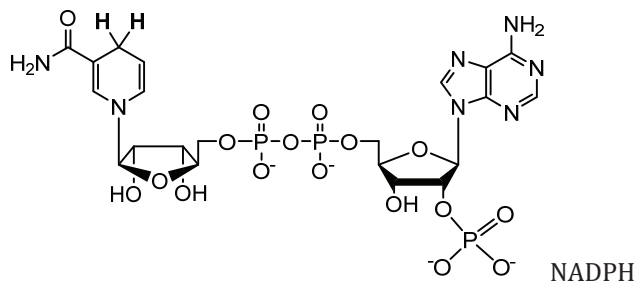
Cytochromes P450 are a superfamily of heme containing enzymes that oxidize organic compounds RH by dioxygen in the presence of sacrificial reducing agent AH_2 , the role of which is commonly played by NADPH:



Cytochromes P450 are *monooxygenases* because one oxygen atom from O_2 is transferred at RH by this differing from *dioxygenases* which transfer both oxygen atoms:



The term "P450" comes from the absorption maximum of the enzyme at 450 nm in the uv-vis spectrum of its reduced state in a complex with carbon monoxide (see below). Cytochromes P450 are three substrate enzymes. They require an H-donor AH_2 which is usually NADPH.

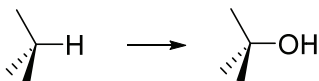


11.2.2. Reactions of Cytochromes P450

Cytochromes P450 are often membrane-bound enzymes of a broad substrate specificity. The enzymes catalyze numerous oxidative processes and have been most actively studied in the mammalian liver

because of their involvement in drug and xenobiotic metabolism. Cytochromes P450 target at hydrophobic, poorly water soluble molecules (steroids, fatty acids). Hydroxylation increases their solubility providing "*membrane detoxification*" because oxidized organic materials (see reactions below) are more hydrophilic than parent hydrophobic compounds and are easier removed.

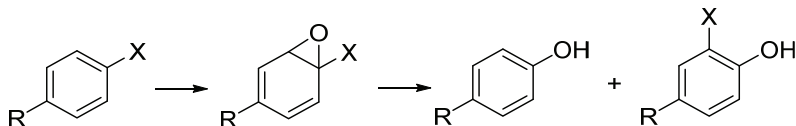
The tremendous attention to cytochromes P450 during several last decades was due to hydroxylation of alkanes involving the activation of sp^3 C-H bonds:



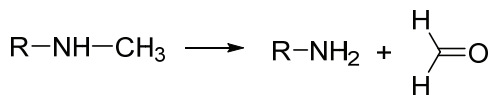
Other reactions to consider are epoxidation of alkenes and oxygenation of alkynes:



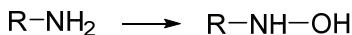
Epoxidation and hydroxylation of arenes/NIH shift (NIH is the National Institute of Health):



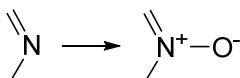
N-Dealkylation:



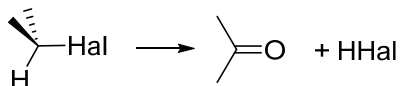
N-Hydroxylation of amines:



N-Oxidation:



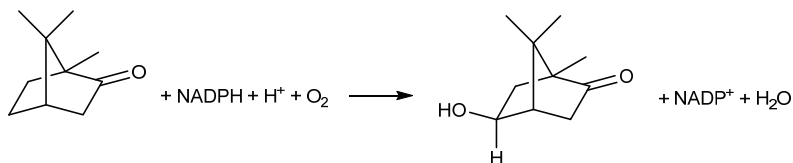
Oxidative dehalogenation:



11.2.3. Composition of Cytochrome P450 (*Pseudomonas putida*)

The X-ray structural information for cytochrome P450 from *Pseudomonas putida* was obtained for its complex with camphor located in the distal zone of the enzyme. The essential compositional elements of cytochrome P450 are the following (principal structural variances with horseradish peroxidase are underlined).

- There is a single polypeptide chain with 414 amino acid residues.
- Heme is a *prosthetic* group as it is tightly bound to the protein via a coordinative Fe-S bond involving proximal cysteine-357.
- Heme is surrounded by apolar residues. Ferryl oxygen of Fe^{IV}=O is accessible to substrates.
- No edge is accessible to the molecular surface; the closest approach to the surface is 8 Å at the proximal face.
- The molecular mass is ca. 45,000 Da.
- Camphor is a substrate (5-6 H₂O's are replaced on binding):

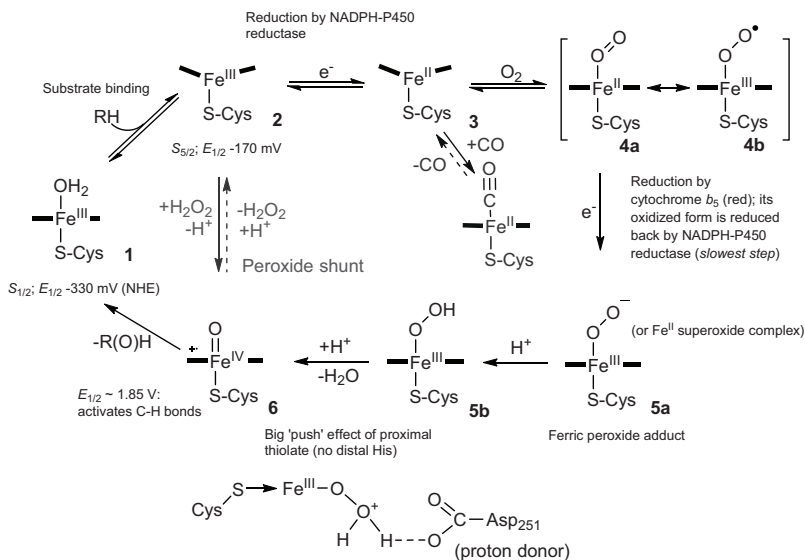


These structural assets, inter alia, make cytochromes P450 an enormously powerful biological oxidizing agent with the reduction potential in the range of 1.8–2.3 V versus NHE between its most oxidized and the resting iron(III) state! This is a key for understanding broad substrate specificity of cytochromes P450 including their ability to cleave nonactivated C–H bonds of organic compounds.

11.2.4. Mechanism of Cytochrome P450

The mechanistic chemistry of cytochromes P450 shown in Scheme 11.2.1 is noticeably more complex than that of peroxidases. Several steps of the cytochrome P450 catalytic machine involve enzymes such as NADPH-P450 reductase and cytochrome b_5 (red). Getting inside the major rules of catalysis by cytochromes P450 makes it more easy understanding catalytic mechanisms of other metal containing oxidizing enzymes that utilize O_2 or H_2O_2 as primary oxidizing agents.

The spin of the resting iron(III) state **1** in Scheme 11.2.1 equals $\frac{1}{2}$ and the $Fe^{III/II}$ reduction potential is rather negative, of -0.33 V vs NHE. Binding of substrate RH to **1** causes a conformational change of the enzyme accompanied by variations of both the spin and $E^{\circ}(Fe^{III/II})$, which in **2** equal $\frac{5}{2}$ and -0.17 V, respectively. Essential is an increase in the potential which makes easier the reduction of iron(III) to iron(II) by NADPH-P450 reductase to form intermediate **3**.



Scheme 11.2.1. Mechanism of catalysis by cytochromes P450.⁹

⁹ Sono M, et al, *Chem Rev*, **1996**, 96, 2841.

First two steps (**1** → **2** and **2** → **3**) are thus required to convert heme Fe^{III} to Fe^{II} . This is essential because iron(II) has a much higher ability than iron(III) to bind O_2 , the primary cytochrome P450 oxidant. Binding of O_2 to **3** gives dioxygen-bound intermediate **4**, which is viewed as either an $\text{Fe}^{\text{II}}-\text{O}_2$ adduct (**4a**) or $\text{Fe}^{\text{III}}-(\text{O}_2^{\cdot-})$, a complex of iron(III) with superoxide anion (**4b**). One electron reduction of **4a/b** into ferric peroxide adduct **5a** (or ferro superoxide complex) is believed to be the slowest step, which is catalyzed by cytochrome $b_5(\text{red})$. The oxidized form of the latter is reduced by NADPH-P450 reductase likewise the **2** → **3** conversion. Protonation of **5a** gives **5b**. A crucial transformation of **5b** into **6**, i.e. cytochrome P450 Compound I, is associated with a "big push effect of proximal thiolate" (bottom of Scheme 11.2.1). Protonated carboxylic group of aspartate 251 delivers the proton at the OOH -ligand of **5b**. This creates water, a good leaving group, and the big push by thiolate forces the heterolysis of the peroxide $\text{O}-\text{O}$ bond and the formation of **6**. Ferry oxygen of this highly oxidizing Compound I is exposed to the surface making feasible hydroxylation of alkanes via the oxygen rebound mechanism (see Section 11.2.6).

Five coordinated intermediate **2** is reminiscent of the iron(III) resting state of peroxidase which reacts directly with H_2O_2 forming Compound I. Similar pathway known as a *peroxide shunt* is operative for cytochrome P450 provided H_2O_2 is present in the system. Hydrogen peroxide intercepts **2** converting it directly to **6**. Thus, cytochromes P450 possess the peroxidatic activity as well (red pathway in Scheme 11.2.1).

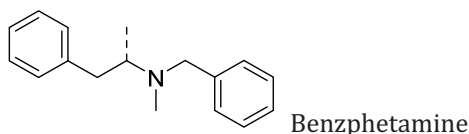
The "carbon monoxide" reason why the name of cytochromes P450 is detailed by *P450* was briefly mentioned above. Scheme 11.2.1 clarifies this. Iron(II) species have much higher ability to bind CO than O_2 . Therefore, iron(II) intermediate **3** will rather form a CO complex (blue pathway in Scheme 11.2.1) than bind O_2 . The CO iron(II) complex has a maximum at 450 nm in its uv-vis spectrum and the enzymes are named cytochromes P450.

11.2.5. Reactivity of Cytochrome P450 Compound I

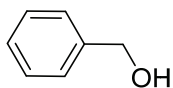
The mechanism of cytochrome P450 catalysis is complex. Reduction of Compound I may not be the rate-limiting step. The data on reactivity of Compound I is scarce. Therefore, a couple of the corresponding

examples will help to get idea about the speed of reactions of cytochrome P450 intermediates.

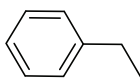
Benzphetamine is classified as an anorectic. The main function is to reduce appetite, which in turn reduces caloric intake. This drug can cause vivid hallucinations if taken for the wrong purpose. It was used for characterizing the reactivity of Compound I of CYP2B4 cytochrome P450. Compound I was made by the laser flash photolysis of Compound II that was prepared by reaction of the resting enzyme with peroxyntirite.¹⁰



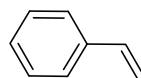
At 22 °C and pH 7.4 the oxidation of benzphetamine follows the Michaelis-Menten kinetics with $K_M = 1.1 \times 10^{-4}$ M and $k_{cat} = 50$ s⁻¹. This corresponds to the second-order rate constant of ca. 5×10^5 M⁻¹ s⁻¹ and demonstrates a high reactivity of the enzyme. However, smaller molecules, viz. benzyl alcohol, ethyl benzene and styrene are oxidized more than ten times slower, the second-order rate constants being in the range of $(0.76 - 2.7) \times 10^4$ M⁻¹ s⁻¹.



$$2.7 \times 10^4$$



$$1.25 \times 10^4$$



$$0.76 \times 10^4 \text{ M}^{-1} \text{ s}^{-1}$$

11.2.6. Mechanism of Hydroxylation of C-H Bonds

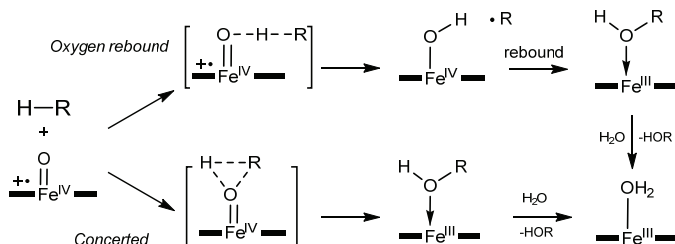
Activation of sp^3 C-H bonds by Compound I of cytochromes P450 to form alcohols (eq 11.2.2) was a true mechanistic challenge.



Debates were centered around two variants shown in Scheme 11.2.2, i.e. concerted *versus* stepwise radical (oxygen rebound) mechanisms.

¹⁰ Newcomb M, et al, *JACS*, **2008**,*130*, 13310; **2009**, *131*, 2971.

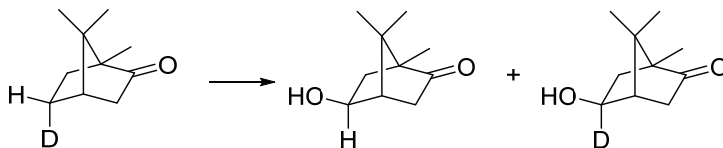
The concerted mechanism in the bottom assumes the insertion of ferryl oxygen into the C–H bond via a three-centered intermediate. No radical intermediates are involved.



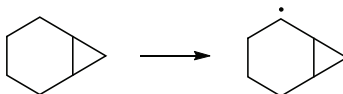
Scheme 11.2.2. Mechanisms of hydroxylation of alkanes by cytochrome P450: concerted versus radical (oxygen rebound) mechanisms.

Instead, there is a homolytic C–H bond cleavage with a concerted migration of hydrogen to form an $\text{Fe}^{\text{IV}}(\text{OH})$ intermediate and an R^\bullet radical. The radical does not go to the bulk but is attacked by the coordinated hydroxyl oxygen (oxygen rebound) to produce, after moving one electron at Fe^{IV} , an alcohol weakly bound to iron(III).

Experimental evidence favors the oxygen rebound model. Such, for example, is (i) a stereochemical scrambling:



(ii) High value of kinetic isotope effect ($k_{\text{H}}/k_{\text{D}} > 11$) observed for camphor derivatives and (iii) detection of trace amounts of the rearrangement products which were observed due to rapid radical isomerization (rate constant $2 \times 10^8 \text{ s}^{-1}$).



Norcarane

11.2.7. Peroxidases versus Cytochromes P450

Peroxidases and cytochromes P450 have a common Compound I intermediate but different chemistry. Structural studies revealed that this is due different accessibility of electron donors AH_2 to the ferryl oxo sites in these enzymes. As it was mentioned above, the site is not exposed to the protein surface of horseradish peroxidase but this is the case for cytochromes P450. Thus, none of the mechanisms in Scheme 11.2.2 is feasible for peroxidases.

There is an enzyme with features typical of both HRP and cytochrome P450. It is a heme chloroperoxidase (CLP) that catalyzes chlorination of C–H bonds of organic molecules AH in the presence of halide ions (Cl^- and Br^-) and peroxides¹¹:



Properties of CLP are somewhere between those of HRP and cytochrome P450:¹²

$$CLP = \frac{HRP + CP450}{2}$$

For example, CLP utilizes H_2O_2 is a primary oxidant as in the HRP case. CLP has a peroxidatic activity in the absence of chloride or bromide. Its heme iron is coordinated via cysteine sulfur as in cytochromes P450.

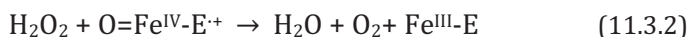
11.3. Catalase: $H_2O_2 \rightarrow \frac{1}{2}O_2 + H_2O$

Catalase is a large enzyme that catalyzes disproportionation of a tiny H_2O_2 molecule into dioxygen and water (eq 10.1.4). It is a tetramer of four polypeptide chains, each over 500 amino acids long. There is one heme per each subunit, iron(III) of which is coordinated to the deprotonated phenolic oxygen of tyrosine. Thus, catalase exemplifies a third scenario of a heme attachment to a protein globule in addition to Fe–N and Fe–S bonding in peroxidases and cytochromes P450, respectively.

¹¹ See Section 4.1 for more information about heme chloroperoxidase.

¹² Sundaramoorthy M, et al, *Structure*, **1995**, 3, 1367.

The catalytic activity occurs through a mechanism shown by eqs 11.3.1 and 11.3.2. The former reveals that, as in the HRP case, the resting state of catalase is oxidized by H₂O₂ into Compound I which is then reduced by the second hydrogen peroxide molecule releasing dioxygen and water.

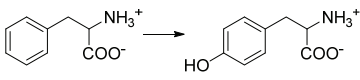
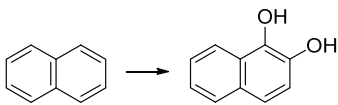
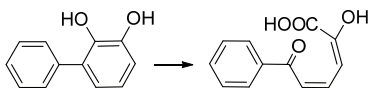
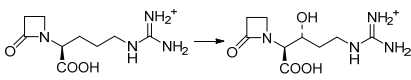


11.4. Mononuclear Non-Heme Iron Enzymes

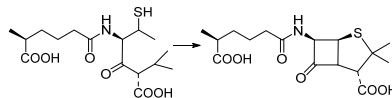
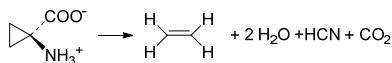
11.4.1. Overview

Nature created not only heme containing oxidizing iron enzymes. There are myriads of iron non-heme proteins. Selected examples of non-heme iron(II) enzymes that use dioxygen as a primary oxidant are shown in Table 11.4.1.¹³

Table 11.4.1. Representative examples of iron(II) non-heme proteins using O₂ as a primary oxidant.

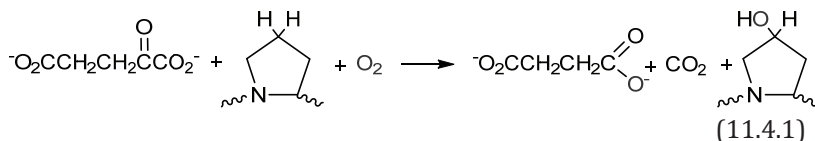
Fe ^{II} /O ₂ process	Enzyme	Catalyzed reaction
pterin-dependent hydroxylation	phenylalanine hydroxylase	
cis-hydroxylation	naphthalene 1,2-dioxygenase	
extradiol dioxygenation	dihydroxybiphenyl dioxygenase	
α-ketoglutarate-dependent hydroxylation	clavaminate synthase	

¹³ Solomon EI, et al, *PNAS*, **2003**, *100*, 3589.

4e oxidative
ring closureisopenicillin *N*-
synthaseascorbate-
dependent 2e
oxidation1-aminocyclo-
propane carboxylic
acid oxidase

11.4.2. PHD: Prolyl Hydroxylase Domain Dioxygenase

To finalize Lecture 11, let us consider in some detail structural features and mechanism of catalysis by an iron(II)/O₂ enzyme with a student-stimulating abbreviation PHD. The PHD acronym arises from *prolyl hydroxylase domain dioxygenase*. In Nature, PHD hydroxylates proline residues of α -subunits of HIF protein (hypoxia-inducible factor) via eq 11.4.1. PHD is a mononuclear iron(II) containing dioxygenase. It uses α -ketoglutarate as a co-substrate, which undergoes sacrificial decarboxylation.¹⁴



The essential compositional elements of PHD are the following.¹⁵

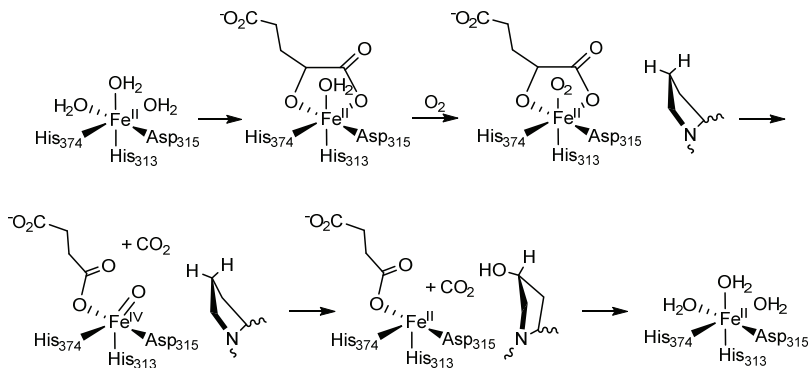
- There are over 400 amino acid residues (407 and 427 in PHD1 and PHD2, respectively).
- PHD2 crystallizes as a homotrimer.
- Six-coordinate iron(II) in the active site of the resting state is *N*-ligated by His313 and His374; it is *O*-ligated by Asp315 and three aqueous ligands.
- The enzyme in its iron(III) state generated by reactive oxygen species (oxidative burst) is inactive.

¹⁴ Fong G-H, Takeda K, *Cell Deat Differentiation* **2008**, *15*, 635

¹⁵ McDonough MA, et al, *PNAS* **2006**, *103*, 9814; Crowdhury R, et al, *Structure* **2009**, *17*, 981

- Low-molecular weight molecules may access the iron center without significant steric restrictions.

A plausible mechanism of catalysis by PHD in Scheme 11.4.1 assumes a chelation of Fe^{II} by α -ketoglutarate. The intermediate formed binds O_2 after which α -ketoglutarate undergoes decarboxylation with the formation of the reactive iron(IV)oxo intermediate which hydroxylates the proline residue via the oxygen rebound mechanism.



Scheme 11.4.1. Plausible mechanism of catalysis by PHD.

Problems

11-1. Make sure that you are now experience no problems with deriving eq 11.1.1 and simplifying it to eq 11.1.2. Rearrange eq 11.1.2 to the typical Michaelis-Menten equation with respect to concentrations of both AH_2 and H_2O_2 . Find expressions for effective values of V_{max} and K_M . Do the same for eq 11.1.1.

11-2. Consider Scheme 11.1.2. Prove that the rate constant k_1 , which describes the speed of formation of Compound I, equals $k_+ \cdot k_- / (k_+ + k_-)$.

11-3. Summarize similarities and dissimilarities of horseradish peroxidase and cytochrome P450.

11-4. Give two examples of none-heme iron containing oxidizing enzymes.

11-5. Summarize three binding modes of heme in peroxidase, cytochromes P-450 and catalase.

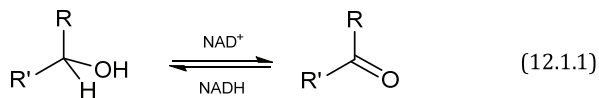
LECTURE 12.

ALCOHOL DEHYDROGENASE (ADH) AND GLUCOSE OXIDASE (GO)

12.1. Alcohol Dehydrogenases

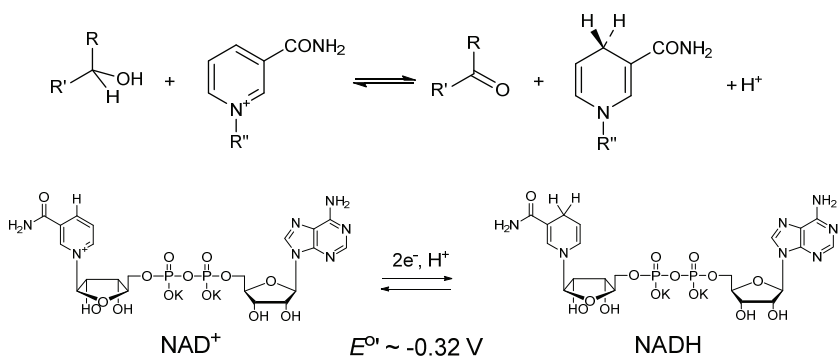
12.1.1. Introduction

Alcohol dehydrogenase (ADH) is the enzyme that makes it possible for humans to drink beer, wine, and other alcoholic beverages. Human ADH catalyzes oxidation of alcohols into aldehydes or ketones in the presence of oxidized cofactor NAD^+ (eq 12.1.1); the enzyme is "reversible", i.e. carbonyl compounds are reduced into alcohols in the presence of reduced cofactor NADH . The reduction is particularly motivating because prochiral carbonyls are converted into optically active alcohols.



Scheme 12.1.1 details eq 12.1.1 by showing all substrate and cofactor atoms involved in the transformation and reminds of that the NAD^+/NADH couple moves hydride or proton and two electrons.

Alcohol dehydrogenases are more substrate-specific enzymes compared to peroxidases and cytochromes P450. There are various other dehydrogenases and their names typically indicate substrates they are targeted at. Examples are lactate, malate, glutamate, etc., dehydrogenases. Several of them together with reactions they catalyze are displayed in Table 12.1.1.

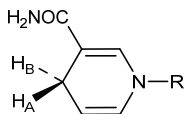


Scheme 12.1.1. Structures of cofactors NAD⁺ and NADH and the ADH-catalyzed reaction showing all key atoms involved.

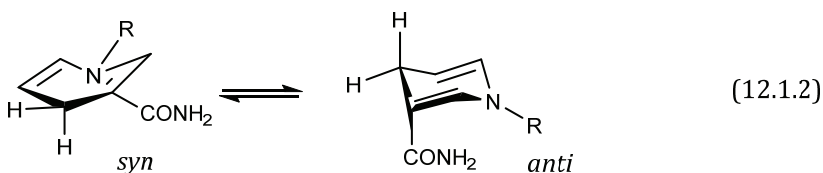
Table 12.1.1. Examples of dehydrogenases and reactions they catalyze.

Dehydrogenase	Class	Catalyzed reaction
alcohol	A	$\text{H}_3\text{CCH}_2\text{OH} \rightleftharpoons \text{H}_3\text{CCHO}$
lactate	A	
malate	A	
glutamate	B	
glucose-6-phosphate	B	
3-glycerol phosphate	B	

The reduced nicotine amide ring of NADH contains prochiral (diastereotopic) hydrogen atoms H_A and H_B . Some dehydrogenases move H_A , some move H_B . They belong to classes A and B, respectively.

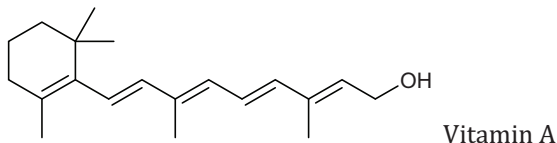


Reactivity of carbonyl compounds in Table 12.1.1 is different. More reactive carbonyls are reduced by dehydrogenases of class A. Correspondingly, less reactive carbonyls are reduced by dehydrogenases of class B. This is due to the fact that the nicotine amide ring of NADH adopts *syn* and *anti* conformations (eq 12.1.2). Interestingly, NADH is more reactive when *anti* and therefore reduces less reactive carbonyls. NADH is less reactive when *syn*. This conformer cannot reduce less reactive substrates and converts only more reactive carbonyl substrates.



12.1.2. Human Alcohol Dehydrogenase

Nature did not probably assume that humans will start to consume ethanol-containing beverages. A biological mission of human ADH is different, viz. to oxidize vitamin A (retinol) in liver.



Human ADH is a two subunit enzyme with a molecular mass of ca. 40,000 each. Each polypeptide chain contains a slightly variable number of amino acid residues (373-379). Polymorphism of the ADH gene gives β_1 , β_2 , and β_3 subunits which differ in a single mutation. In

particular, there is histidine in β_2 instead of Arg47 in β_1 and there is cysteine in β_3 instead of Arg369 in β_1 . A variety of homo- and heterodimeric enzymes $\beta_i\beta_j$ are thus possible. ADH of Chinese and Japanese contains 65% β_2 .

The essential compositional elements of ADH are the following.

- There are two subunits with a molecular mass of ca. 40,000 each.
- There are two Zn ions per subunit: one catalytic and one structural. Catalytic Zn is coordinated by two cysteins, one histidine and one H₂O, the latter being hydrogen-bonded to Ser48.
- The active site consists of the catalytic Zn and two binding domains: for the cofactor and for the substrate ("hydrophobic barrel").
- *Apo* enzyme (protein without bound cofactor) is characterized by $pK_a \sim 9.2$; *holo* enzyme (with bound cofactor) has $pK_a \sim 7.6$ due to a conformational change. It is water coordinated to zinc that undergoes deprotonation.

ADH practices the "ordered" binding of substrates and cofactors; cofactors bind first (Scheme 12.1.2). Steps 12.1.7 and 12.1.4 are believed to be rate limiting for the oxidative and reductive processes, respectively.



Scheme 12.1.2. Ordered binding of substrates in catalysis by ADH.

Effective Michaelis constants $K_{M,eff}$ are noticeably different for NAD⁺ and NADH cofactors, viz. 130×10^{-6} and 0.4×10^{-6} M, i.e. NADH has a higher affinity to the enzyme. It is a matter of common knowledge that Chinese and Japanese are stronger affected by alcohol compared to more alcohol resistant Europeans. The reason for that is the existence of β_1 , β_2 , and β_3 subunits that comprise human ADH. Enzymes composed from different β pairs have variable effective parameters of

the Michaelis-Menten equation 12.1.8 and this accounts for different catalytic activity of human ADH under certain conditions.

$$-\frac{d[\text{EtOH}]}{dt} = \frac{k_{\text{cat,eff}}[\text{EtOH}][\text{ADH}]}{K_{\text{M,eff}} + [\text{EtOH}]} \quad (12.1.8)$$

The data in Table 12.1.2 show that the values of $k_{\text{cat,eff}}$ and $K_{\text{M,eff}}$ vary significantly for alcohol dehydrogenases made of just β_1 and β_3 subunits. Both β_1 and β_3 enzymes function similar at low concentrations of EtOH ($K_{\text{M,eff}} \gg [\text{EtOH}]$) or any other alcohol like vitamin A. Equation 12.1.8 becomes eq 12.1.9.

$$-\frac{d[\text{EtOH}]}{dt} = \frac{k_{\text{cat,eff}}}{K_{\text{M,eff}}} [\text{EtOH}][\text{ADH}] \quad (12.1.9)$$

Thus, enzymatic rates are determined by the $k_{\text{cat,eff}}/K_{\text{M,eff}}$ ratio which does not differ that much for β_1 and β_3 enzymes. When EtOH content in the body is excessive,¹ the rate law changes, i.e. $-(d[\text{EtOH}]/dt) = k_{\text{cat,eff}}[\text{ADH}]$, and the enzymatic rate depends on $k_{\text{cat,eff}}$, which is more than hundred times higher for β_3 than for β_1 enzyme. Chinese and Japanese have lower $k_{\text{cat,eff}}$; their ADH systems is less effective in oxidation of administered ethanol and therefore they are getting intoxicated faster. This is how the Michaelis-Menten equation helps to understand a pseudo-mysterious Asian phenomenon!

¹ Below is official information on alcohol content, which might be interesting. *Blood/Breath Alcohol Concentration* (BAC) is the amount of alcohol in the bloodstream or on one's breath. BAC is the weight of ethanol in g, in 100 mL of blood or 210 L of breath.

0.00 g/210 L of breath is the only safe BAC level.

0.02 g/210 L - At and above this level US federal laws mandate that a person in a safety sensitive transportation job must be removed from the workplace (160 pounds: 2 beers in 1 h \Rightarrow 0.025).

0.04 g/210 L - US federal laws mandate that a person in a safety sensitive transportation job must be sanctioned and may lose the job. Also in most states a person can be convicted of driving under the influence at this level (3 beers in 1 h \Rightarrow 0.049).

0.10 g/210 L - You can be convicted of driving while intoxicated in ALL states.

0.30 g/210 L - Most people will lose consciousness.

0.40 g/210 L - Most people will become comatose and may die (10 Black Russians in 1 h \Rightarrow 0.416).

Table 12.1.2. Effective parameters of the Michaelis-Menten equation 12.1.8 for ADH from different β subunits.

Ethanol substrate	β_1	β_3
$k_{cat,eff}/K_{M,eff}$ ($\text{mM}^{-1} \text{s}^{-1}$)	1.3	0.19
$k_{cat,eff}$ (s^{-1})	0.066	7.0
$\text{pH}_{optimal}$	10.5	7.0

12.1.3. Mechanism of Catalysis by Alcohol Dehydrogenase

The active site of the resting enzyme contains zinc(II) ion, a NAD^+ binding crevice and a substrate binding pocket (Fig. 12.1.1, left). Tetrahedral zinc is coordinated by two cysteine sulfur atoms and one histidine nitrogen. The fourth coordination site is occupied by water which is hydrogen bonded to serine. Binding of NAD^+ increases the acidity of coordinated water and its $\text{p}K_a$ drops to 7.6 due to a conformational change. This prepares the active site for accepting alcohol which binds to zinc as an alkoxide (Fig.12.1.1, right).

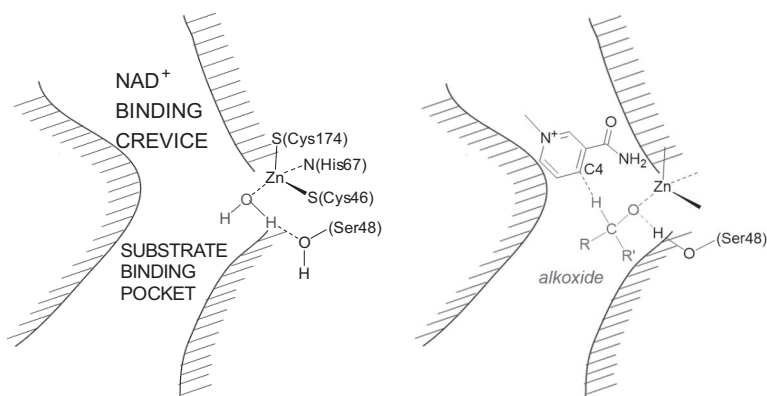
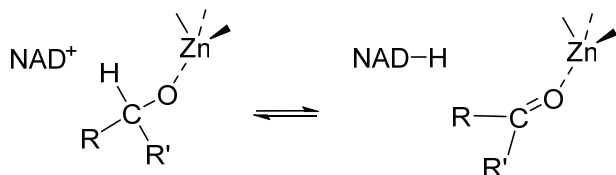


Figure 12.1.2. Mechanism of catalysis by human ADH: resting state (left) and ternary complex (right). See text for details.

The alkoxide model of substrate binding, which endures the proximity of alcohol C–H bond to be cleaved and the C4 carbon of the nicotine amide ring, is supported by the observations of the pK_a values of ethanol and 2-chloroethanol in the holoenzyme, which equal 4.5 and 6.4, respectively. In other words, alcohols turn very acidic and their OH group deprotonation to form alkoxides becomes realistic (cf. with pK_a 's of these free alcohols). The move of hydrogen from alcohol to NAD^+ is characterized by the kinetic isotope effect of 3–5.

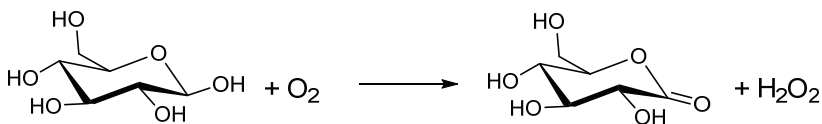


The suggested mechanism of ADH catalysis was supported by the X-ray investigation of the ADH ternary complex with NAD^+ and *p*-bromobenzyl alcohol.² The alkoxide binding of the alcohol was clearly demonstrated. The alcohol oxygen is directly ligated to the catalytic zinc atom. The zinc is tetraordinate and there is no room for a water molecule to make the zinc pentacoordinate.

12.2. Glucose Oxidase

12.2.1. Chemistry and Structure

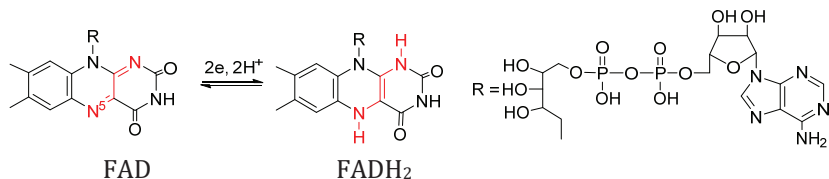
Glucose oxidase (GO) catalyzes the oxidation of β -*D*-glucose by dioxygen into γ -*D*-gluconolactone:



Although GO uses O_2 as a primary oxidant, it is a metal-free enzyme containing flavin adenine dinucleotide (FAD) in the active site. FAD oxidizes *D*-glucose and transforms into $FADH_2$ (Scheme 12.2.1), which is then reoxidized by O_2 into FAD. The E° (FAD/ $FADH_2$) reduction

² Eklund H, et al, *J Biol Chem*, **1982**, 257, 14349.

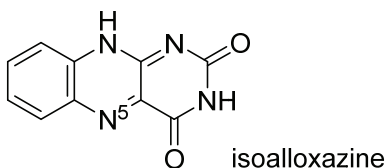
potential, which is associated with the moving of H_2 or two electrons and two protons, equals -0.22 V vs NHE. GO is a stable, resistant to denaturing and inexpensive *ideal* enzyme, as reads the title of a review from 1992.³



Scheme 12.2.1. FAD/FADH₂ couple.

The essential structural and compositional elements of GO are the following.⁴

- The enzyme from *Aspergillus niger* is a 160 kDa dimer.
- There are 120 contact points between the subunits.
- Each subunit has one tightly bound FAD (Fig. 12.2.1); there is a 40 Å separation between FAD molecules in two subunits.
- FAD is deeply buried in the protein globule; the key N5 nitrogen of the isoalloxazine ring of FAD (see Scheme 12.2.1) is separated from the surface by 13–18 Å.



- The active site of GO is at the bottom of a deep pocket, which is funnel shaped and has a cross-section of $10 \times 10\text{ Å}$. The entrance diameter is 10 Å . FAD is close to Asn514, His516, and His559.

³ Wilson R, Turner APF, *Biosens Bioelectron* **1992**, 7, 165.

⁴ Hecht HJ, et al, *J Mol Biol* **1993**, 229, 153.

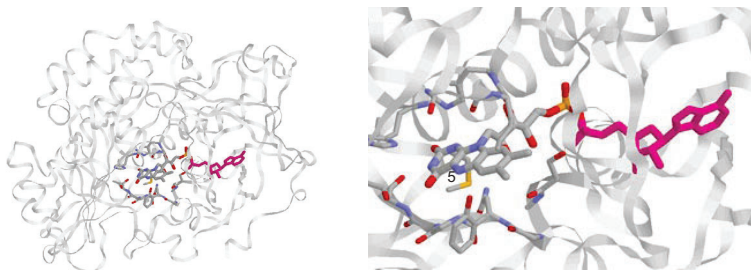
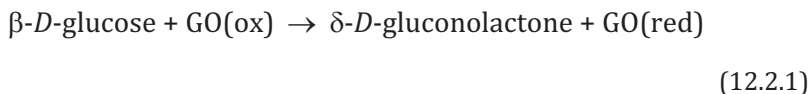


Figure 12.2.1. Subunit of GO from *Aspergillus niger* with FAD hidden inside the protein globule (left) and a FAD area of GO with amino acid residues in an 8.0 Å vicinity from the N5 atom of FAD (right).⁵

Glucose oxidase obeys a classical “ping-pong” mechanism of catalysis, i.e. involves two consecutive independent half-reactions. The native form of the enzyme, FAD-containing GO(ox), oxidizes β -D-glucose into the lactone forming the FADH₂-containing reduced enzyme GO(red), eq 12.2.1. GO(red) is then reoxidized by dioxygen, eq 12.2.2.



Step 12.2.2 is very fast, especially at pH 5, when the enzymatic activity of GO is the highest. The second-order rate constant k_3 equals $1.6 \times 10^6 \text{ M}^{-1} \text{ s}^{-1}$ but decreases more than 100-fold at pH > 8. The oxidation of FADH₂ occurs in two 1e steps. At pH 5.3 the corresponding directly obtained redox potentials for the *Aspergillus niger* enzyme equal -0.048 and -0.050 V versus NHE.

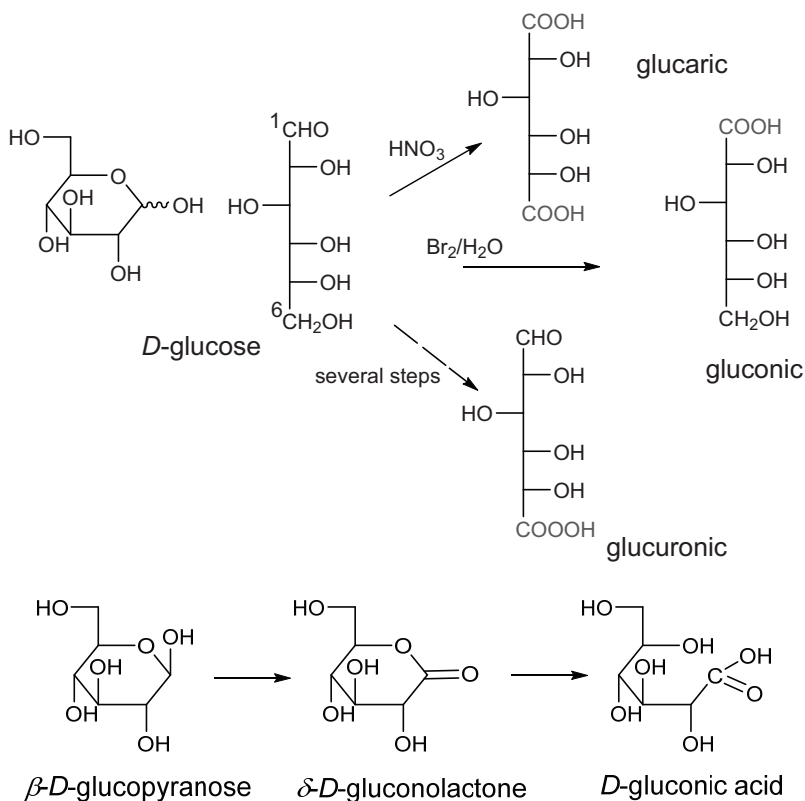
12.2.2. Oxidation of Glucose: Chemical and Enzymatic

There are several pathways of chemical and enzymatic oxidation of glucose (Scheme 12.2.2). Carbon atoms 1 and 6 of glucose bearing formyl and hydroxymethyl groups, respectively, are transformed. Nitric acid oxidizes both of them into carboxyl functions to afford *glucaric* acid. Bromine water is selective to formyl group and converts

⁵ Ryabov AD, *Adv Inorg Chem*, **2004**, *55*, 201.

glucose into *gluconic* acid. It is a delicate work to oxidize just hydroxymethyl group leaving formyl untouched. The product is *glucuronic* acid.

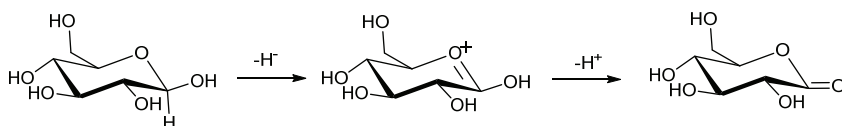
The final product of GO-catalyzed oxidation of glucose is gluconic acid though it is formed from gluconolactone, which is formed first and is not produced when bromine water as an oxidant. Thus, catalysis by GO does not truly match chemical processes. Glucose oxidase is a specific enzyme targeted at β -*D*-glucose. The α -*D*-glucose, *L*-glucose and other pyranoses are significantly less reactive.



Scheme 12.2.2. Oxidation of glucose: chemical (top) and catalyzed by glucose oxidase (bottom). See text for details.

12.2.3. Hydride Mechanism of "Glucose" Half Reaction

There are actually two mechanisms in the ping-pong catalysis by GO which correspond to steps 12.2.1 and 12.2.2. The former deals with the glucose half-reaction. Consider the hydride mechanism shown in Scheme 12.2.3. It assumes the C-H bond cleavage at the anomeric carbon C1. Hydrogen leaves as a hydride to form an oxygen-centered cationic intermediate with a double C=O⁺ bond. Deprotonation of the anomeric hydroxide gives the final lactone. There are consecutive dissociations of hydride and proton. The net result is an abstraction of H₂ consistent with a functioning of the FAD/FADH₂ couple (Scheme 12.2.1).



Scheme 12.2.3. Hydride mechanism of GO-catalyzed oxidation of glucose.

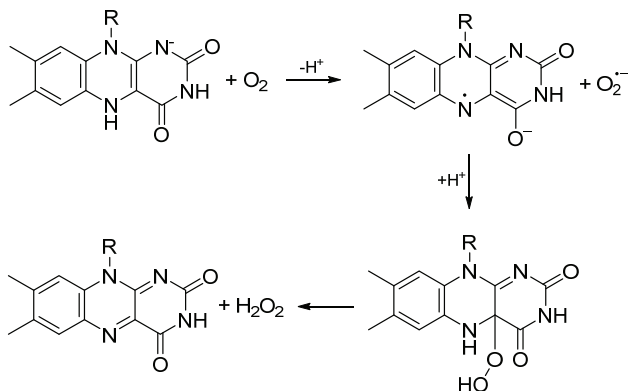
The leaving hydride is directly accepted by the N5 nitrogen of the isoalloxazine ring of FAD. The structural modeling of GO with bound β -D-glucopyranose suggests that the anomeric C-H bond is favorably directed at N5 of the isoalloxazine ring.

12.2.4. Mechanism of FADH₂ into FAD Reoxidation by Dioxygen

The second half-reaction, i.e. reoxidation of FADH₂ into FAD by O₂ in the active site of metal-free enzyme, is mechanistically more challenging because of a spin preservation issue during the oxidation by O₂. Such a problem does not exist for metal-containing enzymes. Glucose oxidase is not the case and therefore the process is worth attention.

It was mentioned above that FADH₂ reacts fast with O₂ under the optimal conditions. Thus, O₂ should act as a 1e oxidant which attacks N-deprotonated form FADH₂ with the formation of the superoxide O₂⁻ and a radical-anion intermediate, i.e. two radical species which may undergo effortless recombination (Scheme 12.2.4). Interestingly, superoxide adds to the carbon atom next to N5 of the isoalloxazine ring

affording a flavin hydroperoxide derivative, which transforms into oxidized FAD after dissociation of H_2O_2 .

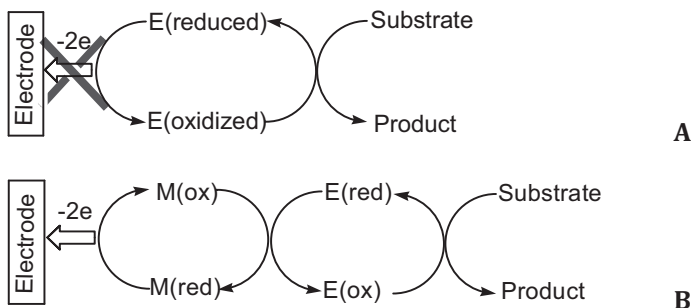


Scheme 12.2.4. Mechanism of the dioxygen half-reaction of glucose oxidase.

12.2.5. Applications of Glucose Oxidase

Glucose oxidase is broadly used due to both its ability to oxidize glucose and reduce O_2 into H_2O_2 . Importantly, GO is inexpensive and resistant to inactivation. Glucose oxidase is a part of bioanalytical amperometric instruments (biosensors), the functioning of which is based on the *mediated electron transfer* (MET). Biosensors are specific and sensitive due to a capability of enzymes to catalyze a particular reaction of a particular compound. Glucose oxidase converts *D*-glucose acquiring two electrons and two protons. These two electrons cannot be removed electrochemically at an anode because the active site sits deeply inside the protein globule. Otherwise amperometric biosensors could function as shown in Scheme 12.2.5A. The $2e$ electron abstraction is performed by O_2 . The job of dioxygen can be carried out by transition metal complexes, which are then oxidized at an electrode (Scheme 12.2.5B). The overall effect is such that electrons move from a substrate to an enzyme, then to a transition metal complex, and finally to an electrode. The electrode recognizes an enzymatic redox reaction and “reports” adequately on a substrate concentration in a sample. Scheme 12.2.5B illustrates principles of MET-based biosensors which consist of (i) an oxidoreductase that catalyzes a redox reaction, (ii) a low-

molecular-weight compound (mediator) that moves electrons between an oxidoreductase active site and an electrode, (iii) a network that keeps together an oxidoreductase and a mediator at the electrode surface.



Scheme 12.2.5. Schematic presentation of direct (non-mediated) electron transfer (A) and mediated electron transfer (B) from enzyme to electrode. M(ox) and M(red) are oxidized and reduced forms of a mediator, respectively.

In 1984 Cass, et al., reported that ferrocene and its derivatives reoxidize GO during the catalytic oxidation of *D*-glucose.⁶ The effect was monitored by cyclic voltammetry and the principal result is shown in Fig. 12.2.2. The current increased dramatically on addition of the enzyme demonstrating a perfect mediating performance of ferrocene carboxylic acid according to the mechanism in Scheme 12.2.5B. Importantly, a registered anodic peak current i_p is a function of a substrate concentration, *D*-glucose in this case. Therefore, the amount of glucose in a sample such as blood can be measured.

⁶ Cass AEG, et al, *Anal Chem* **1984**, 56, 667.

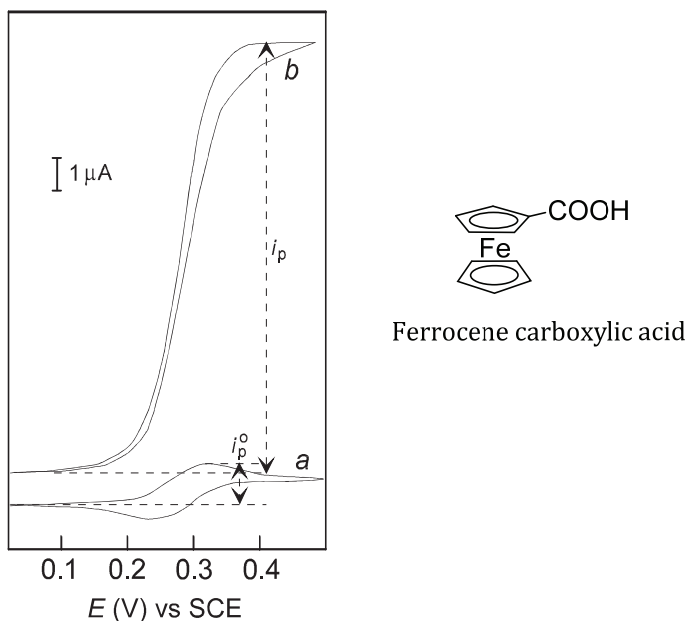
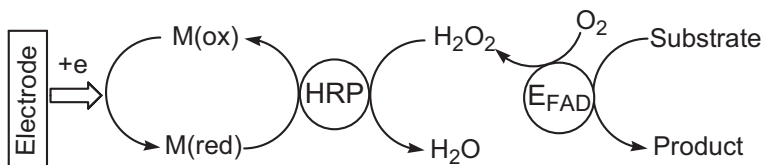


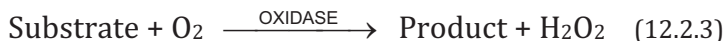
Figure 12.2.2. (a) Cyclic voltammogram of ferrocene carboxylic acid (5×10^{-4} M) at pH 7 and 25 °C, in the presence of *D*-glucose (0.05 M) at a scan rate of 1 mV s^{-1} . (b) As for (a) but with the addition of GO (1.09×10^{-5} M). Reprinted with permission. Copyright 1984 American Chemical Society.

The fact that catalysis by GO is also associated with the production of H_2O_2 is used for construction of bienzyme biosensors containing horseradish peroxidase (HRP), Scheme 12.2.6. Glucose oxidase produces H_2O_2 which oxidizes HRP. The oxidized forms of HRP are reduced by mediators and the oxidized mediators are then reduced at an electrode.



Scheme 12.2.6. Principle of action a bienzyme biosensor incorporating HRP, an oxidase (E_{FAD}), and an electron shuttle.

Many amperometric biosensors incorporated HRP and ferrocenes were designed because the system responds to H₂O₂. Hydrogen peroxide is produced not only by GO but also by other dioxygen-dependent FAD oxidases according to eq 12.2.3.



Thus, an oxidase converts a particular target substrate into a matching product and H₂O₂, the latter oxidizes ferrocene in the HRP-catalyzed process, and ferricenium formed is finally reduced at an electrode. As a result, a catalytic ensemble such as in Scheme 12.2.6 plays a tune of a particular substrate.

Problems

12-1. Compare properties of NAD⁺ and FAD in terms of numbers of electrons and protons moved.

12-2. Explain the fact that though glucose oxidase is a metal-free enzyme, its reduced form reacts rapidly with dioxygen.

12-3. Which features of glucose oxidase account for numerous applications of the enzyme? Name two of such applications.

12-4. Why can't active sites of redox enzymes be easily oxidized or reduced electrochemically at electrodes?

LECTURE 13.

COPPER PROTEINS: TYROSINASE AND LACCASE. BIOLOGICAL GENERATION OF O₂

13.1. Tyrosinase

Tyrosinase is a multicopper oxygenase. The enzyme is involved in the formation of *melanin* (skin and hair pigment). Dysfunction of its production leads to albinism. The most common pigment is *eumelanin*, i.e. cross-linked 5,6-dihydroxyindole and 5,6-dihydroxyindole-2-carboxylic acid polymers (Fig. 13.1.1).

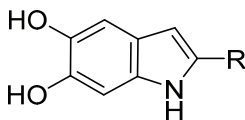
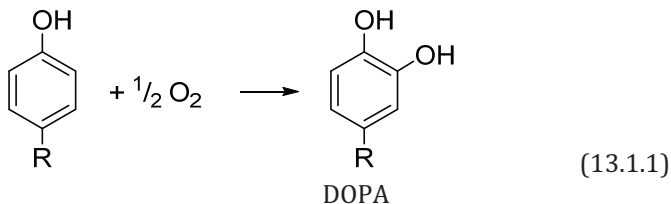
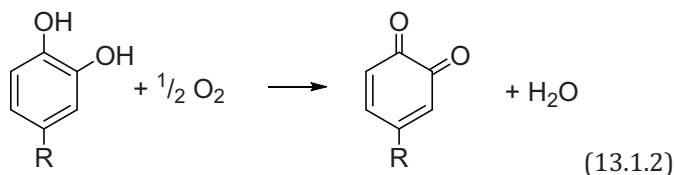


Figure 13.1.1. Eumelanin monomers: 5,6-dihydroxyindole (R = H) and 5,6-dihydroxyindole-2-carboxylic acid (R = COOH).

Tyrosinase displays both *phenolase* (eq 13.1.1) and *catecholase* (eq 13.1.2) activities; the enzyme catalyzes oxidation of tyrosine to DOPA (3,4-dihydroxyphenylalanine) and DOPA to DOPAquinone, respectively.





DOPAquinone

Tyrosinase is a copper-containing enzyme. The active site of the enzyme from *S. castaneoglobisporus* is shown in Fig. 13.1.2. There are two copper ions (type 3 copper) each surrounded by three histidine residues.

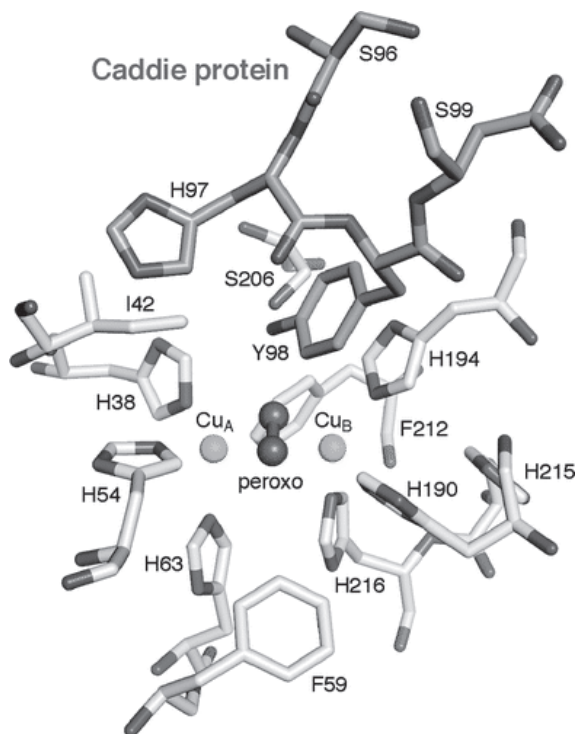
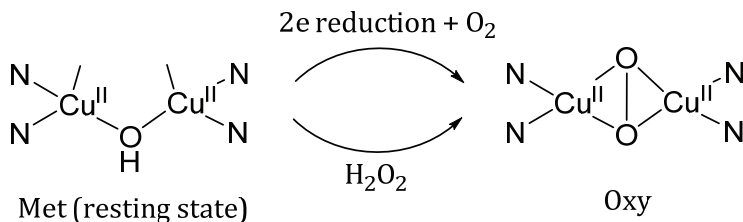


Figure 13.1.2. Oxy form of the active site of bacterial tyrosinase from *S. castaneoglobisporus* with a caddie protein which assists in transportation of two Cu^{II} ions into the catalytic center.¹ Reprinted with permission. Copyright 2007 American Chemical Society.

The resting state of enzyme (met state) contains two Cu^{II} ions bridged by one hydroxide. Their 2e reduction initiates the reaction with O₂ which results in the formation of the oxidized oxy form (Scheme 13.1.1). Note that it is the oxy form that is displayed in Fig. 13.1.2.



Scheme 13.1.1. Met and oxy forms of the type 3 copper active site of tyrosinase.

The mechanism of catalysis by tyrosinase is shown in Fig. 13.1.3.¹ The met form (bottom left) undergoes 2e reduction to form copper(I) deoxy form which accepts dioxygen and is oxidized into oxy form. The latter may display either tyrosinase or catecholase activity by reacting with tyrosine or catechol, respectively. The formation of deprotonated phenol or catechol coordinated to Cu^{II} is postulated in both cases, i.e. of oxy-phenol and oxy-catechol intermediates, respectively. The rearrangement of oxy-phenol to met-catechol features an electrophilic aromatic substitution because the Hammett ρ value equals -1.8 , which was obtained using phenols with variable R groups. Protonation of met-catechol induces intramolecular electron transfer leading to the deoxy form of tyrosinase and the liberation of *ortho*-quinone.

¹ Itoh S, Fukuzumi S, *Acc Chem Res*, **2007**, *40*, 592.

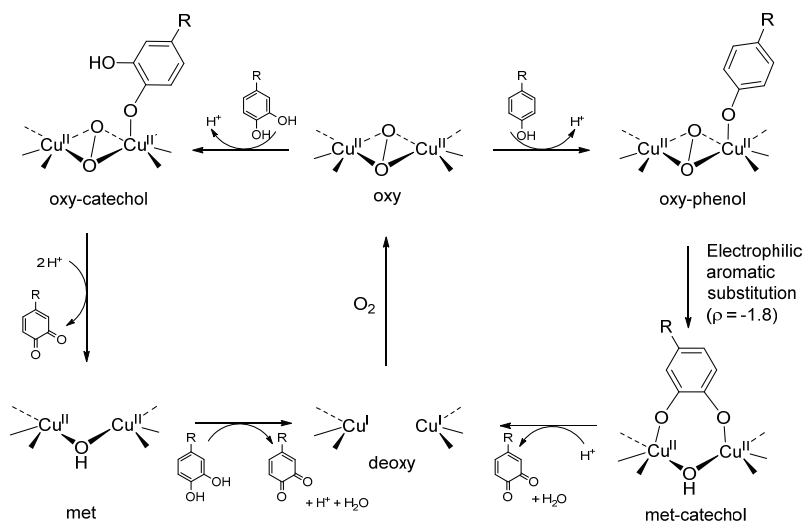
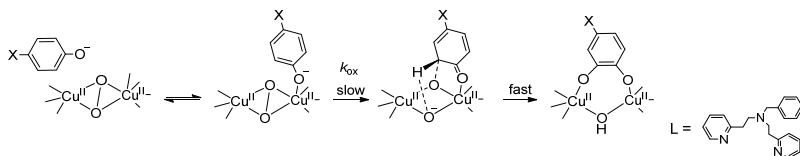


Figure 13.1.3. Mechanism of catalysis by tyrosinase showing both phenolase and catecholase activities.

Mechanistic details of the oxy-phenol \rightarrow met-catechol step were probed using a model system consisting of dinuclear copper(II) complex $[\text{Cu}^{\text{II}}_2\text{L}_2(\mu\text{-O}_2)]^{2+}$ and $\text{XC}_6\text{H}_4\text{OLi}$ (Scheme 13.1.2). The reaction was studied in acetone at -94°C and the following observations were reported. There is a Michaelis-Menten kinetics in phenolate suggesting an intermediate species; the Hammett ρ value for the k_{ox} step is -1.8 which close to the value of -2.8 observed for V_{max} in the enzymatic system; kinetic isotope effect of 1.0 was measured for the chlorophenol derivative. There are two bridging oxo ligands in the complex. One acts as an electrophile attacking the sp^2 carbon of phenolate whereas the second one acts as a base which accepts the leaving proton.



Scheme 13.1.2. Mechanism of formation dinuclear catecholate copper(II) complex from $[\text{Cu}^{\text{II}}_2\text{L}_2(\mu\text{-O}_2)]^{2+}$ and $\text{XC}_6\text{H}_4\text{OLi}$.

13.2. Laccases: a Family of Blue Proteins

Laccases belong to a family of blue copper oxidizing enzymes targeted mainly at phenols. Laccases utilize dioxygen as a primary oxidizing agent. They differ in substrate specificity and oxidizing power, i.e. there are low and high potential laccases with reduction potentials in the range of 0.4-0.8 V versus NHE. Dioxygen is reduced to water and all four oxidation equivalents of O₂ are delivered at a substrate S ($4S + O_2 + 4H^+ \rightarrow 4S^{+} + 2 H_2O$).²

Basic features of laccases are presented in Figure 13.2.1 by the example of laccase from *Coriolus hirsutus* established through an X-ray structural investigation. It is a glycoprotein containing approximately 500 amino acid residues. There are four copper ions of types T₁, T₂ and T₃ in the active site. The T₁ site oxidizes substrates; sites T₂ and T₃ reduce dioxygen and by this restore the oxidizing equivalent at T₁. Dinuclear site with T₃ coppers is similar to that in tyrosinases. Blue color of laccases comes from T₁ site which is responsible for the absorbance maximum at 610 nm.

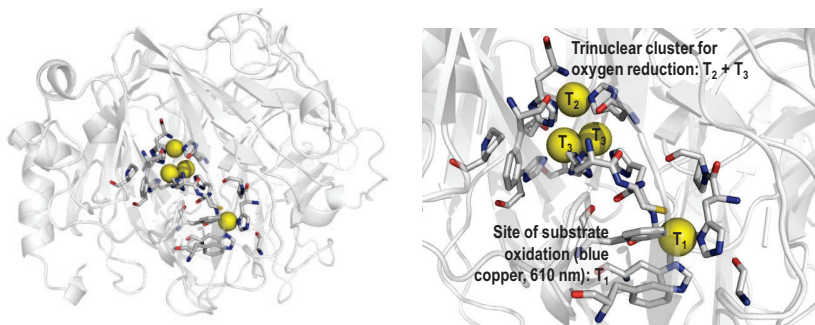
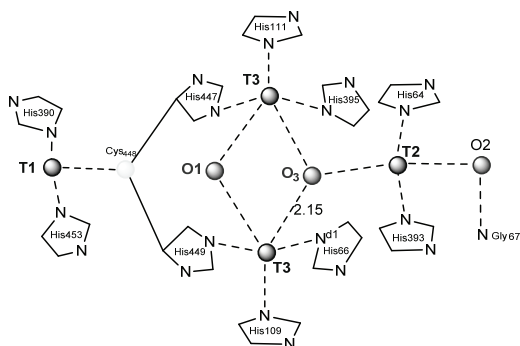


Figure 13.2.1. Structural features of laccase from *Coriolus hirsutus* established by an X-ray investigation.³

Coordination environment of copper ions is shown in Scheme 13.2.1. Note that cysteine sulfur is coordinated to T₁ copper only.

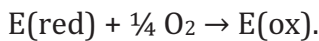
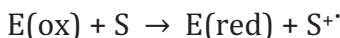
² Solomon EI, et al, *Chem. Rev* **1996**, 96, 2563; Quintanar L, et al, *Acc Chem Res*, **2007**, 40, 445.

³ Pegasova TV, et al, *Acta Cryst, Sect D: Biol Cryst* **2003**, D59, 1459.

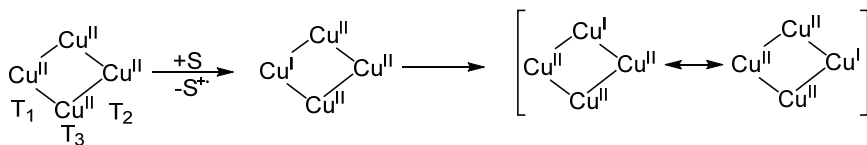


Scheme 13.2.1. Coordination environment of copper ions in laccases.

Laccases practice a ping-pong mechanism of oxidation:



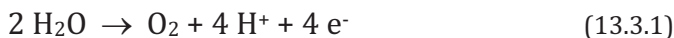
Substrates are oxidized at copper(II) of T₁ first. The lost oxidation equivalent is delocalized over all four copper atoms (Scheme 13.2.2).



Scheme 13.2.2. Delocalization of the lost oxidation equivalent of laccase over all four copper ions

13.3. Biological Generation of O₂

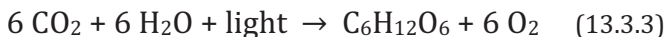
Plants know how to oxidize water into dioxygen via eq 13.3.1. This vital reaction will conclude stories about biological oxidation reactions. Reaction 13.3.1 is one of the most important reactions on the planet, since it is the source of nearly all the atmosphere's dioxygen.



Reaction 13.3.1 is not easy to perform because the reduction potential for the half-reaction 13.3.2 is of 1.229 V (versus NHE), i.e. a very strong oxidizing agent should be generated for performing this redox process.



Reaction 13.3.2 is a part of photosynthesis (eq 13.3.3), a process used by plants and other organisms to convert the energy of light into the energy of chemicals, of saccharides in particular.



Photosynthesis is comprised of two photosystems, i.e. I and II. The photosystem I reduces carbon dioxide into organic matter but consumed electrons are then restored during the oxidation of water via reaction 13.3.1, which is carried out by photosystem II.

Photosystem II is a gigantic dimeric protein complex.⁴ Its dimensions are 105 Å depth (45 Å in membrane), 205 Å length, and 110 Å width. It consists of 16 integral membrane subunits composed of 35 transmembrane helices and three luminal subunits. Reaction 13.3.1 is performed by the deeply buried oxygen evolving complex (OEC), the dimensions of which are incomparably smaller than those of the gigantic protein complex.

OEC consists of four manganese ions and one calcium(II) ion, which are linked by oxo bridges. A crystallographic model of OEC in Fig. 13.3.1 (left) shows that calcium and three manganese constitute a cuban-like Mn₃CaO₄ cluster with the fourth manganese atom attached to it. Calcium(II) does not change its oxidation state during the catalysis and plays a structural role. Nature selected manganese because just this bare ion in the oxidation state 3+ oxidizes water (Lecture 9). The cuban motif is needed for efficient creation and storage of oxidation equivalents, which are finally delivered to water.

The mechanism of photosystem II is displayed in Fig. 13.3.1 (right). There are resting state S₀ and four intermediates S₁–S₄. They all differ

⁴ Ferreira KN, *et al*, *Science* **2004**, *303*, 1831.

in oxidation states of manganese ions. Oxidation states of manganese in S_0 , S_1 and S_2 are identified; those of S_3 and S_4 have to be determined.

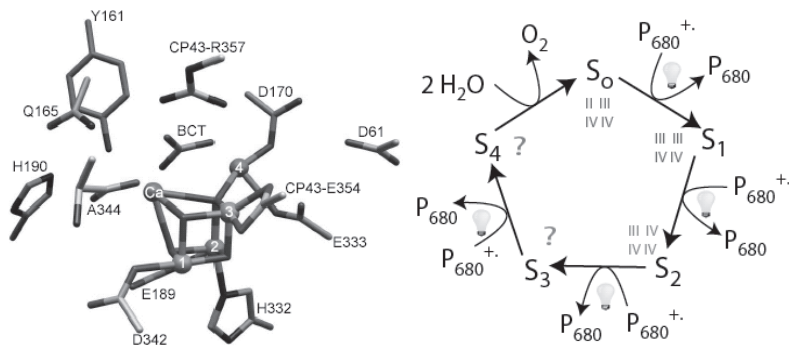
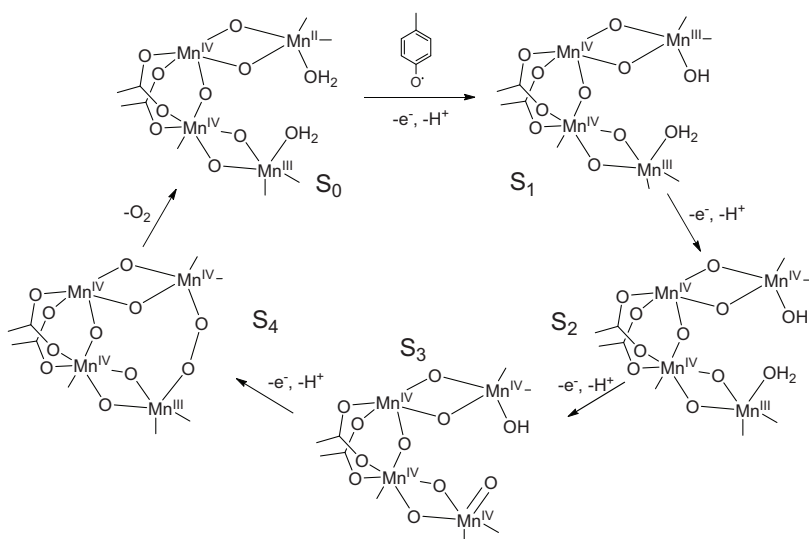


Figure 13.3.1. OEC: crystallographic model (left) and the catalytic cycle (right).⁵

The resting state S_0 is a $Mn_4^{II,III,III,IV}$ state. Two successive $1e$ oxidations convert S_0 to S_1 ($Mn_4^{III,III,III,IV}$) and S_2 ($Mn_4^{III,IV,IV,IV}$) states. The oxidations involve pigment P_{680} , a primary electron donor. Its oxidized form P_{680}^{+} with the reduction potential in the range of 1.3-1.4 V (versus NHE) is photochemically reduced by tyrosine to give a tyrosine radical, which oxidizes manganese ions. The $S_2 \rightarrow S_3$ and $S_3 \rightarrow S_4$ oxidations occur similarly though the exact nature of S_3 and S_4 states is not known yet. In any case S_4 is by four oxidation equivalents above the resting S_0 state, which are required for half-reaction 13.3.1.

Details concerning transformations of manganese centers of OEC presented in Scheme 13.3.1 illustrate how dioxygen is actually produced. Three $1e$ steps lead to S_3 presumably with all four manganese(IV) ions. Note that one Mn^{IV} coordinates hydroxide OH^- and one coordinates oxo O^{2-} ligand. The proton-coupled electron transfer leads to a structure with bridging peroxide, a precursor of the O_2 molecule. The $S_4 \rightarrow S_0$ step can be viewed as a reductive elimination process which lowers the oxidation state of a metal-containing center by two equivalents.

⁵ McEvoy JP, Brudvig GW, *Chem Rev*, **2006**,106, 4455.



Scheme 13.3.1. The mechanistic hypothesis of photosystem II.⁶

Problems

13-1. Compare active sites of tyrosinase and laccase. Identify identical structural motifs.

13-2. What does account for a deep blue color of laccases?

13-3. Explain the choice of Nature: why does manganese comprise the core of oxygen evolving complex?

13-4. Consider Scheme 13.3.1. Explain the fact of deprotonation of the aqua ligand when S₀ is oxidized to S₁.

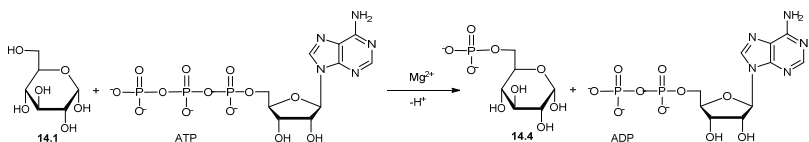
⁶ Tommos C, Babcock GT, *Acc Chem Res*, **1998**, *31*, 18.

LECTURE 14.

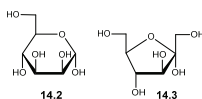
KINASES AND PHOSPHATASES

14.1. Hexo- and Glucokinases

These enzymes¹ catalyze reaction 14.1.1, i.e. the phosphorylation of D-glucopyranose (**14.1**) by adenosine triphosphate (ATP) leading to glucose 6-phosphate (**14.4**) and adenosine diphosphate (ADP). Reaction 14.1.1 occurs in the presence of magnesium ions. Phosphorylation of mannose (**14.2**) and fructose (**14.3**) is also feasible for hexokinases; glucokinases are targeted mostly at glucose. The substrate inhibition by glucose is a common feature of the enzymes.



(14.1.1)



Most native hexokinases from different sources have molecular masses of 50 or 100 kDa, with subunits, when they exist, also with molecular masses of 50 or 100 kDa.² Rather strong inhibition of hexokinases by

¹ Kinases and phosphatases are not oxidoreductases. Though redox enzymes are prioritized in this text, catalysis by kinases and phosphatases is briefly discussed in the final section. This is done due to the understanding of the emerging role of the enzymes in the biological systems because phosphorylation of proteins is directly related to cellular signaling, protein-protein interactions, protein localization and stability, etc. Their dysfunction in human cells is linked to diseases such as cancer and diabetes.

² Cardenas ML, et al, *Biochim Biophys Acta, Mol Cell Res*, **1998**, 1401, 242.

glucose 6-phosphate is a feature of both 50-kDa and 100-kDa enzymes (Table 14.1.1).

Table 14.1.1. Hexokinases: molecular masses, glucose half-saturation concentrations ($K_{0.5}^{\text{Glu}}$)³ and inhibition constants by glucose 6-phosphate (K_i^{Glu6P}).

Enzyme	Mol. mass (kDa)	$K_{0.5}^{\text{Glu}}$ / mM	K_i^{Glu6P} / mM
Rat hexokinase C	99.5	0.007	0.92
Rat hexokinase D	49	5	60
Rat hexokinase B	96	0.23	1.44
Rat hexokinase A	98	0.045	0.21
Loabster hexokinase II	50	0.08	0.8

There are close structural relationships of hexokinase D with the other vertebrate hexokinases. The amino acid compositions of the four isoenzymes is similar, especially those of hexokinases B and D.

Kinetic studies of yeast hexokinase suggested an ordered mechanism catalysis in which the enzyme binds first glucose and then the complex between Mg^{2+} and ATP^4- $\{(\text{Mg-ATP})^2-\}$. The ionic species Mg^{2+} and ATP^4- have only a negligible affinity for the enzyme, or the enzyme-glucose complex.⁴

The structural model of glucokinase was built on the basis of X-ray crystallographic data and computational results. The enzyme is composed of large and small domains. The phosphorylation active site is located in the deep cleft between these two domains (Fig. 14.1.1). The complex $(\text{Mg-ATP})^2-$ is predicted to bind to the left portion of the active site cleft interacting with both domains. The glucose resides in a small pocket providing a favorable microenvironment for its phosphorylation. The γ -phosphate of ATP is close to the C6-OH group of glucose indicating that the γ -phosphate is about to be transferred to glucose.

Lys169 is a key determinant for glucose phosphorylation which might be a *general acid* catalyst to enhance the electrophilicity of the γ -phosphorus atom and by such facilitate the nucleophilic attack of the

³ $K_{0.5}^{\text{Glu}}$ can be viewed as pseudo-Michaelis constants.

⁴ Noat G, et al, *Eur J Biochem*, **1968**, 5, 55

C⁶-OH oxygen at phosphorus. In turn, Asp205 acts as a base that polarizes the O-H bond making the oxygen more nucleophilic.

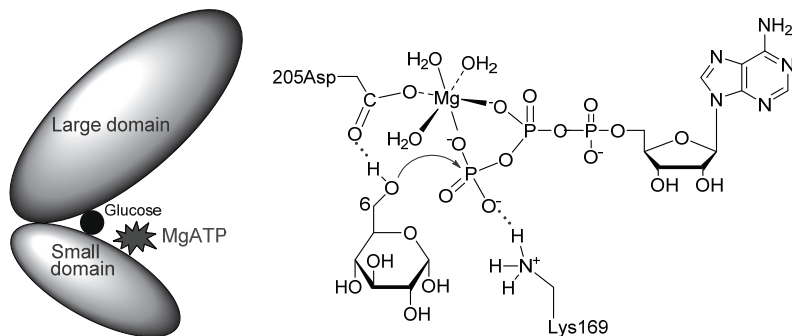


Figure 14.1.1. Structural model of the [glucokinase-(Mg-ATP)²-glucose] complex⁵ and the mechanism of phosphorylation.⁶

14.2. Protein Kinases

Protein kinases are critical for metabolism, cell signaling, protein regulation, cellular transport, secretory processes, etc., and therefore are important for humane physiology. The enzymes phosphorylate hydroxyl groups of serine, threonine and tyrosine residues as it is shown in Fig. 14.2.1. Phosphate is transferred from ATP. Protein kinases are numerous. Among them 85% phosphorylate serine, 11.8% threonine and 1.8% tyrosine.⁷ The former two are referred to as serine kinases; the latter are tyrosine kinases. Remarkably, protein kinases have much lower capacity for phosphorylation of the corresponding free amino acids.

⁵ Zhang J, Li C, Shi T, Chen K, Shen X, et al, *PLoS ONE* 4, **2009**, e6304. doi:10.1371/journal.pone.0006304.

⁶ Wang J, et al, *RSC Adv*, **2015**, 5, 18622.

⁷ Schwartz PA, Murray BW, *Bioorg Chem*, **2011**, 39,192.

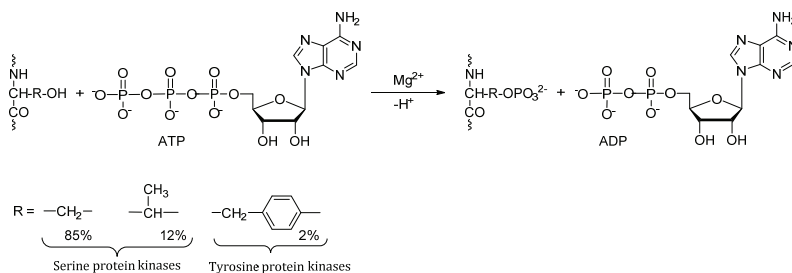


Figure 14.2.1. Hydroxy-group containing amino acid residues phosphorylated by protein kinases.

The substrate specificity of protein kinases is determined by the amino acid residues in the vicinity of a hydroxyl containing residue, which is phosphorylated (P-site). Residues N-terminal to P-site are sequentially numbered P-1, P-2, P-3, etc.; C-terminal residues are P+1, P+2, P+3, etc. Approximately four 'minus' and four 'plus' residues are essential for phosphoryl transfer. Protein kinase A, for example, prefers to phosphorylate serine and threonine of peptides with positively charged residues at P-2 and P-3, whereas P+1 should be a small hydrophobic residue [apply the rule to the synthetic peptide Kemptide (Leu-Arg-Arg-Ala-Ser-Leu-Gly) which is commonly used as a substrate for protein kinase A].

The sequence comparisons of the members of protein kinase family reveal a conserved region of ca. 200–250 amino acids that confers the kinase activity. There is a common kinase domain. Let us consider this by the example of deeply investigated, characterized by X-ray crystallography protein kinase A (PKA). PKA is an adenosine 3',5'-monophosphate-dependent (cAMP, cyclic AMP) heterotetramer composed of a regulatory dimer R₂ and two catalytic subunits 2C. The 2C subunits become catalytically active when cAMP binds to R₂ and induces dissociation of the tetramer. The C-subunit of PKA is comprised of two domains – a small ATP binding domain composed primarily of α helices and a larger substrate binding domain composed mostly of β strands (Fig. 14.2.2). The two domains are connected by a small linker region and generate a binding pocket for the substrate peptide and ATP.

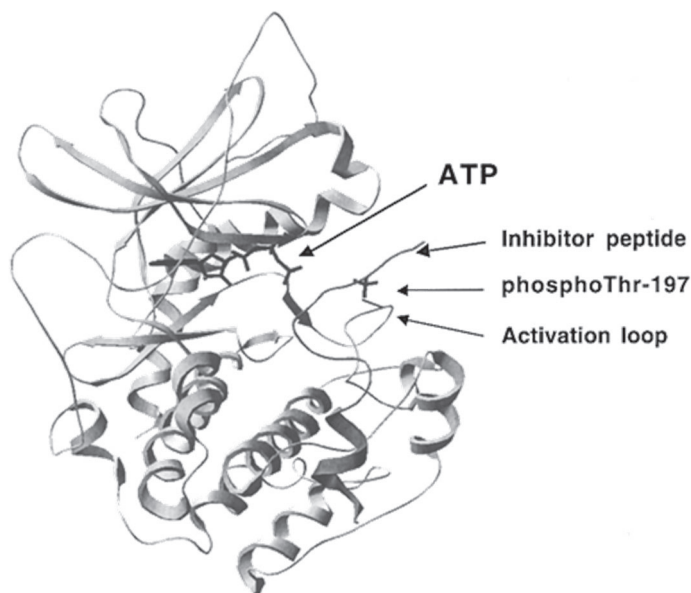


Figure 14.2.2. Ribbon diagram of PKA cocrystallized with ATP and a 20-amino acid inhibitor peptide, PKI (5–24). Arrows point to the activation loop and the phosphorylation site, phosphoThr-197, in the activation loop.⁸ Reprinted with permission. Copyright 2001 American Chemical Society.

The activities of the protein kinases are regulated through an assortment of mechanisms involving regulatory subunits and domains, fatty acid acylation, isoprenylation, and phosphorylation. The phosphorylation is germane and can be correlated with the catalysis. The essential phosphorylation site in PKA, Thr-197, is part of a loop segment known as the activation loop (Fig. 14.2.2). This phosphorylation enhances catalytic activity of PKA by an order of magnitude.⁹ Many protein kinases are also phosphorylated in the activation loop. This residue is far from the site of phosphoryl transfer. The activation loop may function as a “door” to the substrate pocket, a phenomenon which could explain rate enhancements observed upon phosphorylation of the activation loop.

⁸ Adams JA, *Chem Rev*, **2001**, *101*, 2271.

⁹ In terms of k_{cat}/K_M for Kemptide as a substrate.

Figure 14.2.3 shows the active site of PKA and highlights key residue interactions. Asp-184, a strictly conserved residue, interacts with the essential Mg^{2+} (1), which chelates the β and γ phosphates of ATP. Additional stabilization may emanate from the interaction of Lys-72 with α and β phosphates of ATP. The conserved Asp-166 is near the alanine of the inhibitor peptide. Owing to its proximity, Asp-166 may direct the hydroxyl for attack on the γ phosphate of ATP.

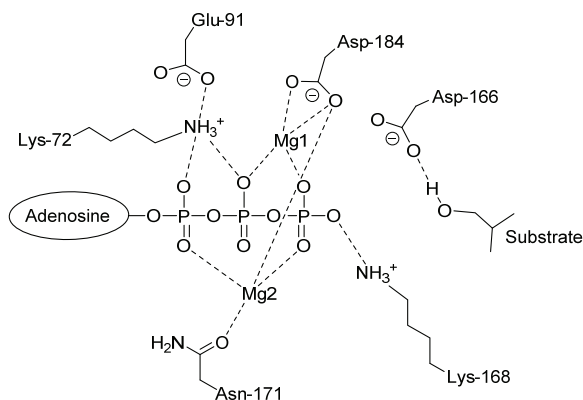


Figure 14.2.3. Key residue interactions in the active site of PKA. Mg^{2+} (1) and (2) represent the PKA-activating (of higher affinity) and PKA-inhibitory (of lower affinity) Mg^{2+} , respectively. The drawing is based on the PKA ternary complex with ATP and a peptide inhibitor. The dotted lines indicate close contacts of less than 2.6 Å but are not drawn to scale.

Lys-168 in PKA makes an electrostatic contact with the γ phosphate and a contact with Thr-201, a residue that forms part of the P+1 binding cleft. In yeast PKA, replacement of this lysine with alanine leads to a mutant protein with a 30-fold elevated K_M for Kemptide and 50-fold reduced k_{cat} . This is consistent with a role for lysine in supporting both the phosphoryl transfer step and possibly peptide binding. It is worth noting that wild type PKA at pH 7 has the following kinetic characteristics: $k_{cat} = 20 \text{ s}^{-1}$, $K_M(\text{Kemptide}) = 2.6 \times 10^{-5} \text{ M}$ and $K_M(\text{ATP}) = 3.8 \times 10^{-5} \text{ M}$. The disordered substrate binding is believed to be typical of PKA though this is not true for all protein kinases.

Chemistry wise, the key transformation in kinases is a nucleophilic substitution at phosphorous(V). The incoming hydroxyl nucleophile ROH replaces the leaving adenosine diphosphate HOADP (Fig. 14.2.4).

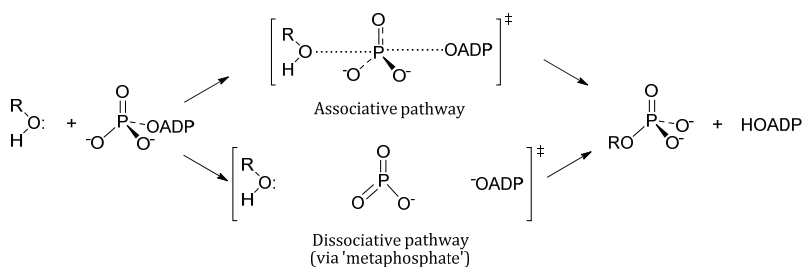


Figure 14.2.4. Associative and dissociative mechanisms of phosphorylation of serine, threonine and tyrosine residues catalyzed by protein kinases.

Two reaction mechanisms of phosphorylation, viz. associative and dissociative pathways, are actively debated (Fig. 14.2.4). The associative concerted pathway involves a synchronous formation of a new O–P bond between the incoming nucleophile and γ phosphate and a cleavage of P–O bond between γ phosphate and ADP. A dominant feature of the dissociative pathway is the cleavage of the γ phosphate–ADP P–O bond to form a hypothetical 'metaphosphate' intermediate. The two limiting cases have obvious mechanistic similarities with the nucleophilic S_N1 and S_N2 substitutions at sp^3 carbon. Discrimination of the two enzymatic mechanisms is a very difficult task due to several objectives. In the PKA case it is even more complicated because the phosphorylation as in Fig. 14.2.4 is not the rate-limiting step (dissociation of ADP from the enzyme-substrate complex is such). The current state of knowledge favors the associative pathway.

Structural features presented in Fig. 14.2.3 are also more consistent with the associative pathway. In fact, the hydrogen bond between conserved Asp-166 and the substrate could polarize the H–O bond, increase an excess negative charge (δ^-) at oxygen and make oxygen more nucleophilic. Second, the electrostatic contact or hydrogen $\text{H}_3\text{N}^+\cdots\text{O}$ bond between Lys-168 and the γ phosphate of ATP could increase an excess positive charge (δ^+) at phosphorous, make the latter more electrophilic and also facilitate the nucleophilic attack.

14.3. Phosphatases¹⁰

Phosphatases catalyze the hydrolysis of phosphate monoesters, the net transfer of the phosphoryl group to water, producing inorganic phosphate (eq 14.3.1). Cautiously, they run a reverse chemistry compared to that catalyzed by kinases.



Phosphatases that transfer the phosphoryl group directly to water possess a binuclear metal center, and the nucleophile is a metal-coordinated hydroxide (i.e. alkaline phosphatase). Other phosphatases follow a two-step overall kinetic mechanism, forming a phosphoenzyme intermediate that is subsequently hydrolyzed by water (i.e. acid phosphatase). The stereochemistry (at phosphorus) is variable. Inversion results from direct phosphoryl transfer to water. A ping-pong mechanism with a phosphoenzyme intermediate will yield a final product with retention of configuration.

14.3.1. Alkaline Phosphatases

Alkaline phosphatases (AP) catalyze the nonspecific hydrolysis of the dianion form of phosphomonoesters ROPO_3^{2-} . The most studied two zinc *E. coli* AP has two identical subunits with 429 amino acid residues. Catalytic rate constants k_{cat} equal 13–45 s^{-1} (pH 8.0) with $K_{\text{m}} \sim 10^{-6}$ M regardless the nature of R. Phosphate is a competitive inhibitor with $K_{\text{i}} \sim 10^{-6}$ M. The pH profile of activity of AP (k_{cat}) is sigmoid and determined by a single event with $\text{p}K_{\text{a}} \sim 7.5$.

The stoichiometric mechanism of AP is shown in Fig. 14.3.1. Here $\text{E}\cdots\text{ROP}$ is a non-covalent enzyme-substrate complex, which undergoes nucleophilic attack by the alkoxide form of Ser-102 to form $\text{E}-\text{P}$ where phosphate is bound to Ser-102. The second nucleophilic attack now at $\text{E}-\text{P}$ results in a cleavage of the serine-phosphate bond and formation of $\text{E}\cdots\text{P}$ where phosphate is bound non-covalently. Dissociation of phosphate finalizes the catalytic cycle.

¹⁰ Coleman JE, *Annu Rev Biophys Biomol Struct*, **1992**, 21, 441; Cleland WW, Hengge AC, *Chem Rev*, **2006**, 106, 3252.

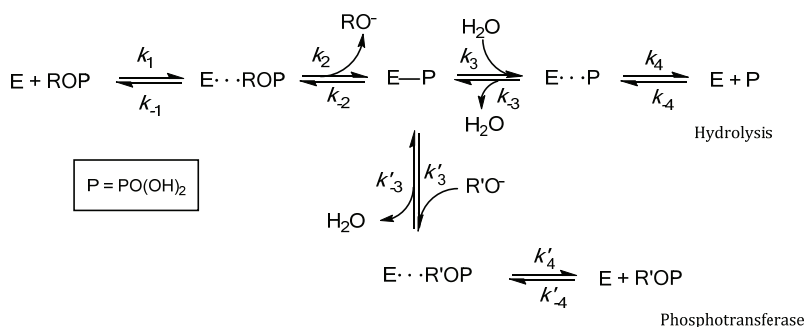


Figure 14.3.1. The stoichiometric mechanism of AP.

At $pH > 7$, the rate-limiting step in the overall mechanism is a release of inorganic phosphate from $E \cdots P$; the hydrolysis of the phosphoserine intermediate $E-P$ is rate-limiting at $pH < 7$.

The active site of the AP from *E. coli* contains two Zn^{2+} ions and one Mg^{2+} ion. The zinc ions are involved in catalysis; the Mg^{2+} functions as a general base provider that deprotonates the Ser nucleophile to form Mg-coordinated hydroxide. All known alkaline phosphatases have this conserved three-metal ion center, as well as an arginine residue (Arg-166 in *E. coli* AP) that plays a role in binding and probably stabilizes the transition state.

Coordinative environment of tetrahedral Zn_1 and Zn_2 is different. Zn_1 is surrounded by Asp-237 and two His (331 and 412). There are two Asp (51 and 369) and His-370 around Zn_2 . The fourth site is occupied by phosphate in $E \cdots P$. Six coordinate Mg is surrounded by Asp-51, Thr-369, His-370 and three water molecules.

Structural and mechanistic details of catalysis by AP are shown in Fig. 14.3.2. Substrate in $E \cdots ROP$ coordinates to both zinc ions and also forms hydrogen bonds with Arg-166. The leaving group oxygen atom is coordinated to Zn_1 and is opposite from Ser-102. Zn_2 favors deprotonation of Ser-102 to form a more nucleophilic serine alkoxide. Zn_1 facilitates P-O bond fission by stabilization of a negative charge on the leaving group oxygen atom. Roles of the two zinc ions reverse in the subsequent hydrolysis of the intermediate $E-P$. After departure of RO^- , water can coordinate to Zn_1 . The Zn_1 -hydroxide attacks the phosphoserine intermediate; its departure is stabilized by

coordination with Zn_2 . There are two nucleophilic attacks at phosphorous, viz. within both $E \cdots ROP$ and $E-P$. Each occurs with inversion providing overall retention of configuration at phosphorous.

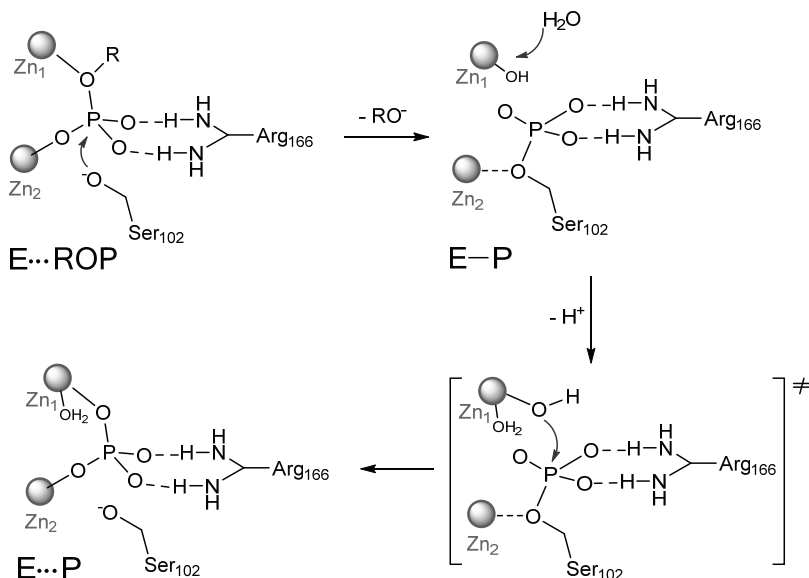


Figure 14.3.2. Structural and mechanistic details of catalysis by AP.

The second nucleophilic attack occurs with OH^- coordinated to Zn_1 . This job can also be performed by external nucleophiles such as alcohols ($R'OH$). This pathway presented at the bottom of Fig. 14.3.1 accounts for the phosphotransferase activity of AP which manifests in the formation of $R'OP$ from ROP and $R'OH$.

Mammalian APs have low sequence identity with the *E. coli* enzyme (25–30%) but the active site residues are conserved and the catalytic mechanism is the same.

14.3.2. Acid Phosphatase

As is the case for alkaline phosphatases, acid phosphatases are nonspecific and catalyze the hydrolysis of phosphomonoesters via a phosphoenzyme intermediate. Acid phosphatases have a conserved

nucleophilic histidine, acidic pH optima and have no metal ions. The catalysis involves a phosphohistidine intermediate and occurs with net retention of configuration.

An X-ray structural study of the rat enzyme with bound vanadate¹¹ identified the likely roles of the conserved His and Asp residues, which are His-257 and Asp-258 in the rat enzyme. In the *E. coli* acid phosphatase, His-303 and Asp-304 correspond to these residues. The Asp residue serves as a general acid to protonate the leaving group in the first phosphoryl transfer step (Fig. 14.3.3). A logical assumption is that the carboxylate -COO^- form of the Asp residue then acts as a general base to deprotonate a nucleophilic water molecule in the second step, hydrolysis of the phosphohistidine intermediate.

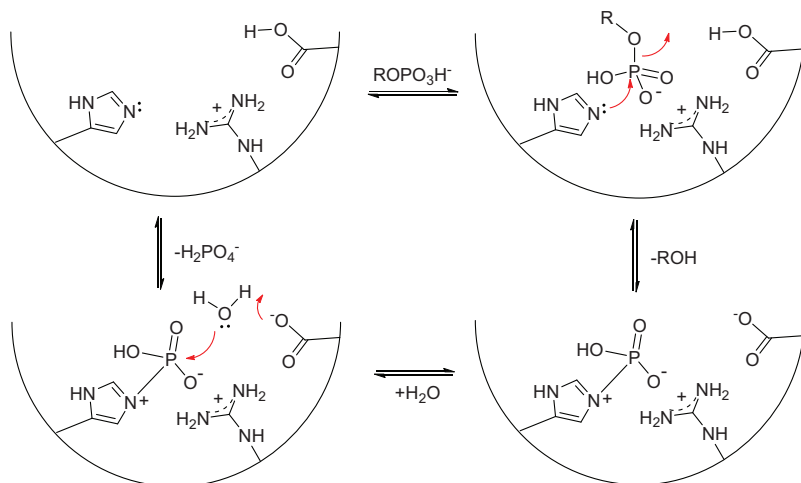


Figure 14.3.3. Mechanism of catalysis by acid phosphatase.¹¹

¹¹ Araujo CL, Vihko PT *Structure of Acid Phosphatases*. In: Millán J. (ed) *Phosphatase Modulators*. Methods in Molecular Biology, **2013**, vol 1053. Humana Press, Totowa, NJ.

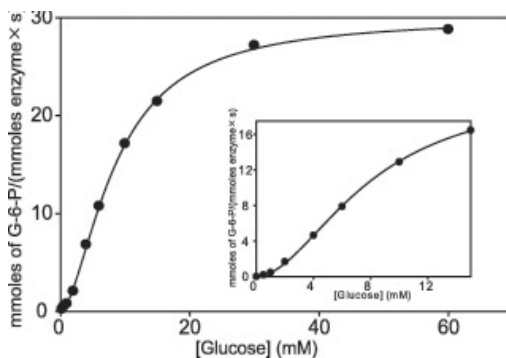
Problems

14-1. Relate the associative and dissociative pathways presented in Fig. 14.2.4 to the S_N1 and S_N2 nucleophilic substitutions at the sp^3 C atom.

14-2. Indicate the difference between hexokinases and glucokinases.

14-3. Find at least two similarities in mechanisms of catalysis by glucokinases and protein kinases by comparing Figs. 14.1.1 and 14.2.3.

14-4. The graph below shows the steady-state rate of the enzymatic reaction catalyzed by the wild-type human glucokinase as a function of glucose concentration.¹² The data and inset in particular reveal an important feature of catalysis by this enzyme. Name this feature.



14-5. Inversion or retention? Suggest stereochemical fate of phosphorus in terms of mechanism of catalysis by acid phosphatase presented in Fig. 14.3.3.

¹² Larion M, Miller BG, *Arch Biochem Biophys*, **2012**, 519, 103.